UNIVERSITÉ
DE STRASBOURG

École doctorale
des Sciences de la Vie et de la Santé

JUSTUS LIEBIG
UNIVERSITÄT

Fachbereich 08
Biologie und Chemie

Institut de génétique et de biologie moléculaire et cellulaire (IGBMC)

Joint PhD THESIS
presented by

Raquel MELA LÓPEZ

To obtain the academic degree of

DOCTOR FROM THE UNIVERSITIES OF STRASBOURG AND GIESSEN
Sciences de la vie et de la santé
Doctor rerum naturalium

Thioredoxin reductase
in *Anopheles gambiae* mosquitoes:
ROLE IN REDOX HOMEOSTASIS MAINTENANCE
AND MANIPULATION FOR VECTOR CONTROL

SUPERVISORS
    Dr. Stephanie **BLANDIN**   Chargée de recherche, Université de Strasbourg
    Prof. Dr. Katja **BECKER**   Professor, Justus Liebig Universität Giessen

RAPPORTEURS
    Prof. Dr. Christopher Horst **LILLIG**   Principle investigator, Universitatsmedizin Greifswald
    Prof. Dr. Hilary **RANSON**   Professor, Liverpool School of Tropical Medicine

EXAMINATEURS
    Dr. Dominique **FERRANDON**   Directeur de recherche, Université de Strasbourg
    Prof. Dr. Tina **TRENCZEK**   Professor, Justus Liebig Universität Giessen

INVITED MEMBERS
    Dr. Elisabeth **DAVIOUD-CHARVET**   Directrice de recherche, Université de Strasbourg

Thioredoxin reductase
in *Anopheles gambiae* mosquitoes:
ROLE IN REDOX HOMEOSTASIS MAINTENANCE
AND MANIPULATION FOR VECTOR CONTROL

PhD thesis

To obtain the degree of doctor at the
Universities of Strasbourg and Giessen

by

Raquel MELA LÓPEZ

Strasbourg, 2019

This doctoral thesis was carried out in the frame of a joint PhD thesis at

Université de Strasbourg, France

under the supervision of Dr. Stéphanie BLANDIN

and

Justus Liebig Universität Giessen, Germany

under the supervision of Pr. Katja BECKER

The experimental work was conducted at the

Insitut the Biologie Moléculaire et Cellulaire, University of Strasboug

and

Institut für Ernährungswissencshaft, University of Giessen

This doctoral thesis was financially supported by

University of Strasbourg

ZikAlliance consortium

Deutsch-Französische Hochschule / Université Franco-allemande

Deutscher Akademischer Austausch Dients

THESIS COMMITTEE

Supervisors

Dr. S. Blandin, Institut de Biologie Moléculaire et Cellulaire, Université de Strasbourg.

Prof. dr. K. Becker, Institut für Ernährungswissenschaft, Justus Liebig Universität Giessen.

Rapporteurs

Prof. dr. C.H. Lillig, Institut für medizinische Biochemie und Molekularbiologie, Universitätsmedixin Greifswald.

Prof. dr. H. Ranson, Liverpool School of Tropical Medicin.

Examinateurs

Prof. dr. T. Trenczek, Institut für Allgemeine Zoologie und Entwicklungsbiologie, Justus Liebig Universität Giessen

Dr. D. Ferrandon, Institut de Biologie Moléculaire et Cellulaire, Université de Strasbourg.

Invited members

Dr. E. Davioud-Charvet, École Européene de chimie, polymerres et materiaux, Université de Strasbourg

•••

Oral examination

Monday 9 December 2019, Institut de Biologie Moléculaire et Cellulaire, Université de Strasbourg.

ACKNOWLEDGEMENTS

Un merci spécial à ma petite pomme, **Pauline**, pour la bonne humeur et le bon travail. Travailler avec toi à vraiment été un plaisir. Tu sais bien que sans ta perseverance il maquerait une bonne partie de cette thèse. **Lilly**, thank you for the work, the ideas and everlasting talks about everything and nothing. I am really happy that you chose to come to Strasbourg because meeting you has really been a pleasure. Thanks to Marina for teaching me how to do the biochemical assays and for all the hard work with the screenings.

Du point de vu personel, je voudrais tout d'abord remercier **Dr. Joern Pütz** pour m'avoir accueilli comme étudiante Erasmus en 2012. Sans tout ton travail je ne serais pas en train d'écrire ces remerciements.

Esta tesis se la debo a **toda mi familia**, sin la cual ni sería ni querría ser como soy. **Abuela**, gracias por el queso y el embutido que me das cada vez que voy y que raciono aquí como si no fuera a volver a probarla. Tío **Javi**, tía **Merce**, gracias por las comidas cuando vuelvo a Madrid. Y por supuesto, esta tesis os la dedico especialmente a vosotras, **Noemi** y **Clara**, porque, literalmente, esto sólo ha sido posible gracias a vosotras.

Carmen y **Luís**, me acuerdo muchísimo de vosotros y de vuestros consejos. Vuestro amor por la biología es la semilla que hoy florece en forma de tesis.

Gracias a mi gran mae, **Pablo**, que en tantas locuras me ha embarcado, y al **resto de amigos** que he hecho a lo largo de esta aventura; gracias por los buenos momentos, sobre todo estos últimos meses que han sido duros. Merci à la **team de Nancy** pour m'avoir accepté les bras ouverts quand j'arrivais à peine à suivre ce qui vous disiez.

Mis chi...cas Alba, Ana C, Ana F, Ana G, Carmen, Esther, Irene y María. Gracias por los millones de mensajes diarios que con elegancia ignoro (pero con cariño, también); me hacen sentir en casa. Me hace muy feliz saber que aunque los años y los kilómetros pasen, siempre estáis ahí, como si nada hubiese cambiado. Gracias por ser como sois.

Dr. Sandra, contigo empezó todo. Gracias por descubrirme el Erasmus prácticas y por amenizarme cultivos aquel año. Me muero de amor con que nos embarcáramos en esta locura juntas y que vayamos a terminarla a la vez. Gracias por los consejos sobre cómo lidiar con la escritura, pero sobre todo gracias por los buenos momentos.

Dr. Marta, contigo también empezó todo. Eres la prueba viva de que madre sí hay más que una. Si alguien me hubiera dicho en 2012 que este iba a ser nuestro camino, creo que me habría dado la risa. Has sido un apoyo y una fuente de inspiración en tantos y tan diversos momentos que sería imposible citarlos, pero gracias por todos y cada uno de ellos.

¡**Simone**!, mi tercer fantástico, mi hermano de otra madre. Ojalá tener una máquina del tiempo y susurrarme al oído que pasaríamos de pedirnos tabaco a pedirnos reactivos. No hacer falta que te diga el enorme apoyo que has sido para mí tanto dentro como fuera del laboratorio. Gracias por tantas discusiones sobre todo lo que hay escrito en esta tesis, pero sobre todo, gracias por ser mi amigo.

A ma deuxième famille, **Rina**, **Jacques**, **Mélina** et **Lola**, qui m'ont toujours donné leur support et qui m'ont fait sentir que j'étais chez-moi dès la première minute. Rina, Jacques, merci d'avoir été mes parents quand les miens étaient à plus de 1500 km. Et surtout… merci pour tout le chocolat que vous m'avez offert pour que je tienne pendant la rédaction!

Papá, **mama**, gracias por absolutamente todo. Por no haberme cortado nunca las alas, por haberme dejado embarcarme en la locura de venir a Estrasburgo. Gracias por acompañarme al teléfono del laboratorio a casa y por darme tanto amor las pocas veces que vuelvo a casa. Prometo que intentaré ir más. **Lala**, sestra mía, gracias por los memes y todas las tonterías que me mandas. Por los momentos juntas estos meses, por ser mi conejillo de indias cada vez que quiero pintar uñas. Gracias por preocuparte por mí y por mandarme fotos de Budy. Y por supuesto, **Budy**, gracias por existir.

Y por último gracias a ti, **Nico**. Merci de m'avoir supporté ces derniers mois malgré tout et merci de m'avoir accompagé dans tout ce voyage. Sé que no ha sido fácil para ti tampoco, pero esto no ha hecho sino reafirmar que tienes el corazón más grande que he visto nunca. Merci pour allés-retours à Giessen et merci de me supporter parler de choses que tu comprends même pas; merci de l'intérêt que tu as toujours montré pour ce que je fais. Nunca me habría imaginado que este sería mi camino ni que sería tan duro a ratos, pero no cambiaría ni uno solo momento porque los hemos vivido juntos.

LISTS OF ABBREVIATIONS

Abbreviations

AChE	Achetylcholinesterase
BSA	Bovine Serum Albumin
CCE	Carboxylesterases
cDNA	Complementary DNA
COPAS	Complex Object Parametric Analyzer and Sorter
CRISPR / Cas9	Clustered Regularly Interespaced Short Palindromic Repeats / CRISPR associated 9
DA	Diamide
DDT	Dichlorodiphenyltrichloroethane
Dhd	Deadhead
dpBF	days post Blood Feeding
dsRNA	double-stranded RNA
DTT	Dithiothreiol
ECT	Electron Transport Chain
EGSH	Glutathione redox potential
FAD	Flavin Adenine Nucleotide
GCL	Glutamate-Cysteine Ligase
GFP	Green Fluorescent Protein
GGT	γ-glutamyltranspeptidases
GMAP	Global Malaria Action Plan
GMEP	Global Malaria Eradication Program
GS	Glutathione Synthetase
GR	Glutathione Reductase
gRNA	Guide RNA
Grx	Glutaredoxin
GSH	Reduced glutathione
GSSG	Oxidized glutathione
GST	Glutathione S-transferase
hGrx1-roGFP2	Human glutaredoxin-1 linked to redox-sensitive green fluorescent protein 2
Hpx	Heme peroxidase
IC$_{50}$	Half maximal inhibitory concentration
Indel	Insertion/Deletion

IRS	Insecticide Residual Spraying
ITN	Insecticide-Treated Net
JH	Juvenile hormone
Kdr	Knock Down Resistance
KO	Knockout
LB	Luria-Bertani
LD$_{50}$	Median lethal dose
LLIN	Long-Lasting Insecticidal Nets
logP	Partition coefficient octanol-water
MRS	Methionine R-Sulphoxide reductase
nAChR	Nicotinic acethylcoline receptor
NADPH	Nicotinamide Adenine Dinucleotide Phosphate
nBF	non Blood-Fed
NEM	N-Ethyl Maleimide
NHEJ	Non-Homologous End Joining
Ni-NTA	Nickel-nitrilotriacetate
NOS	Nitric Oxide Synthase
NOX	NADPH oxidase
NQ	1,4-Naphthoquinone
P450	Cytochrome P450
PBS	Phosphate Buffered Saline
PFA	Paraformaldehyde
Prx	Peroxiredoxine
PTM	Post-Translational Modifications
QA	Quinic Acid
QF	Q transcription Factor
QS	Q Suppressor
QUAS	Q promoter
RNAi	RNA interference
RNS	Reactive Nitrogen Species
roGFP	Redox-sensitive GFP
ROS	Reactive Oxygen Species
Rpl19	60s Ribosomal protein L19
RT-PCR	Reverse Transcription PCR
rxYFP	Redox-sensitive YFP
SOD	Sodium Dismutase

TALEN	Transcription Activator-Like Effector Nuclease
Trx	Thioredoxin
TrxR	Thioredoxin Reductase
TrxR-KO$_{MG}$	Thioredoxin Reductase midgut knockout
WHO	World Health Organization

Abbreviations of oxygen and nitrogen species

H$_2$O$_2$	Hydrogen peroxide
O$_2$	Molecular oxygen
·O$_2^-$	Superoxide anion
·OH	Hydroxyl radical
OH$^-$	Hydroxil anion
ONOO$^-$	Peroxynitrite
NO·	Nitric oxyde
NO$_2^-$	Nitrite
ROO·	Peroxylradical

TABLE OF CONTENTS

LIST OF FIGURES

LIST OF TABLES

INTRODUCTION

1. MOSQUITOES

Mosquitoes, or Culicidae, are a family of insects from the order Diptera that includes around 3000 different species (Rozendaal, 1997). These animals can be found in any latitude, with the exception of regions that are permanently frozen, but they mostly populate tropical and subtropical areas. They present holometabolism, i.e. complete metamorphosis (Fig. I.1). Adult mosquito females lay their eggs on water bodies or areas that will be flooded. Inside, the embryo develops for a variable amount of time (depending on the species and environmental conditions) until a fully formed larva hatches. The larval stage is aquatic and is characterized by a worm-like body shape. Larvae feed on detritus and microorganisms and breathe air, which forces them to stay at the surface of the body of water or close to it. A total of four molts occur during this period; the first three result in very similar looking larvae, while the last one involves rapid development of the imaginal disks and results in a pupa that already comprises many adult features. Pupae are also aquatic and present a very distinctive comma-like body with sexual dimorphism. While the last adult tissues are formed, pupae do not feed and rest by the surface of water where
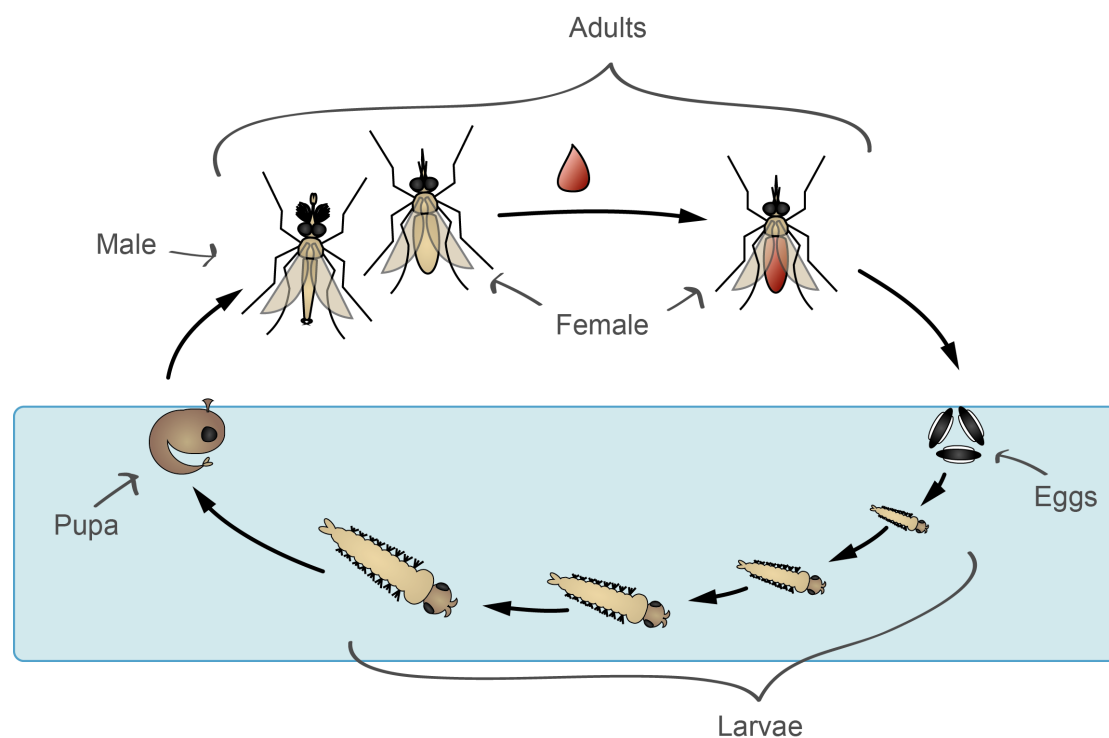
Figure I.1 Mosquito lifecycle. Females lay eggs on water bodies. Larvae hatch from the eggs and undergo four instars with molting in-between. Fourth instar larvae molt into pupae where the last adult tissues are formed. Eventually, a fully formed adult mosquito hatches from the pupa and lives outside of the water. Female adults feed on blood to be able to develop their eggs, closing the cycle.

they can breathe. This process lasts at least one day and results in a fully formed adult, the last stage of the lifecycle and the one that interacts with humans. Adult mosquitoes present an elongated body shape with a long proboscis and sexual dimorphism, as males are smaller in size and present bushy antennae. Their abdomen is also thinner and ends with claspers, which they use to grab on to the female. At this stage, mosquitoes mostly feed on the nectar of plants and contribute to pollination. However, females must feed on the blood of vertebrates to uptake amino acids that are required for egg production. Indeed, very few mosquito species are capable of reproduction without a blood meal. A few days after having fed on blood, females are ready to lay eggs, closing the cycle.

The blood feeding behavior of mosquitoes provides microorganisms with the opportunity to be carried from and to the vertebrate hosts on which they feed. This feature has been exploited by several human pathogens, awarding mosquitoes with the dubious honor of being the deadliest animals on Earth (Gates, 2018). From a biomedical point of view, the most important mosquito vectors fall into three genera: *Anopheles*, *Aedes* and *Culex* (Fig I.2).

A. Anopheles spp.

This genus groups about 380 species, out of which around 60 are important for human health (Rozendaal, 1997). These mosquitoes are characterized by their brown pigmentation and the position they acquire when resting, with the stomach pointing upwards rather than in parallel to the surface (**Fig I.2 A**). They bite from dusk until dawn, inside and outside households.

Although they can also transmit filariasis and some viruses, these mosquitoes are most commonly known as the malaria mosquitoes. The most affected region is Africa, where two major malaria vector species are present: *A. gambiae s. l.* and *A. funestus*. The former is actually a complex of morphologically indistinguishable species that includes *A. gambiae s. s.*, *A. coluzzii* and *A. arabiensis* (Godfray, 2013). These mosquitoes are anthropophilic and can lay their eggs on puddles formed by rain, explaining the higher incidence of malaria during the rainy seasons. Moreover, *A. coluzzii* can also exploit sitting waters derived from human activities such as the small puddles formed by tire traces.

B. Aedes spp.

This genus contains more than 950 different species (Rozendaal, 1997) characterized by the dark pigmentation of the body decorated with light patterns (**Fig I.2 A**). They bite during the day, but their activity peaks at dawn and dusk. Most species breed and bite outdoors.

The main representative of this genus is *A. aegypti*, also known as the dengue mosquito although it can transmit several other viruses such as zika, chikungunya or yellow fever.

A. aegypti mosquitoes are divided into two subpopulations named *A. aegypti formosus* and *A. aegypti aegypti*. The former is found only in Africa and has reduced vectorial capacity. It is proposed that an ancestral *A. aegypti formosus* population evolved to become a human specialist, giving rise to the subspecies *A. aegypti aegypti,* a much more potent vector of human viruses that migrated throughout the tropics (Crawford et al., 2017), explaining why these diseases largely affect the Americas and Asia. These mosquitoes like urban habitats and their eggs can dry and stay so for over a year, hatching when they get in contact with water. Another important species of this genus is the tiger mosquito *A. albopictus*. It is not as efficient a vector as *A. aegypti* but it can still be responsible for outbreaks such as that of chikungunya recorded in Italy in 2017 (Venturi et al., 2017). The danger of these mosquitoes relies also in their wider geographical distribution that extends from tropical to milder climates (Kraemer et al., 2015) and the fact that they keep expanding with the help of human circulation and exchanges.

C. Culex spp.

This genus comprises around 550 species (Rozendaal, 1997). Although they belong to the same *Culicinae* subfamily as *Aedes* mosquitoes, they are similar to *Anopheles* mosquitoes in color; however, as for *Aedes* mosquitoes, their body remains parallel to the surface in resting position (**Fig I.2 A**). They mostly bite indoors during the night.

The two most relevant species are *C. pippiens pippiens*, known as the common mosquito in Europe, and *C. quinquefasciatus*, the common mosquito of the South hemisphere. They usually breed in polluted water, which favors their presence in urban areas. They can transmit filariasis and several viruses such as west Nile virus and Japanese encephalitis.
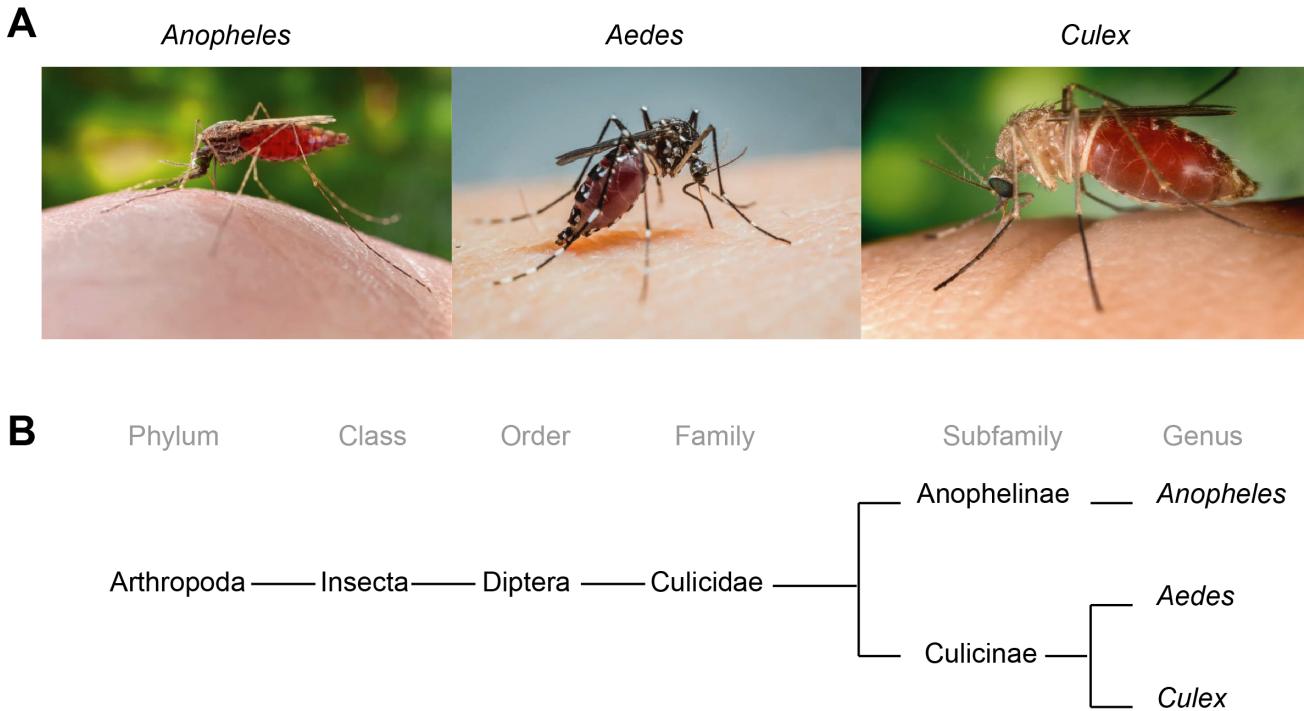
Figure I.2. Mosquito genus of biomedical relevance. (A) Females of the three main vector mosquito genus feeding on a host**.** Pictures taken by James Gathany and Pablo Cabrera (free of copyright); obtained from the Public Health Image Library (http://phil.cdc-gov). **(B)** Phylogenetic tree. Distances are not representative.

2. MALARIA

Malaria is, by far, the deadliest of all vector-borne diseases. In 2017 alone, it caused 435 000 deaths and infected 290 million people in 87 countries. The most affected region is Africa with 92 % of all cases, and the most vulnerable group are children under the age of 5, representing 61 % of all deaths (WHO, 2018).

For the most part, the symptoms of malaria include headaches, fatigue, muscular pain, nausea, vomits and recurring high fever. In the most severe cases, it can also cause anemia and organ failure, including coma that is known as cerebral malaria.

A. *Plasmodium* spp.

The pathogens behind this disease are unicellular protozoans of the genus *Plasmodium*. A total of six species can infect humans, each causing the disease with different levels of severity. The most prevalent species in Africa, South-East Asia, the Eastern Mediterranean and the Western Pacific in *Plasmodium falciparum* (WHO, 2018), that is also the most virulent as it can lead to the most severe symptoms of the disease. On the other hand, the most prevalent species in the Americas is *Plasmodium vivax* (WHO, 2018), which is not as deadly as *P. falciparum* but can form hypnozoites, a dormant form that can stay dormant for months in the liver, leading to malaria relapses. This characteristic is shared by *Plasmodium ovale* parasites as well. *Plasmodium malariae* can lead to asymptomatic blood infections. Finally, there are two simian species also known to infect human hosts, *Plasmodium knowlesi*, which can cause severe malaria (Cox-Singh et al., 2010; William et al., 2011), and *Plasmodium cynomolgi,* the last species described in humans (Ta et al., 2014).

B. Lifecycle

These parasites present a complex lifecycle that involves asexual and sexual replication and takes place in a vertebrate and an invertebrate host, respectively.

(I) Human host

The infection begins with the bite of an infectious *Anopheles* female (Fig. I.3). During blood meals, mosquitoes inject saliva to the host to facilitate the uptake of blood. When mosquitoes are infectious, their saliva contains *Plasmodium* sporozoites, a motile form of the parasite that migrates in the skin and blood vessels of the person until it reaches and infects hepatocytes. Here, a first cycle of asexual multiplication takes place, but it remains asymptomatic. Thousands of merozoites are then released into the blood stream where they can invade erythrocytes. The symptomatic phase of the disease begins. First, merozoites modify the erythrocyte to adapt it to their own needs (ring stage), and use hemoglobin as a major source of nutrients to multiply asexually (trophozoite stage) and undergo schizogony (schizont stage) that

releases several tenths of merozoites upon bursting. These merozoites can in turn infect novel erythrocytes to continue this asexual cycle.

However, some rings exit this cycle and differentiate into gametocytes, the only infectious form to the invertebrate host.
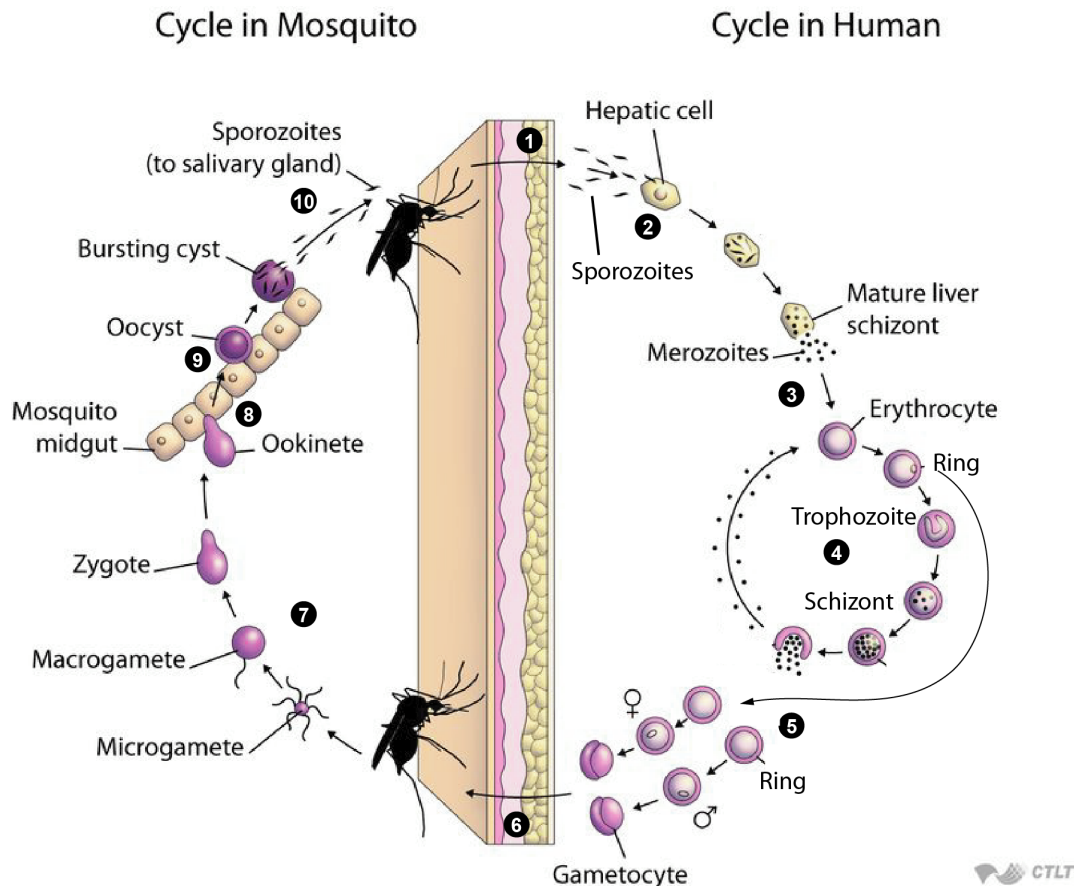
Figure I.3 Lifecycle of *Plasmodium* parasites. **(1)** An infectious mosquito injects sporozoites into the blood stream of a human; **(2)** this form invades hepatocytes where they multiply asexually until **(3)** hepatocytes burst and release merozoites that invade erythrocytes. **(4)** Merozoites invade red blood cells and mture into rings, then trophozoites and schizonts that rupture, releasing several tenths of merozoites produced by asexual multiplications. **(5)** Some rings follow a different pathway and develop into gametocytes **(6)** that are the only forms infectious to mosquitoes. **(7)** In the midgut of the invertebrate, gametocytes rapidly transform into gametes that fuse into a zygote; this zygote turns into an **(8)** ookinete that crosses the midgut epithelium and establishes as a cyst at the basal lamina. **(9)** There, the parasite undergoues numerous asexual divisions within the oocyst that then burst **(10)** releasing sporozoites in the body cavity. Those that invade the salivary glands can be injected into a human host upon the next blood feeding. Figure adapted from "life cycle of the malaria parasite" from Epidemiology of Infectious Diseases (http://ocw.jhsph.edu). Copyright Johns Hopkins Bloomberg School of Public Health. Creative Commons.

(II) Mosquito host

When an *Anopheles* female bites a human whose blood contains gametocytes, the infectious cycle begins in the invertebrate host. The drop in temperature and the presence of certain mosquito factors triggers the process. First, the gametocytes leave the erythrocytes. Male gametes undergo three rapid cycles of genome replication leading to 8 microgametes ready to fertilize the female gamete. When this happens, gametes fuse into a zygote that initiates meiosis and becomes motile, a stage at which it is called ookinete. Ookinetes then cross the peritrophic matrix – a non-cellular structure that is formed in the first hours following blood feeding and that surrounds blood in the gut – and the midgut epithelium to establish the infection at the basal lamina. The parasite then turns into an oocyst that undergoes several cycles of mitotic replication to give rise to sporozoites. When the oocyst bursts, it releases thousands of this motile form that migrate to and invade the salivary glands. During a subsequent blood meal, the female injects the sporozoites together with saliva into a new vertebrate host, closing the cycle.

3. FIGHTING MALARIA

Malaria is an ancient disease closely related to the history of human populations. Mesopotamian clay tablets from 2000 BC already describe deadly fevers that are compatible with malaria symptoms and parasite antigens were found in Egyptian mummies from 3200 BC (Miller et al., 1994). First believed to be a disease arising from the vapors of swamps – *mal'aria* is ancient Italian for "bad air" – *Plasmodium* parasites were not identified as the culprits until the late 19th century, when French military doctor, Alphonse Laveran, observed them in a patient blood sample. A few years later, Sir Manson provided the proof that *Anopheles* mosquitoes are partakers of guilt.

Knowing the etiology of the disease made the development of tools and strategies to fight it efficiently, possible. As a result, the World Health Organization (WHO) launched the Global Malaria Eradication Program (GMEP) in 1955 that resulted in the elimination of the disease in 15 countries and 1 territory and a general reduction of malaria burden in the rest of the world, with the exception the Sub-Saharan region. The program was stopped in 1969 due to funding reduction and a decreased

efficiency of the tools that were being used. The result was a rise in the incidence of malaria during the decades that followed, only reverted by the creation of the Roll Back Malaria partnership in 1998 and the development of the Global Malaria Action Plan (GMAP). The aim was to reduce the death rates to zero and cut the number of cases in a half (Roll Back Malaria Partnership, 2008). Although the overall goal was not achieved, there has been a 51 % drop in malaria deaths and cases since 2000 (Cibulskis et al., 2016).

A. Human focus

Managing malaria cases and treating infected humans is a central strategy in malaria control programs. The first compound to ever be used as a treatment for malaria was quinine. This natural alkaloid is extracted from the bark of cinchona tree, a species endemic to the Americas, and it is responsible for the bitter flavor of tonics. Although its mechanism of action is not fully deciphered, it is assumed to interfere with the hemoglobin digestion and with hemozoin formation, a process that is necessary for the parasite to detoxify free hemes released during hemoglobin digestion. It is active against schizonts and gametocytes, although the latter is not true in the case of *P. falciparum*. The WHO still recommends its use when the first-line treatments for uncomplicated malaria are not an option (Achan et al., 2011).

In 1891, Paul Ehrlich synthesized methylene blue for the first time and paved the way for a new generation of compounds: synthetic antimalarials. Methylene blue is very active against *Plasmodium* parasites, including gametocyte stages, and, although its mechanism of action is not fully elucidated, it can inhibit the glutathione reductase (GR) and interfere with the hemozoin formation (Schirmer et al., 2003). However, it is no longer used due to the length of the treatment (long as its action is slow), its side effects (blue coloring of the sclera and urine) and importantly, the relatively high costs of the synthesis of its heavy metal free form.

The quest for a better antimalarial compound began in the 19th century. With quinine as the starting block; years of research resulted in the synthesis of hundreds of different derivatives, some of which were eventually introduced in the market as antimalarial agents. The best example is chloroquine. Initially ignored for a decade, it was released in the 1940s and quickly became the most widely used drug due to its

fast activity and cheap production. It also hampers the crystallization of heme into hemozoin in the parasite. However, its intense use favored the apparition of resistances 10-20 years after it was released (Slater, 1993). It is still used to treat non-complicated malaria, but its application is dependent on these resistances.

The turning point of antimalarial drug development was the discovery of artemisinin in the 1970s. This compound was isolated from *Artemisia annua*, a plant used in traditional Chinese medicine to treat malaria, and, just like quinine, it served as basis for the development of several derivatives (Faurant, 2011). The mechanism of action is not fully elucidated, but it seems to act via free-radical formation and by inhibiting the parasite proteasome. Artemisinin and its derivatives present a short half-life; therefore, they are not suitable for use in monotherapy. Instead, they are used in combination with other drugs as the first-line antimalarial treatment (Eastman and Fidock, 2009). Artemisinin resistance was first detected in Cambodia in 2009 and is now a major concern for the future of malaria eradication (Fairhurst, Rick M; Dondorp, 2016).

As it is the case for any other infectious disease, having good efficient prophylactic strategies would be key to managing malaria. As such, the development of an efficient and safe vaccine is a major concern and focus of interest of the industry. As of today, the best candidate is the RTS,S/AS01 vaccine from GlaxoSmithKline for which the first pilot vaccination program was launched in Ghana, Kenya and Malawi on April 23rd, 2019. This vaccine targets the circumsporozoite protein of *P. falciparum*, but its efficacy is moderate as suggested by phase III trials where only 30 % and 55 % of children aged 6-12 weeks and 5-17 months, respectively, did not show clinical symptoms of malaria after vaccination (RTS, 2017). Alternatively, antimalarial compounds that target the pre-erythrocytic stages of the parasites can also be used as prophylactics. However, they are mostly recommended for travelers arriving in malaria endemic areas due to their secondary effects when taken for a long time.

B. Mosquito control

Because malaria cannot be transmitted between humans in the absence of a vector, avoiding mosquito bites is the most efficient prophylaxis.

As soon as the role of mosquitoes was discovered, vector control became central to manage malaria. The first strategies focused on larvae. Thus, drainage, oils and larvicides became key tools to fight malaria. The best example of the success of these interventions was the eradication of *A. gambiae s.l.* in northeast Brazil after an accidental introduction of the species. Although several methods were used, most of the strategy relied on Paris Green as a larvicidal compound (Killeen et al., 2002).

Nevertheless, current strategies mainly focus of adult mosquitoes and more particularly they take advantage of two behavioral features of *A. gambiae* and *funestus* species: they bite and rest at night inside households. Hence, insecticide treated nets (ITNs) and indoors residual spraying (IRS) are two major strategies implemented as part of the GMAP (Roll Back Malaria Partnership, 2008). Bed nets have been used for centuries as a simple means to avoid the bother of mosquito bites; however the concept was upgraded (Pryce et al., 2018) during World War II when both German and American troops started to use them in combination with insecticides (Lindsay and Gibson, 1988). These ITNs not only protect people sleeping under them, but they also repel and kill mosquitoes reducing the burden in the whole household and even the community. However, the usability of these ITNs is limited by the fact that they required re-impregnation every 6-12 months, or even before if the nets are washed. This issue was solved in the early 2000s with the development of long-lasting insecticidal nets (LLINs) that have a durability of at least 3 years. IRS, which consists on spraying the walls and ceilings of houses with insecticides, is also commonly used.

(I) Insecticides

In 2019, the WHO recommends the use of 13 insecticides for malaria vector control. These compounds fall into 5 chemical classes with three modes of action, all targeting the nervous system of mosquitoes (**Fig. I.4 A**). All of these insecticides can be used in IRS, however only the pyrethroid class is applied to ITNs (World Health Organization, 2019)

Organochlorines and pyrethroids

Like it was the case for antimalarial drugs, the 1940s also witnessed a revolution from the vector control side. In 1939, Paul Hermann Müller discovered the insecticidal properties of the most famous pesticide in history, dichlorodiphenyltrichloroethane (DDT). This chlorinated hydrocarbon is the only one of its class to be recommended for the control of malaria vectors. This colorless crystal, which had been first synthesized 65 years before, proved to be active against many different pests and showed relatively little toxicity in humans. Moreover, it was very cheap to produce and very efficient in residual spraying. Consequently, it soon became essential in the fight against insect-borne diseases. However, after a period of intensive use in disease control campaigns (including the GMEP) and agriculture, the negative effects of this insecticide on the environment started to be evident. The concern about its safety reached its peak with the publication of Rachel Carson's Silent Spring in 1962, a book where she warned about the environmental impact of this pesticide especially for birds. Indeed, DDT persists very long in the environment and its lipophilicity favors its accumulation in fatty tissues, with heavy consequences in the food chain. Consequently, countries started to restrict and ban its use in the 1970s, a process that ended in 2001 with the approval of Stockholm's Convention on persistent organic pollutants. Nevertheless, the use of DDT is still allowed in the context of disease vector control and the WHO recommends its use in IRS in the case of malaria, as it can last up to 12 months after application to a surface (WHO, 2006).

For their part, the history of pyrethroids is similar to that of the development of chloroquine and artemisinine as they were first isolated from *Chrisanthemum* flowers. These plants have been used as insecticides for centuries, but the first synthetic insecticidal pyrethroids were not developed until the 1970s (WHO, 2005). Pyrethroids are the only chemical class of insecticides recommended for the use in ITNs and therefore the fight against malaria heavily relies on them. They are also used in agriculture and are the major component of household insecticides. The preferential use that is made of these pesticides is due to their high selective toxicity towards insects. Although they also bind to the same target in mammals, the sensitivity is much lower. Thus, these insecticides are considered to be among the safest, although they also have adverse effects on human health (Saillenfait et al., 2015; WHO, 2005).

These two insecticide classes target the sodium channels located in the membrane of axons (Fig. I.4 A), which allow the selective flux of Na^+ ions through a central pore. These channels are activated upon a voltage change. When this happens, a conformational change opens the pore allows Na^+ to enter. The drastic increase of the concentration of this cation leads to the depolarization of the neuron. When the peak of activity is reached, the channel closes itself by physically blocking the pore. As a consequence, Na^+ does not enter anymore and the neuron goes back to its resting potential. This allows the channel to go back to the initial inactive form. DDT acts on the peripheral nervous system by opening the sodium channels spontaneously (Davies et al., 2007). As a consequence, neurons fire randomly, and insects die of excitatory paralysis. Pyrethroids have a very similar mechanism of action too, but they act on both the peripheral and central nervous system. These compounds can be divided in two groups with different effects. Type I pyrethroids induce neuronal firing that leads to insect paralysis. Type II, contain a cyano group and have better killing properties as they irreversibly depolarize axons (Davies et al., 2007).

Organophosphate and carbamates

Organophosphates are organic derivatives of phosphorus, a chemical class where we can find some pesticides but also nerve agents such as sarin. The first pesticides of this class were synthesized in the 1940s and soon became popular after World War II. Popularity increased even further when organochlorines began to be banned. However, these compounds are highly toxic for mammals, which eventually led to the ban of some compounds and a general decrease in the overall use of this class. Interestingly, organophosphates can also be found in nature (Neumman and Peter, 1987), however this discovery came well after the synthesis of the first compounds. Carbamates, that are esters of N-methyl carbamic acid, were first synthesized in the 1950s.

Both these classes target the acetylcholinesterase (AChE) enzyme (Fig. I.4 A), a hydrolase that degrades acetylcholine and other neurotransmitters. It is located in the chemical synapses of cholinergic neurons and muscular junctions and its role is to terminate synaptic transmission. Insecticides bind irreversibly to AChE, which

prevents the degradation of neurotransmitters in the synaptic gap. This hampers the repolarization and eventually results in the death of the animal.

Neonicotinoids

As it will be discussed later, the apparition and spread of insecticide resistances in mosquito populations are major concerns for malaria control programs. As part of the efforts to alleviate this burden, the WHO incorporated the neonicotinoid clothianidin to the list of compounds recommended for IRS in 2017 (World Health Organization, 2019). The first insecticide of this class was synthesized in the 1980s and the first one to be commercialized was released in the 1990s. Since then, they have become one of the most popular insecticide classes. Nevertheless, their use has been largely questioned due to the undesired effect they have on other insects, including bees. Consequently, the European Union agreed to ban their use in 2018.

Neonicotinoids target the nicototinic acetylcholine receptors (nAChRs) (**Fig. I.4 A**), ligand-gated ion channels whose activation relies on the binding of a neurotransmitter such as acetylcholine. When this happens, Na^+ ions enter while K^+ ions exit, depolarizing the cell. The channel remains open as long as the ligand is present. This class of insecticides binds to both insect and mammalian nAChR, however they are selectively more toxic to the former. At low concentrations, they stimulate the receptors whereas at high doses, they block them with the consequent paralysis of the animal (Goulson, 2013).

4. INSECTICIDE RESISTANCE

Resistance, as it is defined by the Insecticide Resistance Action Committee, is "the selection of a heritable characteristic in an insect population that results in the repeated failure of an insecticide product to provide the intended level of control when used as recommended" (Insecticide Resistance Action Committee (IRAC), 2010). Reports on insecticide resistance in mosquito populations date from the 1950s (Gjullin and Peters, 1952), when the popularity of organochlorine insecticides was at its peak. Since then, the situation has only deteriorated; in 2016, 77 % of the countries where malaria is endemic reported resistance to pyrethroids in their mosquito populations and 25 %, to the four commonly used classes

(organochlorines, pyrethoids, carbamates and organophosphates) (World Health Organization, 2018). In the case of *Aedes* species the situation is not encouraging either as resistances have been found in the Americas, Africa and Asia (Moyes et al., 2017).

As these resistance have an impact on the transmission of malaria (Ranson and Lissenden, 2016), the WHO issued a Global plan for insecticide resistance management in malaria vectors in 2012. This action plan was based on 5 key recommendations: (i) manage insecticide resistance, (ii) monitor it, (iii) deepen the knowledge on the mechanisms and the impact, (iv) ensure adequate means and (v) develop new tools for vector control.

Insecticide resistance is a complex phenomenon arising from several mechanisms that act alone or synergistically (Fig. I.4 B).

A. Target-site

Perhaps the most intuitive resistance mechanism is that corresponding to changes in the target that render it less sensitive to the toxicant (Fig. I.4 B.4). As previously described, a given protein can be the target of different insecticide classes, thus this mechanism may result in the resistance to more than one class.

Several point mutations in the sodium channels have been reported to confer resistance to DDT and pyrethroids alone or in combination (Auteri et al., 2018; Du et al., 2016; Rinkevich et al., 2013; Silva et al., 2014). These resistances are commonly known as knockdown resistances (kdr).

Resistances to organophosphates and carbamates associated to changes in the AChE sequence are less common than for organochlorines and pyrethroids. In insects, there are two genes coding for this enzyme (i.e. *AChE-1, AChE-2*). Resistance-conferring polymorphisms in mosquitoes have only been reported for *AChE-1* and thus resistance alleles are called ace-1 and they are usually associated with duplication of the *AcheE-1* gene (Ahoua Alou et al., 2010; Moyes et al., 2017; N'Guessan et al., 2003; Weill et al., 2004).

B. Metabolic

Living organisms possess detoxification pathways that protect them from potentially dangerous chemicals, both endogenous and exogenous. This is attained thanks to a series of complex pathways that involve the introduction of reactive or polar groups into these toxicants (phase I), their conjugation (phase II) and, eventually, their excretion (phase III). Changes in the expression or reactivity of the enzymes that are involved in these pathways can confer an overall increased detoxification capacity that results in the apparition of resistances referred to as metabolic (Fig. I.4 B.3).

Cytochrome P450 (P450) proteins are family of enzymes involved in the biosynthesis of hormones, fatty acids and in the metabolism of xenobiotics (both activating and detoxifying them) (Feyereisen, 1999). They act as monooxygenases and thus take part in phase I detoxification. The overexpression of these enzymes has been associated to pyrethroids, DDT and carbamates resistances (David et al., 2013; Fagbohun et al., 2019; Ibrahim et al., 2016b, 2016a; Ishak et al., 2017; Moyes et al., 2017; Tchigossou et al., 2018); moreover, mutations in the sequence of certain P450s has been associated to pyrethroid resistance (Faucon et al., 2015). Another type of phase I enzymes related to this phenomenon are carboxylesterases (CCEs). Increased activity of these enzymes has mainly been related to organophosphate resistance in *Culex* and A*edes* populations (Grigoraki et al., 2015, 2016; Poupardin et al., 2014; Vaughan et al., 1997).

Glutathione S-transferases (GSTs) belong to the phase II detoxification enzymes. The main role of these enzymes is to catalyze the conjugation of glutathione (GSH) to electrophilic compounds to render them water-soluble and less reactive (Enayati et al., 2005). Increased GST activity has been associated mainly to DDT resistance, but it can also reduce the sensitivity to pyrethroids (Aravindan et al., 2014; Chen et al., 2003; Gunasekaran et al., 2011; Lumjuan et al., 2011; Olé Sangba et al., 2017; Ranson et al., 2000).
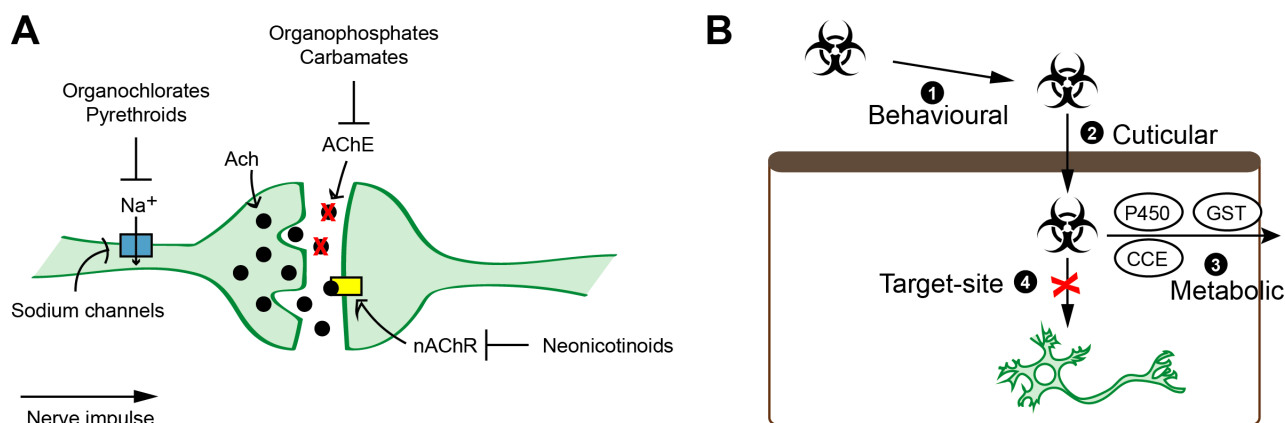
Figure I.4 Mode of action of the insecticides used in malaria control. **(A)** Molecular targets of the different chemical classes of insecticides, all of which participate in the transmission of the nerve impulses. Organochlorates and pyrethoids open the voltage-gated sodium channels located on the axon of neurons, leading to their spontaneous firing. Orgpanophosphates and carbamates target the acetylcholinesterase enzyme (AChE), preventing the degradation of the neurotransmitter acetylcholine. Neonicotinoids open the nicotinic acetylcholine receptors (nAChR) leading to the depolarization of the cell. **(B)** Scheme summarizing the steps followed by an insecticide to cause the death of a mosquito and the changes leading to insecticide resistance. **(1)** Mosquitoes must come into contact with the insecticide, thus changes in their behavior can confer behavioural resistance. **(2)** An insecticide must penetrate the cuticle of the mosquito before reaching its target, thus changes in the thickness and composition of this tegument can result in cuticular resistance. **(3)** Various mosquito enzymes (i.e. cytochrome P450 enzymes (P450), glutathione S-transferases (GST) and carboxylesterases (CCE)) detoxify insecticides. Increased activity of these enzymes can lead to metabolic resistance. **(4)** The insecticide must bind its target, thus changes in the amino acid sequence can also confer target-site resistance.

C. Other

Mosquitoes are exposed to insecticides via topic absorption. This implies that toxicants must first penetrate the cuticle in order to bind their target. Changes in the composition of this external layer can result in less penetration of the toxicants and hence they can confer resistance to insecticides (Balabanidou et al., 2016, 2019; Huang et al., 2018; Vannini et al., 2014) (Fig. I.4 B.2). Moreover, changes in the behavior of mosquitoes (e.g. biting hours) also contribute to these resistance phenomena (Fig. I.4 B.1), for instance by biting earlier and outdoors and thus avoiding contact with insecticide-treated bednets (Carrasco et al., 2019).

5. REDOX HOMEOSTASIS

A. Oxidants

For the vast majority of organisms, life is mostly dependent on the metabolism of molecular oxygen (O_2). This molecule diffuses across biological membranes and provides large free energy release when it is reduced, being the final acceptor of electrons in the mitochondrial respiratory chain. Moreover, despite being a diradical in its ground state, O_2 is stable as their unpaired electrons are in parallel spins. However, this is a double-edged sword (**Fig I.5**) as partial reduction leads to the apparition of the free radical superoxide anion ($\cdot O_2^-$) and further dismutation of this molecule, to hydrogen peroxide (H_2O_2). H_2O_2 is relatively stable and can thus diffuse (Pryor, 1986), however it is converted to hydroxyl radical ($\cdot OH$) in the presence of metal ions such as iron (Fe^{2+}). This is the most dangerous of these reactive oxygen species (ROS) (Nordberg and Arnér, 2001) and its half-life is only 10^{-9} sec, which means it reacts within 5 molecular diameters from their formation site (Pryor, 1986). At the same time, reaction of these ROS with lipids (Reed, 2011) and proteins (Davies, 2016) can lead to the apparition of peroxyl radicals ($ROO\cdot$), which are also very reactive.

In eukaryotes, most of the energy produced in the cells comes from the electron transport chain (ECT) of mitochondria. This ECT consists of a series of redox complexes in the inner mitochondrial membrane that transfer electrons from donors to acceptors while pumping H^+ to the intermembrane space. If any of these electrons leaks from the chain and is caught by O_2, it results in $\cdot O_2^-$ formation. This failure occurs constantly on the ECT, mainly at complexes I and III (Brand, 2010), and thus the mitochondrion is the major site of ROS production in eukaryotic cells. Because redox processes are essential in diverse compartments and processes in all living organisms, ROS can be significantly generated in other organelles as well (Dansen and Wirtz, 2001; Gross et al., 2006). For instance, the uncoupling of the regular catalytic cycle of P450s leads to the production of $\cdot O_2^-$ and H_2O_2 in the endoplasmic reticulum (Hrycay and Bandiera, 2012; Lewis, 2002). Additionally, ROS production can be enhanced by external factors such as UV light (Heck et al., 2003), ionizing radiation (Riley, 1994), pollutants (Gurgueira et al., 2002) and chemicals such as paraquat (Winterbourn, 2008). ROS can also be produced on purpose by

nicotinamide adenine dinucleotide phosphate (NADPH) oxidases (NOXs) (Panday et al., 2015) (**Fig I.5**). These enzymatic complexes transfer one electron from NADPH to O_2 to form $\cdot O_2^-$. This is known as respiratory burst and is typical of phagocytes as part of the immune response (Thomas, 2017), including insect hemocytes (Lavine and Strand, 2002).

Oxygen-based radicals are not the only oxidizing species that can be formed in biological systems. Reactive nitrogen species (RNS) are also very important (**Fig I.5**). Nitric oxide ($NO\cdot$) is a diatomic molecule with one unpaired electron. Despite this, it is not a very reactive species and its biological importance mainly radiates from its role as a neurotransmitter (Vincent, 2010). However, it can react to form more dangerous RNS. Upon reaction with $\cdot O_2^-$, it gives rise to peroxynitrite ($OONO^-$) and its autoxidation leads to the formation of nitrite (NO_2^-) (Lundberg et al., 2008), both of which can damage biomolecules (Bian et al., 2003; Crawford et al., 2017; Radi, 2018).
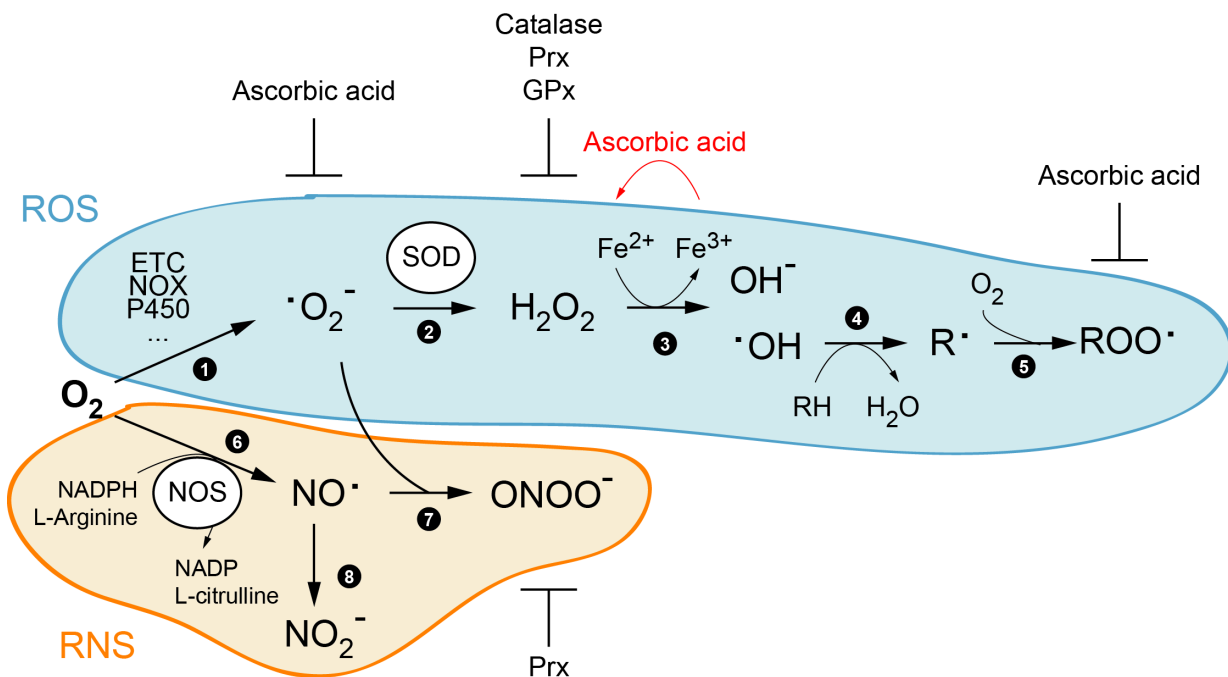
Figure I.5 Production and scavenging of reactive oxygen species (ROS) and reactive nitrogen species (RNS). The reactions are not balance and only the most physiologically relevant species and scavengers are shown. **(1)** Molecular oxygen (O_2) can be oxidized to superoxide anion ($\cdot O_2^-$) in the electron transport chain (ETC), by NADPH oxidases (NOX), cytochrome P450 (P450) and other reactions. $\cdot O_2^-$ can be scavenged by ascorbic acid. **(2)** $\cdot O_2^-$ is dismutated to hydrogen peroxide (H_2O_2) by sodium dismutases (SOD). H_2O_2 can be scavenged by catalase, peroxiredoxs (Prx) and glutathione peroxidases (GPx); otherwise, **(3)** it can lead to the production of hydroxyl anions (OH^-) and hydroxyl radicals ($\cdot OH$) catalyzed by metals (Fe^{2+}). **(4) (5)** $\cdot OH$ engages in further oxidative reactions leading to oxidation of proteins, lipids and nucleic acids. **(6)** Production of nitric oxide ($NO\cdot$) by nitric oxide synthase (NOS). **(7)** The reaction of $NO\cdot$ with $\cdot O_2^-$ produces peroxynitrite ($ONOO^-$) that can be scavenged by Prx. This RNS can lead to protein damage. **(8)** The autoxidation of $NO\cdot$ generates nitrite (NO_2^-) that can also damage proteins. Red color indicated pro-oxidant activity of scavengers.

NO· is endogenously produced by nitric oxide synthases (NOS) from L-arginine and O_2 with the help of NADPH, flavin adenine dinucleotide (FAD), flavin mononucleotide and tetrahydrobiopterin (Lundberg et al., 2008). Whereas mammals possess three isoforms, insects only seem to have one, whose activity is regulated by Ca^{2+}-calmodulin (Ribeiro and Nussenzveig, 1993).

Both ROS and RNS can inflict irreversible damage to biomolecules such as lipids (Halliwell and Chirico, 1993; Stubbs and Smith, 1984), DNA (Pogozelski and Tullius, 1998) and proteins (Pogozelski and Tullius, 1998). However, as it will be further discussed in section C, they are also important in several immune processes and participate in cell signaling through post-translational modifications (PTM) in cysteines (**Fig. I.8**).

B. Antioxidants

To deal with challenge that the paradoxical roles of ROS/RNS entail, cells have developed antioxidant systems to counteract them and repair their damage. The balance between oxidants and antioxidants is what is commonly called "redox homeostasis" and the negative consequences of an imbalance that favors oxidants, "oxidative stress". Keeping a correct intracellular nucleophilic tone through antioxidants is essential for cell viability.

Antioxidant systems are extremely complex, and form interconnected networks. Several types of molecules can act as antioxidants in cells by direct scavenging of ROS/RNS or by repairing the oxidative damage generated by them.

(I) Low molecular weight antioxidants

Ascorbic acid is a water-soluble vitamin (vitamin C) that can directly scavenge ROS such as $\cdot O_2^-$ and ROO·, protecting biological membranes (Buettner, 1993) (**Fig. I.5**). However, ascorbic acid can also act as a pro-oxidant molecule as it reduces metals like iron (Fe^{3+}) and copper (Cu^{3+}), which can then generate ·OH (Putchala et al., 2013). Vitamin C can be up taken from the diet or synthesized *de novo*, in a process that seems dependent on glycogenolysis (Braun et al., 1994). More energetically

advantageous is the enzymatic recycling of the oxidized form (dehydroascorbate) to the active reducing form by thioredoxin reductase (TrxR) (May et al., 1998a), glutaredoxins (Grxs) (Wells et al., 1990) and GSTs of the omega class (Whitbread et al., 2005). On their part, tocopherols and tocotrienols (vitamin E) are lipid-soluble antioxidants with similar antioxidant activity as ascorbic acid (Tappel, 1962) that are uptaken from the diet.

The most abundant thiol antioxidant in cells, GSH, is also a low molecular weight antioxidant. However, due to its importance, its role in the antioxidant network will be discussed in a separate section.

(II) Enzymatic antioxidants

Superoxide dismutases (SODs) are metal-containing enzymes that catalyze the dismutation of $\cdot O_2^-$ into H_2O_2 (**Fig I.5**). They are located in the nucleus, the cytoplasm, mitochondria and the extracellular space and, as metal cofactors, they can either use copper-zinc or manganese (Zelko et al., 2002). *Anopheles gambiae* mosquitoes code for 2 nucleocytoplasmic cuSODs, one extracellular cuSOD and one mitochondrial MnSOD.

Catalase converts H_2O_2 to H_2O and O_2 (**Fig. I.5**) and, in most eukaryotes, including insects, it is encoded by one single gene and the protein localizes in peroxisomes.

(III) Thioredoxin system

Thioredoxins

Thioredoxins (Trxs) are a class of small (12 kDa) thiol-active proteins present in all living organisms. They contain a thioredoxin domain, like other proteins that will be described in this introduction (peroxiredoxins (Prxs), Grxs and GSTs). These proteins are involved in DNA synthesis (Zahedi Avval and Holmgren, 2009) and can reduced disulfide bridges in proteins (**Fig. I.6**), thus being involved in protein folding (Berndt et al., 2008). Moreover, as it will be discussed in section C, they play key roles in cell signaling processes. Trxs also play an antioxidant role (**Fig. I.6**) by reducing Prxs and methionine R-sulphoxide reductase (MRS) (Lu and Holmgren, 2014) and, in

insects, they are responsible for the recycling of oxidized glutathione (GSSG) to GSH as there is no glutathione reductase in these animals (Bauer et al., 2003a; Kanzok et al., 2001).

Disulfide reduction is mediated by an active motif that is highly conserved across various species (-Cys-Gly-Pro-Cys-) (Eklund et al., 1991). In *A. gambiae* there are three genes coding for thioredoxins, two of which have predicted mitochondrial import signals. Only the cytoplasmic one, Trx1 (AGAP009584), presents the conserved redox-active motif as such, whereas the other two have Ala and Asp residues instead of Pro. In mammals, Trx1 has 5 Cys residues in total. The first two (active site) confer the disulfide-reductase activity, but they are also important in other protein protection mechanisms such as denitrosylation and reduction of sulfenic acid to thiols (Wu et al., 2011). The other three Cys modulate the activity of the protein as they can undergo several PTMs. Moreover, the only Tyr residue of these proteins can be nitrated (Wu et al., 2011). In mosquitoes and flies, only one of the Cys outside the active site is conserved whereas the Tyr is present in mosquitoes, but not in the fuitfly.

The genome of *D. melanogaster* flies codes for more Trxs than other insects', probably due to duplication events after divergence from mosquitoes (Corona and Robinson, 2006). Within these additional genes, there are two sex-specific Trxs (Deadhead, dhd, CG4193; TrxT, CG331) that are present in the nuclei of nurse cells and spermatocytes, respectively (Pellicena-Pallé et al., 1997; Salz et al., 1994; Svensson et al., 2007).

Peroxiredoxins

Prxs, also known as thioredoxin peroxidases, are another class of small (20-30 kDa) thioredoxin-fold proteins. They are very abundant in mammalian cells where they account for up to 1 % of the total amount of the soluble protein fraction (Chae et al., 1997). These proteins reduce H_2O_2, organic hydroperoxydes and peroxynitrite (Fig. I.5), and obtain the reducing equivalents from thioredoxins (Chae et al., 1994) (Fig. I.6), hence they are key players in the antioxidant network.

Prxs are classified into two groups depending on the number of active Cys. 2-Cys Prxs possess a peroxidatic and a resolving Cys, and most of them form homodimers

were each of the Cys assists the corresponding one in the other monomer (Perkins et al., 2014). 1-Cys Prxs lack the resolving Cys and thus require assistance by other thiol-containing proteins. In *D. melanogaster,* these Prxs display Trx-independent peroxidase activity (Radyuk et al., 2001). The genome *A. gambiae* mosquitoes contains 5 Prxs genes (3 1-Cys, 2 1-Cys) coding for cytosolic, mitochondrial and extracellular proteins. In *D. melanogaster* Trx2 is a substrate of Prx1, whereas Trx1 is not, thus showing that there is a functional differentiation between possible Trx/Prx couples (Bauer et al., 2002).

Glutathione peroxidases

Glutathione peroxidases (GPx) are a family of phylogenetically related proteins that reduce H_2O_2 and hydroperoxydes (Little and O'Brien, 1968; Mills, 1957) (**Fig. I.5**), thus exerting similar antioxidant roles as Prxs. In vertebrates, these proteins have a seleno-cysteine (Sec) and obtain their reducing equivalents from GSH, thus the name. However, most invertebrate GPxs contain Cys instead of Sec and display thioredoxin peroxidase activity (Maiorino et al., 2007) (**Fig. I.6**). To our knowledge, *Rhodnius prolixus*, the kissing bug, is the only insect where a Sec-containing GPxs has been described (Dias et al., 2016). In *A. gambiae* there are three predicted GPx genes, all of them potentially lacking selenium.

Thioredoxin reductase

TrxR is a homodimeric flavoenzyme that transfers electrons from NADPH to Trxs via the prosthetic group FAD. Thus, TrxR is considered as the recycling enzyme of the Trx system (**Fig. I.6**). Additionally, TrxRs can also reduce other substrates such as H_2O_2 (Zhong and Holmgren, 2000), lipid peroxydes (Björnstedt et al., 1995) and dehydroascorbate (May et al., 1998b) and Grx2 (Johansson et al., 2004).

As a result of evolution, there are two different types of TrxRs. Prokaryotes, archea and lower eukaryotes present small TrxRs with a molecular weight of 35 kDa. The catalysis of these low M_r TrxR relies on the FAD prosthetic group and neighbor thiol-active site that is conserved among species (-Cys-Val-Asn-Val-Gly-Cys-) (Williams, 1995). Higher eukaryotes have larger TrxRs (55 kDa) with an additional C-terminal interface domain that contains another redox-active disulfide. Interestingly, this active motif, encoded by the last C-terminal amino acids of the protein, is not conserved

among species. Indeed, this redox center can have three different forms. In most cases (including mammals), the catalysis relies on the presence of selenium (-Gly-Cys-Sec-Gly) (Arscott et al., 1997; Luthman and Holmgren, 1982) whereas the orthologs in *P. falciparum* and insects are selenium-independent. In Apicomplexan parasites this second site is similar to the N-terminal one (-Gly-Cys-X-X-X-X-Cys-Gly) (Miiller et al., 1996) whereas insects the two Cys are adjacent (-Thr/Ser-Cys-Cys-Ser) (Bauer et al., 2003b, 2003a). Of note, high M_r TrxRs are closer in their sequence to glutathione reductases (recycling enzyme of the glutathione system) than to low M_r TrxRs (Gasdaska et al., 1995). All TrxR homodimerize in a head-to-tail conformation and in higher M_r TrxRs, electrons flow between both monomers.

D. melanogaster possess two genes coding for TrxRs, whereas *A. gambiae* mosquitoes only have one gene. *AgTrxR* gives rise three splice variants that code for two cytoplasmic and one mitochondrial form (Fig. 2.1) that have been biochemically characterized (Bauer et al., 2003a), but whose biological functions *in vivo* have not been explored.
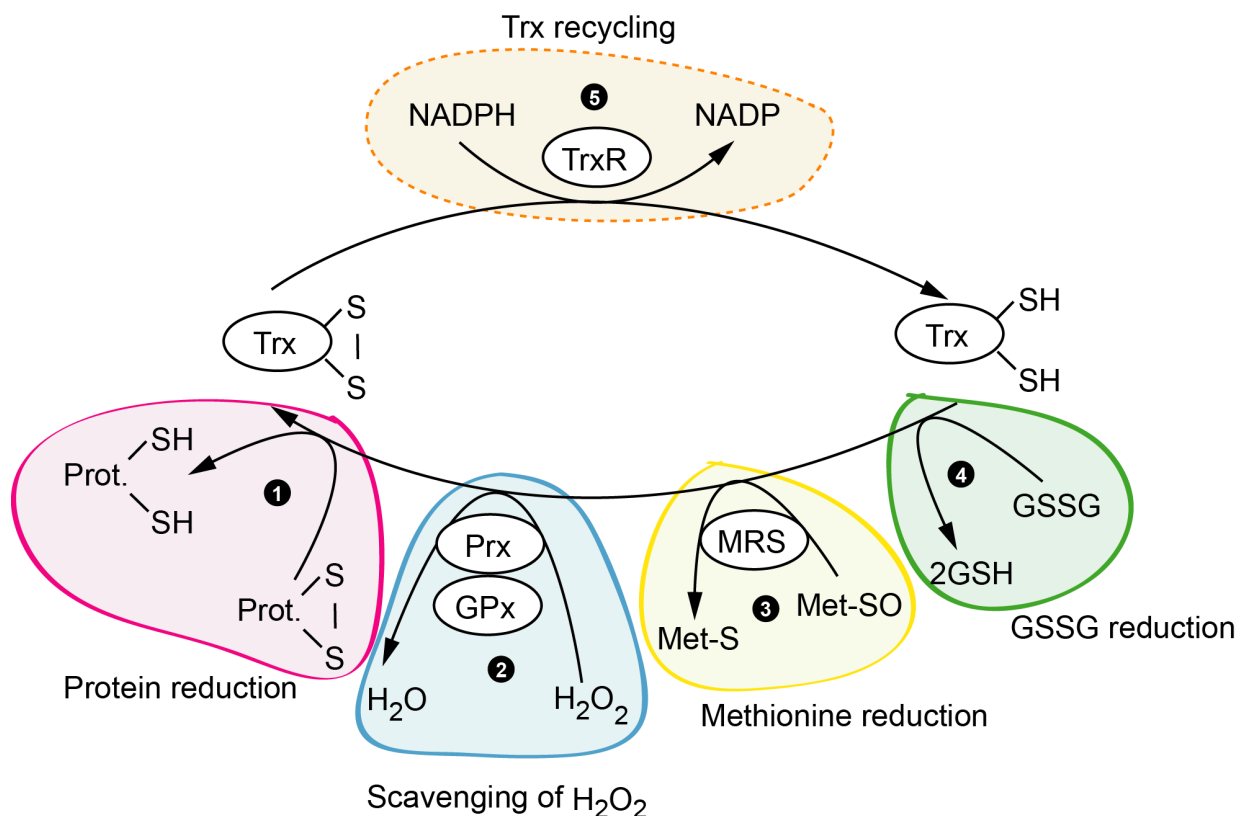
Figure I.6. Thioredoxin system in insects. (1) Thioredoxins can reduce disulfide bridges in proteins; they also give electrons **(2)** to peroxiredoxins (Prx) and glutathione peroxidases (GPx) to scavenge hydrogen peroxide (H_2O_2) and **(3)** to methionine sulfoxide reductase (MRS) to reduce oxidized methionine residues. **(4)** They can also reduce oxidized glutathione (GSSG) to the active form (GSH). **(5)** Thioredoxins obtains the reducing equivalents from NADPH in a reaction mediated by thioredoxin reductase (TrxR). Reactions are not balanced.

(IV)   Glutathione system

Glutathione

GSH is a widely distributed antioxidant in living organisms. It is present in millimolar concentrations in most cells, is thus considered as a major actor in redox homeostasis. This tripeptide is formed by cysteine, glycine and glutamate and is both a reductant and a nucleophile. In cells, it is also present as GSSG; however, the reduced form is much more abundant (Abdu et al.; Hazelton and Lang, 1984). The ratio between these two is generally used as measure of oxidative stress in cells. Almost 90 % of the total amount of GSH/GSSG is found in the cytoplasm; around 10 %, in the mitochondria (Jocelyn and Kamminga, 1974) and a small percentage, in the endoplasmic reticulum, where both forms are almost equally as abundant (Hwang et al., 1992).

GSH is synthesized *de novo* intracellularly from the three constituent amino acids in a two-step process that requires ATP (Fig. I.7 A). The first step is catalyzed by the enzyme glutamate-cysteine ligase (GCL), formerly known as γ-glutamylcysteine synthetase as it gives rise to the formation of γ-glutamylcysteine from glutamate and cysteine. GCL is formed by two subunits encoded by different genes and it is the rate-limiting enzyme of the biosynthetic process. The second enzyme involved in the synthesis of GSH is the GSH synthetase (GS) that catalyzes the reaction between γ-glutamylcysteine and glycine to yield GSH (Lu SC, 2013). In *A. aegypti* mosquitoes the biosynthesis of GSH decreases upon ageing, resulting in an overall drop the in total amount of GSH in this species (Hazelton and Lang, 1983, 1984).

Because glutamate and cysteine are linked through a peptide bond with the γ-carboxyl group of glutamate, the degradation of GSH cannot be mediated by regular hydrolases. The only enzymes capable of such activity are γ-glutamyltranspeptidases (GGTs) (Fig. I.7 A), that are membrane-bound proteins with the catalytic site facing towards the extracellular space. Hence, GSH and GSSG must first be exported in order to be degraded. The name of these enzymes is due to their capacity to transfer the γ-glutamyl group to peptides and amino acids in a transpeptidation reaction. Alternatively, they can also use water as acceptor, generating glutamate (Bachhawat and Kaur, 2017). The resulting amino acids can be retaken by the cell to synthesize more GSH (Bachhawat et al., 2013).
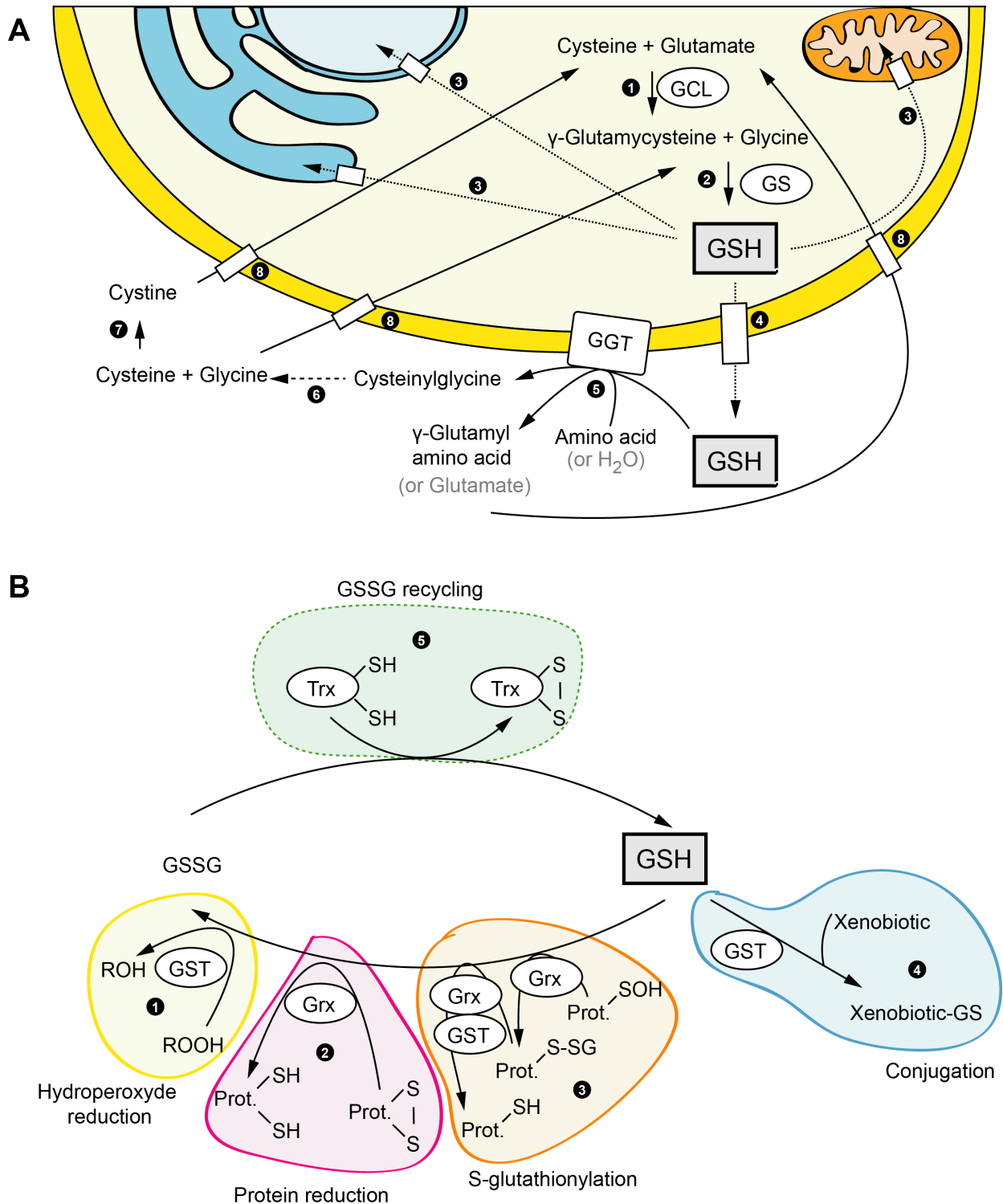
Figure I.7. Glutathione system in insects. (A) Glutathione (GSH) is synthesized in the cytoplasm of cells whereas its degradation occurs in the extracellular space. **(1)** Glutamate cysteine ligase (GCL) produces γ-glutamylcysteine from glutamate and cysteine. **(2)** Glutathione synthase (GS) produces GSH from γ-glutamylcysteine and glycine. **(3)** GSH import into other organelles and **(4)** export out of the cell. **(5)** γ-glutamyltranspeptidases (GGT) catalyzes the transfer of the γ- glutamyl group from GSH to amino acids or H_2O forming γ- glutamyl amino acids or glutamate, respectively. **(6)** The remaining group, cysteinylglycine, is broken into cysteine and glycine **(7)** Cysteine is oxidized to cystine in the extracellular space. **(8)** The three constituent amino acids are imported into the cell and can be reused to synthesize more GSH. **(B)** Reduced glutathione (GSH) can be used by **(1)** glutathione S-transferases (GSTs) to reduce organic hydroperoxides and **(2)** glutaredoxins (Grx), to reduced disulfide bridges in proteins. Moreover, **(3)** it can be used to protect damaged proteins by S-glutathionylation that is mediated by Grxs and GSTs. Finally, it can also be used **(4)** by GSTs to detoxify xenobiotics. **(5)** Oxidized glutathione (GSSG) can be reduced by thioredoxins (Trx). Reactions are not balanced.

Importantly, GSH can be imported and exported from the cell (**Fig. I.7 A**). Moreover, because its biosynthesis takes place in the cytoplasm, it must be imported into other organelles. This processes are mediated by various transporter families, depending on the tissue and the species (Bachhawat et al., 2013). GSH can directly scavenge hypochlorous acid (HOCl) (Haenen and Bast, 2014). However, the major antioxidant functions of this tripeptide come from its use by antioxidant proteins such as Grxs (**Fig. I.7 B**). It also serves as a protection of partially oxidized thiols when it is conjugated (S-glutathionylation) and is a protagonist in xenobiotic detoxification mediated by GSTs.

As mentioned before, most organisms possess a GSSG recycling enzyme called GR. This flavoenzyme is similar to TrxR in its structure and catalysis (Thieme et al., 1981) but is absent in insects. In these organisms, the Trx/TrxR system is believed to be responsible for the recycling of GSSG instead (Bauer et al., 2003a; Kanzok et al., 2001) (**Fig. I.7 B**).

Glutaredoxins

Grxs are another class of small thiol-active proteins that contain a thioredoxin domain. Grxs are divided into two groups depending on the number of Cys present in the active site. Dithiol Grxs (Cys-X-X-Cys) transfer electrons from GSH to a variety of substrate proteins (**Fig. I.7 B**), and are implicated in the regulation of processes such as proliferation, apoptosis and transcription (Hanschmann et al., 2013) (see section C). Alternatively, they can also be reduced by TrxR (Johansson et al., 2004). The other type of Grxs are monothiol Grxs (Cys-X-X-Ser), which seem to be implicated in iron metabolism rather than redox signaling (Berndt and Lillig, 2017).

The genome of *A. gambiae* mosquitoes codes for 4 Grx genes. Three of them are dithiol Grxs and one is a monothiol one with a predicted mitochondrial import signal. To our knowledge, their products and roles have not been investigated.

Glutathione S-transferases

As introduced in the metabolic insecticide resistance section, GSTs are phase II detoxification enzymes that conjugate GSH to xenobiotics (**Fig. I.7 B**). In addition,

they can participate in the antioxidant defense by reducing organic hydroperoxides (Hayes et al., 2005; Lee, 1991).

GSTs can be divided into three families according to their cellular localization. Cytosolic and mitochondrial GSTs have similar 3D structures whereas the microsomal family does not. The cytosolic family is the most diverse one with six different classes in insects (delta, epsilon, zeta, theta, sigma and omega) (Ding et al., 2003; Ketterman et al., 2011), but eight additional classes have been identified in other species (alpha, mu, pi, beta, lambda, phi, tau and "u") (Hayes et al., 2005). In general, these GST classes are encoded by multigene families and an even greater diversity can be achieved by alternative splicing (Ranson et al., 1998). In *A. gambiae* the largest classes are GSTd and GSTe, clustered in chromosomes 2R and 3R, respectively (Ding et al., 2003).

C. Biological relevance of the antioxidant network

In the beginning, ROS were seen as harmful molecules that were randomly produced in cells. Nowadays, we know that they also play key roles in cell signaling (Finkel, 2011; Holmström and Finkel, 2014) and immunity (Fang, 2011; Han et al., 2000; Peterson et al., 2007).

The former role is mostly due to the reversible oxidation of reactive Cys residues in proteins (Fig. I.8). Non-radical oxidation (i.e. transfer of two electrons) of thiols (-SH) leads to sulfenic acid (-SOH) formation, which is not very stable, unless the microenvironment allows it. Further oxidation leads to sulfinic acid (-SO$_2$H) and eventually, to sulfonic acid (-SO$_3$H), both of which are irreversible. To protect proteins from this fatal destiny, -SOH can be protected by GSH upon S-glutathionylation (Fig. I.8) mediated by Grxs (Gravina and Mieyal, 1993; Thomas et al., 1995) (Fig. I.7 B); the inverse process (deglutathionylation) is also catalyzed by Grxs (Peltoniemi et al., 2006) as well as GSTs of the omega class (Menon and Board, 2013) (Fig. I.7 B). Alternatively, -SOH can also form disulfide bridges (-S-S-) with other thiols (Fig. I.8); of note, disulfide bridges can be formed directly upon the attack of ·OH and from S-glutathionylated intermediates. Both Trxs (Fig. I.6) and Grxs (Fig. I.7) can mediate the reduction of -S-S- to –SH. On the other hand, radical oxidation of –SH (i.e. transfer of 1 electron) leads to the formation of thiyl radicals (-S·) that can be N-

nitrosylated (-SNO) upon reaction with NO· (Jourd'heuil et al., 2003) (Fig. I.8). The inverse mechanism is less understood, but is mediated by denitrosylases (Benhar et al., 2009).

These modifications serve as switches that can activate and deactivate proteins from several signaling pathways (e.g. MAPK, NF-kB, Keap1-Nrf2, PI3K-Akt, etc) thus playing essential roles in physiological processes such as autophagy, apoptosis, cell proliferation, ageing, immunity and development (Hernández-García et al., 2010; Lin and Scott, 2012; Mhamdi and Van Breusegem, 2018; Redza-Dutordoir and Averill-Bates, 2016; Scherz-Shouval et al., 2007; Thannickal and Fanburg, 2010; Torres and Forman, 2003; Zhang et al., 2016a). Since the redox homeostasis of cells relies on its antioxidant network, these molecules control these processed indirectly, extending their importance beyond the antioxidant defense itself. Moreover, the GSH and Trx systems have a direct role, as previously described.
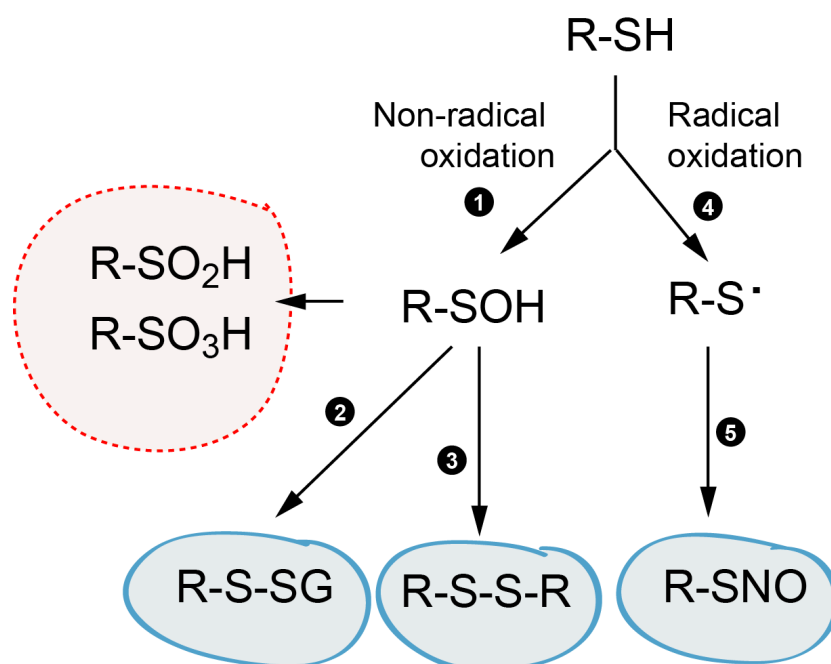
Figure I.8. Post-translational modifications in cysteines. (1) Non-radical oxidation of cysteine thiols (-SH) can lead to the apparition of sulfenic acid (-SOH) that can undergo further oxidation to sulfinic acid (-SO$_2$H) and sulfonic acid (-SO$_3$H); this oxidation states are irreversible and may lead to function loss in proteins. Alternatively, -SOH can be protected by **(2)** S-glutathionylation (-S-SG) or **(3)** forming a disulfide bridge (-S-S-) with another thiol. **(4)** Radical oxidation of –SH can give rise to thiyl radicals **(5)** that can be S-nitrosylated (-SNO).

(I) Biological relevance in insects

The role of low antioxidant molecules (i.e. vitamincs C and E) has mostly been studied in hervivorous lepidotperans where they are important to face the pro-oxidant effect of dietary polyphenols (Barbehenn et al., 2001) as well as for growth and development (Fraenkel and Blewett, 1946; House, 1966; Popham and Shelby, 2009), adult emergence and the antiviral response (Popham and Shelby, 2009). Moreover, ascorbic acid levels and/or dihydroascorbate reductase activity are higher in non-diapause larvae, suggesting a protective role against metabolic oxidative stress (Jena et al., 2013; Jovanović-Galović et al., 2004). On the contrary, sodium ascorbate, a sodium salt of this antioxidant that is commonly used in the food industry, has a deleterious effect on mosquitos and sandflies upon oral uptake, possibly due to its pro-oxidant activity (McDermott et al., 2019).

On the other hand, cuSOD2 modulates the immune system in *D. melanogaster* flies (Pragya et al., 2014) and enhances survival during diapause in *C. pippiens* (Sim and Denlinger, 2011), while MnSOD is up-regulated 24 h after blood feeding in *A. gambiae* mosquitoes (Ribeiro, 2003). In humans, lack of catalase activity is not deadly, but it has been related some to age-dependent disorders (Góth and Nagy, 2013). *D. melanogaster* mutants are also viable, but lack of catalase activity below a certain threshold reduces the lifespan of the flies (Sun et al., 2002). In *A. aegypti* mosquitoes, catalase is induced upon blood feeding and favors dengue prevalence (Oliveira et al., 2017) whereas in *A. gambiae*, knocking down catalase increases mortality upon blood feeding (Magalhaes et al., 2008). Likewise, catalase is also an important defense in herbivorous lepidopterans (Felton and Duffey, 1991).

With regard to the Trx system, Prxs are among the most studied redox-active proteins in insects. Their role in immunity and the antioxidant defense as well as their response to different challenges has been studied and characterized in flies (Odnokoz et al., 2017; Radyuk et al., 2009, 2010, 2013), bees (Huaxia et al., 2015; Yan et al., 2014; Yao et al., 2013), lepidopterans (Cao et al., 2018; Lee et al., 2005; Shi et al., 2012; Wan et al., 2014) and aphids (Zhang and Lu, 2015). In *A. stephensi* Prx1 is induced upon infection with Plasmodium parasites to protect cells from nitrosative and oxidative damage (Luckhart, 2008) and in *A. gambiae* Prxs are upregulated upon blood meal (Ribeiro, 2003). As for Trxs themselves, dhd is required for meiosis and embryonic development in *D. melanogaster* (Pellicena-Pallé

et al., 1997; Salz et al., 1994) whereas TrxT ablation has no impact (Svensson et al., 2003). DmTrx2 mutants (ortholog of AgTrx1) have a reduced lifespan whereas its overexpression confers higher tolerance to oxidative stress (Svensson and Larsson, 2007); the ortholog in *Helicoverpa armiguera* is also involved in the antioxidant and antiviral responses (Zhang et al., 2015). Finally, TrxR is essential for development in *D. melanogaster* and hypomorphic mutations severely reduce the lifespan of adult flies (Missirlis et al., 2002).

Regarding the GSH system, little research has been done on the role of insect Grxs. In *Helicoverpa armiguera*, Grxs seem to be involved in the antioxidant defense (Zhang et al., 2016b) whereas in *D. melanogaster*, Grx1 seems to play a role in copper homeostasis (Mercer and Burke, 2016). On the contrary, the role of GSTs in insects has been largely studied, mostly in the context of insecticide resistance as it was described before. Most evidence of this role comes from measuring an increase in the total GST activity, which can be due to gene amplification or to increased transcription; alternatively, this role can be inferred from the synergism between GST inhibitors and insecticides, thus it is difficult to attribute such phenomena to a specific GST. The contribution of GSTs to insecticide resistance is double, they can directly detoxify them and also alleviate the oxidative damage (Enayati et al., 2005; Pavlidi et al., 2018). Moreover, in *D. melanogaster*, GSTs are also involved in the synthesis of hormones, thus playing a key role in development (Enya et al., 2017).

Of note, ROS and RNS can exert direct roles in the immune response as they are toxic to pathogens (Fang, 2011; Han et al., 2000; Peterson et al., 2007). In *Anopheles* mosquitoes, NOS is strongly upregulated in midgut cells that are traversed by parasites, or in close proximity to these, and probably contributes, together with NOX5/HPX2, to protein nitration at the site of infection (Han et al., 2000; Kumar et al., 2004). Likewise, NOX5, together with the heme peroxidase (HPX2), mediate protein nitration at the site of parasite invasion in the mosquito midgut, a step that is essential to trigger an efficient antimalarial response in *A. gambiae* mosquitoes (Kumar et al., 2001; Molina-Cruz et al., 2008).

D. Cross-talk between the Trx and GSH systems

In many aspects, the Trx and GSH systems are similar, both in terms of mechanisms and functions (**Fig I.9**). These two networks can interact with each other (**Fig. I.9 A**) as demonstrated by the fact that human TrxR can reduce Grx2 (Johansson et al., 2004) that can itself reduce Prx3 (Hanschmann et al., 2010); moreover, they can act as backup of each other, which suggest they are (partially) redundant (Du et al., 2012; Eriksson et al., 2015; Reichheld et al., 2007; Tan et al., 2010).

This cross-talk between the system is more evident in the case of insects (**Fig. I.9 B**) where the lack of GR is compensated by Trxs themselves (Bauer et al., 2003a; Kanzok et al., 2001). Thus, in these organisms TrxR is the only enzyme reducing both Trx and GSH systems (**Fig. I.8 B**). This particularity of the antioxidant defense of insects, added to the role of these systems in insecticide resistance, offers an interesting new lead to develop insecticides. Moreover, the fact that TrxR is essential for viability in *D. melanogaster* suggests that TrxR might be a good target candidate. Thus, the aim of my PhD was to assess the suitability of this enzyme as a target to develop novel insecticides against disease-transmitting mosquitoes. To that end, I addressed three main questions:

What are the general redox dynamics of glutathione in mosquitoes?
(CHAPTER 1)

▪ ▪ ▪ ▪

What is the role of TrxR in *A. gambiae*?
(CHAPTER 2)

▪ ▪ ▪ ▪

Do chemical modulators of TrxR kill mosquitoes?
(CHAPTER 3)
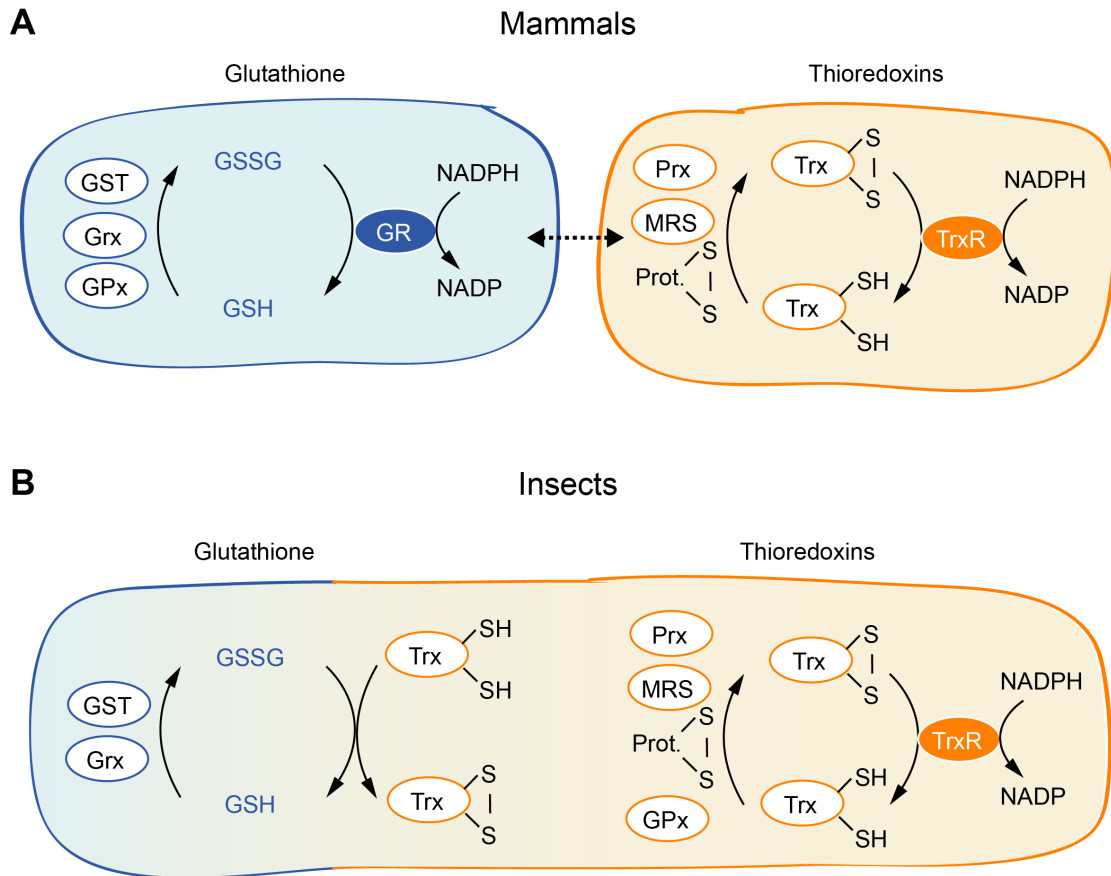
Figure I.9 Cross-talk between the glutathione and thioredoxin systems. (A) In mammals, glutathione is used by glutathione s-transferases (GST), glutaredoxins (Grx) and glutathione peroxidases (GPx) and is recycled by the glutathione reductase (GR). On the other hand, thioredoxins reduce disulfide bridges in proteins and are used by peroxiredoxins (Prx) and methionine sulfoxide reductases (MRS) and are recycled by thioredoxin reductase (TrxR). These two systems are separate, but they can interact and back up each other. **(B)** In insects, there is no GR; instead Trx are responsible for the recycling of GSSG. Moreover, GPx use Trx instead of GSH. In these animals, the glutathione system is dependent on the Trx one.

1

CHAPTER

Redox dynamics of glutathione
in mosquitoes

1. INTRODUCTION

Monitoring and measuring redox processes in the natural context of cells is a challenging task long hampered by the technical difficulties inherent to the nature of redox chemistry. Typically, glutathione is measured by HPLC (Hazelton and Lang, 1984), which entails the disruption of cells with the consequent formation of oxidation artifacts and loss of cellular resolution. Moreover, HPLC-based methodologies are not suitable for dynamic measurements. Alternatively, redox-active dyes can be directly applied to cells (Sebastià et al., 2003), but they are irreversible, partially non-specific and do not attain subcellular resolution.

The discovery (Ormö et al., 1996) and further application (Chalfie et al., 1996) of the green fluorescent protein (GFP) to image living organisms was a revolution in the field of microscopy. Since, many groups have used this highly stable protein to engineer new fluorescent tools, including enhanced versions, new colors (Zhang et al., 2002) and probes to detect intracellular signals such as Ca^{2+} (Miyawaki et al., 1997). Redox biology also found the answer to some of its technical challenges with the development of the redox-sensitive YFP (rxYFP) (Østergaard et al., 2001) and, soon after, the GFP versions (roGFPs) (Hanson et al., 2004).

The wildtype GFP presents fluorescence thanks to a chromophore formed of three cycled amino acids (S65/Y66/G67). The excitation maximum of this protein depends on the protonation state of the phenol group of Y66. In its neutral form, the peak is at 395 nm, whereas in the de-protonated one, at 475 nm. However, when the neutral form is excited, it transfers a proton to E222, thus converting to the excited anionic form. Consequently, both protonation states, and excitation wavelengths, result in the emission of a green light of 509 nm.

In roGFPs, the predominant form of the chromophore depends on the oxidation state of two cysteines that have been introduced in positions S147 and Q204. For roGFP2 (derived from enhanced GFP) the predominant form is the anionic one, but it shifts towards the protonated one upon disulfide formation. Because the oxidation is reversible, this property can be exploited to follow redox changes in living cells (Fig. 1.1). Due to the ratiometric nature of such measurements, this method is also insensitive to photobleaching and differences in the concentration of the probe or thickness of the cell.

In the context of cells, this oxidation is predominantly due to the interaction with GSSG and mediated by Grxs (Dooley et al., 2004; Hanson et al., 2004). Coupling of roGFP2 with Grx1 (Dooley et al., 2004; Hanson et al., 2004) results in a probe (Grx1-roGFP2) that is more specific and catalytically self-sufficient and therefore more reliable to record the dynamics of glutathione (Gutscher et al., 2008). The proposed mechanism for this probe consists of three steps: (1) the active cysteine C23 of Grx1 reacts with GSSG and forms a mixed Grx1-glutathione disulfide; (2) this intermediate reacts with one of the engineered cysteines of roGFP2 and S-glutathionylates it; (3) eventually, roGFP2 reorganizes itself to form an internal disulfide bridge. The three steps are fully reversible (Meyer and Dick, 2010) (**Fig. 1.1 A**).

A

B
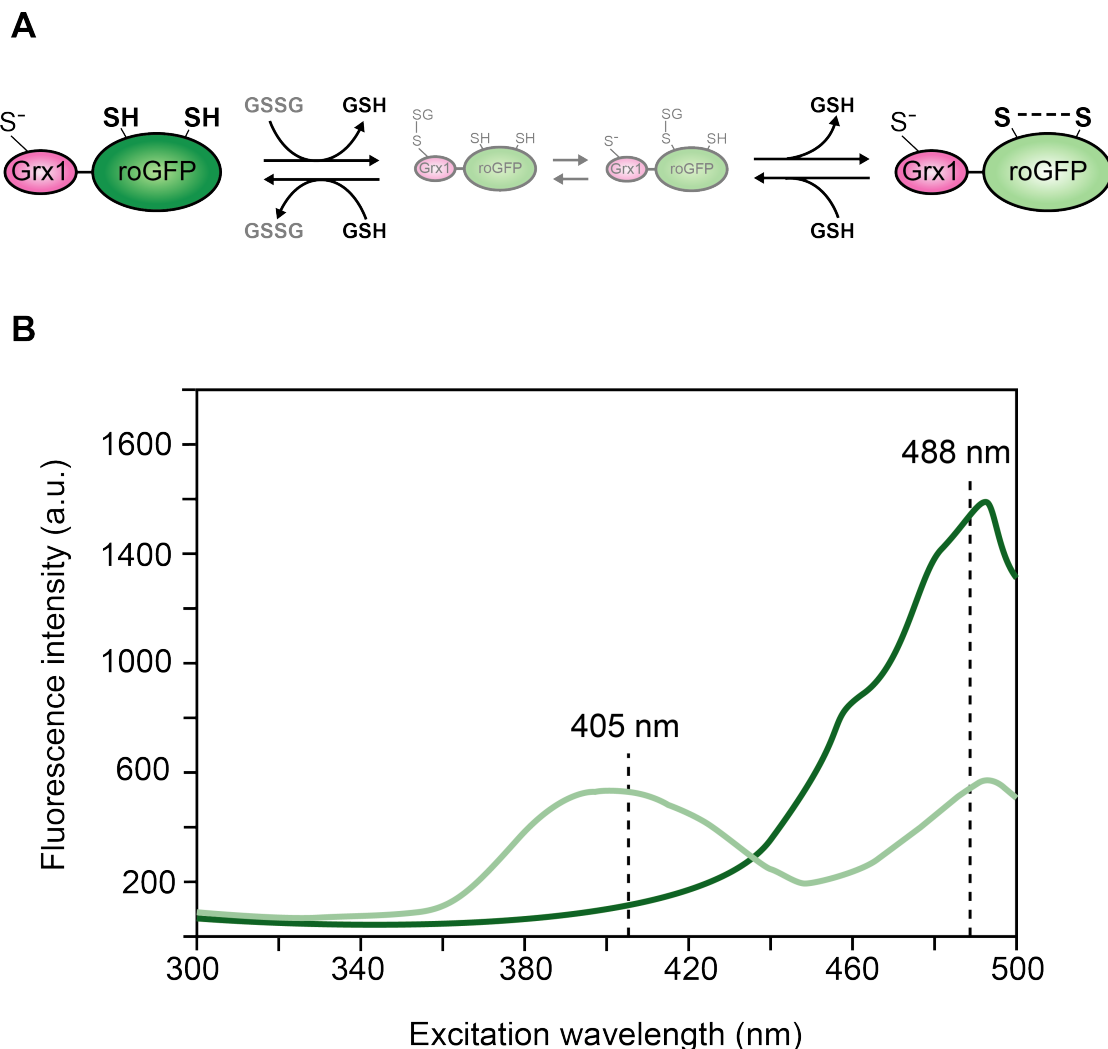
Figure 1.1. Mechanism of action of Grx1-roGFP2 probes. (**A**) The active cysteine of glutaredoxin-1 (Grx1) reacts with oxidized glutathione (GSSG) to form a mixed disulfide, which yields a molecule of reduced glutathione (GSH). In a second step, this intermediate S-glutathionylates one of the engineered cysteines of roGFP2; finally, roGFP2 reorganizes to form an internal disulfide bridge with the other engineered cysteine, liberating another molecule of GSH. All these steps are reversible. (**B**) Reduced roGFP2 presents a peak of excitation around 488 nm (dark green). Upon oxidation, roGFP2 loses part of its excitability at 488 nm and gains some at 405 nm (light green).

hGrx1-roGFP2 has proved to be a very useful tool to follow the dynamics and assess the response of the glutathione pool in several organisms, including *Drosophila melanogaster* flies (Albrecht et al., 2011) and *Plasmodium falciparum* parasites (Kasozi et al., 2013). However, to our knowledge, it has never been applied to mosquitoes.

The aim of this chapter was to establish new transgenic mosquito lines expressing hGrx1-roGFP2 in order to explore the dynamics of glutathione in mosquitoes and its response to different oxidative challenges.

2. RESULTS

A. Expression roGFP2 in enterocytes in *Anopheles gambiae*

The midgut of *Anopheles gambiae* mosquitoes is responsible for two key processes in the biology of this insect: blood digestion and the early antiplasmodial response. Furthermore, several promoters driving expression in this tissue had already been characterized (Volohonsky et al., 2015) while no ubiquitous promoter had been reported. Thus, we reasoned that a transgenic line expressing hGrx1-roGFP2 in the midgut would be of use. To that end, we generated a line expressing the construct under the control of the *Drosophila* actin 5c promoter (GC4027), known to be able to drive the expression of fluorescent probes in the midgut of *A. gambiae* mosquitoes at all developmental stages (Volohonsky et al., 2015). We first cloned hGrx1-roGFP2 (Kasozi et al., 2013) under the control of the actin 5c promoter into a transgenesis vector that contained an attB site for phage Φ31 recombination, then we injected the construct into the X1 mosquito line carrying an attP site in chromosome 2L. The resulting line presented strong, green fluorescence in the midgut through all developmental stages for both sexes. The probe was localized both to the cytoplasm and the nucleus, with a higher signal being detected in the latter (**Fig. 1.2 A**).
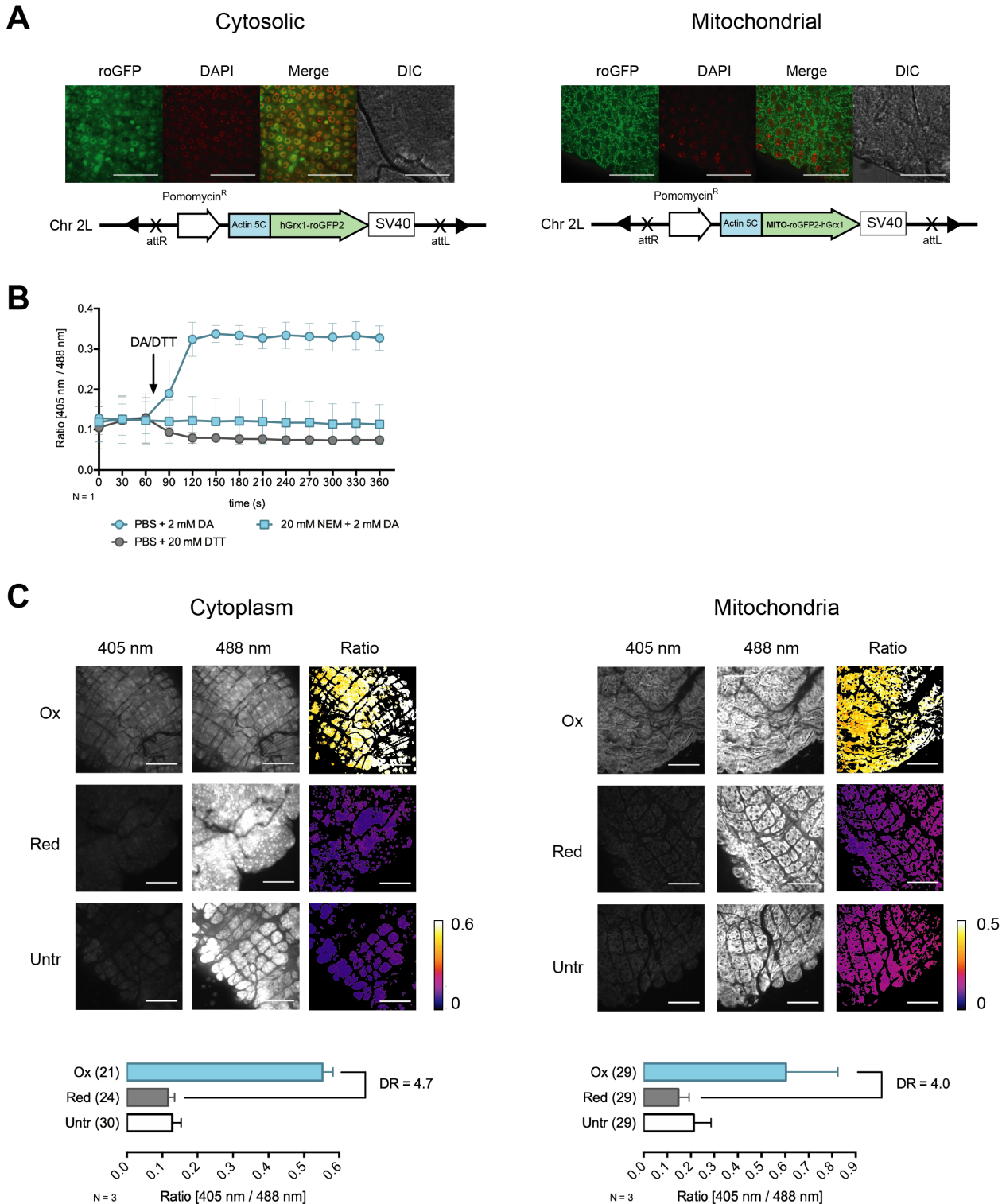
Figure 1.2. The glutathione pool is mostly reduced in the cytoplasm, nucleus and mitochondria of enterocytes in *Anopheles gambiae* females. (A) hGrx1-roGFP2 and mito-roGFP2-hGrx1 were cloned under the control of the *Drosophila melanogaster* Actin 5C (CG4027) promoter, and then inserted into the genome of *Anopheles gambiae* mosquitoes by phage Φ31 recombination with a docking site in chromosome 2L. The resulting lines express the construct in enterocytes with nucleo-cytoplasmic and the mitochondrial localization, respectively. **(B)** The midgut of adult females (cytoplasmic probe) was dissected in PBS and imaged for 1 minute; then, they were exposed to either 20 mM dithiotheiol (DTT) or 2 mM diamide (DA) and imaged for 5 more minutes to assess their responsiveness to reduction and oxidation. Additionally, some midguts were dissected in 20 mM N-ethylmaleimide (NEM) and the DA experiment, repeated to assess the efficiency of NEM to block oxidation. Error bars represent the SD of three midguts. The experiment was performed once (N). **(C)** Midguts were dissected and incubated in DA (ox), DTT (red) or NEM (untr) and the dynamic range and the basal state of the probe were assessed. Scale bars, 100 μm. Bars and error bars represent the mean and SD of three independent experiments (N), respectively. The total number of midguts is indicated in brackes.

40

To assess the response of the probe, we dissected females in PBS and imaged their midguts for 1 min, then added diamide (DA, oxidant) or dithiothreiol (DTT, reducer) and imaged for 5 more min. We calculated the ratio of the intensities obtained when the tissue was excited at 405 nm and 488 nm for each time point. In both cases, the maximum response was attained in 1 min. Upon DA exposure there was a 2.78-fold increase in the 405 nm / 488 nm ratio. On the contrary, DTT reduced this value 0.84 times (**Fig. 1.2 B**). This suggests that the basal state of the probe in enterocytes is close to the lower end of its dynamic range; i.e. that the pool of glutathione in these cells is highly reduced. Next, we tested whether the probe could be protected from oxidation by alkylating the free thiols as described by Albrecht et al (Albrecht et al., 2011). To that end, midguts were dissected in PBS containing 20 mM N-ethymaleimide (NEM) and the DA experiment, repeated. Midguts did not show any changes in the 405 nm / 488 nm ratio, confirming that even short incubation in NEM is enough to protect the probe from oxidation.

Next, we assessed the basal state of glutathione in fixed tissues. To that end, we dissected and incubated midguts in NEM prior to fixation. In parallel, we prepared fully reduced and oxidized controls by dissecting and incubating the tissues in DTT and DA prior to NEM blocking. With the ratios obtained for these controls, we could calculate that the maximum dynamic range of the probe in these conditions was 4.7 (**Fig. 1.2 C**). Consistent with the observations for unfixed tissues, the redox potential of glutathione was found to be close to the lower end of the probe both in the cytoplasm and the nucleus, with an average degree of oxidation of 11 %. Assuming that the midpoint redox potential of roGFP2 is -280 mV (Meyer and Dick, 2010) and a cytosolic pH of 7.2 this would correspond to a E_{GSH} of -316 ± 5 mV.

Because mitochondria are the major ROS producers in cells, we decided to explore their glutathione pool as well. Hence, we amplified the mito-roGFP2-hGrx1 transgene from *Drosophila melanogaster* (Albrecht et al., 2011) and then repeated the same process as for the cytoplasmic line. The resulting transgenics presented the same overall pattern with fluorescence being restricted to the mitochondria (**Fig. 2 A**). Again, we assessed the basal state of the glutathione pool in this compartment as we did for the cytoplasm. The dynamic range of the probe was 4, slightly lower than that of the cytoplasmic one (**Fig. 2 C**). The average degree of oxidation of the probe was higher than in the cytoplasm (24 %), which corresponds to a redox potential of -295 ± 5 mV.

B. Dynamics of glutathione in the midgut during the lifecycle of A. gambiae

Next we explored whether the high GSH/GSSG ratio observed in adults was kept throughout mosquito development. To that end, we dissected larvae at their 4th instar and pupae and we compared them to adults. In general, the redox potential of both glutathione pools was higher at the pupal stage and high variability between individuals was observed (**Fig. 1.3 A**). The statistical significance of these changes varied among experimental repeats, but the mean was consistently higher than that of the other two stages. Interestingly, the redox potential of the mitochondrial pool was often higher than the cytoplasmic one in larvae and adults, but not in pupae. Because the pupal stage is a period of intense tissue remodeling, we hypothesize that the observed increase in glutathione oxidation is due to these changes, and that the high variability of the measures in pupae is likely linked to variation in the pupae age upon dissection as we did not specifically control this.

Oxidative changes are known to occur upon ageing (Albrecht et al., 2011) and they have been suggested to trigger senescence (Holmström and Finkel, 2014). Hence, we next addressed if there was an increase in the redox potential of glutathione as mosquitoes became older. To that end, we dissected and imaged the midgut of females and males during the first, the second and the third weeks after emergence (Fig. 1.3 B). In females, no difference in the GSH/GSSG ratio was observed between time points. Consistent with our previous observations, the mitochondrial pool was slightly more oxidized that the cytoplasmic one at all ages. Unlike females, males presented a more variable oxidation of their glutathione pools, both in the cytoplasm and the mitochondria, but we did not find a clear correlation with ageing when analyzing different repeats (**Fig. 1.3 B'**). Indeed, taken independently, experiments showed two different tendencies for the cytoplasm and the mitochondria. In the former, the direction of the changes (more reduced or oxidized) varied among repeats. In the case of mitochondria, changes were consistent in two of the three repeats, but antagonistic in time; during the first 2 weeks there was an increase in the redox potential of glutathione whereas the opposite effect was observed during the last week (**Fig. 1.3 B' repeat 2 and 3**). The sample size of the remaining repeat was very small and conclusions are difficult to draw; nonetheless, with the exception of one midgut at week three, the rest of the tissues analysed seemed to follow the same tendency as the one observed in the other repeats (**Fig. 1.3 B' repeat 1**).
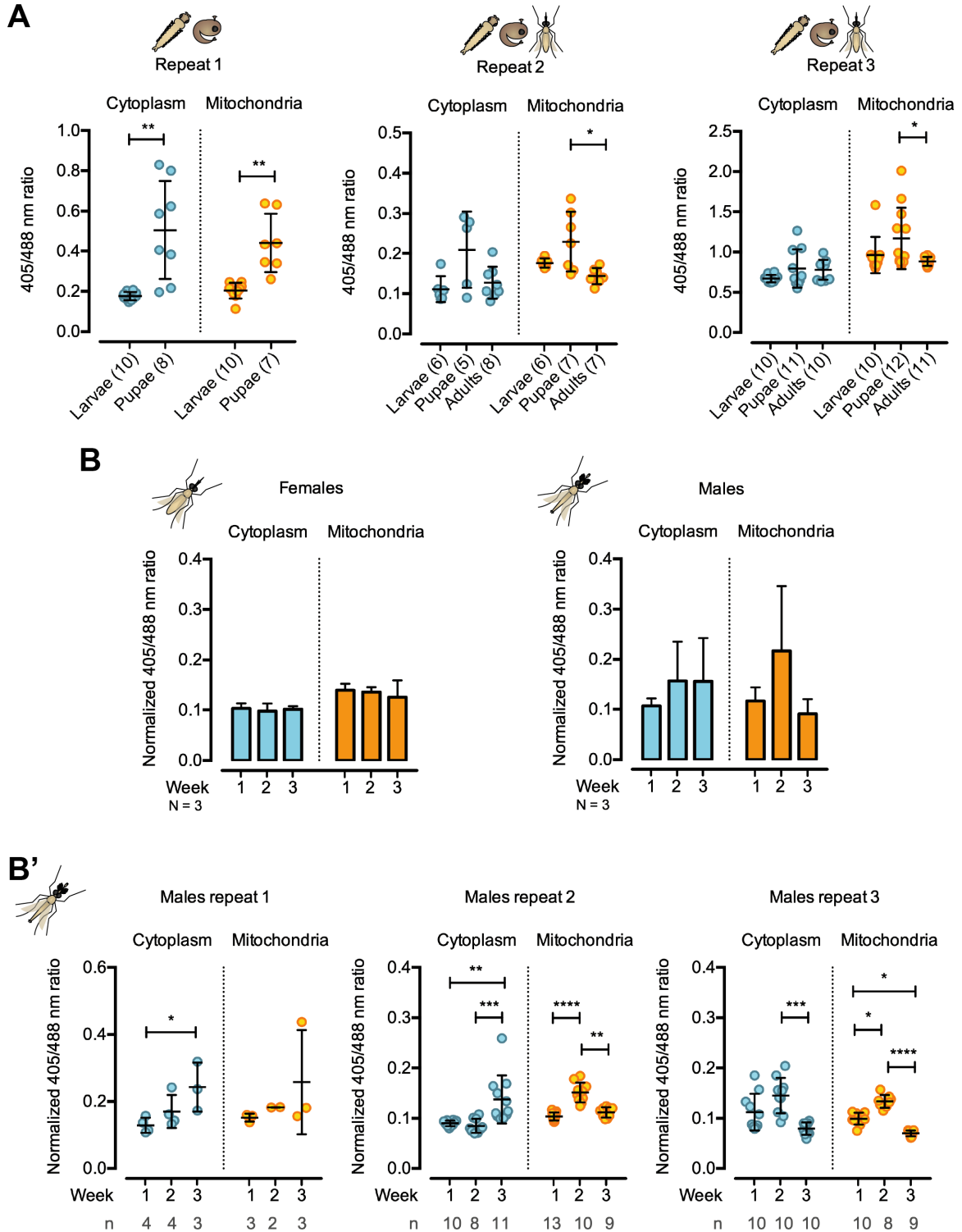
Figure 1.3. The pool of glutathione undergoes oxidation during the pupal stage and is very dynamic in adult males upon ageing. Midguts of mosquitoes were dissected and analyzed at different developmental stages and ages. **(A)** Changes during development. 4th instar larvae, pupae and young adults were compared in three independent repetitions. Horizontal and error bars indicate mean and SD, respectively; dots represent values for individual mosquitoes and the total number of mosquitoes is indicated in brackets. **(B)** Adult mosquitoes were dissected during the 1st, 2nd and 3rd week after emergence and their midguts were analyzed depending on the sex. Bars and error bars indicate mean and SD of three independent repeats, respectively **(B')** For males, the three independent repeats are shown in separately in **(B)** where horizontal and error bars indicate mean and SD, respectively; dots represent values for individual mosquitoes and the total number of mosquitoes is indicated in brackets. For pair-wise comparisons, statistical analyses were performed using unpaired t-test with Welch correction; for multiple comparisons, Kruskal-Wallis was used followed by Dunn post hoc. *p = 0.05; **p = 0.01; ***p = 0.001; **** p = 0.0001. Only significant comparisons are indicated.

From these experiments, we concluded that redox maintenance systems are more robust in females than they are in males and that oxidative stress does not correlate with ageing in mosquitoes.

C. Response of glutathione in the gut to natural and artificial oxidative challenges

During blood feedings, females ingest large amounts of hemoglobin, releasing free heme, the prosthetic group of hemoglobin and a potent pro-oxidant molecule (Ryter, S, W. Tyrrell, R, 2000). Most free heme is converted to hematin that adheres to the mosquito peritrophic matrix and is excreted with blood meal remains. Still, blood meal heme is the major source of iron for female mosquitoes (Zhou et al., 2007), and uptaken iron may induce oxidative stress in midgut tissues, as well as the increased metabolism during blood digestion. To measure the impact of blood feeding on the glutathione redox homeostasis, we allowed females to feed on naïve mice and analyzed the fluorescent signal of roGFP2 24 h later. The redox potential of the mitochondrial pool was unaffected by blood digestion at this time point (**Fig. 1.4 A**); however a slight oxidizing impact was detected on the cytoplasmic pool, although we did not observe this effect in all the independent repeats that we performed (**Fig. 1.4 A, A'**).

To further explore the robustness of this redox buffer, we challenged female mosquitoes in an artificial manner. To that end, we supplemented the feeding sucrose solution with hydrogen peroxide (H_2O_2) and dissected the midgut 24 h later. No oxidation was observed in either glutathione pool. We repeated the experiment using paraquat (N-N'-dimethyl-4,4'-bipyridinium dichlore), an herbicide commonly used to induce oxidative stress (Castello et al., 2007; Shivanandappa, 2017). Again, we did not measure any signs of glutathione oxidation; instead we observed a slight, but significant decrease in the redox potential of the mitochondrial pool. Taken together, these results may confirm the robustness of the mosquito antioxidant system, maintaining a reduced environment despite oxidative assaults and suggest that the cytoplasmic and mitochondrial pools are independently regulated. Alternatively, one may hypothesize that the involvement of the glutathione pool in intracellular redox maintenance is limited, or that the different assays we used were not adequate to detect its involvement.
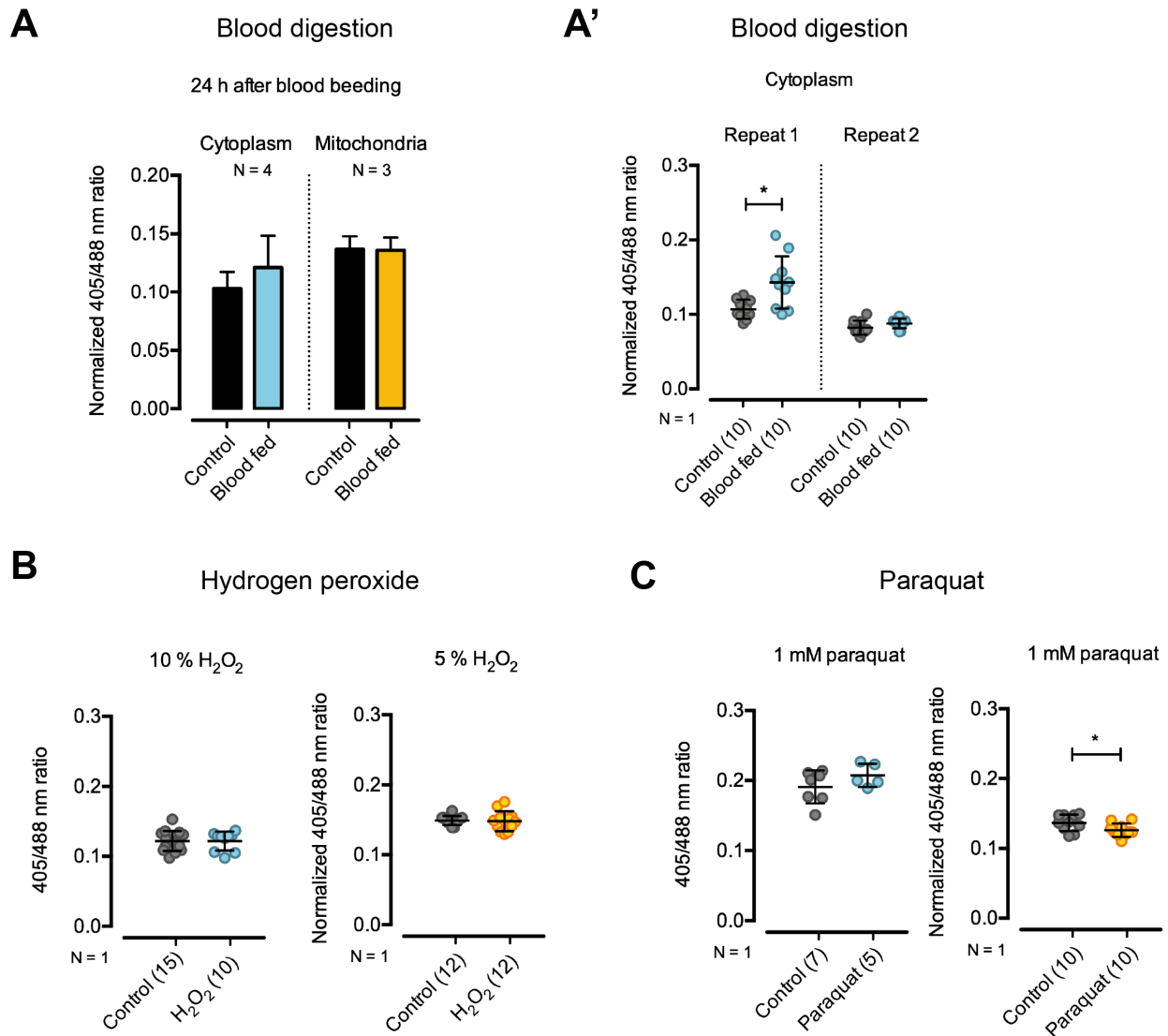
Figure 1.4. Glutathione is a robust redox buffer in *Anopheles gambiae* females. Adult females were challenged with different oxidants and their midguts analyzed 24 h later. **(A)** Females were fed on a naïve mouse and dissected 24 h later in parallel with unfed siblings (control). Bars and error bars indicate mean and SD of three independent repeats (N), respectively. For the cytoplasm, two of the repeats are shown in **(A')**, where horizontal and error bars indicate mean and SD, respectively; dots represent values for individual mosquitoes and the total number of mosquitoes is indicated in brackets. **(B)** The sugar feeding solution was supplemented with 5 % or 10 %hydrogen peroxide (H_2O_2) or **(C)** 1 mM paraquat (N,N'-dimethyl-4,4'-bipyridinium dichlore) and mosquitoes were dissected 24 h later in parallel with unchallenged siblings (control). Horizontal and error bars indicate mean and SD, respectively; dots represent values for individual mosquitoes and the total number of mosquitoes is indicated in brackets. The experiments were only performed once (N). For pair-wise comparisons, statistical analyses were performed using unpaired t-test with Welch correction. *p = 0.05. Only significant comparisons are indicated.

D. Response of glutathione to P. berghei ookinete invasion

The midgut epithelium is the first tissue that *Plasmodium* parasites must cross in order to establish an infection in mosquitoes. Moreover, this invasion triggers the immune response of the insect which, in its early steps, is known to be mediated by ROS and RNS (Han et al., 2000; Kumar et al., 2004). Thus, we wondered what impact this response had on the pool of glutathione. To that end, we infected mice with a transgenic *P. berghei* strain that constitutively expresses mCherry, and then we allowed females expressing hGrx1-roGFP2 to feed on them. We dissected their midguts 20 - 24 h after the blood meal and we imaged them from the basal lamina to the lumen in the Z-axis. 78 % of the parasites that had reached the basal lamina co-localized with round cells extruding from the epithelium (**Fig. 1.5 D - H**). Moreover, most of these cells displayed an oxidized pool of glutathione (**Fig 1.5 F''**). On the contrary, midguts having been in contact with uninfected blood presented a reduced glutathione potential and did not show any signs of cell extrusion (**Fig. 1.5 A – C**). Most of the protruding cells that we found formed groups that co-localized with one single parasite (**Fig. 1.5 F**). This observation is consistent with the fact that *P. berghei* parasites move laterally from cell to cell during the process of invasion (Han et al., 2000). Considering this and the fact that extruded cells leave a characteristic scar in the epithelium (Han et al., 2000), we could presume the order in which parasites had invaded these groups of cells (**Fig. 1.5 F'**). When we compared this with the degree of oxidation of each enterocyte, we did not observe any correlation (**Fig. 1.5 F', F''**). Furthermore, some of the extruded enterocytes presented signs of apoptosis such as nuclear condensation (**Fig. 1.5 F'''**). Again, this feature did not reflect time elapsed since invasion, and while most protruding/apoptotic cells were highly oxidized, we could also detect some with no obvious sign of glutathione oxidation (**Fig 1.5 F', cell 1**).

Han et al (Han et al., 2000) described the presence of round, extruding cells that were positive for NOS in the midgut of *A. stephensi* females after *P. berghei* infections. Because our highly oxidized cells showed the same phenotype, we wondered whether the difference in the redox potentials was due to the overexpression of NOS. To gain resolution, we decided to detect the presence of parasites using antibodies against the *P. berghei* surface protein 21 (Pbs21). This approach has the additional advantage that it reveals the existence of lysed parasites in cells (Han et al., 2000). As expected, we detected NOS signal in all the midguts
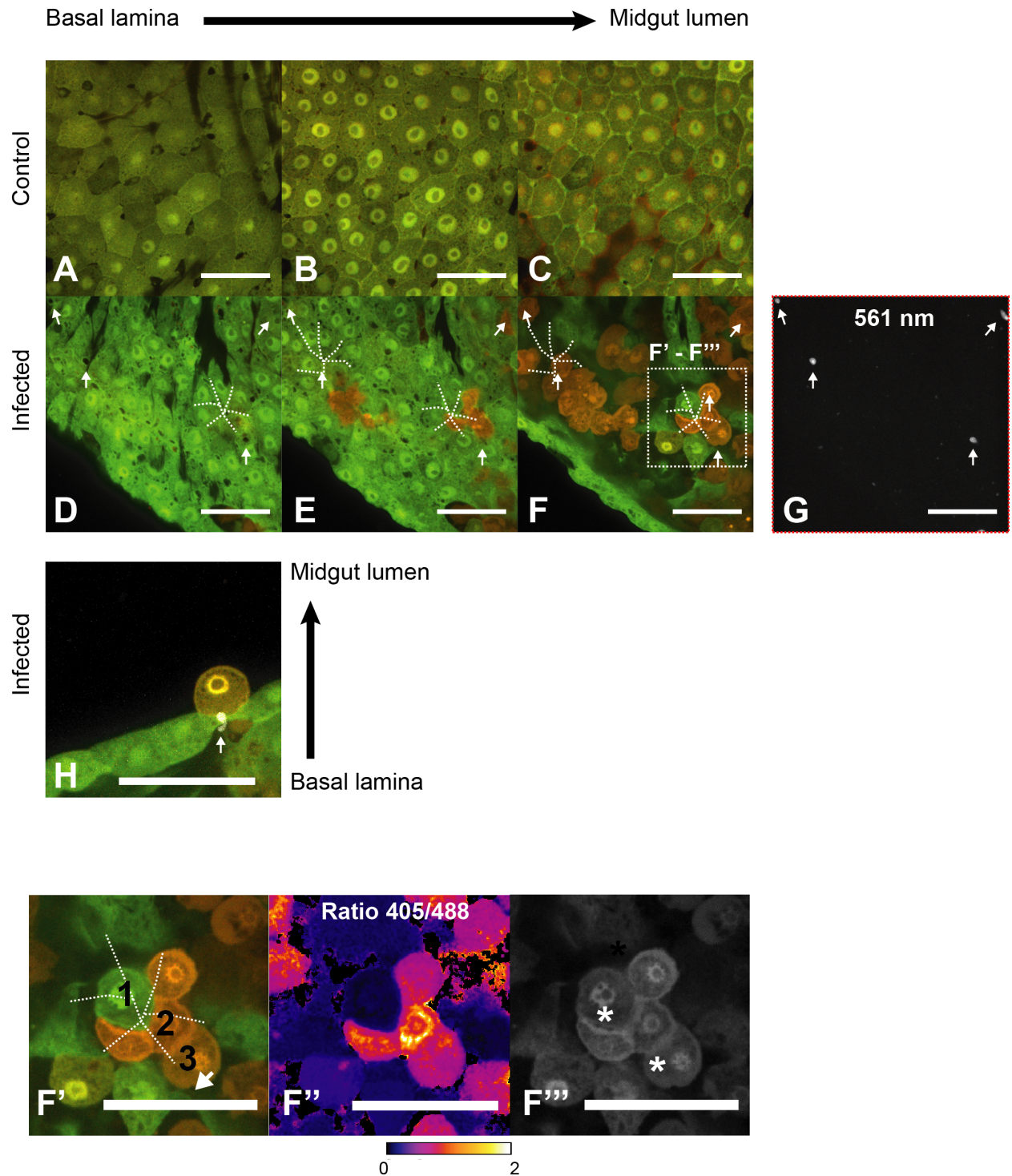
Figure 1.5. *Plasmodium berghei* infections lead to the apparition of highly oxidized enterocytes extruding from the epithelium. Transgenic *Anopheles gambiae* females expressing hGrx1-roGFP2 in the cytoplasm of enterocytes were fed on mice infected with transgenic *P. berghei* parasites expressing mCherry (infected) or non-infected mice (control). 20-24 h later midguts were dissected and analyzed. **(A – F)** Two midguts shown at three different positions in Z-axis: **(A, D)** basal lamina, **(B, E)** epithelium plane and **(C, F)** midgut lumen. **(G)** Parasites in the basal lamina and epithelium plane of the infected midgut **(D, E)**. **(H)** Lateral view of an oxidized, protruding cell that co-localizes with a parasite in the basal lamina. **(F' – F''')** Close-up of area within the white square in **(F)**. **(F')** Numbers indicate the presumed order of invasion by the parasite. **(F'')** 405 nm / 488 nm ratio. **(F''')** Stars indicate cells with signs of nuclear condensation. White arrows and white dotted lines indicate the presence of parasites and the scars left by extruded cells, respectively, in the basal lamina or the epithelium plane. Unless otherwise indicated, images are a merge of the ones obtained with the 488 nm (green) and the 405 nm (red) lasers. Scale bar, 50 µm.
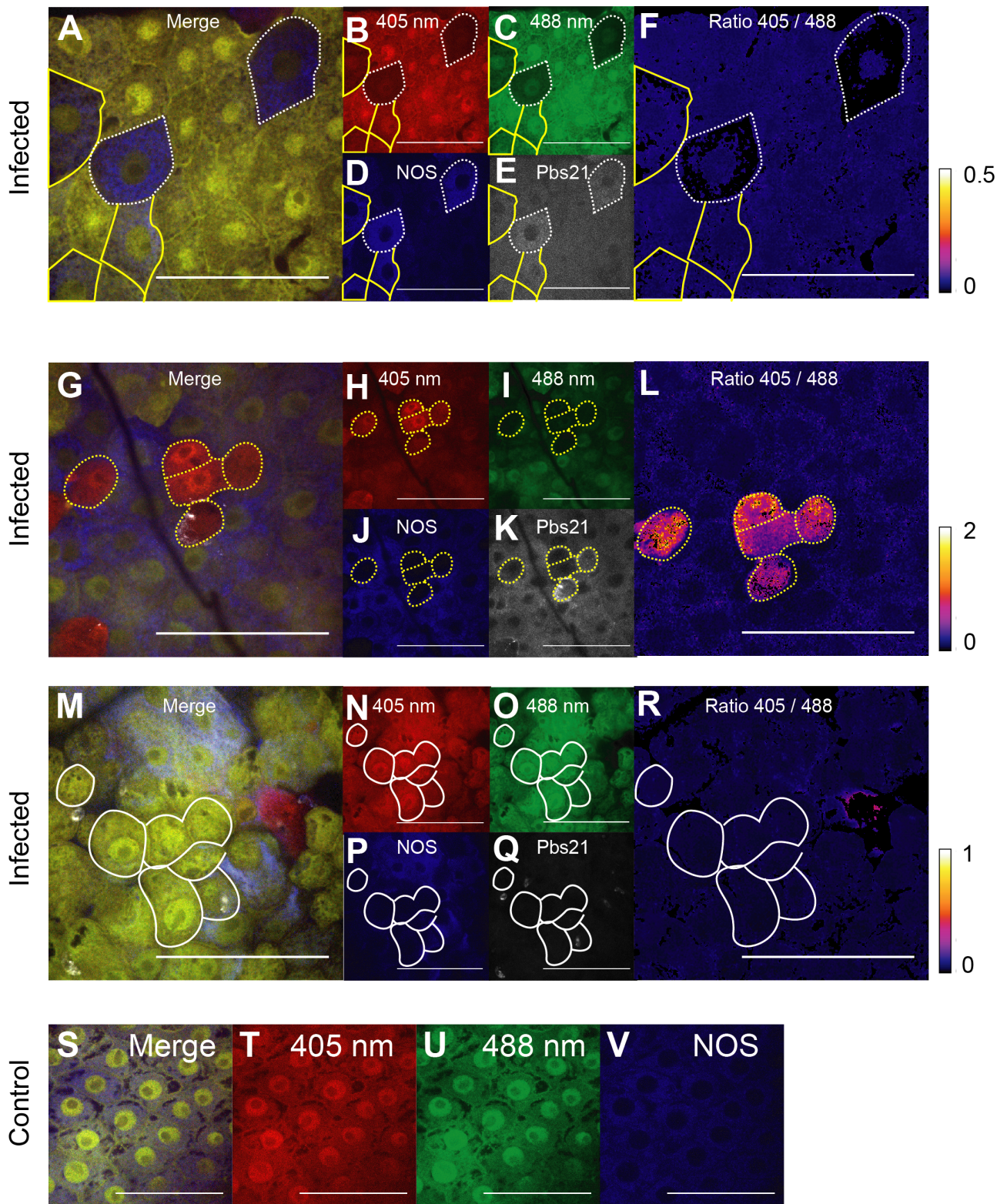
Figure 1.6. The oxidative state of cells does not correlate with the levels of nitric oxide synthase. *Anopheles gambiae* females expressing cytoplasmic hGrx1-roGF2 were fed on a *Plasmodium berghei* infected or a naïve mouse. 24 h later, midguts were dissected and stained with antibodies against nitric oxide synthase (NOS) and *P. berghei* surface protein 21 (Pbs21). **(A − F)** Infected midgut. Lines indicate the presence of cells overexpressing NOS that are roGFP negative (white dotted) or positive (yellow). **(G − L)** Infected midgut. Yellow dotted lines indicate the presence of cells negative for NOS that are extruding and oxidized. **(M − R)** Infected midgut. White lines indicate the presence of cells negative for NOS that are extruded and reduced. **(S − V)** Uninfected midgut. **(A, G, M, S)** Merge of the 405 nm and 488 nm images. **(B, H, N, T)** Images obtained with the 405 nm laser. **(C, I, O, U)** Images obtained with the 488 nm laser. **(D, J, P, V)** NOS expression. **(E, K, Q)** Traces of *P. beghei* parasites. **(F, L, R)** Ratio between the images obtained with the 405 nm and the 488 nm laser. Scale bar, 100 µm.

that were analyzed, including naïve-fed controls (**Fig. 1.6 D, I, P, V**). This is consistent previous observations that NOS is constitutively expressed in blood-fed mosquito midguts (Han et al., 2000). Additionally, infected midguts contained cells overexpressing the enzyme (**Fig. 1.6 D**); most of them were in close contact with parasites or were positive for Pbs21, i.e. most likely cells where parasites had been lysed (**Fig. 1.6 D, E**). In 77% of these NOS-overexpressing cells, roGFP was quenched and therefore their cytoplasmic redox state could not be analyzed (**Fig. 1.6 B, C, F white dotted lines**); most of those that did express roGFP were reduced (**Fig. 1.6 B, C, F yellow lines**). Inversely, we also found cells that were negative for NOS (**Fig. 1.6 J, P**). 96% of these cells were protruding to the midgut lumen and were reduced (**Fig. 1.6 N**) or oxidized in the same proportion (**Fig. 1.6 B L**). Altogether, these results suggest that the differences in the redox state of the extruded cells is not directly caused by the overexpression of NOS and that the midgut reaction to parasite invasion is a complex process at the tissue level.

Another interesting organ from the point of view of *Plasmodium* infections is the salivary glands. After ookinete maturation and final release of sporozoites in the mosquito body cavity, this motile form of the parasite must cross the salivary gland epithelium in order to be inoculated into the vertebrate host. To investigate the redox response of these cells, we cloned the cytoplasmic hGrx1-roGFP2 probe under the control of the anopheline antiplatelet protein (AAPP; AGAP009974) promoter and inserted it into the same genomic locus as before. The resulting line expressed the construct in the nucleus and cytoplasm of the salivary gland epithelium (**Fig. 1.7 A**). To characterize the response of the probe and the basal state of glutathione in this tissue, we dissected young females (3-5 days old) and followed the same protocol as for the midgut lines. The dynamic range of the probe in this tissue was virtually the same as for the other lines (4.2) and the redox potential close to the lower end of the probe (**Fig. 1.7 B**). We have thus established another biosensor line that measures the redox potential of glutathione in salivary glands and therefore that will help us characterize the *Plasmodium-Anopheles* interactions further.

A

B
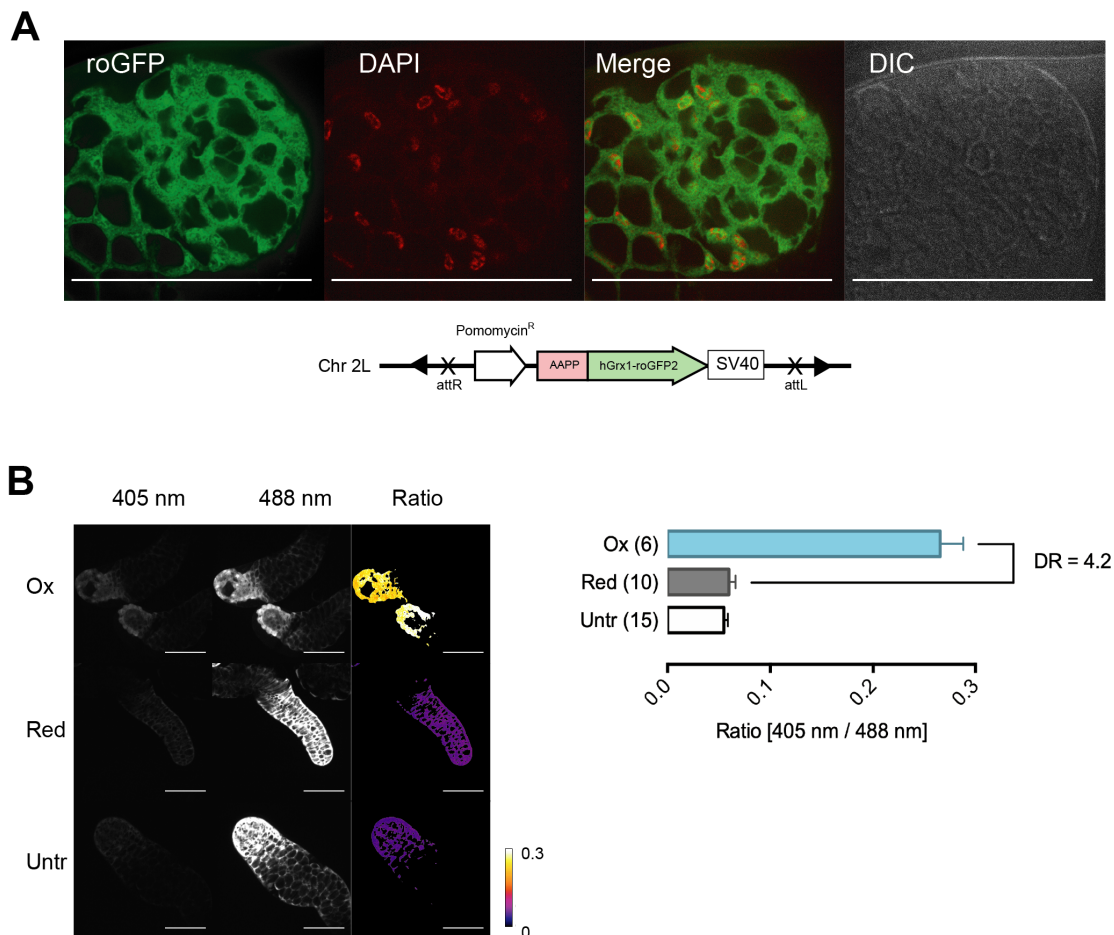
Figure 1.7. Glutathione is highly reduced in the nucleus and cytoplasm of epithelial cells in the salivary glands of _Anopheles gambiae_ females. (A) hGrx1-roGFP2 was cloned under the control of the salivary gland-specific AAPP (AGAP009974) promoter, and then inserted into the genome of _Anopheles gambiae_ mosquitoes by phage Φ31 recombination with a docking site in chromosome 2L. The resulting line expresses the construct in the cytoplasm and nucleus of epithelial cells in salivary glands. **(B)** Salivary glands were dissected and incubated in diamide (ox), dithiothreiol (red) or N-ethylmaleimide (untr) and the dynamic range and the basal state of the probe were assessed. Scale bars, 100 μm. Bars and error bars indicate the mean and SD of one single experiment; total number of midguts indicated in brackets. DR = dynamic range.

E. Expression of hGrx1-roFGP2 in Aedes aegypti mosquitoes

Another mosquito species of biomedical relevance is the dengue mosquito _Aedes aegypti_. In this species, blood meals are known to induce an antioxidant response, which has been suggested to play a role in the susceptibility of these insects to the viruses they transmit (Bottino-Rojas et al., 2018; Oliveira et al., 2017). Thus, we reasoned that having transgenic _A. aegypti_ lines expressing hGrx1-roGFP2 would be relevant to the field and might help elucidate the antiviral response in these

mosquitoes. Because viruses establish systemic infections, we cloned the hGrx1-roGFP2 probe under the poly-ubiquitin promoter (AAEL0003867), known to drive robust EGFP expression in almost every tissue at all developmental stages (Anderson et al., 2010). In the absence of docking lines and of efficient knock-in in this species, we chose to use the piggyBac system that leads to random integration in the genome. With one transgenic female that we obtained, we established a homozygous line expressing the construct in all tissues but the ovaries. However, within tissues, the expression was not homogenous, and presented patches of roGFP-negative cells (**Fig. 1.8 A, C**). Because other lines in the laboratory expressing GFP under the same promoter do not present this phenotype, we concluded that it was due to the genomic locus where the transgene landed. To study the response of the probe and the basal state of glutathione we chose two tissues, the midgut and the malpighian tubules. Indeed, the latter have been proposed to be key players in heme detoxification and the antioxidant response upon blood meal (Piermarini et al., 2017). We dissected midguts and malpighian tubules and exposed them to DA, DTT or directly NEM, fixed them and measured the 405 nm / 488 nm ratio. As expected, the dynamic range of the probe in the midgut was 4 and the basal state of glutathione close to the lower end of the probe (**Fig. 1.8 B**). In two of the repeats the average redox potential was – 297 ± 2 mV whereas in the third one the degree of oxidation of the probe was below 5 %, thus suggesting a potential close to – 320 mV. Surprisingly, the dynamic range of the probe in malpighian tubules was only 2 (Fig. 1.8 B). The cells that compose this tissue present granules in the cytoplasm that are auto-fluorescent when excited with the 405 nm laser (**Fig. 1.8 C, white lines**). Of note, the intensity of this auto-fluorescence is not the same in all cells (**Fig. 1.8 C, yellow lines**), probably as a result of different concentrations or compositions. DTT-treated samples show homogenous, reduced nuclei, but not cytoplasms (**Fig. 1.8 C**), suggesting that this auto-fluorescence is altering the signal coming from roGFP and leads to an artificially high glutathione oxidation signal in the cytoplasm. We thus concluded that in this tissue, it might only be possible to investigate the roGFP oxidation level in nuclei. Nevertheless, the line will be useful to study the antiviral response of the gut in future experiments, and most likely, in other tissues as well.
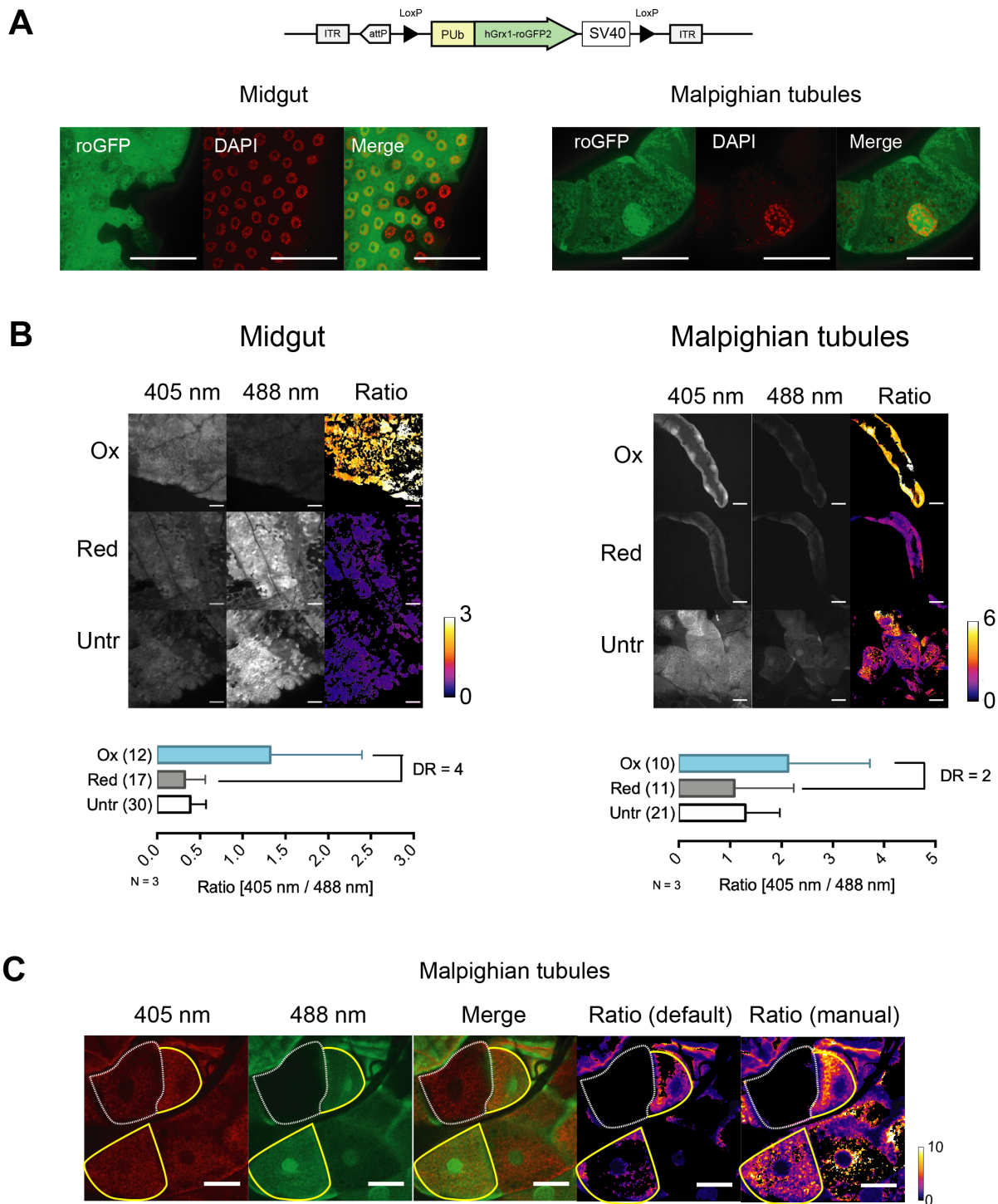
Figure 1.8. hGrx1-roGFP2 can be successfully applied to *Aedes aegypti* enterocytes, but not the malpighian tubules. (A) hGrx1-roGFP was cloned under the control of the poly-ubiquitin promoter (AAEL003867), then inserted randomly into the genome of *Aedes agypti* mosquitoes by piggyBac transgenesis. The resulting line expressed the construct in several tissues in a patchy manner. The probe localizes to the nucleus and the cytoplasm in both midguts and malpighian tubules**. (B)** Midguts and malpighian tubules were dissected and incubated in diamide (ox), dithiothreiol (red) or N-ethylmaleimide (untr) and the dynamic range and the basal state of the probe were assessed. Bars and error bars indicate the mean and SD of three independent experiments (N); total number of mosquitoes indicated in brackets. DR = dynamic range. **(C)** Auto fluorescent granules in a malpighian tubule treated with dithiothreiol (DTT, reductant). Default ratio refers to the processing of the images with the default setting suggested by ImageJ; manual ratio refers to a manual processing adapting the setting for optimal resolution of the least fluorescent cells. White dotted line indicates a roGFP-negative cell; yellow lines, two positive cells with different auto fluorescence. Scale bars, **(A, C)** 100 μm and **(B)** 50 μm.

3. DISCUSSION

Despite the biological relevance of oxidative stress, little is known about redox homeostasis in mosquito vectors. This gap in our knowledge of these insects contrasts with the roles that oxidants and antioxidants play in key processes such as immunity (Bottino-Rojas et al., 2018; Han et al., 2000; Kumar et al., 2003, 2004; Molina-Cruz et al., 2008; Oliveira et al., 2013, 2017) and insecticide resistance (Oliver and Brooke, 2016; Ranson et al., 2001; WHO, 2012). Moreover, insects lack the major antioxidant enzyme glutathione reductase (Kanzok et al., 2001) and therefore we cannot extrapolate findings in other organisms to this particular case. In the past, the study of such systems was hampered by technical difficulties, however the development of redox-sensitive fluorescent probes and of mosquito transgenesis has opened new opportunities in this regard.

Here we have, for the first time, expressed the glutathione biosensor hGrx1-roGFP2 in different cellular compartments, tissues and mosquito species thereby offering novel tools to measure and study the dynamics of E_{GSH} in real time. Likewise, we have shown that the redox potential of glutathione in the cytoplasm of enterocytes and the salivary glands epithelium are within the measurable range of roGFP2. In the midgut, the E_{GSH} was found to be -316 ± 5 mV, in *A. gambiae,* and between -297 mV and -320 mV, in *Aedes aegypti*, In *A. gambiae* salivary glands, it was also close to -320 mV. These measurements are consistent with previous observations made in other eukaryotes using roGFP tools such as in *D. melanogaster* where it was reported to be below -300 mV (Albrecht et al., 2011), in HeLa cells (between -315 and -325 mV) and in *P. falciparum* (-314 mV). Moreover, we calculated the E_{GSH} in the mitochondria of enterocytes in *A. gambiae* and found that it is slightly less reducing (-295 ± 5 mV). This is consistent with the idea that mitochondria are the major ROS producers in cells (Diebold and Chandel, 2016), however it does not seem to be the case in all species. For instance, this phenomenon holds true in mouse neurons (Wagener et al., 2016) but not in *Arabidopsis thaliana* (Rosenwasser et al., 2010) or HeLa cells (Dooley et al., 2004). Moreover, in *D. melanogaster*, differences in the redox potential of glutathione in the cytoplasm and the mitochondrial depend on the tissue (Albrecht et al., 2011). Likewise, in our studies we found sex-based differences in this relationship. Whereas females consistently displayed a higher potential in mitochondria, males did not.

In general, males showed much more dynamic pools of glutathione, which is consistent with the observations that, in general, they possess lower levels of antioxidants and produce more ROS (Ide et al., 2002; Niveditha et al., 2017). This was patent in our ageing studies where we did not find any changes in either pool in the case of females, but large variability in males. In the cytoplasm, these changes did not follow any trend, but rather depended on the experimental repetition; on the contrary, findings in mitochondria were more reproducible, but antagonistic in time as the redox potential increased during the first 2 weeks, then decreased during week 3. These observations contradict the oxidative damage theory of ageing (Harman, 2003) and suggest that this variation in males derives from other related or unrelated phenomena. Mosquitoes are known to fight bacteria by producing ROS (Molina-Cruz et al., 2008), thus one plausible explanation is that the observed dynamics in the midgut glutathione pool oxidation are a consequence of differences in the midgut microbiota composition or number.

During the pupal stage, mosquitoes undergo metamorphosis and complete the formation of the last adult tissues. This process entails the elimination of the former larval midgut to form the adult organ. In *A. aegypti* this remodeling is mediated by autophagic cell death (Fernandes et al., 2014), a process that is triggered by a decrease in GSH levels accompanied by a decrease in the GSH/GSSG ratio (Desideri et al., 2012; Kiššová and Camougrand, 2009; Mancilla et al., 2015). Consistent with this, we found that *A. gambiae* pupae presented a much more oxidizing E_{GSH} as compared to larvae and adults. The differences in the degree of oxidation that we observed among individuals and experimental replicates suggest that this process takes place gradually in a very specific timeframe. In order to address this, the experiments should be repeated controlling precisely for the time of dissection after pupation.

During blood meals, female mosquitoes uptake several times their body weight of blood. The digestion of these meals takes place in the midgut and releases large amounts of heme, the prosthetic group of hemoglobin. This molecule promotes oxidation (Sahoo et al., 2016), thus blood-sucking arthropods have developed adaptations to protect themselves from heme toxicity (Graça-Souza et al., 2006). In *A. gambiae*, several antioxidant genes are upregulated after a blood meal (Molina-Cruz et al., 2008; Ribeiro, 2003) whereas *A. aegypti* seems to reduce ROS production to avoid dangerous heme-derived products (Oliveira et al., 2011). Here we have assessed the implications that blood digestion has on the glutathione pool

of enterocytes. When comparing the mitochondria of unfed and blood-fed females 24 h after the meal, we did not find any differences. In the case of the cytoplasm, an overall slight increase in oxidation was observed, but no statistical significance was found. This experiment was repeated 4 times in total; when we investigated the results of each of these independent repeats separately, we found that this increase was apparent and significant only in two of them. The absence of clear signs of oxidation in the glutathione pool suggests that mosquitoes have a strong antioxidant response to blood digestion although we cannot exclude that oxidation may occur at other levels such as lipid peroxidation. The variability and minor nature of the changes observed in the cytoplasm suggest that it might not be a consequence of blood digestion *per se* but rather derived from differences in the mosquito populations, possibly again in the composition of the gut microbiota or differences in the ingested blood.

Here, we also assessed the response of *A.* gambiae females to artificial oxidative challenges. Feeding them with H_2O_2 did not have any oxidizing effect on either glutathione pool. This is consistent with previous observations in *D. melanogaster* where H_2O_2 production and GSH/GSSG imbalance do not correlate (Albrecht et al., 2011). Unexpectedly, paraquat feeding led to a small reduction of the GSH potential in mitochondria. This herbicide leads to the production of superoxide anions in mitochondria, thus inducing oxidative stress. Our observation could result from a strong antioxidant response in the mitochondria to counteract this increase in ROS. Of note, paraquat-induced oxidative stress was recently shown to be regulated by the endoplasmic reticulum response, rather than cytoplasmic/mitochondrial glutathione (Tarimo et al., 2018). Still these assays were only repeated once with a small number of mosquitoes, and should thus be repeated to draw solid conclusions. Testing different concentrations of these compounds, several timepoints and other chemicals (such as diamide or tert-butyl hydroperoxide) will give us a more precise description of how mosquitoes deal with these challenges.

Another question that we addressed in the present work was the effect of the antiplasmodial response on redox homeostasis. 20 - 24 h after infection with *P. berghei* parasites, we observed the presence of protruding cells in the midgut lumen, most of which presented an oxidized cytoplasmic glutathione pool and co-localized with parasites. Because the antiplasmodial response in *A. gambiae* triggers the overexpression of NOS (Han et al., 2000), we immunostained infected midguts with antibodies against this enzyme to further investigate the response. Interestingly,

most NOS-overexpressing enterocytes were negative for roGFP. Parasite invasion is known to lead to tyrosine nitration (Kumar et al., 2004) in enterocytes and nitrite ($NO_2\cdot$) quenches GFP fluorescence upon nitration of Y66 (Espey et al., 2002). This is consistent with the idea that parasite nitration is mediated by NO_2^- and not peroxynitrite ($ONOO^-$). In this context, nitration is possible thanks to a two-step process: first, enterocytes overexpress NOS to produce NO, and then an oxidase and a peroxidase likely NOX5 and HPX2 (de Almeida Oliveira et al., 2012) catalyze the conversion of NO to NO_2^- (Kumar et al., 2004). Again, this is consistent with the fact that we found various levels of roGFP fluorescence in NOS-overexpressing enterocytes. Interestingly, we detected few of these cells in the midgut lumen; instead, most of them were in the epithelium plane and, for the most part, they retained a geometrical shape. This is suggestive of two things: (i) that the observed cells were at an early stage of the antiplasmodial response and (ii) that NOS signal is lost as the extruding process goes on. Indeed, this phenomenon would render these cells undetectable to our assay if they also lacked the roGFP signal. This is coherent with the fact that we did find NOS-negative extruded cells that conserved their roGFP fluorescence. Extruded cells displayed both reduced and oxidized glutathione redox pools and signs of apoptosis, but we did not find any clear correlation between these two or the time elapsed since invasion. Apoptosis can be initiated by oxidative stress through imbalance of the glutathione buffer (Hall, 1999); interestingly, in human pheocromocytoma cells, hydroperoxide-induced apoptosis leads to a rapid increase in GSSG levels followed by a recuperation of the redox potential (Pias and Tak Yee, 2002). We can thus hypothesize that the oxidizing E_{GSH} observed in some cells might be transient. Nevertheless, in our assays we studied a narrow timeframe and we did not investigate other effectors such as NOX5/HPX2. Further studies are necessary to better elucidate the exact mechanisms, localization and timeframe of the observed processes. For instance, using the H_2O_2-biosensor Orp1-roGFP2 probe might help us understand the nature of this process from the point of view of the oxidants.

Finally, we also investigated the E_{roGFP2} in the malpighian tubules of *A. aegypti* mosquitoes. Unfortunately, the dynamic range of the probe was smaller than that observed in enterocytes in both *A. aegypti* and *A. gambiae*. This could be indicating a higher concentration of glutathione in this tissue. However, we also found that the roGFP signal with the 405-nm laser was distorted by the autofluorescence of the granules present in the cytoplasm of this cell type, thus interfering with the ratio. Because the concentration of these inclusions is not uniform in the tissue, we could not draw any conclusions and we did not investigate them any further. The origin of

these granules is not clear, although some authors have proposed that they are by-products of metabolism (Wessing and Zierold, 1999). Starvation prior to dissection might therefore decrease autofluorescence, however this may also interfere with redox homeostasis. Alternatively, higher expression of roGFP2 would increase the signal-to-noise ratio. Of note, as nuclei of the malpighian cells are devoid of these inclusions, it might be possible to use them to measure GSH/GSSG ratios in this tissue, however, the image analysis in this case would be more laborious.

In conclusion, hGrx1-roGFP2 has proven to be a useful method to follow the dynamics of glutathione oxidation in the midgut of two different mosquito species as well as in salivary glands of *A. gambiae* females. We have shown that both cytoplasmic and mitochondrial glutathione pools are mostly reduced and kept so even when exposed to oxidative challenges. These observations indicate that either mosquitoes have powerful antioxidant systems that maintain the glutathione pool reduced, or that the glutathione pools is not sensitive to / not involved in the mosquito intracellular homeostasis maintenance, at least in the midgut. hGrx1-roGFP2-expressing mosquitoes will help us further investigate oxidative stress in mosquitoes and characterize their antioxidant systems. Additionally, introgressing this transgene into insecticide-resistant strains may also serve to assess some of the molecular mechanisms underlying insecticide resistance and help develop new tools to counteract them.

2

CHAPTER

The role of thioredoxin reductase
in *Anopheles gambiae*

INTRODUCTION

It is generally believed, that the absence of the key antioxidant GR in insects is compensated by the Trx/TrxR system. In *D. melanogaster* and *A. gambiae,* Trxs can efficiently reduce GSSG *in vitro* (Bauer et al., 2003a; Kanzok et al., 2001) and the knockdown of TrxR in the imaginal disks of the former leads to an increase in the GSSG/GSH ratio (Albrecht et al., 2011). The role of *TrxR1* has been investigated in the fruitfly where it is essential for development; however, the role of TrxR in mosquitoes remains uncharacterized.

The genome of *A. gambiae* codes for one single *TrxR* gene on chromosome X (Fig. 2.1). This gene is composed of 4 exons and 3 introns and gives rise to 3 isoforms by alternative splicing. Most of the protein sequence is coded on exon 4, the only one that is common to the three isoforms. The other 3 exons code for the 5' UTR and the first amino acids of each isoform, including a mitochondrial targeting peptide for one of them. We proposed to investigate the role of this gene in the malaria mosquito *A. gambiae* by studying the phenotype of TrxR-deficient mosquitoes.

Producing gene knockouts in mosquitoes has only been recently possible with the development of Transcription Activator-Like Nucleases (TALENs), and more recently, with the discovery and further application of the clustered regularly interspaced palindromic repeats / CRISPR associated 9 (CRISPR/Cas9) system to gene-editing that has entailed a revolution in the field of molecular biology as it allows for an easy manipulation of the genome at any given sequence (Charpentier and Doudna, 2013) (Fig. 2.2). In brief, the Cas9 endonuclease produces a double-strand break in the
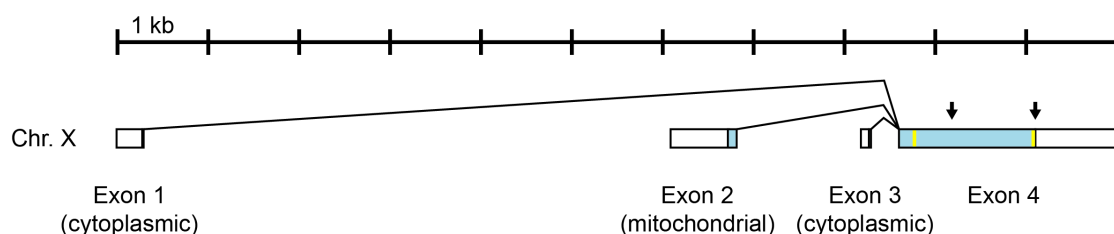
Figure 2.1 *Thioredoxin reductase* **genomic locus in** *Anopheles gambiae.* Thioredoxin reductase is encoded by one single gene on chromosome X in *A. gambiae.* This gene comprises 4 exons and 3 introns and gives rise to three isoforms that have the 4th exon in common. Yellow lines indicate the active sites in the protein product. Arrows indicate the peptides used to rise antibodies against the protein. ORF are shown in blue.

genome at the locus indicated by a guide RNA (gRNA) that must then be repaired by the cell. The damage can be mended by homologous recombination with the sister

chromatid, a system that can be exploited to knock-in any desired sequence into the genome. Alternatively, reparation can be achieved by non-homologous end joining (NHEJ, i.e. directly ligating the two broken ends), a mutagenic pathway that introduces errors like small insertion-deletions (indel); when this mutations are non-synonymous they can lead to functional knockouts (KO) where the gene is present in the genome, but it does not yield any functional protein product (Dong et al., 2018).
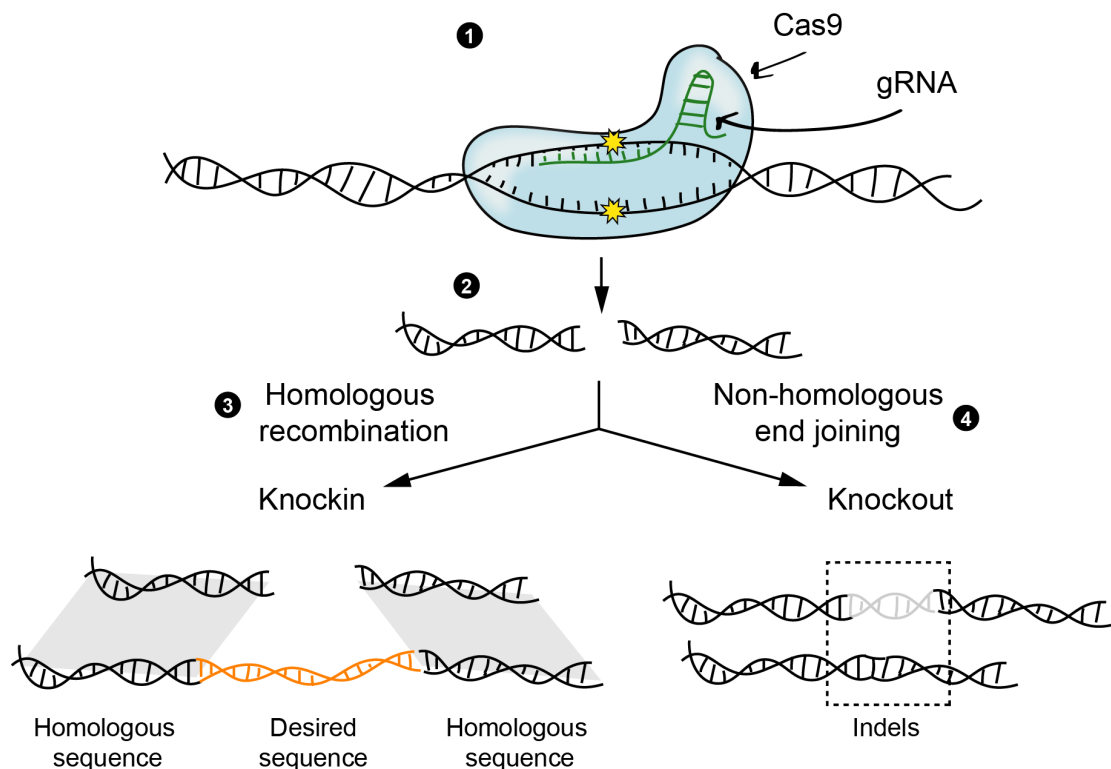
Figure 2.2 CRISPR/Cas9 mutagenesis. (1) The Cas9 endonuclease produces a double-strand break on DNA. The location of the cut is dictated by a guide RNA (gRNA) with complementarity to the target sequence. **(2)** As a result, DNA is broken and must be repaired. To that end, the cell has two options. **(3)** It can repair the break by homologous recombination using its sister chromatid. This pathway is not mutagenic and can be exploited to introduce a given desired sequence in that position. **(4)** Alternatively, the break can be repaired by ligating the two broken ends by non-hoologous end joining. This generally leads to the insertion and/or deletion of nucleotides; if these indels are non-synonymous, a functional knockout is produced.

4. RESULTS

A. Polyclonal antibodies against insect thioredoxin reductase

Most of the commercially available antibodies against TrxR recognize mammalian proteins and none of them have been designed against insect TrxRs. Thus, to be able to study this protein in mosquitoes, we first produced polyclonal antibodies (Fig. 2.3). To that end, we immunized rabbits with 20 amino acid-long peptides and then, purified the serum on an affinity column containing these same peptides. We

Anopheles gambiae female midgut
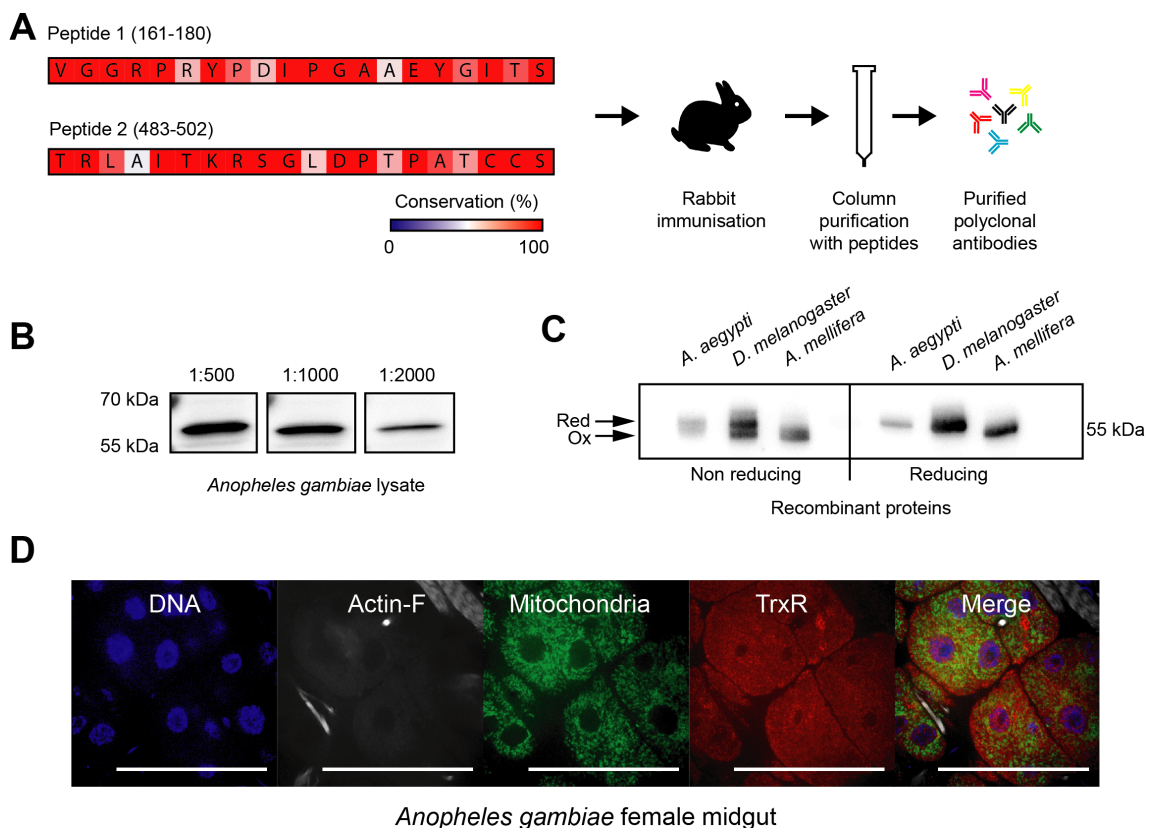
Figure 2.3 Polyclonal antibodies against insect thioredoxin reductase. (A) Two 20 amino acid-long peptides of *A. gambiae* thioredoxin reductase (TrxR) were chosen based on their predicted immunogenicity and conservation in other insect species. Positions with regard to AgTrxR (AGAP00565-RC, Vectorbase) are shown in brackets. The peptides were used to immunize rabbits whose serum was purified in affinity columns containing the same peptides. **(B)** The antibodies recognize a ~60 kDa protein in *A. gambiae* extracts when tested in 1:500, 1:1000 and 1:2000 dilutions. **(C)** The antibodies also recognize recombinant TrxRs from *A. aegypti* mosquitoes, *D. melanogaster* flies and the honeybee *A. mellifera* that were produced in bacteria. Under non-reducing conditions, a second smaller band (~55 kDa) corresponding to the oxidized form, can be observed. **(C)** The antibodies recognize a ubiquitous protein in enterocytes when used in immunostaining assays. DNA (DAPI), Actin-F (Phalloidin), mitochondria (mito-roGFP2-hGrx1).

selected these peptides on two criteria: (i) to increase our chance that the chosen sequences would be immunogenic, we used online prediction tools to generate a list of candidates, and (ii) to ensure that the antibodies would cross-react with other insect species, we aligned several insect TrxR sequences and looked for the degree of conservation of the generated peptide list. As a result, we chose two highly conserved sequences, VGGRPRYPDIPGAAEYGITS and TRLAITKRSGLDPTPATCCS (Fig. 2.3 A). The final purified product recognized a protein of approximately 60 kDa, consistent with the size of AgTrxR (Bauer et al., 2003a), in standard western blot conditions (Fig. 2.3 B). As expected, these polyclonal antibodies also recognized other insect TrxRs (Fig 2.3 C). Interestingly, under non-reducing conditions, a second band of slightly less than 55 kDa was also detected, most likely corresponding to the oxidized form of the protein (Fig. 2.3 C). Moreover, these antibodies can also be used in immunofluorescence assays. With the exception of the nucleolus, TrxR can be detected quite uniformly in midgut cells (Fig. 2.3 D).

B. Silencing of thioredoxin reductase by RNA interference

To assess the role of TrxR in adult *Anopheles gambiae* mosquitoes, we first silenced TrxR by RNA interference (RNAi). To that end, we synthesized dsRNA against a 594 bp-long sequence of *TrxR* exon 4 and we injected females with 200 ng of the final product. 72 h after the injection, TrxR protein levels were only partially decreased in adult females (50 ± 6.2 % here, Fig. 2.4 B). We reasoned that this reduction could still be sufficient to detect a phenotype, especially if exposed to an oxidative stress. The lifespan of dsTrxR-injected mosquitoes was not affected compared to control dsLacZ-injected mosquitoes (Fig. 2.4 C). To push the antioxidant response, we let both groups feed on blood 3 days after injection and followed their survival for 30 days. The median survival of dsTrxR-injected mosquitoes was the same as controls (20 days) but their survival was significantly lower after 21 days (log-rank test), suggesting that the loss of TrxR might be detrimental in old mosquitoes (Fig. 2.4 D). Finally, we did not detect any impact of TrxR partial silencing on the redox potential of glutathione using roGFP2 mosquitoes (Fig. 2.4 E, and see Chapter I) and on parasite development in the mosquito midgut after infection with *P. berghei* (Fig. 2.4 F). Because TrxR silencing was only partial in dsTrxR-injected mosquitoes, we could not exclude that the absence of clear phenotype was due to the remaining protein.
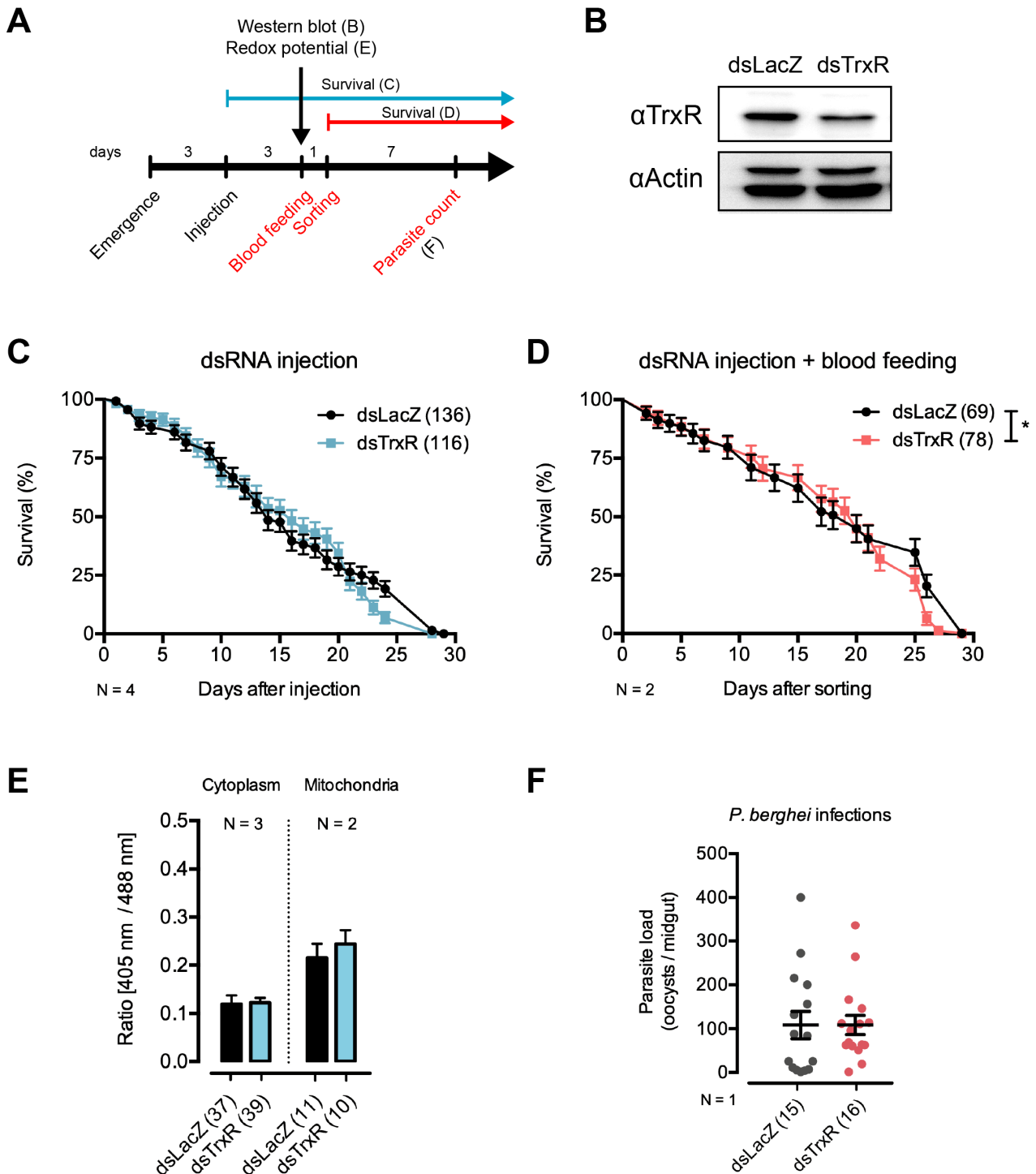
Figure 2.4. Limited silencing of TrxR does not affect mosquito phenotype. (A) Scheme summarizing experimental procedures. Letters shown in brackets refer to the panel where results are displayed. **(B)** 3 days after injection with dsRNA targeting TrxR, whole mosquito extracts show 50 % reduction in TrxR protein levels. **(C)** This partial TrxR silencing does not have an impact on the survival of the mosquitoes. **(D)** Upon blood meal, dsTrxR-injected mosquitoes die faster from day 20 when compared to control dsLacZ-injected mosquitoes. **(E)** Partial silencing of TrxR has no impact on the oxidation level of the cytoplasmic or mitochondrial glutathione pools and **(F)** on the parasite load one week after infection. Horizontal and error bars represent mean and SEM, respectively. Each dot indicates the number of oocysts in one migut. Survival curves were compared by the Log-rank method; pair-wise comparisons, by Mann-whitney. *p < 0.05. Only significant comparisons are shown.

We tried to improve TrxR silencing by increasing the amount of dsRNA delivered and targeting other sequences within the gene, however the outcome was consistently the same, indicating either that some tissues are refractory to gene silencing by dsRNA injection, or that the TrxR protein has a slow turn over. We therefore aimed to study the phenotype of TrxR knock out mosquitoes.

C. Knockout of the thioredoxin reductase gene in Anopheles gambiae

(I) Role of thioredoxin reductase during development

To knock out the TrxR gene, we made use of the CRISPR/Cas9 system. In our laboratory, CRISPR/Cas9 mutagenesis in *A. gambiae* mosquitoes is achieved by crossing a mosquito line expressing Cas9 protein to a line expressing gRNAs against the target gene. Several transgenic mosquito lines expressing the Cas9 protein under the control of the Vasa promoter, known to drive expression in the germline (Papathanos et al., 2009) and to mediate CRISPR/Cas9 mutagenesis when provided with guide RNAs (Dong et al., 2018), have been generated in our laboratory.

To increase our chances to obtain *TrxR* knockouts, we targeted the *TrxR* gene at 4 different points in exon 4 (**Fig. 2.5 A**). We reasoned that the cutting of the gene at different levels could result in the loss of a significant portion of the piece of DNA between two double stranded breaks was removed, or at least, that it would increase the chances that non-synonymous mutations would occur. We designed the 4 gRNAs (**Fig. 2.5 B**) with the help of online tools and we cloned each one under the control of the U6 small nuclear RNA polymerase III promoter (AGAP013557). The construct was integrated at an attP docking site on chromosome 3R using phage Φ31 integrase recombination (**Fig. 2.5 A**). Because the Vasa protein is maternally transmitted (Papathanos et al., 2009), the direction of the crosses between the Cas9 and guide lines mattered (**Fig. 2.5 C**). Indeed, when using Vasa::Cas9 males for the cross, mutations were expected to only occur in the germline; however, Vasa::Cas9 females may lead to somatic mutations during embryogenesis. Thus, should our hypothesis that TrxR is essential for development in mosquitoes be true, the outcome of each of these crosses would be different. Whereas the F1 progeny

coming from the cross between U6::gRNA females and Vasa::Cas9 males should be viable, the progeny of the reciprocal cross would not develop. We performed the crosses in both directions three times with very reproducible results. As expected, the crosses using Vasa::Cas9 females laid regular amounts of eggs, but very few larvae hatched from them. We found a total of 15 larvae, none of which survived for more than three days. However, the reciprocal crosses (**Fig. 2.6 A**) did not lead to the expected outcome. Instead, we observed a developmental delay of about 3 days that resulted in no functional adults. Most individuals died as pupae, during hatching or as adults with the legs trapped in the pupal case (**Fig. 2.6 C**, compare Cas9 and gRNA). Western blot analyses revealed a significant decrease in TrxR protein levels in whole pupae lysates (**Fig. 2.6 A**), indicating that, in contrast to our expectation, somatic mutations had occurred during development. We analyzed different tissues in the few surviving F1 adults of this cross, and showed that TrxR knockout had not occurred in all tissues with the same efficiency (**Fig. 2.6 A**). For instance, the
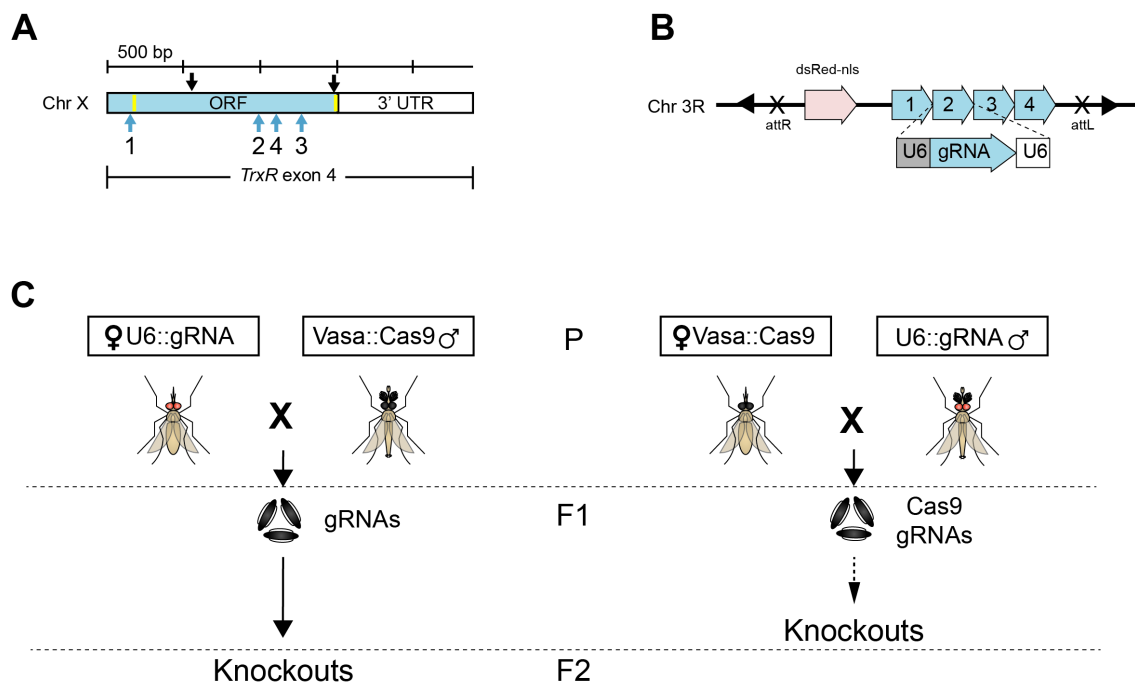
Figure 2.5 Developmental knockout strategy. (A) Four guide RNAs (gRNA; blue, bottom arrows) targeting the exon 4 of the thioredoxin reductase gene (*Trxr*) in *A. gambiae*. Yellow lines indicate TrxR redox active sites. Black, top arrows indicate the peptide sequences recognized by the antibodies. **(B)** gRNAs were cloned under the control of the U6 promoter and integrated into a docking site on chromosome 3R. Triangles indicate the leftovers from the transposon used to integrate an attP site in the genome and attR/attL are the scars left by the recombination event at this site. dsRed-nls is the transgenesis marker. **(C)** gRNAs are expressed ubiquitously (U6 promoter) whereas Cas9 is only expressed in the germline (vasa promoter); additionally, Cas9 is deposited in the eggs of Vasa::Cas9 female mosquitoes. Crossing gRNA females and Cas9 males is expected to lead to a F1 generation where gRNAs and Cas9 are only expressed together in the germline and thus only this cell line will carry mutations in *TrxR*. Knockouts from these mutation events are recovered in the F2 generation. Alternatively, crossing Cas9 females and guide males leads to a F1 generation where both gRNAs and Cas9 are present in the eggs, thus allowing for mutations during embryonic development of F1 mosquitoes. Homozygous U6::gRNAs are detectable by the red fluorescent signal in their eyes and ventral nervous chain.

malpighian tubules were not affected. These results are consistent with a leaky expression of the Vasa promoter in somatic tissues during development as reported by other groups (Champer et al., 2017). Furthermore, the observed lethal phenotype confirms that TrxR is essential during *A. gambiae* development. Interestingly, sexing pupae and adults revealed a strong sex bias in favor of females (around 80 %). To assess the origin of this disparity, we crossed our U6::gRNA females with males carrying the Vasa::Cas9 transgene and a fluorescent marker at the Y chromosome. This allowed us to count the proportion of both sexes during the whole developmental series. Our data show that the sex bias appears in the course of larval development, and increases at each larval molting (**Fig. 2.6 B**). In newly hatched larvae we found 129 males and 125 females, whereas after the first molt the proportion of females was 75%. To make sure that this phenotype was due to the reduction in TrxR levels and not off-target effects on other genes, we repeated the crosses with a line expressing an enhanced version of Cas9 (eSpCas9) that is known to be more specific (Slaymaker et al., 2016). The outcome of the cross of eSpCas9 females with gRNA males was the same as the one observed for Cas9, however the cross between U6::gRNA females and eSpCas9 males gave a progeny that did not show any developmental delay and where most individuals reached the adult stage, with some being functional (i.e. ability to fly). We repeated the cross in parallel with the Cas9 one. This experiment was performed once, allowing mosquitoes to lay eggs twice and analyzing the results of both progenies together (**Fig. 2.6 C − G**). The cross of gRNA females with Cas9 males showed the same developmental delay as before, whereas the progeny from the cross with eSpCas9 males developed at the same time as the controls. Regarding the lethal phenotype, the cross with Cas9 gave rise to a single functional adult that could fly while that with eSpCas9 led to 17 % of functional adults (**Fig 2.6 C, E**). Again, 90 % of the adults coming from the Cas9 cross were females, whereas the eSpCas9 progeny showed a 50:50 ratio; however, a 100 % of the functional adults were females in both crosses (**Fig. 2.6 E**). Finally, most of the eSpCas9 individuals reached adulthood and hatched from the pupae, whereas the Cas9 progeny mostly died as pupae or during emergence (**Fig. 2.6 C**). Independently of the cross, the adult mosquitoes that could not leave the breeding water did not die immediately, but lived for a few days floating on the water, suggesting they were dying of starvation rather than from mutations in TrxR. To check if they would survive out of the water, we carefully detached them from pupal cases and placed them into cages containing sugar solutions. However, these mosquitoes never stood up, indicating troubles with their movements. Regarding the functional adult females collected from the eSpCas9 cross, some of
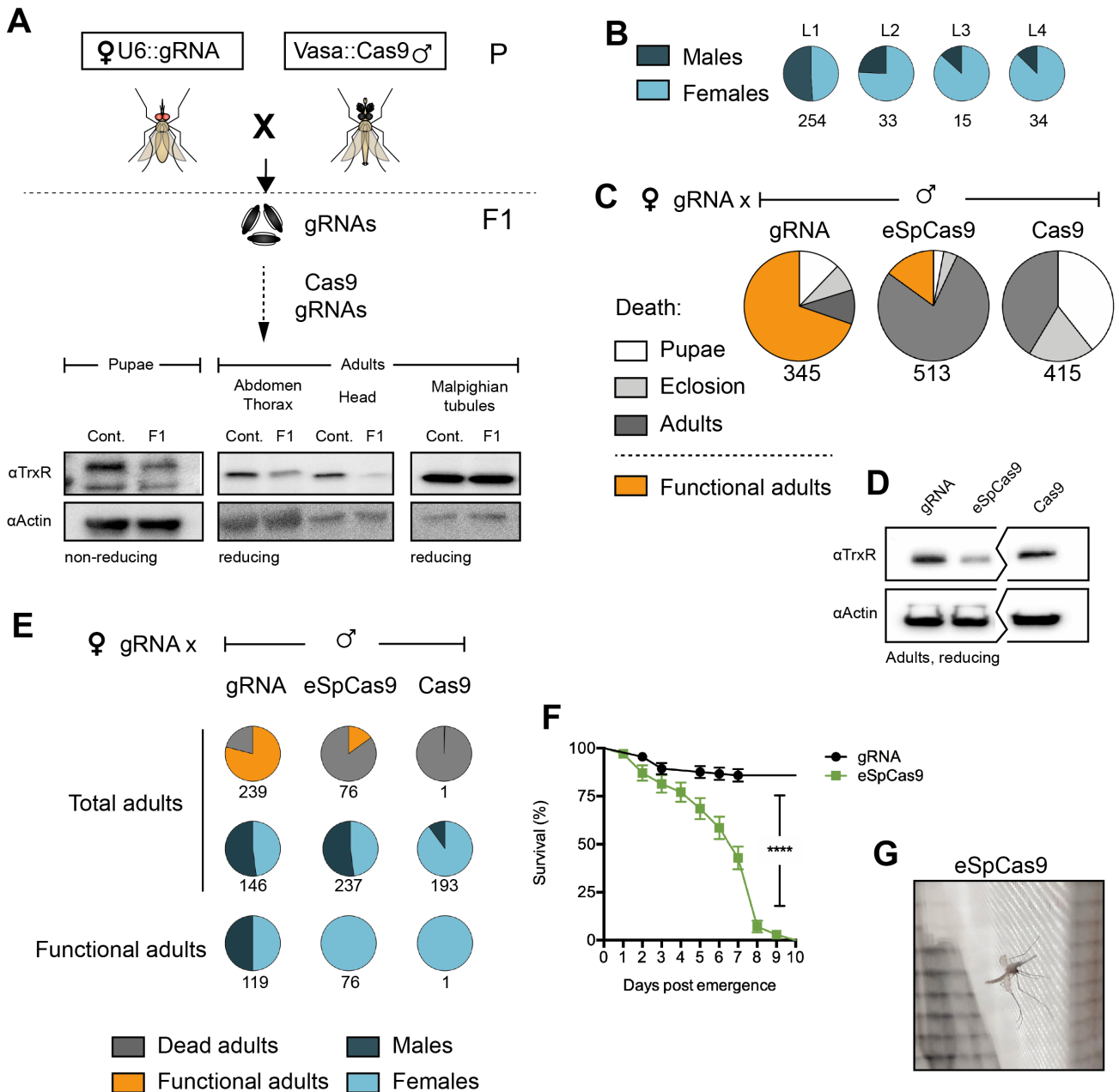
Figure 2.6 Thioredoxin reductase is essential for development. (A) When gRNA females are crossed to Cas9 males, the F1 progeny shows a developmental delay and dies as larvae, pupae or adults that cannot leave the breeding water. In these mosquitoes, TrxR levels are reduced in the abdomen, throax and the head, but not the malpighian tubules as revealed by western blot analysis. **(B)** Proportion of males (dark) and females (light) at the 4 different larval instars. The total amount of individuals counted is indicated below each pie chart. **(C)** Proportion of adults that can fly (functional adults; orange) in crosses using gRNA females and gRNA, eSpCas9 or Cas9 males. The proportion of dead individuals at different developmental stages is shown in different shades of grey. The total amount of individuals is indicated below each pie chart. **(D)** TrxR levels in whole mosquito extracts from each cross. **(E)** Proportion of functional adults (orange; the total number is indicated below each pie chart) and females (light blue; the total number is indicated below each pie chart) within the total number of adults. Proportion of females (light blue; the total number is indicated below each pie chart) within the total number of functional adults. **(F)** Lifespan of adult females coming from the crosses of U6::gRNA females with the U6::gRNA or Vasa::eSpCas9 males. Survival was assessed every 24 h and curves were compared by the Log-rank test; **** $p < 0.0001$. **(G)** Picture of a deformed F1 adult female with a curved abdomen and open wings from U6::gRNA females crossed with Vasa::eSpCas9 males.

them presented functional adult females collected from the eSpCas9 cross, some of them presented severe morphological deformations such as a curved abdomens and tendency to leave their wings open when resting (**Fig. 2.6 G**), to stay at the bottom of the cage and walk or to fly in circles. Moreover, their lifespan was severely reduced compared to controls from the gRNA cross, all of them dying within 10 days (**Fig. 2.6 F**). We concluded that TrxR is essential for mosquito development and that it is not possible to study the role of TrxR in adult mosquitoes by these means.

(II) Role of thioredoxin reductase in the midgut of adult mosquitoes

To circumvent this issue, we performed a somatic knockout at the adult stage. For this, we needed to express Cas9 and/or the gRNAs under the control of a promoter that was not expressed at the larval and pupal stages. Very few promoters have been characterized in *A. gambiae* (Volohonsky et al., 2015) and our choice was laid on the promoter of the G12 protein (AGAP006187) whose expression is undetectable during development and strongly induced in the midgut of female adults upon a blood meal (Volohonsky et al., 2015) (**Fig. 2.7 A**). Although this would not lead to a complete knockout in all tissues, we reasoned that the midgut would be an interesting tissue to study the role of TrxR as it is responsible for blood digestion and the early antiparasitic response. We therefore cloned eSpCas9 under the control of the G12 promoter and integrated it into the genome of *A. gambiae* at the X1 docking site in chromosome 2L (Volohonsky et al., 2015). As expected, the resulting line expressed Cas9 in the midgut after a blood meal, with a peak of expression at 24 h (**Fig. 2.7 B**). We crossed this line with the U6::gRNA line resulting in a progeny that developed normally; adults were allowed to feed on mice and their midguts analyzed for TrxR expression on a western blot 3 and 7 days after, however no decrease was found (**Fig. 2.7 C**). According to the VectorBase (release VB-2019-08) there are five U6 genes in *A. gambiae*. In *D. melanogaster* different U6 promoters drive CRISPR/Cas9 mutagenesis in somatic tissues with different efficiencies (Port et al., 2014); thus, we concluded that the absence of mutagenesis in our system could be due to the absence of expression of our U6 promoter in midgut cells.

To make sure that both eSpCas9 and gRNAs would be expressed concomitantly in enterocytes, we decided to place gRNAs under the control of the G12 promoter as well. However, this is a polymerase II promoter and thus RNAs expressed from it are exported to the cytoplasm. To avoid it, we used a tRNA-gRNA tandem system that had been successfully applied to other organisms (Dong et al., 2017; Port and Bullock, 2017; Zhang et al., 2019b) (**Fig. 2.8 A**). In brief, gRNAs are flanked by tRNAs and transcribed as a single RNA molecule by RNA Pol II. The endogenous machinery recognizes the tRNA folds and processes the RNA molecules, liberating both tRNAs and gRNAs in the nucleus. To shorten the construct, we decided to express only 3 of the 4 gRNAs that were used in the U6::gRNA line. To select the 3 best gRNAs, we evaluated two parameters for each guide: (i) the predicted efficiency and (ii) putative off targets with the help of an online tool (**Table 2.1**). All the gRNAs
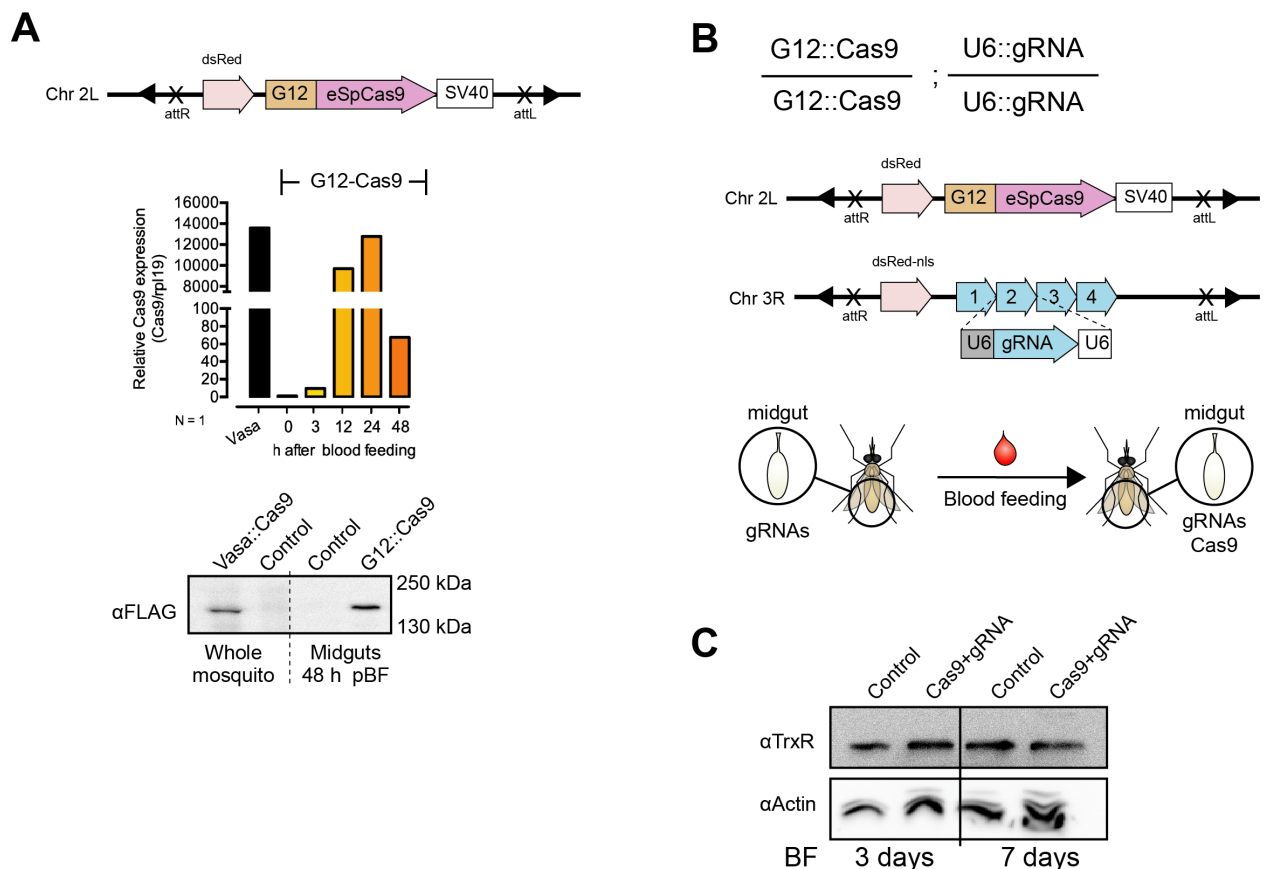
Figure 2.7. The G12 promoter leads to strong expression of Cas9 in the midgut 24 h after blood feeding, but it does generate mutations with gRNAs driven by the U6 promoter. (A) eSpCas9 was cloned under the control of the G12 promoter and inserted into a docking site on chromosome 2L. Triangles indicate the leftovers from the transposon used to integrate an attP site in the genome and attR/attL are the scars left by the recombination event at this site. dsRed-nls is the transgenesis marker. The line expresses *Cas9* after blood feeding, with the peak being at 24 as revealed by qPCR analyses on whole mosquito extracts. At the protein level, Cas9 is also present after blood feeding. **(B)** In G12::Cas9/U6:.gRNA mosquitoes, Cas9 expression is triggered in the midgut by a blood meal while gRNAs are expressed ubiquitously, esulting in TrxR-KO in midgut cells. **(C)** TrxR protein levels in the midgut of G12::Cas9/U6:.gRNA females 3 and 7 days after blood feeding.

had putative off-targets with at least two miss-matches, thus excluded that with the lowest predicted efficiency (i.e. gRNA number 4) and we cloned the other three in order as before, flanked by tRNA$_{Gly}$, under the control of the G12 promoter. The resulting construct was integrated in the genome in the same locus as the G12::Cas9 transgene (**Fig. 2.8 A**).

We then crossed the G12::eSpCas9 and the G12::gRNA lines and obtained a progeny that developed normally. We evaluated the TrxR protein levels in the midgut, malpighian tubules and the rest of the body of adult females before a blood meal and 3 days after (**Fig. 2.8 B**). As expected, TrxR levels were strongly and specifically reduced in the midgut of adult mosquitoes expressing both Cas9 and gRNAs, however this was true not only true in fed females, but also in non-fed ones. Thus, we concluded that there is a basal expression of G12 in the enterocytes of adult females that is sufficient to drive CRISPR/Cas9 mutagenesis before a blood meal. At the cellular level, most cells showed a severe reduction of TrxR, although some of them were still positive (**Fig. 2.8 C**). Of note, remaining TrxR in the midgut of Cas9+gRNA mosquitoes could either be the full-length functional protein or products of mutations leading to partial (in the case of premature stop codons) or unfunctional TrxR.

To assess whether the loss of TrxR in the midgut had any fitness cost, we monitored the lifespan of the midgut TrxR-knockout (TrxR-KO$_{MG}$) mosquitoes under different conditions (**Fig. 2.8 D – H**). To minimize genetic and environmental variations

Table 2.1. Design and evaluation of guide RNAs against *TrxR* (AGAP000565)

Guide	Sequence	Location	Rank.	Off-targets (miss matches)				Efficiency
				0	1	2	3	
1	GGCACCAAGTGGGGCCTGGG	X:10030632	67	0	0	0	1	61.93
2	GAACGTGCCGCACATCTACG	X:10031471	193	0	0	1	2	77.34
3	GCGCTACTGCTACCTGAAGG	X:10031753	171	0	0	2	0	71.83
4	GCGCATGGACTACGCGGACG	X:10031588	150	0	0	0	2	58.12

Designed using CHOPCHOP v2 (http://chopchop.cbu.uib.no)

between groups, most of the experiments were conducted on siblings that were bred in the same water. In brief, both parental strains mated randomly, and the progeny was bred as one; at the adult stage, the two control genotypes (Cas9 with red eyes, and gRNAs with turquoise eyes) and the knockouts (TrxR-KO$_{MG}$ with red and turquoise eyes and carrying both Cas9 and gRNAs) were separated and phenotyped. First, we showed that TrxR-KO$_{MG}$ have the same lifespan as controls (**Fig. 2.8 D**). Unexpectedly, when we let them feed on mouse blood, we observed a significant increase in the lifespan of blood-fed TrxR-KO$_{MG}$ mosquitoes as compared to blood-fed controls, as well as a non-significant increase when compared to the non-blood-fed TrxR-KO$_{MG}$ (**Fig. 2.8E**). These unexpected results suggested that (i) the changes that occur in response to blood meals and/or (ii) the nutritional contribution of blood were beneficial to TrxR-KO$_{MG}$ mosquitoes, and/or (iii) TrxR-KO$_{MG}$ mosquitoes are more resistant to the oxidative stress generated during blood digestion. To investigate whether TrxR-KO$_{MG}$ mosquitoes were more resistant to other oxidative stresses, we challenged mosquitoes with artificial compounds that do not provide nutrients. For this, we supplemented their sugar-feeding solution with H_2O_2 or paraquat and monitored their survival. When feeding H_2O_2, both TrxR-KO$_{MG}$ and control mosquitoes underwent a severe reduction of their lifespan as compared to their sugar-fed siblings; however, TrxR-KO$_{MG}$ and control mosquitoes behaved similarly (**Fig. 2.8 F**). In contrast, TrxR-KO$_{MG}$ mosquitoes had a better fitness than control mosquitoes upon feeding on 1 mM paraquat (**Fig. 2.8 G**). Taken altogether, these results suggest that the loss of TrxR in the midgut is beneficial for mosquito survival upon several oxidative challenges, especially blood feeding, either directly or indirectly, by triggering compensation mechanisms that are beneficial to mosquitoes when they face these challenges.

We next explored whether the loss of TrxR in the midgut would also impact the vectorial capacity of TrxR-KO$_{MG}$ mosquitoes. To that end, TrxR-KO$_{MG}$ and control mosquitoes expressing Cas9 or the gRNAs only were infected with *P. berghei* parasites and the number of parasites per midgut was counted at 7 days post infection (**Fig. 2.8 H**). When the experiment was performed on mosquitoes bred separately, Cas9 mosquitoes were more infected that gRNAs and TrxR-KO$_{MG}$ mosquitoes. Still, the three groups had a similar phenotype when larvae were bred in the same water, suggesting that the previous results were an artefact originating from the different environments larvae encountered during their development, leading, for instance, to different midgut microbiota (Boissière et al., 2012; Linenberg et al., 2016). These results indicate that the absence of TrxR in the gut of mosquitoes
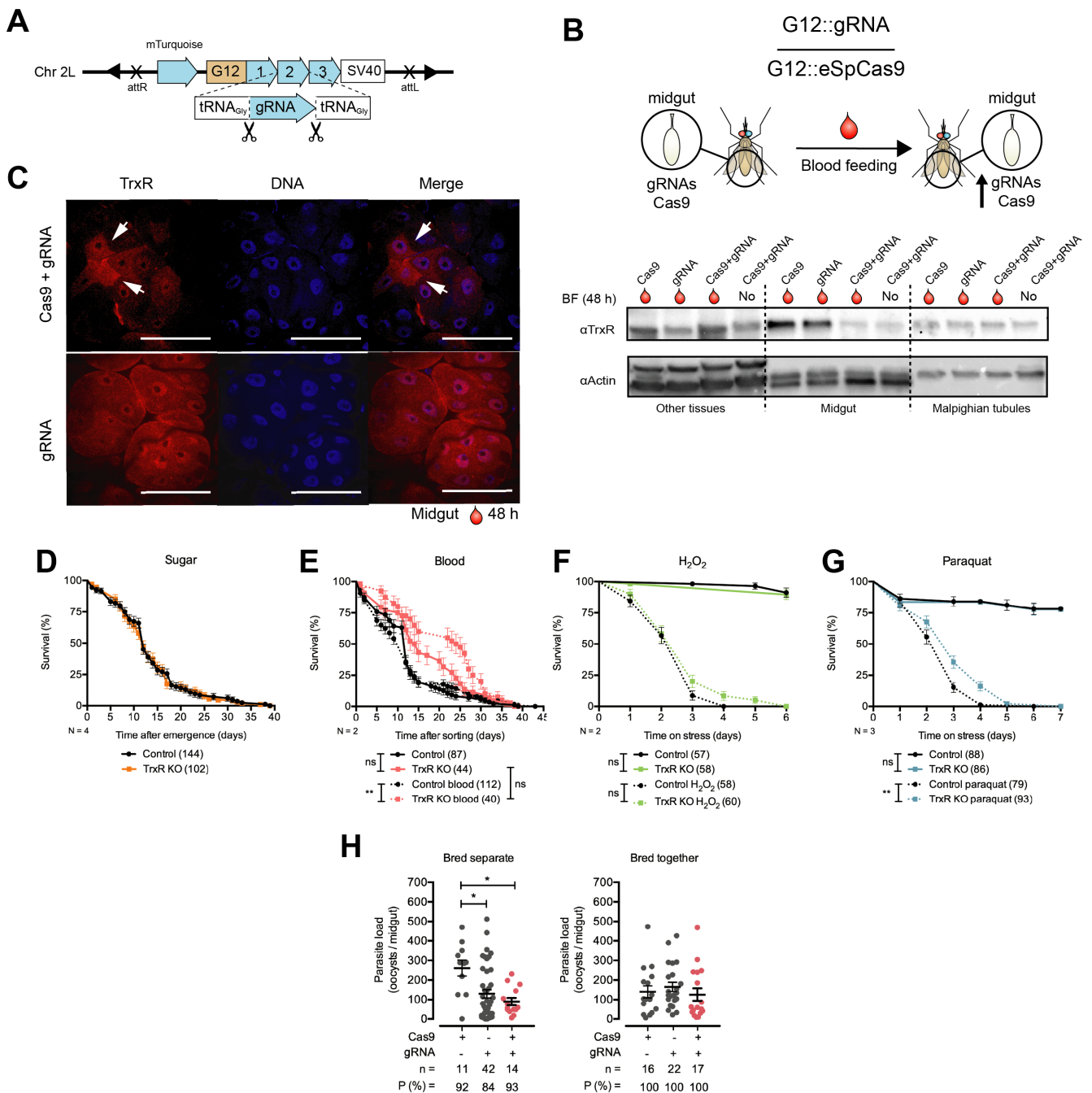
Figure 2.8. Thioredoxin reductase is not essential in the midgut of *A. gambiae* mosquitoes and its absence increases the tolerance to oxidative stress. (A) 3 guide RNAs (gRNAs) against exon 4 of the *thioredoxin reductase (TrxR)* gene were cloned under the control of the G12 promoter flaked by tRNA$_{Gly}$ sequences, thus leading to the processing and release of the gRNAs in the nucleus. The transgene was inserted into the X1 docking site on chromosome 2L, and the resulting line crossed to a line expressing eSpCas9 under the same promoter. Triangles indicate the leftovers from the transposon used to integrate an attP site in the genome and attR/attL are the scars left by the recombination event at this site. mTurquoise is the transgenesis marker. **(B)** TrxR protein levels in the midgut, malpighian tubules and rest of the body of control (Cas9, red eyes; gRNA, blue eyes) and knockout (Cas9+gRNA, blue and red eyes) mosquitoes. All samples were collected 48 h after a blood meal, except for the knockouts where "no" is indicated. **(C)** Immunostainings showing the level of TrxR in control (gRNA) and knockout (Cas9+gRNA) midguts 48 h after blood feeding. TrxR was detected with polyclonal antibodies and DNA was stained with DAPI. Arrows indicate the presence of TrxR positive cells in knockout mosquitoes. The lifespan of control (Cas9 and gRNA) and knockout (Cas9+gRNA) mosquitoes was monitored every 24 h **(D)** without challenge, **(E)** after blood feeding, **(F)** feeding on 1 % hydrogen peroxide (H_2O_2) and **(G)** feeding on 1 mM paraquat. Total number of mosquitoes is shown in brackets. Survival curves were compared by the Log-rank test; group comparisons, by Kruskal-Wallis followed by Dunn post hoc. ** $p <$ 0.01; ns = non significant. Comparisons not shown were non significant. **(H)** Number of oocysts per midgut 7 days after feeding of a *P. beghei* infected mouse. Horizontal and error bars represent the mean + SEM, respectively. Dots represent the number of parasites in single midguts. Group comparisons were performed using Kruskal-Wallis followed by Dunn post hoc. * $p <$ 0.05; only significant comparisons are shown. n = total number of mosquitoes. N = number of independent repeats. P = prevalence

74

keeping environmental conditions as close as possible to be able to compare mosquito groups, even in the relatively well-controlled laboratory environment.

Finally, to test our hypothesis that TrxR control the GSH buffer in mosquitoes, we decided to cross our midgut KOs with a roGFP-expressing line (see Chapter I). However, the three transgenes (Cas9, gRNAs and hGrx1-roGFP2) were inserted into the same X1 genomic locus. To circumvent this issue, we inserted the hGrx1-roGFP2 construct into the E locus (Pondeville et al., 2014) on chromosome 3R (the same one used to integrate the U6::gRNAs transgene). As expected, the resulting line expressed roGFP2 in the nucleus and cytoplasm of enterocytes, however, the level of fluorescence was lower than when the construct was inserted in the X1 locus, and not all the cells were positive (**Fig. 2.9 A**). Differences in roGFP2 expression from these two loci indicate a clear position effect and that the X1 locus is more accessible than the E locus in enterocytes. Next we crossed the (act5::hGrx1-roGFP2)$_E$ line with the (G12::Cas9)$_{X1}$ and the (G12::gRNA)$_{X1}$ lines separately, we homozygotized them, and we crossed the two resulting lines to obtain roGFP-positive mosquitoes lacking TrxR in the midgut (G12::gRNA/G12::eSpCas9; Act5:.hGrx1-roGFP2/ Act5:.hGrx1-roGFP2). We then measured the GSH/GSSG ratio in the midgut of 3 and 7 day-old mosquitoes that had not been fed on mice (different batches), and of 9 day-old mosquitoes, 48 h after blood feeding. Unfortunately, due to technical issues, the three genotypes could not be bred together during larval development. The results showed a significant oxidation in 7 day-old TrxR-KO$_{MG}$ mosquitoes that had not been fed on blood and the opposite effect in 9 day-old 48 h after blood feeding, with a significant decrease in their GSH oxidation levels (**Fig 2.9 B**). These experiments were only conducted once and with mosquitoes bred separately, they should thus be repeated in better conditions, but our preliminary data suggest that TrxR is not essential for the control of the GSH pool oxidation level. Altogether, the characterization of the TrxR-KO$_{MG}$ mosquitoes suggests that TrxR is not essential in the mosquito midgut and that its absence even provides a fitness advantage upon certain challenges, in particular blood feeding. In the same line, TrxR-KO$_{MG}$ did not lead to a major increase in the oxidation level of the glutathione pool, opening several questions: (i) Is the GSH pool maintained reduced by Trx or by other means? (ii) How do mosquitoes control their intracellular redox homeostasis in the absence of both GR and TrxR in enterocytes? (iii) Are there compensatory mechanisms that are triggered in the absence of TrxR in the midgut of TrxR-KO$_{MG}$ mosquitoes?
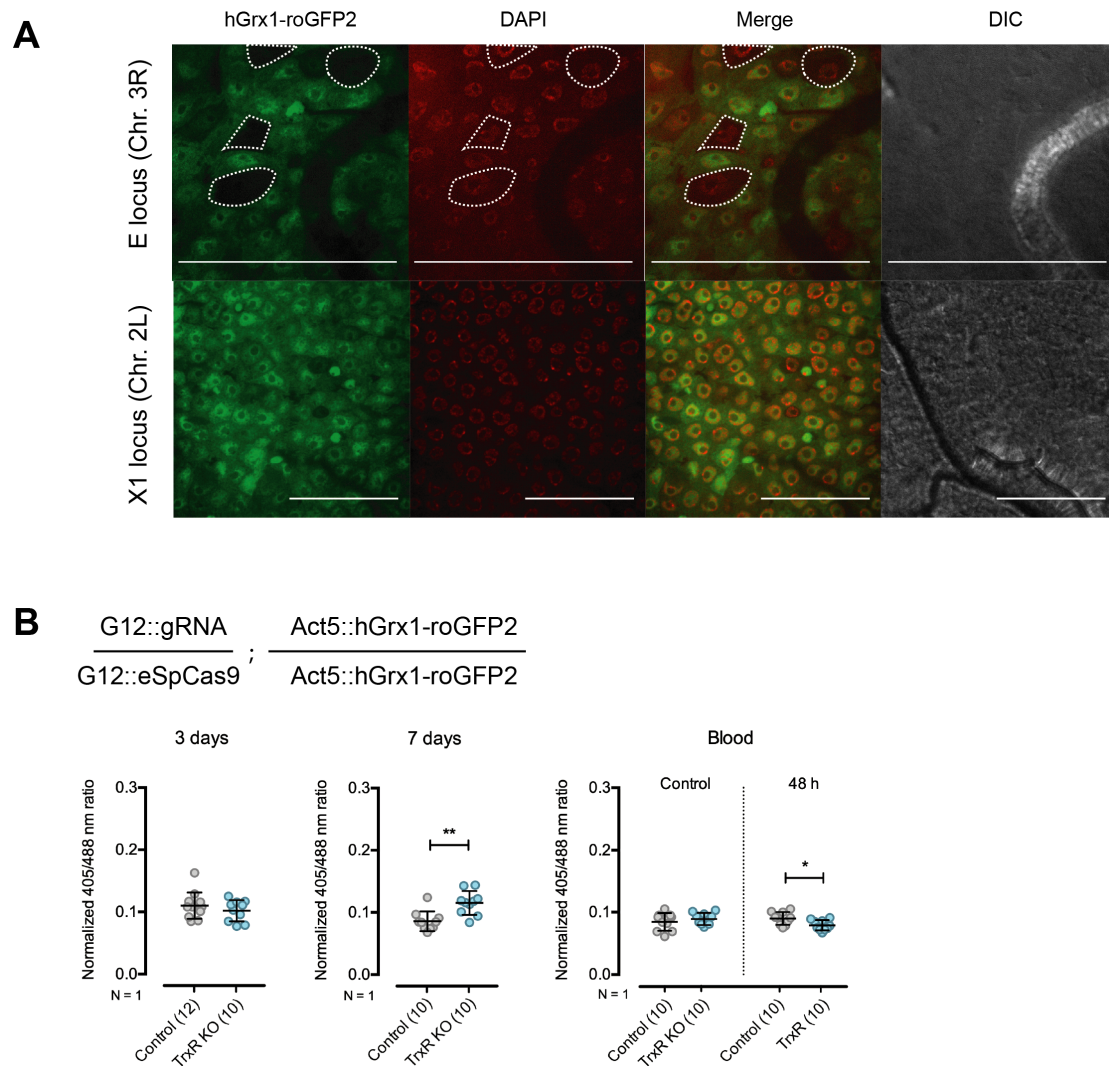
Figure 2.9 Impact of the loss of thioredoxin reductase (TrxR) on the oxidation of the cytoplasmic pool of glutathione in enterocytes. **(A)** roGFP2 fluorescence in enterocytes of transgenic mosquitoes expressing hGrx1-roGFP2 under the control of the *Drosophila* actin 5C promoter inserted in two different loci. Note the overall lower expression and the presence of roGFP2 negative cells when the construct was inserted in the E locus as compared to X1 locus. White dotted lines indicate negative cells. Scale bar = 100 µm. **(B)** The ratio between reduced (GSH) and oxidized (GSSG) glutathione was measured in the midgut of TrxR knockout mosquitoes (TrxR-KO) at different ages and 48 h after blood feeding. Pairwise comparisons performed using Mann-Whitney; * $p < 0.05$; **$p < 0.001$. Non-significant comparisons not indicated.

D. Transcriptome of thioredoxin reductase knockout midguts

To look for these potential substitutes for TrxR in the enterocytes of TrxR-KO$_{MG}$ mosquitoes, we compared the transcriptome of TrxR-KO$_{MG}$ midguts to that of control mosquitoes expressing Cas9 or gRNAs only. We reasoned that, if another protein or group of proteins was compensating for the loss of TrxR, they could be

overexpressed in TrxR-KO$_{MG}$ mosquitoes. Because the phenotype with and without blood feeding was different, we compared the transcriptomes in three different conditions: before blood feeding, 3 days after blood feeding and 1 week after blood feeding (**Fig 2.10 A**). To this end, Cas9 and gRNA mosquitoes were allowed to mate randomly and the progeny was bred together until day five after emergence. On this day, individual mosquitoes were assigned to each population according to the fluorescence of the eyes and we collected the non-blood fed samples (nBF). The rest of mosquitoes were allowed to feed on the same mice and we collected the samples 3 and 7 days after (dpBF). Unfortunately, the Cas9 population was smaller so the last time point could not be collected for this group. In parallel, we confirmed the absence of TrxR in TrxR-KO$_{MG}$ midguts for nBF and 3 dpBF samples by western blot (**Fig. 2.10 B**). We treated midguts as described in Materials and Methods and sequenced the resulting libraries on an Illumina Hiseq 4000.

Sequencing reads were quality filtered and aligned to the *A. gambiae* geneset and compared pairwise between KOs and each parental strain for each time point. We considered a twofold ratio (log2 fold change > 1) and more than 50 transcripts per million (TPM) as a highly expressed, up-regulated threshold (**Fig. 2.10 C**). In general, few transcripts were up-regulated at each time point. Interestingly, the number of up-regulated transcripts in TrxR-KO$_{MG}$ midguts increased with time, doubling between the nBF and 3dpBF, and between the 3dpBF and 7dpBF. Because samples were collected once only, we could not estimate the statistical significance of the up-regulated transcripts. Instead, we reasoned that, if there was a mechanism compensating for the loss of TrxR, the genes involved in this mechanism should be up regulated in several comparisons, thus we compared all time points and genotypes to each other, i.e. # comparisons. A total of 85 transcripts were up regulated in KO mosquitoes, but none of them in all tested conditions. 33 % of the transcripts were up regulated in at least 2 conditions, but 71 % of them were genotype-dependent (i.e. not similar in the comparison of TrxR-KO$_{MG}$ midguts with Cas9 and gRNA ones). Out of the 8 remaining transcripts, 3 were only up regulated after blood feeding. Aga-mir-281 (AGAP005579) is a midgut-specific miRNA (Feng et al., 2018; Winter et al., 2007) with pro-viral functions in *A. albopictus* (Zhou et al., 2014) and the pigment dispersing hormone (AGAP005776) is a neuropeptide expressed by visceral neurons (Renn et al., 1999; Talsma et al., 2012). Interestingly,
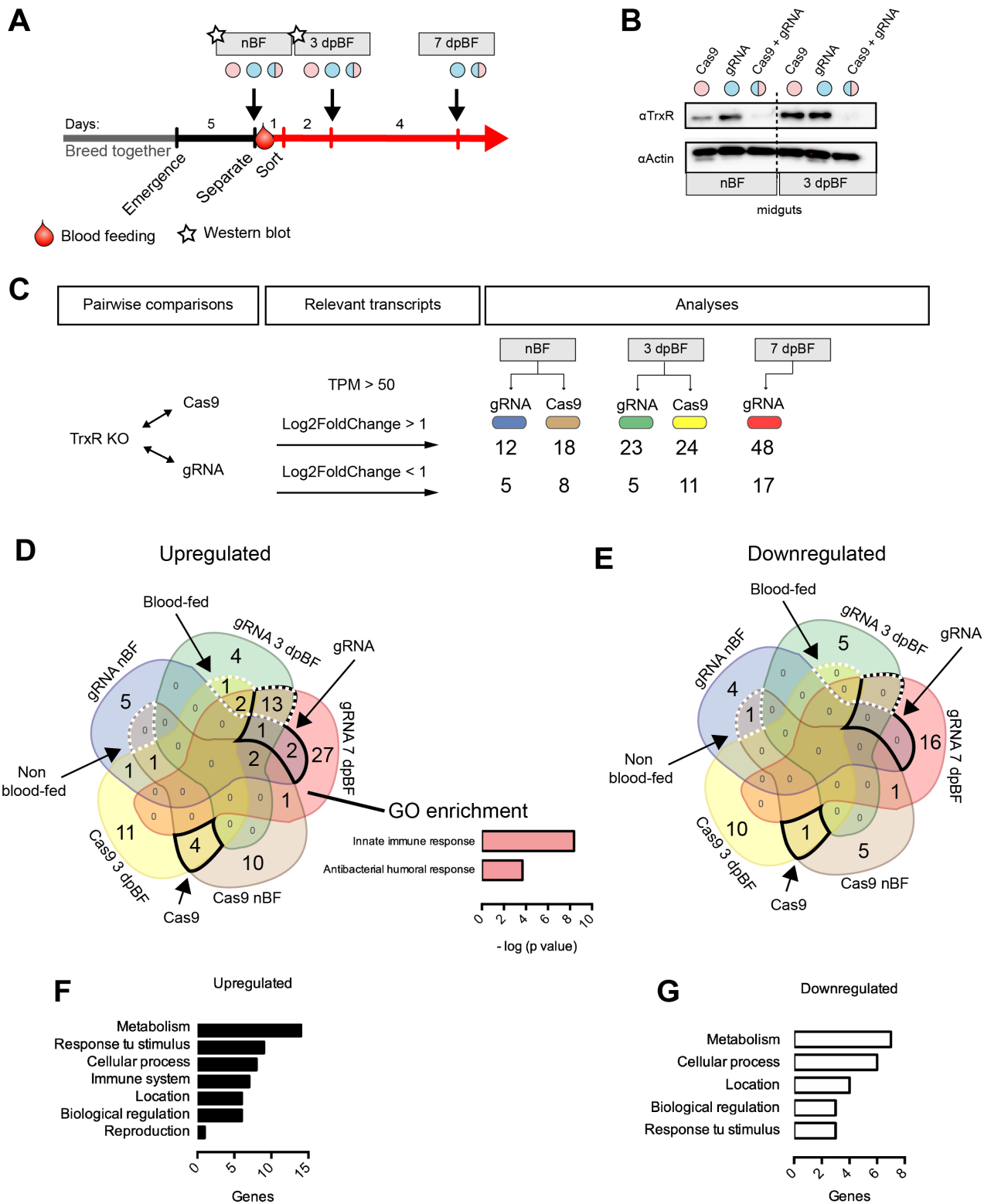
Figure 2.10. Transcriptome of the midgut of mosquitoes lacking thioredoxin reductase (TrxR) in this tissue. **(A)** Scheme of the experimental procedure to collect and analyze samples. The genotype of the mosquitoes is indicated by colored circles, G12::gRNA/G12::gRNA (blue), G12:.eSpCas9/G12::eSpCas9 (red) and G12:.gRNA/G12:.eSpCas9 (blue and red) **(B)** TrxR levels analyzed by western blot in control (Cas9, gRNA) and knockout (Cas9+gRNA) midguts before blood feeding and three days after. **(C)** The transcriptome of TrxR-KO midguts was compared to that of Cas9 and gRNA midguts by time point (before blood feeding, 3 days and 7 days after blood feeding). Transcripts expressed > 50 times per million (TPM) and twice as much in knockouts than controls (log2foldchange < 1) were considered up-regulated; those expressed twice as little (log2foldchange < 1), down-regulated. **(D, E)** Venn diagrams of the up- and down-regulated transcripts, respectively. Comparisons by genotype are indicated with black lines; comparisons before and after blood feeding are indicated with white, dotted lines. Gene ontology (GO) enrichment was performed in all the lists. **(F, G)** Biological processes in which the up- and down-regulated transcripts are involved, respectively.

78

GST d3 (AGAP004382) was up regulated 3 dpBF. Finally, 2 transcripts were up regulated in all conditions, except at 3 dpBF when compared to Cas9. The product of AGAP008648 is not characterized, but it has a farnesoic acid O-methyl transferase domain,that is known to be involved in the biosynthesis of juvenile hormone. This gene is also up-regulated after ivermectin ingestion (Seaman et al., 2015). AGAP012798, a gene non-localised on the genome (UNKN chromosome) and with 40S ribosomal proteins S11 as paralogues and orthologues, is also up-regulated 3 dpBF when compared to Cas9, but it is below the threshold. Gene ontology (GO) analysis only detected enrichment in the 7 dpBF comparison, probably because this category had most genes (**Fig. 2.10 D**). Unexpectedly, the enrichment was for immunity-related genes. Next, we repeated the same pairwise comparisons, but looked for down-regulated genes (log2 fold change < 1); a total of 43 different transcripts were found, 93 % of which were only found in one dataset. (**Fig. 2.10 E**).

Next, we analyzed all up- and down-regulated transcripts (**Table 2.2**). Most of them were related to metabolism, suggesting a remodeling of some metabolic pathways in the absence of TrxR. Moreover, we found that several detoxification enzymes were up-regulated. 4 P450 genes (P450-6M2, P450-6M4, P450-9J3, P450-6P3), two GSTs (GSTd3 and GSTo) and the ABC transporter C11 were up-regulated in at least one condition. On the contrary, P450-6P3 and the ABC transporter C9 were down-regulated at day 3 and day 7 pBF, respectively, when compared to gRNAs. With regard to other participants of the GSH system, apart from the two aforementioned GSTs, cystinosin (AGAP004115), a lysosomal transporter protein that exports cystine (i.e. the oxidized dimer of Cys) (Sumayao et al., 2018), was up-regulated in TrxR-KO$_{MG}$ before blood feeding when compared to gRNA; on the contrary, GGT (AGAP006915) was down-regulated at day 7 pBF. With regard to other effectors of the Trx system, MRS and Prx4 were down-regulated when compared to gRNAs before blood feeding and at day 3 pBF, respectively.

Surprisingly, TrxR did not show up in our pairwise comparisons. As we did not detect traces of the protein in our TrxR-KO$_{MG}$ samples, we expected the mRNA to be strongly down-regulated in KOs. To elucidate the origin of this discordance, we investigated the alignment of our reads to the *TrxR* gene. First we noticed that there was indeed a down-regulation, but that it was below our threshold. Second, all the transcripts that were present showed indel mutations around the sequences targeted by guides 2 and 3, but not guide 1. Most of these mutations generated early stop codons, probably leading to partial TrxR proteins that are quickly discarded, as we

did not detect them by western blot. This observation is in good agreement with the gRNA efficiency prediction that was lower for gRNA1 compared to gRNAs 2 and 3 (Table 2.1) although we cannot exclude that indels generated by gRNA1 in the 5' end of the gene could lead to the absence of mRNA production.

The transcriptomic analyses we performed did not lead to the identification of any putative compensating enzyme, but they suggested changes in the detoxification pathways, the immune system and metabolism. The fact that two GSTs were up-regulated after blood feeding suggests that the GSH pool is still functional in TrxR-KO$_{MG}$ midguts and that it could be compensating for deficiencies in the Trx system.

E. Developing a conditional CRISPR/Cas9 system

To address whether TrxR dispensability in adult mosquitoes is a general feature or if it is restricted to the midgut, we aimed at knocking out the gene in all tissues. As previously mentioned, this entails the use of a promoter whose expression is strictly restricted to the adult stage and, because our aim is a complete KO, it must also be ubiquitous. Because no endogenous *Anopheles gambiae* promoter with such characteristics has been characterized, and because promoter leakiness is likely sufficient to generate a gene KO when driving Cas9, we evaluated the use of artificial systems. The Q system is based on the regulatory genes of the Qa cluster of *Neurospora crassa* and consists of a promoter (QUAS), a transcription factor (QF) and a suppressor (QS). QF is required to drive expression from QUAS and QS hampers its activity; thus, when the three components are present, the expression of genes downstream of QUAS is repressed. However, QS is released from QF upon interaction with a small molecule called quinic acid (QA) (Fig. 2.11 A). The system was successfully applied to *D. melanogaster* flies, where expression from the QUAS promoter can already be observed 24 h after addition of QA to the food (Potter et al., 2010). Q system-based transgenic *A. gambiae* lines have been used in the past (Riabinina et al., 2016), however not for conditional expression. For our purpose, we decided to express Cas9 under the control of this system. To that end, we cloned eSpCas9 under the control of the QUAS promoter and QF and QS under a ubiquitous promoter in the same construct. To make sure that the production of QF would not exceed that of QS and drive expression in the absence of QA, we
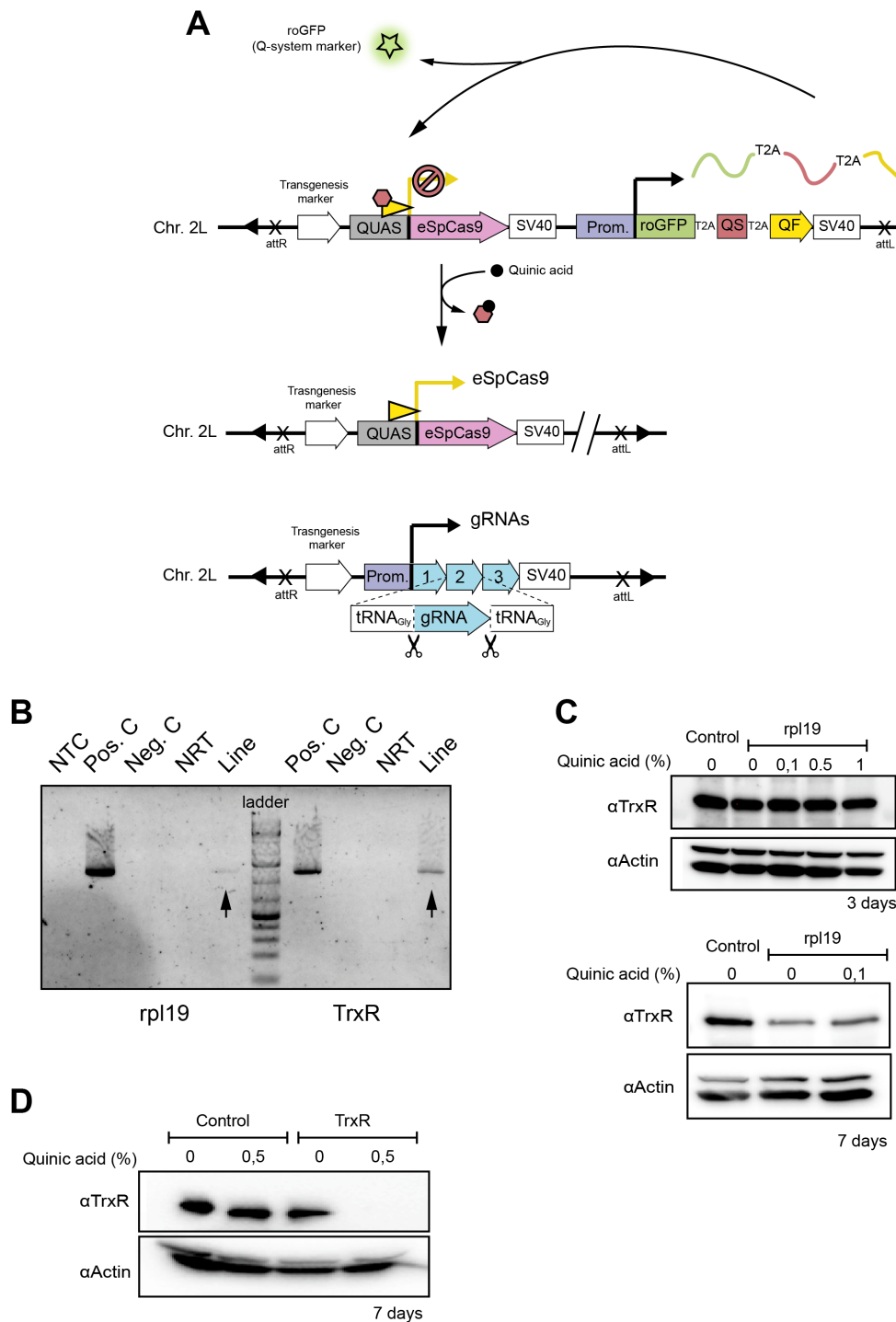
Figure 2.11. Conditional knockout of thioredoxin reductase (TrxR) using the Q system. (A) Scheme of the transgenes and the expected mode of action. hGrx1-roGFP2 (roGFP) was cloned followed by the Q suppressor (QS) and the Q transcription factor (QF), all separated by T2A self-cleavable peptides (black, dotted lines). eSpCas9 was cloned under the control of the Q promoter. QS and QF bind the Q promoter hampering Cas9 expression. Upon addition of quinic acid (QA), QS is released and Cas9 transcribed. The transgene was inserted into the X1 docking site on chromosome 2L, and the resulting line crossed to the G12::gRNA line. Triangles indicate the leftovers from the transposon used to integrate an attP site in the genome and attR/attL are the scars left by the recombination event at this site. mTurquoise is the transgenesis marker. **(B)** RT-PCR amplification of the roGFP-QS-QF transcript (black arrows) in a line where it expression is driven by the rpl19 promoter and a line where it is driven by the TrxR promoter. **(C)** TrxR protein levels evaluated by western blot in the rpl19-driven line after feeding on different concentrations of quinic acid for different amounts of time. **(D)** TrxR protein levels in the TrxR-driven line after feeding on 0.5 % (w/v) of quinic acid for 1 week.

expressed them as one single transcript separated by the "self-cleavable" peptide T2A (Liu et al., 2017). Finally, to be able to visualize where the system was

expressed and to measure the effect of TrxR-KO on the oxidation of the glutathione pool in these cells, we added hGrx1-roGFP2 into the same transcript. In summary, we aimed at expressing roGFP, QS and QF (in this order) as a single transcript under the control of an *Anopheles gambiae* promoter. The addition of T2A sequences between these three elements, allows generating three independent proteins from the same transcript. roGFP2 would indicate where the system was express and provide us a means to measure the impact of TrxR knockout on the glutathione system; QS and QF would bind to the QUAS promoter, thus repressing Cas9 expression. Upon QA feeding, QS would be released leading to Cas9 accumulation in the cell and to the KO of TrxR provided that gRNAs are present in the same cell (**Fig. 2.11 A**).

Another issue with our approach was the lack of knowledge of ubiquitous promoters in *Anopheles gambiae*. Therefore, to drive the Q system we decided to clone a 1500-bp region upstream of the 1st exon of *TrxR,* increasing our chances that the system is expressed where *TrxR* is expressed. Additionally, we tested the promoter driving the expression of the 60s ribosomal protein L19 (rpl19, AGAP004422), a gene that is strongly expressed and commonly used as housekeeping in qPCR assays. To that end, the 1500-bp region upstream of rpl19 was cloned. In parallel to the construction of the Cas9 lines, we also cloned the tRNA-gRNA array used in midgut KOs under the *TrxR* and *rpl19* promoters.

After egg injection and selection of transgenic mosquitoes using the relevant transgenesis markers, we did not notice any roGFP expression for either of the promoters driving the expression of the roGFP-QS-QF transcript. To investigate whether the issue was due to the absence of activity of the regions that were cloned as promoters, or to an issue with the processing of the polycistronic transcript, we extracted RNA and amplified the polycistronic mRNA by RT-PCR. A band of the expected size was detected in both lines for both promoters, although rpl19 was clearly fainter than for the TrxR promoter (**Fig. 2.11 B**), suggesting that both promoter region drive mRNA expression, with TrxR promoter more efficient than rpl19. Thus, the absence of roGFP fluorescence could be due to (i) a faulty translation of the transcript (notably with the T2A skip peptides) or (ii) a defect in roGFP itself. Hence, to check if the rest of the system was working, we crossed the

Cas9 and gRNA lines, fed adults with QA and checked if there was a reduction in TrxR levels. In the rpl19 transgenics, TrxR levels remained the same as in controls 72 h after the supplementation of the feeding solution with different amounts of QA, or upon feeding with 0.1 % QA for 7 days (**Fig. 2.11 C**). In contrast, in the TrxR line, we did not detect any TrxR in extracts of whole mosquitoes 1 week after supplementation of the sugar solution with 0.5 % QA (Fig. 2.11 D). This indicates that the Q system works when driven by the *TrxR* promoter, possibly because it drives a higher expression of the Q system than the *rpl19* promoter, but further assays under similar conditions are required before concluding. The absence of roGFP fluorescence despite the production of functional QS and QF, and thus probably the correct translation of hGrx1-roGFP2, could be due to the presence of a 17 amino-acid tail corresponding to the N-term of the T2A skip peptide that stays attached to the protein upstream. Nevertheless, these results are preliminary as the experiments were performed once with a limited number of mosquitoes. Further tests are required to confirm the efficiency of the system and, should it be the case, the phenotype of such mosquitoes.

Table 2.2. List of up- and down-regulated genes in thioredoxin reductase midgut knockout mosquitoes

| Transcript | | nBF | | 3 dpBF | | 7 dpBF | GO, system |
ID	Name	Cas9	gRNA	Cas9	gRNA	gRNA	
AGAP000376	Transferrin			-2.22			
AGAP000604		-1.28					
AGAP000605		-7.90					
AGAP000692	cecropin anti-microbial peptide					1.01	Immune process, response to stimulus
AGAP000693	cecropin anti-microbial peptide					2.85	Immune process, response to stimulus
AGAP000694	cecropin anti-microbial peptide					2.31	Immune process, resonse to stimulus
AGAP001047	inositol polyphosphate 1-phosphatase					-2.69	Cellular process, metabolism
AGAP001190	Female reproductive tract protease GLEANR_896				-1.51		
AGAP001212	peptidoglycan recognition protein (long)					1.21	Biological regulation, immune process, response to stimulus
AGAP001352				1.19		-1.13	
AGAP002058	beta-galactosidase		1.96	-2.18			
AGAP002093				-2.15			Cellular process, localization
AGAP002582		-4.48					
AGAP002629		-3.96			2.27		
AGAP002643					1.25	1.31	Metabolism
AGAP002847	Niemann-Pick Type C-2					-1.17	Localization
AGAP002851	Niemann-Pick C2 protein		-1.17				Localization, metabolism
AGAP002865	cytochrome P450	1.78			-1.25		
AGAP003051	stearoyl-CoA desaturase (delta-9 desaturase)					1.12	Cellular process
AGAP003328	NADH dehydrogenase 1 alpha subcomplex 6					-2.51	Response to stimulus
AGAP003352	Stomatin (EPB72)-like 3			-1.07		1.33	
AGAP003900	NADH dehydrogenase 1 alpha subcomplex 7	3.13					Localization, metabolism
AGAP003906	WASH complex sub 4	3.16				-1.05	Cellular process, localization
AGAP003927	Insulin-like peptide 5			1.13			
AGAP004115	cystinosin		2.50				Localization, GSH
AGAP004199	solute carrier family 5 (sodium-coupled monocarboxylate transporter), member 8	1.31		1.03	-1.21		
AGAP004382	glutathione S-transferase delta class 3			2.07	1.76		Metabolism, GSH
AGAP004636	sodium-independent sulfate anion transporter			1.20			
AGAP004748						-1.09	
AGAP004880	L-lactate dehydrogenase				2.30	1.74	Metabolism
AGAP004882	transmembrane 9 superfamily member 3				1.72		Localization

Red indicates up-regulated transcripts. Blue indicates down-regulated transcripts. Samples were compared to the two parental strains (gRNA and Cas9) at three different timepoints: before blodd feeding (nBF), 3 days after blood feeding (3dpBF) and 7 days after blood feeding (7 dpBF)

Table 2.2. (continued)

| Transcript | | nBF | | 3 dpBF | | 7 dpBF | GO, system |
ID	Name	Cas9	gRNA	Cas9	gRNA	gRNA	
AGAP004916					1.14	1.50	
AGAP004918	fibrinogen					1.53	
AGAP005065		1.62		1.75		-1.07	
AGAP005334	C-type lectin (CTL) - mannose binding					1.65	Resonse to stimulus
AGAP005335	C-type lectin (CTL)					1.11	Cellular process, localization, response to stimulus
AGAP005579				1.50	2.42	2.52	
AGAP005749	glutathione S-transferase omega class 1		-1.09			1.33	GSH
AGAP005776	pigment dispersing hormone			1.12	1.67	1.90	
AGAP006121						1.19	
AGAP006177			1.30	1.17			
AGAP006191	chitinase			-2.21			
AGAP006194						1.00	
AGAP006195						1.32	
AGAP006202		1.30					
AGAP006342	peptidoglycan recognition protein (short)				2.38	3.11	Biological regulation, immune process, response to stimulus
AGAP006343	peptidoglycan recognition protein (short)					3.99	Biological regulation, immune process, response to stimulus
AGAP006367		1.38				1.40	
AGAP006432						1.06	
AGAP006707	serine-type enodpeptidase				2.94	1.22	
AGAP006709	Chymotrypsin-1		1.48		1.29	1.31	
AGAP006710	chymotrypsin			-1.26			
AGAP006711	Chymotrypsin-2				1.33	1.40	
AGAP006793					1.32	1.49	
AGAP007140	Ser/Thr protein phosphatase/nucleotidase			1.48			
AGAP007165	Late trypsin			3.48			
AGAP007292	inhibitor of apoptosis 3	1.13		1.57		-1.18	Biological regulation, cellular process, metabolism
AGAP007293	inhibitor of apoptosis 7						Metabolism
AGAP007347	C-type lysozyme				1.09	3.74	
AGAP008212	cytochrome P450	1.41					
AGAP008214	cytochrome P450			1.06			
AGAP008436	ATP-binding cassette transporter family C member 11				2.78	1.55	
AGAP008502	L-xylulose reductase		2.16				Metabolism
AGAP008645	gambicin anti-microbial peptide					1.61	
AGAP008648	Farnesoic O-ethyl transferase domain	3.16	2.07		1.99	2.10	
AGAP008659	SWI/SNF				1.44	1.30	
AGAP008915	gamma-glutamyltranspeptidase					-1.51	
AGAP009049	Chitinase			3.33			
AGAP009053	lipopolysaccharide-induced TNF-alpha transcription factor (LITAF-like 3)					1.04	Immune process
AGAP009122		6.56					
AGAP009159	AMP dependent ligase					2.24	
AGAP009313						1.42	
AGAP009592		-1.77	-1.90	1.00			
AGAP010328		3.78					Metabolism, reproduction
AGAP010363				2.34			

Table 2.2. (continued)

Transcript		nBF		3 dpBF		7 dpBF	GO, system
ID	Name	Cas9	gRNA	Cas9	gRNA	gRNA	
AGAP010594	Protein CWC15 homolog A			1.43			Metabolism
AGAP011053				-1.76			
AGAP011098	Isoaspartyl-peptidase/L-asparaginase	1.25	1.19	1.00			Cellular process, metabolism
AGAP011294	defensin anti-microbial peptide					3.55	
AGAP011326	inhibitor of apoptosis 2			-1.31			Biological regulation, cellular process, metabolism
AGAP011352	glucosamine-fructose-6-phosphate aminotransferase	1.13					Cellular process, metabolism
AGAP011477	Eupolytin	1.08				2.80	
AGAP011615					1.93		
AGAP011630						1.47	
AGAP011805	ornithine decarboxylase			-1.31		1.04	Metabolism
AGAP011806	ornithine decarboxylase			-2.88		1.73	Metabolism
AGAP011820						-1.07	Cellular process
AGAP011824	thioredoxin peroxidase 4			-1.30			
AGAP012291	Cytochrome P450				1.10	1.09	
AGAP012349		-1.04	1.58			1.04	
AGAP012395	peptide-methionine (S)-S-oxide reductase		-1.51		1.50		Response to stimulus, Trx
AGAP012445	phosphatidate phosphatase					1.09	Metabolism
AGAP012449		2.77				-2.92	
AGAP012798		1.25	1.04		1.19	1.69	
AGAP012818	V-type proton ATPase subunit a	7.49		2.17		-1.26	Biological regulation
AGAP012879	60S ribosomal protein L18a (partial)			-1.62			
AGAP013066						1.14	
AGAP013318	outer membrane lipoprotein Blc		1.81			1.38	Metabolism, response to stimulus
AGAP013329				2.67			
AGAP013359						2.91	
AGAP013543						1.26	
AGAP013569		-1.92			5.82	-7.23	
AGAP013748	mitochondrial import receptor subunit TOM7 homolog					-1.01	
AGAP028128	ATP-binding cassette transporter family C member 9					-1.02	
AGAP028369	adenosine triphosphatase subunit 8	1.22				-1.50	
AGAP028383	NADH dehydrogenase subunit 4L					-1.70	
AGAP028541		4.17	3.24		1.01		
AGAP028568						1.12	
AGAP028764			-3.22				
AGAP029277				1.12			
AGAP029298					-1.15		

5. DISCUSSION

Apart from the lack of GR in insects, little is known about intracellular redox maintenance systems in these animals. It is generally believed that the absence of this key antioxidant is compensated by the Trx/TrxR system and therefore that TrxR is essential. However, to our knowledge, the role of this protein has only been assessed in *D. melanogaster* during development (Missirlis et al., 2001, 2002).

Here we have developed polyclonal antibodies against AgTrxR that recognize a ~60 kDa protein in *A. gambiae* protein extracts and recombinantly produced insect TrxRs from *A. aegypti, D. melanogaster* and *A. mellifera*. These broad-spectrum polyclonal antibodies will be instrumental in the future to study TrxR in other insect species. Moreover, a second smaller band of slightly less than 55 kDa, corresponding to the predicted protein size (54.5 kDa) was detected when performing western blots in non-reducing conditions. Because this band is never observed in reducing conditions, we concluded that it corresponds to the oxidized form of TrxR. This shift is also observed in other thiol-active proteins such as Trxs (Du et al., 2012; Ragu et al., 2014; Wang et al., 2012) and can be exploited to know the oxidative status of the proteins in redox western blots.

The CRISPR/Cas9 mutants of *TrxR* generated in this study shed light into the role of this protein in mosquitoes. The presence of both CRISPR/Cas9 partakers (i.e. Cas9 and gRNAs) in mosquito eggs led to the abrogation of embryonic development. In contrast, in *D. melanogaster,* the absence of a functional *TrxR* gene at the embryonic stage does not hamper development of this stage as *TrxR* mRNA is maternally transmitted (Missirlis et al., 2001), however, the deposition of TrxR underlines the importance of this protein in embryos. Of note, TrxR is also essential in embryonic development in mammals (Bondareva et al., 2007; Jakupoglu et al., 2005), where Trxs are indispensable as they are involved in cell proliferation and apoptosis (Matsui et al., 1996; Nonn et al., 2003). When Cas9 was expressed later during larval development, the resulting partial somatic knockouts showed a strong lethal phenotype. When we used Cas9 to drive mutagenesis, we obtained mosquitoes with a developmental delay of 3 days that mostly died as pupae or adults with the legs trapped in the pupal case. When we used eSpCas9, the delay disappeared and 17 % of the progeny became functional adults; nonetheless, most of them died, as they could not leave the breeding water. These phenotypes are similar to those found for

D. melanogaster carrying hypomorphic mutations of *TrxR1* (i.e. that cause partial loss of the gene function). Missirlis et al (Missirlis et al., 2001, 2002) generated two hypomorphic lines showing different degrees of larval lethality; in one of them, 20 % of the progeny became functional adults and the rest died as pharate adults in the pupal case, whereas in the other one only 2 % of pupae hatched. In our assay, the variability of the observed phenotypes could be due to a variable number of cells presenting TrxR defects and/or to the generation of hypomorphic alleles. Further biochemical characterization of TrxR activity in these progenies will help elucidate this point. Moreover, the two types of mutants that we generated with Cas9 and eSpCas9 presented a strong sex bias in favor of females. Since *TrxR* is coded on chromosome X in *A. gambiae* mosquitoes, we hypothesize that this biais is due to the fact that mutagenesis events in males are more likely to lead to a reduction in TrxR activity as they have a single copy of the gene. Another plausible explanation, that does not exclude the previous one, is that females are more prepared to face the consequence of this loss. The functional adult females obtained with eSpCas9 died within 10 days after emergence, later that the hypomorphic fruitflies that die within 2-3 days (Missirlis et al., 2002). Western blot analyses on Cas9-derived adults showed an unequal loss of TrxR in different tissues, thus the longer lifespan of our mosquito mutants could be due to the fact that the protein function is still intact in some tissues. Of note, hypomorphic mutant fruitflies were not morphologically distinguishable from wild types, whereas our *TrxR* mutant adults presented serious deformations and impaired movement. These differences in the phenotype of *TrxR* mutants in mosquitoes and flies could be due to the fact that mosquitoes only possess one *TrxR* gene whereas *D. melanogaster* has two. The physiological reasons behind the lethal phenotype remain elusive. The Trx/TrxR system is known to play an important role in cell proliferation and apoptosis (Lu and Holmgren, 2012; Muri et al., 2018; Peng et al., 2016; Silva-Adaya et al., 2014; Sun and Rigas, 2008; Yoo et al., 2013), thus it is plausible that our phenotype is the outcome of defective larval growth; however, our mutants did not show differences in size when compared to wild types at any developmental stage. On the contrary, the main defects correlated with molting processes. *C. elegans* worms are unable to reduce cuticle components when TrxR and GR activities are decreased and this phenotype correlates with impaired molting (Stenvall et al., 2011); thus we hypothesize that the phenotype observed in *A. gambiae* mosquitoes defective for TrxR might be due to molting issues rather than to cell proliferation. This hypothesis is also coherent with the morphological defects observed in some of the functional adults and the fact that the non-functional ones had their legs trapped in the pupal case.

At the adult stage, our data demonstrate that TrxR is dispensable in the midgut. The severe reduction of TrxR levels in this tissue by CRISPR/Cas9 mutagenesis had no impact on the survival or the vectorial capacity of the insect. Surprisingly, TrxR-KO$_{MG}$ mosquitoes lived longer than wild types after blood feeding and upon feeding on 1 mM of the pro-oxidant paraquat, suggesting that they are more resistant to oxidative stresses. To elucidate the origin of this unexpected outcome, we performed transcriptomic analyses in pools of midguts at three different time points and conditions (nBF, 3 dpBF and 7 dpB). In general, few transcripts were up- or down-regulated in knockouts as compared to controls, and most of them were found in only one of the comparisons. Interestingly, some of the up-regulated hits corresponded to detoxification enzymes, which could explain the increased tolerance of TrxR-KO$_{MG}$ mosquitoes to blood digestion and paraquat. This phenomenon was also found in TrxR1-deficient mouse hepatocytes as being mediated by the Nrf2 pathway (Suvorova et al., 2009). Indeed, this transcription factor is sensitive to redox changes and is known to regulate the expression genes involved in detoxification (Kobayashi et al., 2004; Wang et al., 2014), metabolism (Fu et al., 2019; Mitsuishi et al., 2012; Ohl et al., 2018; Wang et al., 2018), and also immune genes (Thimmulappa et al., 2016). In the same direction, we also found that most up- and down-regulated transcripts were related to metabolism and that there was an enrichment for immune-related and anti-bacterial genes among the upregulated transcripts 7 dpBF. The Nrf2 signaling pathway is activated upon oxidative stress (Vomund et al., 2017), thus our results could be indicative of such an imbalance in TrxR-KO$_{MG}$ midguts. Alternatively, the Trx/TrxR has also been proposed to activate Nrf2 (Schmidt, 2015), thus our findings could be the result of an overall decreased activity of this system. In the future, measuring the concentration of different ROS and analyses of the redox state of Trxs will help elucidate the origin of this activation. Of note, our transcriptomic analyses did not include experimental replicates and thus, some of the responses that we observed might be due to other factors independent of the loss of TrxR. More samples should be sequenced in order to confirm the statistical significance of the detected changes. In yeast, the transcription of Prxs is increased in the absence of TrxR (Carmel-Harel et al., 2001); in our analyses, the results showed rather the opposite effect as Prx4 was downregulated 3 pBF in one of the comparisons. This is in line with the findings in mice embryos defective for TrxR (Bondareva et al., 2007), thus suggesting this response is not conserved between yeast and animals.

Knocking out *TrxR* in hGrx1-roGFP2 mosquitoes did not lead to any major changes in the redox balance of glutathione. Young mosquitoes did not show any difference as compared to wild types, and blood fed mosquitoes even showed a slightly more reduced GSH pool than controls. Only 1-week-old mosquitoes showed mild oxidation. On the contrary, knocking down TrxR in the imaginal disks of *D. melanogaster* leads to a severe decrease of the GSH/GSSG ratio. The fact that the GSH pool is still mostly reduced in enterocytes that do not express TrxR is consistent with our transcriptomic data. After blood feeding, two GSTs were upregulated; this phenomenon was also observed in yeast and mice (Bondareva et al., 2007; Carmel-Harel et al., 2001), where it was hypothesized that it could be indicative of a shift of the redox homeostasis burden towards the GSH system. Although these experiments were only performed once, they suggest that (i) the Trx/TrxR system is not (the only) responsible for the recycling of GSSG in *A. gambiae* mosquito midgus and/or (ii) there are other mechanisms replenishing the GSH content of the midgut cells. In mouse hepatocytes lacking both TrxR and GR, redox homeostasis is sustained by the GSH biosynthetic pathway (Eriksson et al., 2015). In mosquito TrxR-KO$_{MG}$ enterocytes, this model would be supported by the fact that cystinosin and GGT were up- and down-regulated, respectively, although only in one comparison each. In the future, blocking the activity of the enzymes that contribute the biosynthesis of GSH in TrxR knockouts will help us elucidate if such is the case. Alternatively, GSH could be imported from other tissues where the Trx/TrxR system is still working. The conditional expression of the CRISPR/Cas9 components using the Q system will help us reduced the TrxR activity in all tissues at the adult stage, and hence, clarify this possibility. Finally, it is also possible that the recycling of GSSG in mosquitoes is not (entirely) due to the Trx/TrxR system. Although we would have expected to see an increase in the expression of the responsible protein(s), such regulation could be post-transcriptional thus not observable in a transcriptomics assay. Proteomic analysis might therefore be more helpful in this case, however PTM regulation might also be complicated to detect in such case. Eventually, we could also scan the genome for potential candidates that could be tested on RNAi assays in hGrx1-roGFP2-expressing mosquitoes.

In this chapter we also provide new insights on the tools and methods that can be used to target genes by CRISPR/Cas9 in *A. gambiae*. First, we showed that the expression of Cas9 under the control of the vasa promoter leads to somatic mutations during development, which should be taken into account when analyzing the phenotype of mutant lines obtained by these means. Moreover, the absence of

TrxR mutants in mosquitoes expressing gRNAs under the control of the U6 promoter AGAP013557, strongly suggests that this promoter is not expressed in enterocytes. As an alternative, we reported for the first time the suitability of the tRNA-gRNA array system to drive mutagenesis in somatic tissues in this species. Using Cas9 and eSpCas9 led to the same overall phenotypes during mosquito development, but with important differences. eSpCas9 is known to reduce off-target mutagenesis (Slaymaker et al., 2016) and therefore differences could be indicative of a contribution of some off-targets to the developmental delay and lethal phenotype, which should be confirmed by sequencing of the predicted off-target loci and rescue experiments. Still, the eSpCas9-derived phenotype is very similar to that observed in Cas9 mosquitoes, but delayed compared to it, and it is similar to TrxR defective *D. melanogaster*. Thus, another plausible explanation is that eSpCas9 has reduced on-target efficiency in *A. gambiae* mosquitoes as compared to Cas9. This decreased activity combined with the fact that eSpCas9 is only expressed in small amounts in some cell types could result in delayed mutagenesis with regard to Cas9. To elucidate the time course of the mutagenesis, we unsuccessfully tried to measure TrxR levels in western blot at different larval stages. In the future, this should be repeated by sequencing of the TrxR locus instead. In our transcriptomic analyses on midgut *TrxR* knockouts we could only detect a mild down regulation of TrxR at the mRNA level. Still, these transcripts contained non-synonymous indel mutations around the positions of gRNAs 2 and 3. This is commonly observed in CRISPR/Cas9 mutants (Tuladhar et al., 2019) and in our case, it led to mRNAs that were not translated into proteins otherwise, we would have detected a partial TrxR protein with our polyclonal antibodies as one of the antigenic peptides used to produce them, lies upstream of the two guides. Since the two positions were close to each other we were expecting that the fragment lying between the two guides would be lost. The fact that we do not observe such phenomenon might be indicative of each cleavage happening at different moments rather than simultaneously, for instance, if both gRNAs have different efficiencies. On the contrary, we did not detect any mutation event for gRNA 1; this could be due to a complete loss of functionality of alleles mutated at this point or to the nature of the sequence itself as this guide was predicted to be the least efficient. These results should be taken into account for the design of gRNA is the future and further highlight the importance of selecting more than one guide when targeting a gene with the CRISPR/Cas9 system. We have also reported a different expression pattern and efficiency in the midgut for transgenes inserted in the *E* (Pondeville et al., 2014) and *X1* loci (Volohonsky et al., 2015). This should be taken into account when designing transgenic lines in the future, especially

for CRIPR/Cas9 mutagenesis. Moreover, this phenomenon could also be contributing to the unequal efficiency of our CRISPR/Cas9 system in different tissues during development. Indeed, the U6::gRNA transgene was inserted into the less efficient and more variable E locus. Finally, the difficulty to find robust and strong endogenous promoters to drive transgene expression ubiquitously in *A. gambiae*, and the disparity observed between the expression of these endogenous genes and that of transgenes placed under the control of the corresponding promoters is suggestive of a complex gene regulation, probably requiring long distance enhancer sequences.

In conclusion, we have shown that TrxR is essential for embryonic and larval/pupal development, but dispensable in the midgut of adult mosquitoes. In the future, knocking out the gene in all adult tissues will help elucidate if this dispensability is a general feature in *A. gambiae* or just a particularity of some tissues. Surprisingly, our data suggested that the absence of TrxR in the midgut might be compensated by the GSH system, opening the question of who is responsible for the maintenance of this buffer in the absence of both TrxR and GR. A deeper characterization of the role of other effectors of the GSH pathway will shed light into the mechanisms that regulate the redox homeostasis in insects. The role of TrxR in *D. melanogaster* has only been studied in development, thus we do not know if the observed dispensability of TrxR at the adult stage is a common feature in insects or rather a particularity of mosquitoes, a question that will be worth answering.

3

CHAPTER

Chemical inhibition
of thioredoxin reductase

1. INTRODUCTION

As mentioned in the introduction section, TrxR belongs to the family of dimeric flavoenzymes. This oxidoreductase obtains the reducing equivalents from NADPH and has three domains: the pyridine nucleotide-binding domain, a flavin-binding domain and the interface domain. All TrxRs have at least two active sites (FAD and redox-active disulfide), but high M_r TrxRs (i.e. those present in higher eukaryotes) possess an additional C-terminal redox site.

In high M_r TrxRs electrons flow from NADPH to FAD and then to the N-terminal disulfide of the same monomer, which is adjacent to the flavin. The N-terminal dithiol reduces the C-terminal active site of the other monomer and finally, this site reduces the oxidized substrate Trx-$(S)_2$. Prior to catalysis, the enzyme is reduced to a 2-electron reduced state by 1 equivalent NAPDH and then, to a 4-electron reduced state by a second NADPH equivalent during catalysis. The enzyme oscillates between these two states (Bauer et al., 2003b, 2003a; Zhong et al., 2000).

The N-terminal active site (-CVNVGC-) is conserved among species. However, the C-terminal one is not. In most organisms, this site is formed by a –Gly-Cys-Sec-Gly sequence; however, in insects, it consists of two adjacent Cys flanked by Ser (Thr and Ser in the case of *A. gambiae*) (Bauer et al., 2003b, 2003a; Kanzok et al., 2001). Interestingly, Sec $\rightarrow$ Cys mutants have a very low catalytic efficiency (Zhong et al., 2000), whereas insect TrxRs are virtually as active as the mammalian ones with regard to Trx reduction (Arnér et al., 1999; Bauer et al., 2003a; Kanzok et al., 2001); nevertheless, this is not the case with other substrates such as dehydroascorbate, for which reduction the Sec residue seems to be key (Gromer et al., 2003). The extraordinary performance of insect TrxRs is explained by the microenvironment that is formed around the C-terminal disulfide. In the model proposed for *D. melanogaster* TrxR (Gromer et al., 2003), the adjacent Ser assist each Cys residue. Indeed, Cys[490'] is deprotonated to a thiolate that attacks the disulfide bridge of Trx-$(S)_2$ and subsequently, the thiolate resulting from Cys[489'] cleaves the intermolecular disulfide bridge to release the reduced substrate Trx-$(SH)_2$. Moreover His[106] has been proposed to help in this process (Huang et al., 2008).

The essential role of TrxR in different organisms and pathogenic cells has been gaining attention in biomedicine. Several TrxR inhibitors have been studied as

medical drugs against bacteria (Harbut et al., 2015; Owings et al., 2016; Zou et al., 2018), protozoan parasites - including *Plasmodium falciparum* (Andricopulo et al., 2006; Davioud-Charvet et al., 2003; Debnath et al., 2013; McCarty et al., 2015; Tiwari et al., 2016), fungi (Regina et al., 2019) and cancer (Urig and Becker, 2006; Zhang et al., 2019a).

The aim of this chapter was to explore the potential of AgTrxR as a target for new molecules that would sensitize mosquitoes to the oxidative stresses they encounter during their life. To that end, we first produced recombinant TrxR and Trx from 4 insect species (*Anopheles gambiae, Aedes aegypti, Drosophila melanogaster* and *Apis mellifera*) and then tested a library of compounds for their ability to inhibit these enzymes. Finally, we fed mosquitoes with the best hit from this assay to assess the toxicity and impact on redox homeostasis.

2. RESULTS

A. Screening to identify thioredoxin reductase inhibitors

(I) Comparison of the thioroedoxin reductase sequence of different insect species

Current insecticides produce off-target effects in other insect populations, which contributes to major issues such as the colony collapse disorder in bees. Thus, additional efforts should be made when designing novel insecticides to make them as specific to the target species as possible.

Species-specificity is hard to reach when organisms are phylogenetically closely related. Thus, we first assessed the degree of conservation of TrxR among insects. To that end, we blasted the sequence of AgTrxR (AGAP000565-RC) to retrieve orthologs in other insect species; then, we aligned the top 30 (including AgTrxR) and colored the resulting consensus sequence according to the degree of conservation (**Fig 3.1 A**). Within the same family, the percentage of identity of TrxR is around 80 %; when comparing different families and orders, this conservation is between 60 and 70 %, thus confirming that TrxR is a highly conserved enzyme. Despite this low

variability, some regions show a sequence identity below 50. The most variable sequence is the N-terminal one, most likely due to the fact that we retrieved and aligned both cytoplasmic and mitochondrial TrxRs. In the C-terminal active site, the
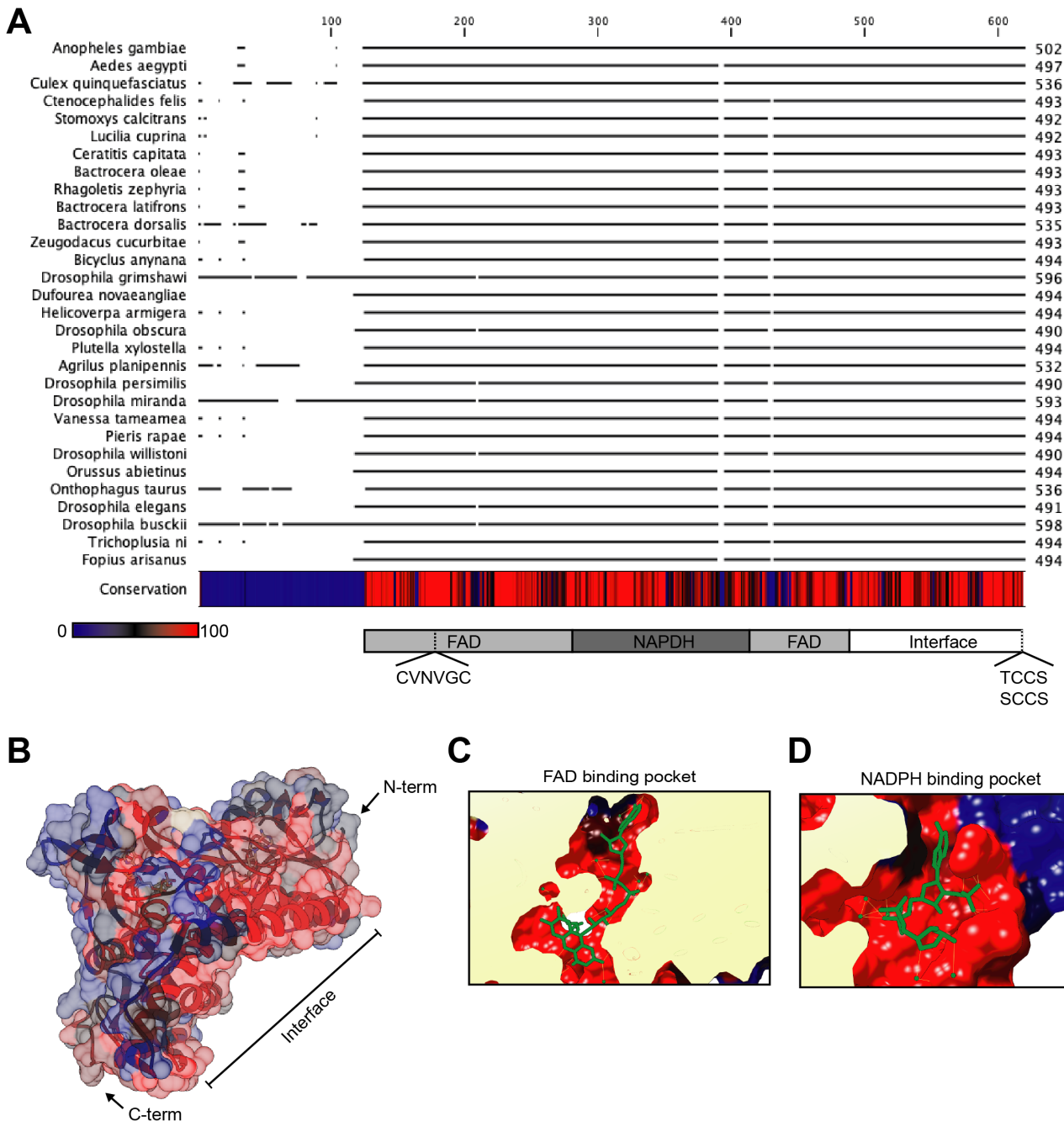
Figure 3.1. Thioredoxin reductase (TrxR) is highly conserved in insects. The sequence of *Anopheles gambiae* TrxR (AGAP000565-RC) was blasted to retrieve orthologs in insects, and then **(A)** all sequences were aligned and colored according to the degree of conservation. TrxR is highly conserved among insect species (>50 %). However, some regions of the FAD and the NADPH binding domains show conservation below 50. Moreover, some dipterians present a Thr residue instead of Ser at the first position of the C-terminal active site (*Anopheles gambiae, Aedes aegypti, Culex quinquefasciatus, Ceratitis capitata, Bactrocera oleae, Rhagoletis zephyria, Bactrocera latifons, Bactrocera dorsalis* and *Zeugodacus cucurbitae*). **(B)** The 3D structure of *Drosophina melanogaster* TrxR monomer (2nvk) was obtained from the protein data bank and colored according to the degree of conservation calculated for TrxR in insects. Most of the residues showing conservation below 50% are located in the surface of the protein. **(C)** The FAD and **(D)** NADPH-binding pockets are highly conserved, with the exception of several residues not interacting directly with either molecule.

conservative S499T substitution observed in *Anopheles gambiae* is also present in other mosquito genus (*Aedes* and *Culex*) and dipterian families (*Ceratitis, Bactrocera, Zeugodaucus*). Still, the C-terminal portions of the FAD- and the NADPH-binding domains present some variability (**Fig 3.1 A**). To further explore the potential relevance of these differences, we colored the 3D structure of DmTrxR (2nvk), the only insect TrxR structure that is available, according the degree of conservation in insects. Most of these variable sequences are placed in the exterior surface of the monomer. Regarding the FAD- and the NAPDH-binding pockets, only few amino acids are not conserved and none of them is in direct contact with these cofactors (**Fig 3.1 B, C, D**). Altogether, this analysis suggests that species-specific inhibitors might be difficult to design. Nevertheless, human TrxR1 and TrxR2 (cytoplasmic and mitochondrial, respectively) are highly conserved, yet they show different inhibitor specificities (Rackham et al., 2011). Thus, we hypothesized that the differences we found might be sufficient to identify mosquito-specific TrxR inhibitors.

(II) Recombinant thioredoxin and thioredoxin reductase from different insect species

To test our hypothesis experimentally, we decided to screen for the inhibitory capacity of a library of selected compounds on different insect Trx/TrxR systems. We first aimed to express and purify recombinant TrxR and the major cytosolic Trx from three mosquito species (*Anopheles gambiae, Aedes aegypti, Culex pipiens*) and two other insects (*Drosophila melanogaster* and *Apis mellifera*, the honey bee).

Anopheles gambiae and *Drosophila melanogaster*

Both AgTrxR and DmTrxR, as well as their respective major cytosolic Trxs, had already been expressed and purified from *E. coli* (Bauer et al., 2003a; Kanzok et al., 2001) using the pQE30 expression system. In brief, this method is based on the T5 promoter transcription-translation system and adds a 6xHis tag at the N-terminal of the protein for purification in nickel-nitrilotriacetic (Ni-NTA) affinity columns. pQE30 vectors coding for DmTrxR, DmTrx and AgTrxR were already available at Prof. Katja Becker's laboratory. Hence, we only amplified the *AgTrx1* sequence from mosquitoes

and cloned it into the same vector. Then, we transformed M15 *E. coli* bacteria and we followed the recommended protocol for pQE30 expression. In brief, bacteria were grown in LB medium and expression induced upon addition of IPTG at 37ºC for 4 h. The proteins retained in the Ni-NTA column were eluted with increasing concentrations of imidazole (10-200 mM). To identify the fractions containing the proteins, we loaded 10 µL of each into SDS-PAGE gels. We noticed that the *D. melanogaster* orthologs were expressed in high amounts, however neither *A. gambiae* protein could be detected.

To optimize the expression protocol of the mosquito proteins, first we unsuccessfully repeated the processed using a rich medium (i.e. 2xYT) and inducing expression at room temperature overnight. Bauer et al (Bauer et al., 2003a) expressed the proteins from a cloning strain of *E. coli*, thus we transfected XL1-blue bacteria with each pQE30 plasmid and pREP4 (required repression vector for expression with T5 promoter) and repeated the expression protocol in rich medium for 4 h. We did not detect a band with increased intensity at the expected size. However, some of the fractions looked slightly yellow. This pigmentation is typical of FAD-containing proteins like TrxR. Thus, to increase the sensitivity of detection, we tested for the presence of AgTrx1 and AgTrxR on a western blot using anti-His antibodies (**Fig 3.2 A**). Both proteins were present in the 100 mM imidazole fraction in very low concentrations. Additionally, they were also detected in the flow-through and AgTrx1, in the buffer-only fraction, suggesting a poor retention in the column. Because mosquitoes and bacteria do not use the same codons at the same frequency, we co-transfected bacteria with the expression vectors and pRARE II, a plasmid coding for rare tRNAs, to facilitate translation. A faint band corresponding to the AgTrxR size was detected in the fraction containing 100 mM imidazole (**Fig 3.2 B**). Thus, we concluded that the translation of the recombinant proteins was likely hampered by codon-use differences and that pRARE II was not enough to help in this process.

Therefore, we ordered codon-optimized versions of both genes, cloned them into pQE30 and expressed them with the standard expression protocol. Both AgTrxR and AgTrx1 were present in all imidazole-containing fractions at high concentrations (**Fig 3.2 C**) (Supplementary S1, S2).
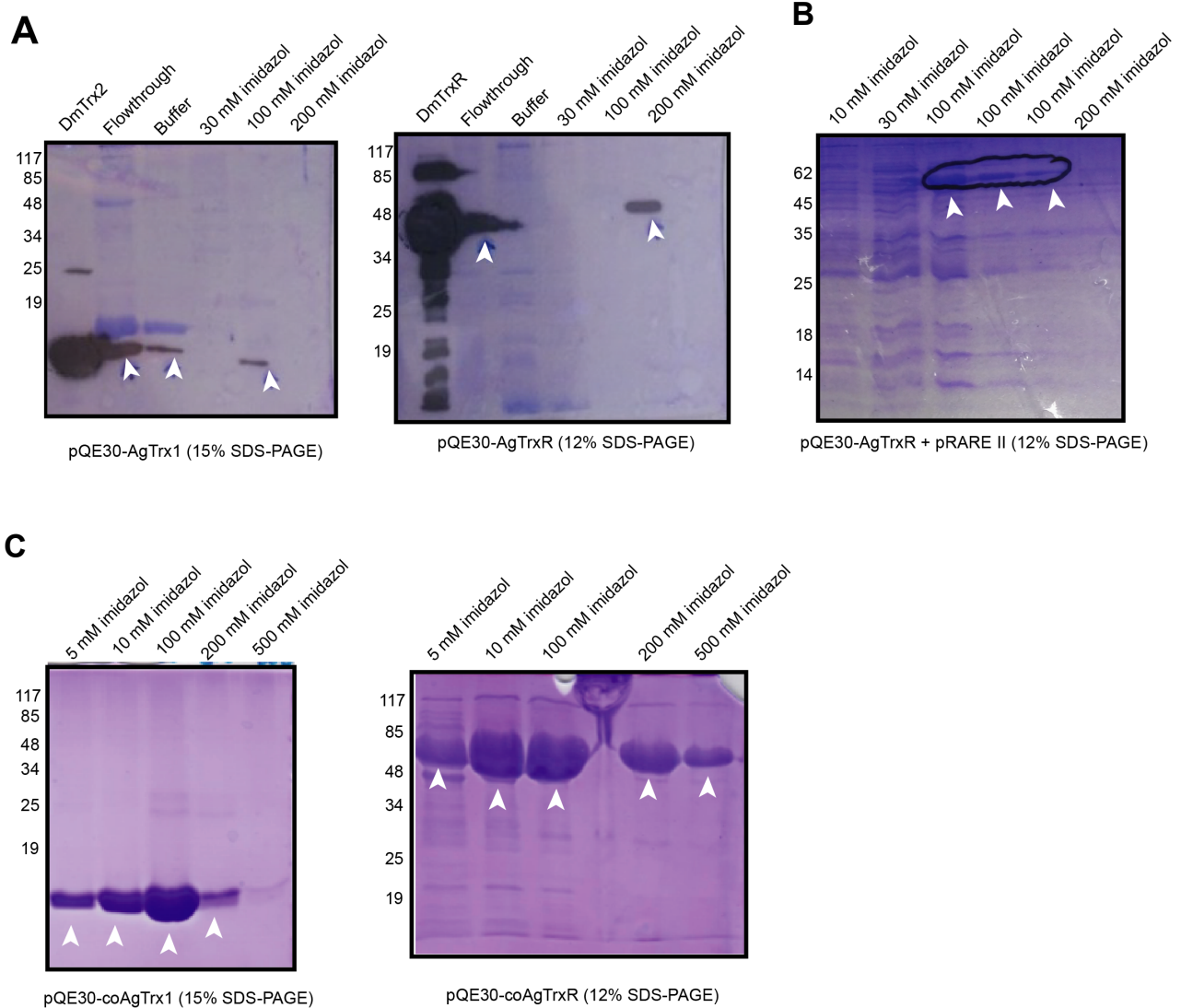
Figure 3.2. *Anopheles gambiae thioredoxin reductase* and *thioredoxin* require codon-optimization for expression in *E. Coli*. *E. coli* bacteria were transformed with pQE30 vectors coding for AgTrxR or AgTrx and grown in liquid culture. After protein expression, cells were lysed and the supernatant loaded into Ni-NTA columns. Retained proteins were eluted with increasing concentrations of imidazole. Fractions were loaded in SDS-PAGE gels and stained with Coomasie Blue. **(A)** Proteins produced from the endogenous gene sequences could only be detected by western blot (black bands) using antibodies against the N-terminal His tag. **(B)** The presence of a band could be detected in the gel upon co-transfection with a plasmid coding for rare tRNAs; however, in low amounts **(C)** Codon-optimized versions of the genes led to high protein expression and purification in all imidazole-containing fractions. White arrows indicate the presence of the proteins.

Aedes aegypti, Culex pipiens *and* Apis mellifera

To our knowledge, the remaining 6 proteins had never been expressed in *E. coli*. Therefore, we cloned them into pQE30 and repeated the expression protocol. For AmTrx2, AmTrxR and AaTrxR we obtained high amounts of the proteins with the standard protocol. However, AaTrx1, CpTrxR and CpTrx1 were not detectable in

SDS-PAGE assays, as it was the case of the *A. gambiae* proteins. Hence, we concluded that the absence of expression was likely due to the codon use. Since we already had the AaTrxR protein, we order a codon-optimized version of *AaTrx1* and expressed the protein from it (Supplementary S3). Codon optimization has not yet been done for *CpTrxR* and *Cptrx1*.

(III) Pilot screening in vitro

To identify specific modulators of AgTrxR, we selected and screened a total of 37 compounds (Table 3.1) for their ability to inhibit the different TrxR proteins in quasi-physiological conditions (i.e. phosphate buffer pH 7.4, NADPH and Trx as substrate). These compounds were selected and provided by Dr. Elisabeth Davioud-Charvet (ECPM in Strasbourg), based on their potential redox reactivity and/or their similarity to some insecticidal molecules. When screening for TrxR inhibitors, 5,5′dithio-bis(2-nitrobenzoic acid) (DTNB) is the most frequently used substrate in the literature (Fang et al., 2005; Liu et al., 2008; Tuladhar and Rein, 2018; Wazen et al., 2014). This low molecular weight chemical, also known as the Ellman's reagent, is a highly reactive disulfide that can be reduced at the N-terminal site of TrxRs (Lacey et al., 2008). Thus, we decided to perform the screenings using DTNB as well. At the end, all compounds were tested once with each TrxR in the presence of its corresponding Trx or DTNB, except for DmTrxR that was only tested with DmTrx2. Using Trx as substrate for AgTrxR, DmTrxR and AmTrxR, the screening was first performed in a microplate reader to identify molecules with inhibitory activity, and the assay was repeated for those molecules using a spectrophotometer to calculate the half maximal inhibitory capacity (IC_{50}) more precisely. Likewise, the DTNB assay with AmTrxR was performed using this strategy. For both AaTrxR screenings and AgTrxR using DTNB, compounds were directly assayed in the spectrophotometer. All the compounds were tested at 10 different concentrations (300 μM – 15 nM).

In total, 21 compounds showed inhibition in at least one of the assays (Table 3.1 and Supplementary S4); several of these chemicals were known TrxR inhibitors, thus validating our approach:

- **Auranofin** (S-triethyl- phosphinegold(I)-2,3,4,6-tetra-O-acetyl-1-thio-b-D-glucopyranoside; compound 30) inhibited all TrxRs with Trx or DTNB as

substrates; moreover, it proved to be very active despite the absence of selenium in these enzymes (IC$_{50}$ = 130-20 nM).

- The other gold(I) complex tested, **GoPI-Sugar** (1-phenyl-bis(2-pyridyl)phosphole gold chloride thio-β-d-glucose tetraacetate ; compound 31), showed a low IC$_{50}$ for AgTrxR and AmTrxR with their cognate Trxs (30 and 50 nM, respectively), but this is 10 times higher than that observed for the human ortholog (4.3 nM) (Jortzik et al., 2014) suggesting that selenium plays an important role. In the case of AaTrxR, it was more efficient in the DTNB-reductase assay (IC$_{50}$ = 90 nM) than the Trx one (1 μM), unlike for the other two TrxRs.

- **Curcumin** inhibited AaTrxR and DmTrxR in the presence of their Trxs (IC$_{50}$ = 36.5 and 42.4 μM), but, again, this compound is 10 times more active against seleno-TrxRs like the rat's (3.6 μM) (Fang et al., 2005).

- The 1,4-naphthoquinone (**NQ**; compound 28) was also very active against AgTrxR, AaTrxR and AmTrxR, showing inhibition in the nanomolar range when tested with the endogenous substrates (IC$_{50}$ = 280 – 410 nM). These values are lower than those observed for other selenium-independent oxidoreductases like the TrxR of *P. falciparum* (750 nM) or the human GR (1.3 μM) (Morin et al., 2008). Interestingly, the IC$_{50}$ in the DTNB-reductase assay was higher in all the cases, suggesting that NQ is more active against the C-terminal active site.

The rest of the compounds identified in the screening showed inhibition in the low micromolar range.

Overall, the different TrxRs seemed to react similarly, but the only compound that showed inhibition of all TrxRs in the two assays was auranofin (GoPI-Sugar and compound 24 as well, if we only consider the Trx assay). Interesting differences in the inhibitory properties of the compounds are the following:

- Compounds 3 and 19 inhibit AgTrxR/DTNB but not AaTrxR/DTNB.

Table 3.1. Tested compounds and IC$_{50}$ values (µM) on different insect TrxR using the cognate Trx or DTNB as substrate

#	Mw (g/mol)	Anopheles gambiae		Aedes aegypti		Drosophila melanogster	Apis mellifera		
		Trx	DTNB	Trx	DTNB	Trx	Trx	DTNB	
1	414,93		> 300	162,90	> 300				Only *Aedes* + C-term?
2	486,55		94,88	46,21	82,16			109,90	
3	271,39		147,70	> 300	> 300				Only DTNB *Anopheles*
4	514,67		243,70	> 300	388,30				Only DTNB mosquitoes
5	275,22		> 300	> 300	> 300				
6	310,27		> 300	172,40	73,75				Only *Aedes*
7	267,22		94,38	> 300	146,70				Only DTNB mosquitoes
8	467,22		> 300	93,90	> 300	26,70			C-term?
9	460,51		98,62	66,45	63,39				Only DTNB mosquitoes + *Aedes* Trx.
10	342,35		> 300	> 300	> 300				
11	403,52		> 300	> 300	> 300				
12	260,25		> 300	> 300	> 300				
13	486,55		197,50	124,10	84,59				Only DTNB mosquitoes + *Aedes* Trx.
14	245,20		> 300	> 300	> 300				
15	229,23		> 300	> 300	> 300				
16	152,15		> 300	> 300	> 300				
17	248,2		> 300	> 300	> 300				
18	264,24		24,80	133,90	43,02			72,00	More active with DTNB
19	254,36		295,20	> 300	> 300				Only DTNB *Anopheles*
20	335,47		> 300	> 300	> 300				
21	336,19		55,90	41,78	55,58		112,10*	169,70	More active on mosquitoes
22	344,07		> 300	> 300	> 300	> 300			
23	338,52		> 300	317,10	233,10				Only *Aedes*
24	344,52	44,80	35,80	47,48	66,46	31.70 *	61,50*	> 300	More active on mosquitoes with DTNB
25	220,36		> 300	> 300	> 300		> 300		
26	264,33		> 300	> 300	> 300				
27	368,38		73,97	36,47	> 60	42,40		91,78	**Curcumin**
28	158,16	0,28	1,15	0,37	89,77		0,41	308,20	**NQ**, C-term?
29	172,18	285,00	> 300	> 300	> 300	128,00	120,70		**Menadione**, C-term?
30	678,49	0,11	0,02	0,02	0,13	0,11	0,11	0,099*	**Auranofin**
31	928,74	0,03	0,12	1,00	0,09		0,05	65,39	**GoPI-Sugar**. More active on mosquitoes with DTNB
32	373,9		> 300	> 100	> 300	327,00	> 300		**Methylene blue**
33	357,2		> 300	78,73	> 200		210 *		C-term?
34	341,2		111,00	95,06	54,38		49,78		
35	355,18		> 300	27,09	278,00		25,17		C-term?
36	322,44		71,04	222,20	44,73		114,50		
37	354,51		88,29	137,40	70,01		> 300		Only DTNB mosquitoes + *Aedes* Trx.

Values determined in spectrophotometer except for * where determined in microplate reasder.
Left-most column indicated observations on specificity and potential mode of action. Name of known compounds shown in bold. Backgound color indicates IC$_{50}$ < 1 µM; < 10 and < 100 µM (from darker to lighter).

- Compounds 1, 6 and 23 were specific to AaTrxR.
- Compounds 1, 8, 33 and NQ probably target the C-term of the tested TrxR as they are more active on TrxR in combination with Trx than with DTNB.
- Compounds 21, 24 and GoPI-Sugar are clearly more active on mosquito TrxR in combination with DTNB.
- Compounds 4, 7, 9, 13 and 37 were active on both mosquito TrxR in combination with DTNB. Moreover, compounds 9, 13 and 37 were also active on AaTrxR with Trx, but not AgTrxR.

These results suggest it is possible to improve the specificity of the inhibitors.

B. Toxicity of inhibitors upon injection

To assess whether the TrxR inhibitors that we identified in our pilot screening had mosquitocidal activity, we tested them *in vivo* on *A. gambiae* adults. To increase the chance that the compounds would reach their inhibitory concentration range in the mosquito's body, we decided to test compounds whose IC_{50} in the AgTrxR/AgTrx1 assay were in the nano molar range (i.e. NQ, auranofin and GoPI-sugar). To make sure that the compounds were efficiently delivered, we first injected them directly into the hemolymph.

We dissolved the compounds in 100% DMSO to a final concentration of 100 mM, then we prepared 7 different solutions (10 mM - 0.1 mM) keeping the DMSO concentration constant (10 %). Unfortunately, GoPI-sugar was not soluble in these conditions and was therefore excluded from the assay. 1 week-old female mosquitoes were injected with 69 nL of each of these concentrations of auranofin or NQ. A control group was injected with 10% DMSO in each assay. We monitored lethality every 24 h for 1 week. Both compounds showed a lethal effect during the first 24 h of the assay (**Fig 3.3 A**). For the rest of the week, there was no significant mortality for either compound at any concentration, suggesting they are metabolized within 24 h. Moreover, this toxic effect seemed to be dose-dependent, with three exceptions. The mortality of the 0.1 mM NQ-injected group was abnormally high (60 %) as compared to other low doses; likewise, the DMSO control of the auranofin experiment was also very high (40 %). Injecting mosquitoes is a complicated process that requires optimal conditions to guarantee a good survival of the individuals;

parameters such as the thickness of the needle, the ressure exerted, or the entry point have a decisive role in the rate of success. Hence, we concluded that this high mortality was probably due to the injection process rather than the injected compounds themselves. Finally, the 8 mM auranofin solution – second most concentrated – had an abnormally low lethality (26.7 %). This mortality was similar to that observed for the second lowest concentration (considering the 0 mM control) (20 %). Because these two concentrations were placed in the second position of the dilution series from each end, it is plausible that a mistake was made when loading the injection needle and that the 0.1 mM solution was injected instead of that corresponding to 8 mM.

A

B
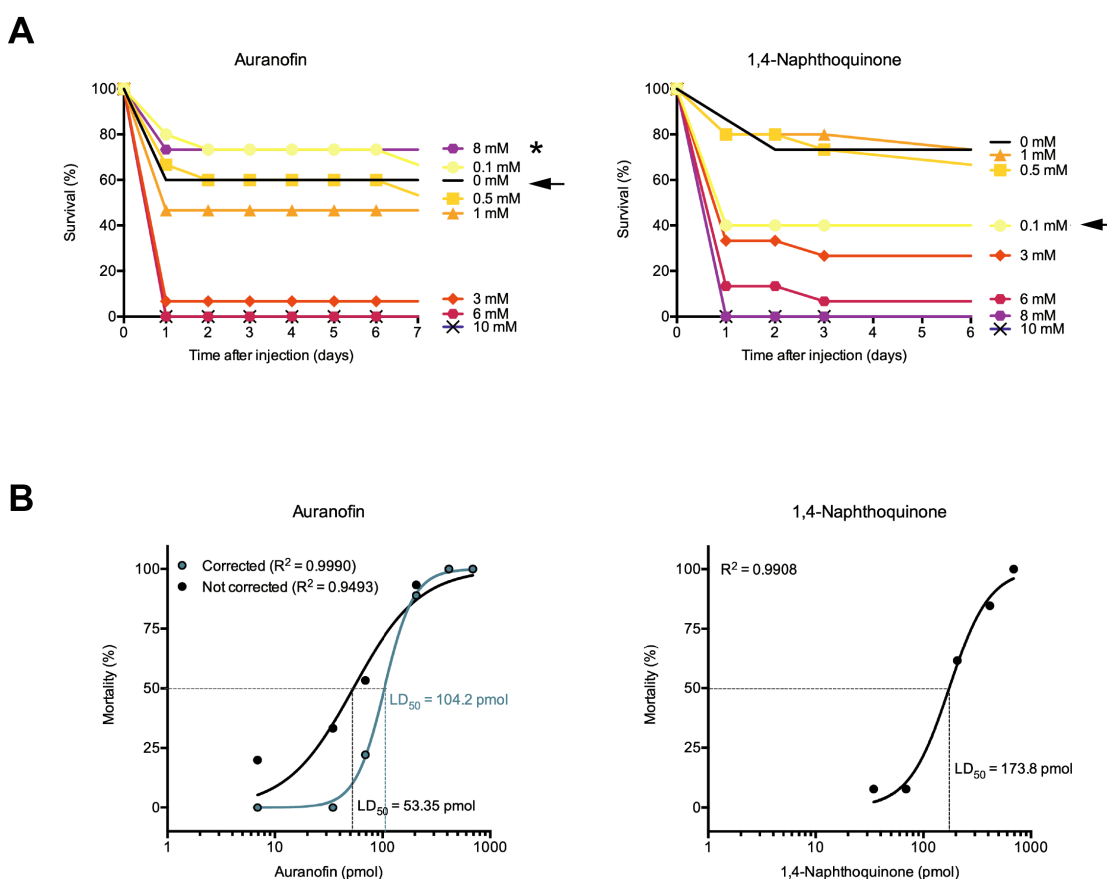
Figure 3.3. Injected auranofin and 1,4-naphthoquinone kill *Anopheles gambiae* mosquitoes in a dose-dependent manner in 24 h. (A) Mosquitoes were briefly anesthetized to receive injections with different doses of each compound. Their survival was followed for a week. Most individuals died within the first 24 h. Black arrows show doses with abnormally high lethality and stars, abnormally low as compared to similar doses in the same experiment. These doses were excluded for further analyses. **(B)** Lethality at 24 h correlates with the dose of the compound. For auranofin, the dose-response curve was estimated with the raw data (not corrected) or taking into account the high mortality of the control group (corrected). We calculated the LD_{50} for each situation (104.2 pmol or 56.11 ng/mg and 53.35 pmol or 28.73 ng/mg, respectively). For 1,4-naphthoquinone, the ED_{50} was 173.8 pmol or 14.86 ng/mg. Data represent one single experiment with 15 mosquitoes per group. R^2 represents the coefficient of determination.

Considering the mortality recorded at day 1, we estimated the lethal dose (LD$_{50}$) of each compound in these conditions (**Fig 3.3 B**). To do so, we excluded the above-mentioned groups and we corrected the mortality rates of the rest with that of the control groups; in the case of auranofin, we also did the calculations without correction. The LD$_{50}$ of NQ was 173.8 pmol, which corresponds to 14.86 ng of substance/mg of mosquito. Taking as a reference the ratio between hemolymph volume and body weigh estimated in A. *stephensi* (0.25 µl/mg) (Mack et al., 1979), this translates into a concentration of 23.48 µM. In the case of auranofin, it was 104.2 pmol (56.11 ng/mg; 20.67 µM) when we corrected the mortality and 53.35 pmol (28.73 ng/mg; 10.58 µM), when we did not. Thus, these two molecules appear to be toxic to mosquitoes in a dose-dependent manner when delivered in the body cavity by injection. These experiments should obviously be repeated to confirm the results but we decided to test the compounds in more realistic conditions than injection. Because auranofin had a lower IC$_{50}$ both *in vitro* and *in vivo* we chose this molecule for further characterization.

C. Effect of inhibitors upon oral administration

Current mosquitocides exert their toxic affect upon topic absorption. In order for a molecule to be active by this means, it must first penetrate the cuticle of he insect. This hard integument is composed of chitin, lipids and proteins covered by a thin layer of hydrocarbons that prevents desiccation. Thus, the capacity of a compound to penetrate this tissue depends on its lipophilicity. The most commonly used measure of lipophilicity in drug and pesticide design is the logarithm of partition coefficient octanol-water (logP), which is defined as the ratio between the concentrations of a given solute in these two solvents. The higher the value of logP, the more lipophilic a compound is and the more likely it will penetrate the cuticle (Webb and Green, 1945).

With the help of an online tool, we estimated that the logP of auranofin was 0.58, indicating rather low lipophilicity. Thus, we concluded that the toxicity of auranofin upon topic exposure would probably be hampered by a poor absorption. Therefore, we decided to test our compound upon oral entry. Although this is not the way in which insecticides are delivered to mosquitoes, this strategy can also be used when targeting pests, especially crawling insects. Moreover, our roGFP lines expressed

the construct in the midgut, thus we reasoned that this method would be best to assess the impact this molecule might have on the midgut glutathione pool.

Our first concern regarding this administration was the fact that it requires mosquitoes to actively uptake it. Thus, we first run a preliminary test to assess whether they would. *Anopheles gambiae* and *Aedes aegypti* females were starved for 6 h, then allowed to feed on a solution containing sugar, blue food coloring and 500 µM of auranofin. 24 h later, the cups containing *A. gambiae* mosquitoes were full of blue dots, suggesting females had fed on the solution properly. Additionally, some mosquitoes had blue abdomens and their midguts contained the blue solution (**Fig 3.4 A**). In contrast, 10 minutes after the beginning of the experiment, most of the *A.*

A

B

C
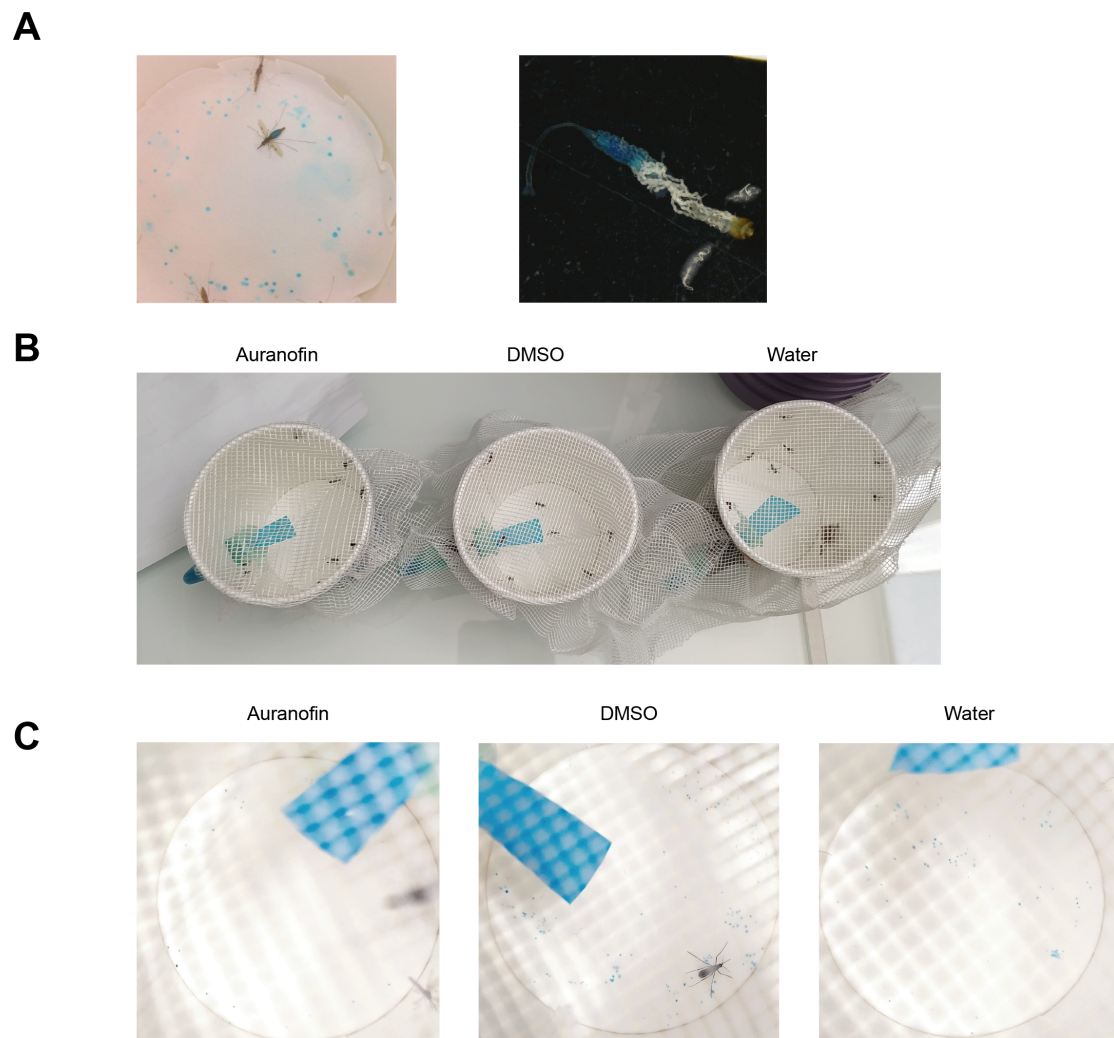
Figure 3.4. *Anopheles gambiae* mosquitoes, but not *Aedes aegypti*, feed on auranofin. Mosquitoes were starved for 6 h and allowed to feed on a solution containing auranofin (500 µM), DMSO 0.5% (v/v), sugar (5%, w/v) and blue food coloring (0.1%, v/v) for 24 h. Two controls were made in parallel: one did not contain auranofin and the other one did not contain auranofin or DMSO. **(A)** *Anopheles gambiae* females fed well on auranofin as demonstrated by the presence of blue dots at the bottom of the cup and blue coloring in the midgut. **(B)** 10 minutes after having been placed in the cups, most *Aedes agypti* females avoided contact with the auranofin-containing solution and **(C)** 24 h later they had barely fed on it as suggested by the very few blue dots at the bottom of the cup.

aegypti females present in the auranofin-containing cup rested as far as possible from the solution (**Fig 3.4 B**). 24 h later, only a few blue dots were present at the bottom of this cup (**Fig 3.4 C**), suggesting that females had barely fed on the solution. Therefore, we tested oral administration of auranofin on *A. gambiae* mosquitoes.

(I) Toxicity

To assess the toxicity of auranofin, we fed 8-10-day old mosquitoes with 7 different concentrations of the drug (500 - 5 µM) for 24 h. The compound showed a dose-dependent lethal effect in the micro molar range (LD_{50} = 277.6 ± 1.12 µM). For the lowest doses (5 - 25 µM) mortality was close to 0; for the two highest concentrations (250 µM and 500 µM), mortality higher, but in most cases, it did not reach 100% (**Fig 3.5 A**). We next repeated the assay using younger mosquitoes (3-5 day old). Since we did not reach a plateau for 100 % mortality in the previous experiment, we decided to include a higher concentration (1000 µM) this time. Again, auranofin showed a dose-dependent lethal effect on mosquitoes; however, we could not reach 50 % lethality within the range of concentrations that were tested (**Fig 3.5 A**). We thus hypothesized that young mosquitoes are less sensitive to auranofin.

To explore this, we fed mosquitoes at different ages with the same doses of auranofin (200 µM) or DMSO as control. 21-day-old mosquitoes showed higher mortality when fed with the vehicle than the other groups, although this difference was only statistically significant when compared to the youngest group (**Fig 3.5 B**). This phenomenon led to an average mortality of 30 ± 17.63 % in 21-day-old mosquitoes, which is above the percentage acceptable for a valid assay (i.e. 20 %). However, since the rest of the groups had mortalities between 0 % and 20 %, we exceptionally accepted these controls for comparison. As suggested by our previous experiments, susceptibility to auranofin increased with ageing, but it was only statistically significant when the oldest and youngest groups were compared. The mortality of the groups fed during the 2nd week post emergence was highly variable across experimental replicates (**Fig 3.5 B**). These differences were also observed in the dose-response assays (**Fig. 3.5 A**) and suggest that the changes leading to this age-dependent susceptibility might be occurring around this age.

In order to assess whether this lethal effect was due to the targeting of TrxR, we fed our TrxR KO_{MG} mosquitoes with auranofin. As presented in Chapter II, these mosquitoes lack the enzyme in enterocytes at the adult stage, as a result of somatic CRISPR/Cas9 mutagenesis. Although other tissues do express TrxR, we reasoned that the oral entry of auranofin would first impact enterocytes; thus, should TrxR be the main target mediating auranofin toxicity, we would expect to see a reduction in the mortality of the KOs as compared to control mosquitoes expressing TrxR. To test the hypothesis, we fed 1-2 week old TrxR KO_{MG} and control mosquitoes with 500 µM auranofin or just DMSO, and we counted the number of dead mosquitoes 24 h later. The experiment was repeated three times and in two of them, death was also recorded at 48 h. In two of the replicates, the mortalities of each group were similar and thus numbers were pooled; in the other one, mortality was lower and thus results analyzed separately. In both cases, TrxR KO_{MG} mosquitoes were less sensitive to auranofin during the first 24 h (p = 0.0009 for the non-pooled experiment and 0.0105, for the other two as determined by Fisher's exact test). On the contrary, at 48 h no difference was found (p = 0.0872) (**Table 3.1**). These results suggest that TrxR is at
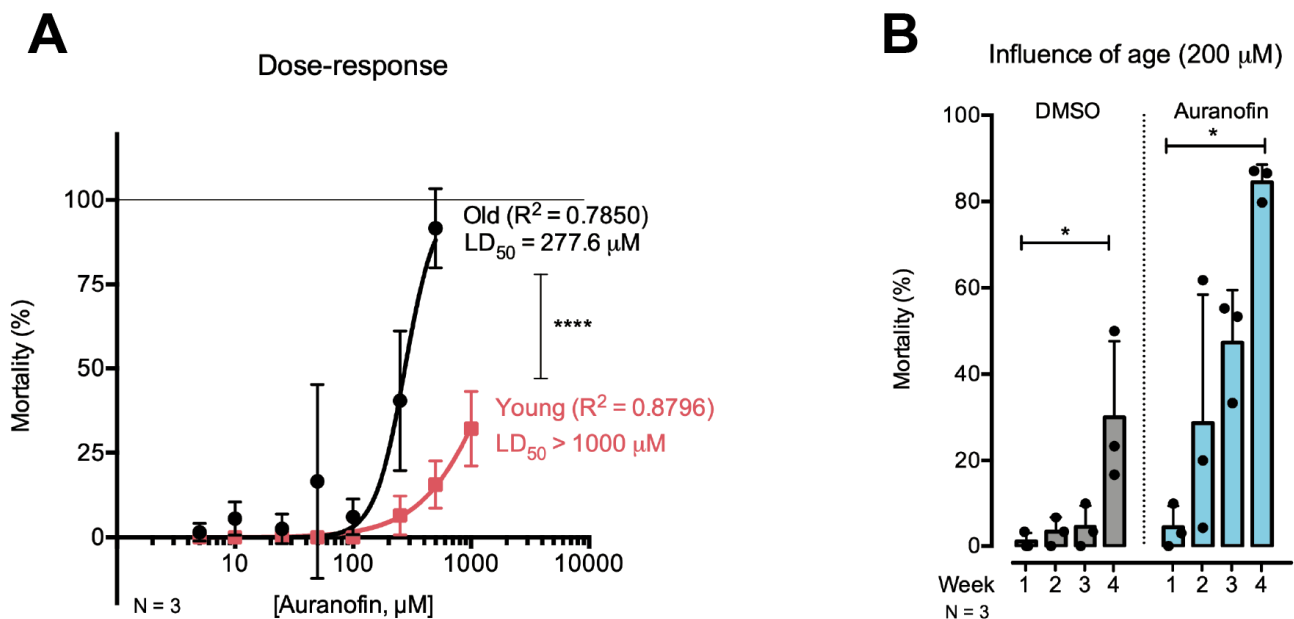
Figure 3.5. Auranofin is toxic to *Anopheles gambiae* mosquitoes upon feeding in dose- and age-dependent manner. (A) Dose-response toxic effect of auranofin in adult mosquitoes at two different ages upon feeding. Old (8-10 days post emergence) and young (3-5 days post emergence) *Anopheles gambiae* females were fed with auranofin at different concentrations (500 – 5 µM and 1000 – 5 µM, respectively). Groups fed with the solvent (DMSO) were used as controls. 24 h later, dead mosquitoes were counted. Dose-response curves were fitted using the Hill equation and curves compared using F-test. Points represent the mean of independent experiments (N) and error bars, SD. ****p < 0.0001. R^2 = coefficient of determination. **(B)** The sensitivity of adult mosquitoes to auranofin increases with the age. Females were fed with 200 µM auranofin or DMSO (control) at different weeks post-emergence. 24 h later, dead mosquitoes were counted. Bars represent the mean of three independent experiments (N; dots); error bars, SD. Statistical analyses were performed within each treatment group (DMSO or auranofin) using Kurskal-Wallis followed by Dunn post hoc. *p = 0.05. Comparisons not indicated were non-significant.

least partially responsible for the toxicity observed for auranofin in mosquitoes. The loss of effect of the TrxR KO with time could be explained by the diffusion of the compound to other tissues, or by the activity of the compound on other enzymes present in the mosquito gut.

Table 3.2. Lethality of 1-week-old control and midgut thioredoxin reductase (TrxR KO$_{MG}$) mosquitoes upon feeding with 500 µM auranofin.

Repetition	1		2 & 3			
Time point	24 h		24 h		48h	
Outcome	Dead	Alive	Dead	Alive	Dead	Alive
Control (n)	17	13	31	9	38	2
TrxR KO$_{MG}$ (n)	4	26	19	21	32	8
	Fisher's exact test *****p = 0.0009**		Fisher's exact test ***p = 0.0105**		Fisher's exact test p = 0.0872	

The experiment was repeated 3 times. For repetition 2 and 3 the results were similar and thus pooled for further analyses. For comparison, Fishers's exact test was performed. Significant p values indicated in bold.

(II) Redox homeostasis

Since we observed a toxic effect of auranofin upon oral administration, we next investigated whether it also had an oxidizing effect on the GSH pool. To that end, we fed groups of 1-week old cyto-roGFP and mito-roGFP mosquitoes with the same concentrations of auranofin as in the toxicity assays. 24 h later, we counted dead mosquitoes and dissected the midgut of the survivors to measure the 405 nm / 488 nm ratio. The 500-µM solution killed 100 % of the mosquitoes and thus we could not analyze the impact this dose had on glutathione. The cytoplasmic pool of glutathione displayed a dose-dependent increased oxidation (R^2 = 0.8655, p = 0.0071) (**Fig 3.6 A B**). In general, the degree of oxidation was more variable with higher doses suggesting unequal feeding among individuals. With regard to the mitochondrial pool
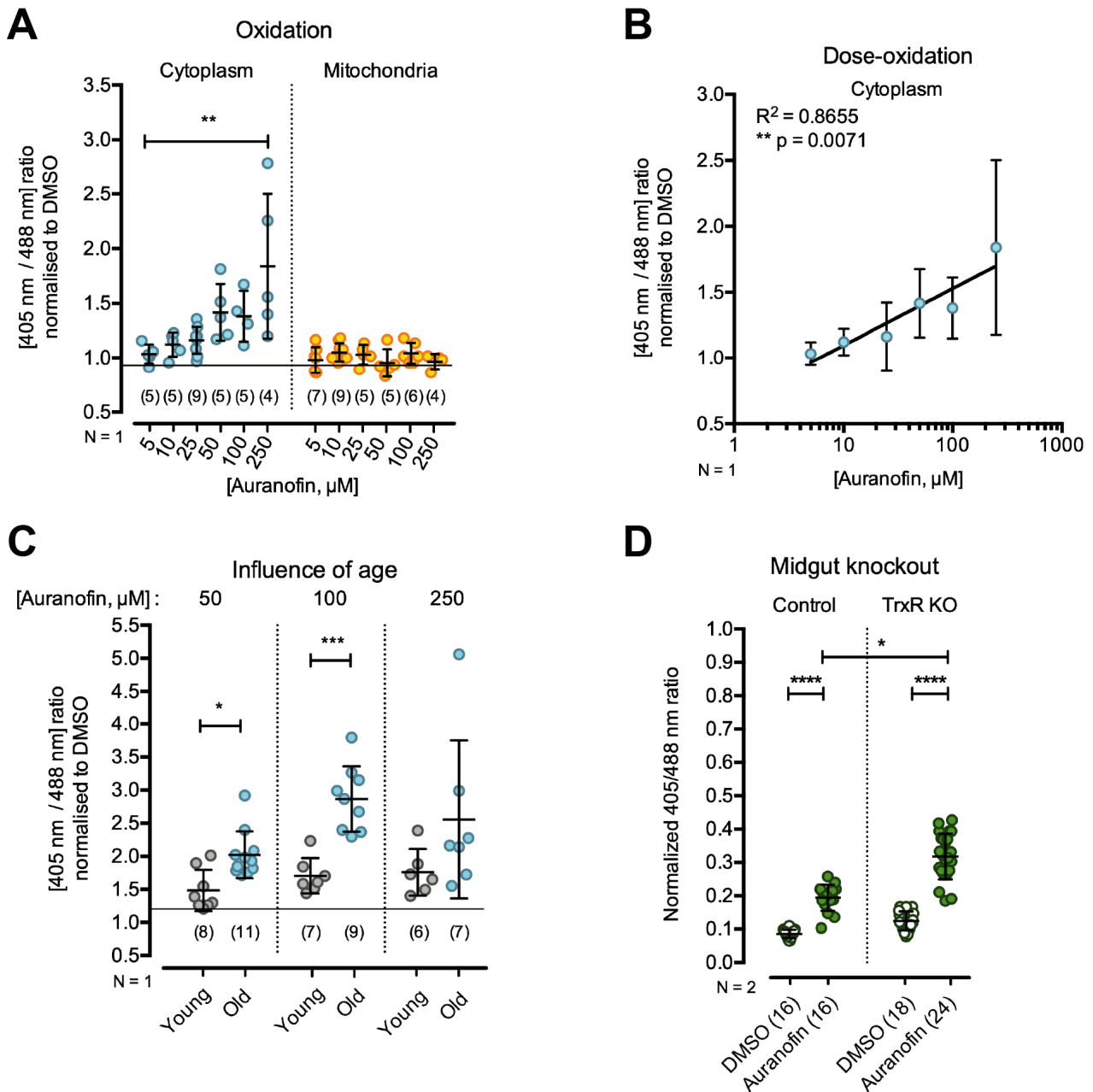
Figure 3.6. Auranofin induces age-dependent oxidation in the cytoplasm by a mechanism that is independent of thioredoxin reductase (TrxR) inhibition. Adult *Anopheles gambiae* females expressing hGrx1-roGFP2 in enterocytes were fed with auranofin and the redox state of the survivors analyzed by confocal microscopy 24 h later. The intensities obtained with the 405 nm laser were divided by those obtained with the 488 nm one and the resulting ratio was used as a measure of roGFP2 oxidation. **(A)** 3-5 day old females show an increase in oxidation in the cytoplasm, but not mitochondria. Mosquitoes were fed with auranofin at different concentrations (5 – 250 µM) or DMSO (control). The ratio for each concentration was divided by that of the DMSO controls. For the cytoplasmic line, **(B)** the average oxidation was plotted according to the dose and shows positive correlation; correlations was calculated using linear regression and the statistical significance of the slopes was calculated using F-test. R^2 = coefficient of determination. **(C)** The degree of oxidation depends on the age of the mosquitoe. Young (3-5 day old) and old (8-10 day old) mosquitoes were fed with auranofin at three different concentrations (50, 100 and 250 µM). **(D)** Mosquitoes lacking TrxR in the enterocytes are more susceptible to auranofin-induced oxidation. 8-10 day old females expressing (control) or not (TrxR KO) TrxR in enterocytes were fed with 200 µM auranofin or DMSO and the degree of oxidation 24 h later was normalized to a fully-reduced control. In all dot plots, horizontal and error bars represent mean and SD, respectively; dots represent values for individual mosquitoes and the total number of mosquitoes is indicated in brackets. Statistical analyses were performed using Kruskal-Wallis followed by Dunn post hoc. Only significant comparisons are indicated (*p < 0.05; **p <0.01; ***p <0.001; ****p < 0.000.1). N indicates the number of independent repeats.

glutathione, no oxidative effect was observed with any of the concentrations that were tested (**Fig 3.6 A**).

To investigate whether this effect on the cytoplasm was also dependent on the age of the mosquitoes, we repeated the experiment with 3-5 day old (young) and 8-10 day old (old) mosquitoes and the three highest concentrations of auranofin that we could analyze in the previous experiment (50 µM, 100 µM and 250 µM). For al the doses, the average oxidation was higher in older mosquitoes; these differences were only statistically significant for the 50 µM and 100 µM, probably due to the death of the most oxidized old mosquitoes before dissection (**Fig 3.6 C**).

To assess the role of TrxR in the auranofin-induced cytoplasmic oxidation, we fed 8-10 day old TrxR KO$_{MG}$ mosquitoes expressing roGFP (see Chapter II) with 200 µM auranofin or DMSO. As controls we used mosquitoes expressing only Cas9 or the gRNAs along with roGFP and we treated them with the same solutions. 24 h later, we dissected the mosquitoes and analyzed their midguts by microscopy. As expected from our previous data, control mosquitoes fed with auranofin showed oxidation in the cytoplasmic GSH pool. As we had previously shown that TrxR KO$_{MG}$ mosquitoes were less sensitive to auranofin, we expected a parallel reduction in GSH oxidation in TrxR KO$_{MG}$ midguts. In contrast, TrxR KO$_{MG}$ mosquitoes showed higher oxidation after auranofin feeding than control mosquitoes (**Fig 3.6 D**), suggesting that GSH oxidation upon auranofin treatment is likely due to the targeting of another protein and that TrxR alleviates this burden. It also indicates that increased GSH oxidation and mortality are not directly linked.

3. DISCUSSION

The toxic effect of TrxR inhibitors and their potential to act as medical drugs has been studied in the context of various pathologies (Andricopulo et al., 2006; Becker et al., 2000; Davioud-Charvet et al., 2003; Debnath et al., 2013; Harbut et al., 2015; McCarty et al., 2015; Owings et al., 2016; Regina et al., 2019; Tiwari et al., 2016; Urig and Becker, 2006; Zhang et al., 2019a; Zou et al., 2018). To our knowledge, and despite the catalytic differences between the insect and mammalian orthologs, their insecticidal potential had never been assessed before.

Here we have, for the first time, produced and purified TrxR and the major cytosolic Trx from *Aedes aegypti* mosquitoes and the honeybee *Apis mellifera*. Future characterization of the kinetics of these TrxRs will shed light on the mechanistic differences between selenium-dependent and –independent TrxRs and will guide us on the quest for more specific inhibitors.

We have designed and developed an efficient *in vitro* screening to detect inhibitors of insect TrxRs. Two different approaches were used. In most cases, the library was first tested on a microplate reader to discard the non-inhibitory compounds, and then positive hits were further characterized using a spectrophotometer. In general, the IC_{50} calculated with the microplate reader were lower than those obtained with the spectrophotometer for a given molecule. Still, the fact that we were able to identify more inhibitors in the spectrophotometer assays where the pre-screening was not performed, suggests that we may have overlooked the inhibitory capacity of some compounds when prescreening with a microplate reader, although probably not those in the low micromolar range and below. In the future, this should be taken into account when designing screenings.

A total of 21 compounds inhibited at least one insect TrxR in the nanomolar or low micromolar range using their endogenous substrates or DTNB. The lack of Sec in the C-terminal active site of insect TrxRs is compensated by a specific conformation that favors the protonation of the Cys residue; as a result this binding pocket and the mammalian one are different (Eckenroth et al., 2007) and insect TrxRs are not inhibited, or not as efficiently, by the most commonly used disulfide reductase inhibitors (Kanzok et al., 2001). Hence, the results of our screenings provide valuable

information on inhibitors that could be used against these species as well as on their modes of action.

In most assays, the IC_{50} of auranofin (compound 30) was around 100 nM. This is similar to its IC_{50} for the Sec $\rightarrow$ Cys mutant of the human enzyme (Lothrop et al., 2009) and low Mr TrxRs (Harbut et al., 2015; Owings et al., 2016), suggesting that auranofin is equally active against all selenium-independent TrxR. Still, the IC_{50} against AaTrxR (Trx assay) and AgTrxR (DTNB assay) was 5 times lower, similar to that found against wild type human TrxRs with selenium (Gromer et al., 1998). These assays should be repeated to confirm the observed difference and, if possible, in parallel with both wildtype and mutant human TrxR. Should the low IC_{50} be confirmed in these insect TrxRs, it would be interesting to crystallize them in the presence of auranofin to better understand their high reactivity against specific selenium-independent oxidoreductases.

Sequence alignment of several insect TrxR showed a high conservation of this enzyme (>60 %). Consistently, our screenings showed that, in general, insect TrxRs react similarly; however only auranofin (compound 30) was active against all of them with the two different substrates that we tested (i.e. Trx and DTNB). Further biochemical characterization of the mode of action of these inhibitors and potentially crystallization of the enzymes in their presence would help us to gain insight into this specificity and guide us into a more rational design of specific modulators. This pilot screen shed light into the specificity of some molecules. Based on the structure of the differential inhibitors, new molecules with different substituents should be tested. Of note, NQ inhibited most enzymes in the nanomolar range, whereas menadione, which contains an additional methyl group in position 2, did not. Thus minor changes the structure of the molecule might lead to great improvements in their reactivity against TrxRs.

We have further studied the potential of TrxR inhibitors to be exploited in an insecticidal strategy against malaria mosquitoes. First, we showed that both auranofin and NQ are toxic in a dose-dependent manner when they reach low micromolar concentrations in the hemolymph. To better characterize this phenomenon, we studied the effect of auranofin into more detail. This gold salt was originally approved as a treatment against rheumatoid arthritis under the name Ridaura; however, in the recent years its therapeutic applications have been intensively studied in the context of other pathologies such as cancer (Carlos Lima and Rodriguez, 2012; Onodera et al., 2019; Ralph et al., 2019), HIV (Diaz et al.,

2019) and fungal (Wiederhold et al., 2017), parasitic (Capparelli et al., 2016; Fan et al., 2017; Jones et al., 2016) and bacterial (Jang and Eom, 2019; Marzo et al., 2018) infections. In our assays, auranofin was delivered to mosquitoes by feeding. Surprisingly, this compound seemed to have a repellent effect on *A. aegypti* mosquitoes but not in *A. gambiae.* This conclusion was drawn from the observation that mosquitoes avoided contact with solutions containing this molecule and did not feed well on them. In the future, experiments should be repeated with different doses and in parallel with other TrxR inhibitors to elucidate the behavioral bases of this phenomenon and whether this is particular to auranofin or it is common to other TrxR inhibitors as well. In *A. gambiae* mosquitoes older than one week (after emergence), auranofin was toxic in a dose-dependent manner with an IC_{50} = 277 µM. In younger mosquitoes, the dose-dependent toxicity was still present but the IC_{50} was over 1 mM (maximum concentration tested). This age-dependent effect was further confirmed by feeding mosquitoes during the 1st, 2nd, 3rd and 4th week after emergence with the same amount of auranofin. This phenomenon was also observed for current insecticides (Collins et al., 2019; Machani et al., 2019; Mbepera et al., 2017; Rajatileka et al., 2011), thus suggesting that it might be due to an overall decrease of their capacity (i) to detoxify xenobiotics and/or (ii) to overcome the inflicted damage. Moreover, the great variability observed among experimental repeats of the groups fed during the 2nd week (4 – 62 %) suggests that these changes might occur at this period. In the future, it would be interesting to repeat the experiments controlling for the age in a more specific manner in order to elucidate the origin of these differences. *P. falciparum* parasites must develop during more than one week in the mosquito's body before they become infectious to humans; thus specifically targeting mosquitoes older than one week could limit the selective pressure for resistances, as they would still have time to reproduce.

In rats, auranofin is known to target TrxR and exerts its toxic effects on cells upon disruption of the mitochondrial function followed by apoptosis (McKeage et al., 2002; Rigobello et al., 2002, 2004). This is concomitant with an increase in mitochondrial H_2O_2 levels (Rigobello et al., 2005). Surprisingly, in mosquitoes, auranofin led to a dose-dependent oxidation of the cytoplasmic pool of GSH but not the mitochondrial one, indicating that the compound does not target mitochondria as efficiently or that the GSH oxidation observed in cells is due to TrxR-independent mechanisms. Other mechanisms associated with auranofin treatment (e.g. apoptosis) should be assessed to better understand its mechanism of action in mosquitoes. Mosquitoes that do not express TrxR in enterocytes were less susceptible to auranofin during the

first 24 h of treatment, but not 2 days after. These results suggest (i) that the toxic effect that we observe for auranofin is due, at least partially, to the targeting of TrxR and (ii) the midgut plays an important role when the drug is administered orally. Testing this compound in complete TrxR knockouts and/or in combination with other TrxR inhibitors will help elucidate whether the observed mortality at day 2 is due to the inhibition of other enzymes or to TrxR in other cell types.

The fact that mosquitoes lacking TrxR in enterocytes displayed higher cytoplasmic oxidation of the GSH pool than wildtypes, but lower lethality indicates that lethality is not a consequence of GSH oxidation. It further implies that the GSH oxidation is due to another target than TrxR and that TrxR alleviates this oxidation either by directly controlling the GSH pool or scavenging ROS (e.g. H_2O_2 through peroxiredoxins). The lack of mitochondrial oxidation could be explained by the absence of this target in this organelle. Repeating these experiments in combination with inhibitors of the GSH biosynthesis pathway or other redox enzymes may shed light into the origin of this oxidation.

In conclusion, we have developed an efficient *in vitro* assay to identify inhibitors of insect TrxRs and we have provided with new insight on the inhibitory capacity of several known and novel compounds. Likewise, we have shown that the TrxR inhibitor auranofin has mosquitocidal activity upon oral ingestion, which could be exploited to develop sugar baits. In the future, auranofin and other TrxR inhibitors that may be more lipophilic, should be tested upon topic exposure assays to assess the aptitude to be used in conventional delivery methods (i.e. ITNS and IRS). Moreover, it would also be interesting to test it in combination with current insecticides to see if it has a synergistic effect, especially in metabolic resistant strains. Interestingly, human GST P1-1 is a target of auranofin (De Luca et al., 2013), thus this compound might help break GST-dependent resistances.

CONCLUSIONS

This thesis explored the role of thioredoxin reductase in the disease-transmitting mosquito *Anopheles gambiae* and its potential as a novel insecticide target. The findings of this project contributed to a better understanding of the regulation and of the physiological relevance of the glutathione redox couple in insects and questioned its direct relationship to the thioredoxin system, and provided new insecticidal leads.

Previous data obtained in *D. melanogaster* and *A. gambiae*, suggested that, in absence of GR, oxidized glutathione is recycled by Trx. Indeed glutathione is found in high quantity in mosquito species, most of it in being in the reduced form (Abdu et al.; Hazelton and Lang, 1984). *In vitro*, the Trx/TrxR systems from *D. melanogaster* and *A. gambiae* show efficient GSSG-reductase activity and, in lysates, GSSG reduction can only be attained upon addition of Trxs (Kanzok et al., 2001). Moreover, knocking down TrxR in the imaginal disks of *D. melanoasgter* results in increased GSH oxidation (Albrecht et al., 2011).

Consistently with a putative role of glutathione as a redox buffer, we show that, in the midgut, both the cytoplasmic and mitochondrial glutathione pools are mostly reduced and quite stable over time, even when mosquitoes are exposed to oxidative challenges (e.g. blood feeding, and hydroperoxide and paraquat feeding). We however identified three noticeable exceptions with clear increase in the oxidation of the glutathione pool: (i) during pupation, at a time when the larval midgut tissue is destroyed and replaced by the adult tissue, (ii) in midgut cells undergoing cell death that are expelled from the midgut epithelium upon parasite infection, and (iii) in aging male mosquitoes, although the oxidation levels were more variable there. Increased oxidation in these cases is likely linked to tissue remodeling, autophagy and/or cell death, possibly a consequence rather than the cause, a hypothesis that will be interesting to investigate experimentally. Of note, males generally have more variable levels of glutathione oxidation compared to females, especially during aging as mentioned above. Whether these differences are due to a differential regulation of the glutathione pool itself between males and females (e.g. lower biosynthetic capacity of males), to a different antioxidant capacity in general (e.g. lower levels of other antioxidants), and/or whether they are linked to early cell death linked to their shorter lifespan, remains elusive.

In contrast to our starting hypothesis, our data suggest that the glutathione pool is not maintained reduced by the TrxR/Trx system in the midgut, or at least not exclusively. Indeed, the knockout of TrxR in enterocytes does not lead to an increase

of the oxidation of the glutathione pool, leading to the question of how this pool is maintained reduced in the absence of both GR and TrxR. Our first hypothesis was that another oxidoreductase was responsible for the recycling of glutathione in *A. gambiae* mosquitoes; however, we did not detect any up-regulation of potential candidates in our transcriptomic analyses. Another possibility is that high GSH levels are maintained by the biosynthesis pathway as it has been reported in mouse hepatocytes (Eriksson et al., 2015), or that it is imported from other tissues that express TrxR. In favor of the former, cystinosin was upregulated in non-blood fed TrxR KO$_{MG}$ midguts and GGT, downregulated 7 pBF. Blocking the glutathione biosynthesis pathway in TrxR-KO$_{MG}$ will help us elucidate this point. Moreover, we have now developed a conditional system to express the CRISPR/Cas9 effectors at the adult stage and in all tissues, which will be instrumental to test whether TrxR is indeed fully dispensable in adults. Combined with the ubiquitous expression of the hGrx1-roGFP2 reporter, it will also allow us to investigate the link between the glutathione and thioredoxin systems in other tissues and confirm/infirm their independence. Of note, a recent paper described a new redox sensitive reporter (TrxRFP1), similar to the hGrx1-roGFP2, but in equilibrium with the Trx pool and coupled with a red fluorescent reporter (Fan et al., 2017). This reporter would have to be adapted in order to be used in *A. gambiae*, however it would be instrumental to follow the oxidation of the Trx pool in Trx-KO cells, and would allow us to follow the oxidation of both the glutathione and the Trx pools when used in combination with hGrx1-roGFP2, a key experiment to further investigate the link between the two systems. In the future, studying other partakers of the redox network could help elucidate how mosquitoes maintain their redox homeostasis, notably in the absence of GR and TrxR, for instance, using H_2O_2 redox sensors (i.e. Orp1-roGFP2) or measuring the expression levels of different antioxidants or their antioxidant capacity in biochemical assays.

Consistently with the absence of an increase in glutathione oxidation in TrxR-KO enterocytes, TrxR-KO$_{MG}$ mosquitoes have no fitness issue. In contrast, they are even more resistant to oxidative stresses such as blood feeding and feeding on paraquat. These unexpected results could be explained by the up-regulation of detoxification enzymes (i.e. P450s, GSTs and ABC transporters) in the midgut of TrxR KO$_{MG}$ females. Additionally, our transcriptomic analysis also detected changes in metabolic networks, which could contribute to a better use of the nutritional content of blood feedings resulting in extended lifespan. The transcriptional signatures observed in TrxR-KO$_{MG}$ midguts, with the upregulation of genes involved in metabolism, immunity

and detoxification are reminiscent of the overactivation of the Nrf2 transcription factor. This could be the result of an increase in oxidative stress (Vomund et al., 2017) and/or a direct effect of a TrxR deficiency (Schmidt, 2015). The transcriptomic analysis will be repeated and resulting hypotheses validated, for instance by silencing candidate genes using RNA interference.

The phenotype of TrxR mutants during development was more striking than when limited to enterocytes in adult mosquitoes. Indeed, mutagenesis of TrxR in *A. gambiae* egg led to complete abrogation of the embryonic development, a role of TrxR that is conserved in mice (Bondareva et al., 2007; Jakupoglu et al., 2005) and most likely *D. melanogaster* where maternal transmission of TrxR mRNA sustains early development, underlying the importance of this enzyme at this stage (Missirlis et al., 2001). Mutating *TrxR* at a later timepoint during development led to a delay in larval development and severe lethality during pupation and adult emergence. We hypothesize that this phenotype could be due to deficiencies in the molting process. Moreover, most of the individuals that reached the adult stage had their legs trapped in the pupal case and presented severe morphological deformations. This phenotype is similar to that observed in mosquitoes treated with juvenile hormone (JH) analogs (Spielman and Williams, 1966). JH is a key hormone in insects that sustains larval development; JH levels must therefore decrease at the end of the last larval instar in order for the insect to undergo pupation (Goodman and Cusson, 2012; Zhu and Noriega, 2016). Thus, a plausible explanation for the developmental phenotypes of TrxR-KO would be a defect in the decrease of JH levels. Of note, AGAP008648 was up-regulated in TrxR KO_{MG} midguts in 4 of the 5 comparisons that we performed in our transcriptomics analyses. The product of this gene has a predicted farnesoic acid O-methyl transferase domain, known to be involved in the biosynthesis of juvenile hormone. To elucidate whether this is the cause of our phenotype, JH levels could be tittered during development and metamorphosis in wildtype and TrxR-KO mosquitoes. Alternatively, JH analogs and antagonists might also be of use. Should JH be involved in our phenotype, this finding would uncover a novel role of the TrxR/Trx system in hormonal control in insects. In any case, the essentiality of this gene during development suggests it could also be a target for larvicides.

Furthermore, we provided a proof of principal that the oral administration of a small molecule targeting TrxR, in this case auranofin, has mosquitocidal activity against *A. gambiae* adults. The fact that TrxR-KO_{MG} mosquitoes are less sensitive to auranofin during the first 24 h confirmed that TrxR is indeed a target of auranofin in the midgut,

although we cannot exclude that other enzymes are targeted. This and the increased oxidation of the glutathione pool in TrxR-KO$_{MG}$ mosquitoes upon auranofin treatment contrast with their improved fitness upon oxidative challenges. The discrepancy could be due to the progressive adaptation of KO mosquitoes to the absence of TrxR activity that results in a normal lifespan and better protection of enterocytes from oxidative challenges. In favor of this hypothesis is the observation that auranofin treatment also led to an increase in GSH oxidation that was enhanced in the absence of TrxR, suggesting that TrxR-KO cells may rely more heavily on GSH-based mechanisms to deal with the induced oxidative stress. Alternatively, both oxidation and lethality could be linked to the inhibition of a different target. To elucidate the mode of action of auranofin in mosquitoes, these experiments should be repeated in combination with other TrxR inhibitors as well as other molecules targeting detoxification enzymes. Should the higher glutathione oxidation be due to another molecular target it will help us elucidate the regulation of GSH homeostasis in mosquitoes and provide us with new insecticidal targets.

We also developed an efficient screening assay to identify inhibitors of insect TrxRs *in vitro*. As a result, we identified several inhibitors, providing valuable information on molecules that could be used to inhibit TrxR in insects and potential hits to look for species-specific inhibitors. In order to perform these screenings, we also produced, for the first time, the major cytosolic Trx and TrxR from the honeybee *Apis mellifera* and from the disease-transmitting mosquito *Aedes aegypti*. In the future, the biochemical characterization of these enzymes will contribute a better understanding of the catalysis of selenium independent TrxRs.

Finally, we also contributed to the development and characterization of novel tools for mosquito transgenesis and CRISPR/Cas9 gene editing, notably to generate mutants in an inducible and tissue-specific manner in adult mosquitoes. This has often been a try/fail and try again story, but we are confident these tools will be useful to mosquito community.

MATERIALS AND METHODS

MOSQUITOES

1. Rearing

Mosquitoes were reared in an insectarium with a relative humidity of 75%, a temperature of 27 ± 2 ºC and 12 hours day/night cycle. Larvae were grown in deionized water for eight to ten days and fed with TetraMin grinded fish food. Prior to emerging, pupae were placed in cages with mosquito nets and adults were fed with a 10% sucrose solution.

Blood meals were done on anesthetized CD1 mice. For this, mice were anaesthetized via an i.p. injection of 8.5 mg/kg of xylazine (Rompun) and 42.5 mg/kg of a mix of tiletamine and zolazepam (w/w 1:1, Zoletil) diluted in saline solution (85 ul of the mix injected per 10 g) and exposed to mosquito bites for 15 min. Two days after blood feeding, females were allowed to lay eggs on a filter paper soaked in deionized water; 2 days later, newly hatched larvae were placed in a container with deionized water to begin the cycle again.

All experiments using mice (including infections, see below) were performed at the Institut de Biologie Moléculaire et Cellulaire (Strasbourg, France), using facilities and protocols adhering to national regulations of laboratory animal welfare in France. Facilities and protocols have been certified by the regional veterinary services (authorization N° F67-4822) and by the national ethics committee in animal experimentation (authorization for project APAFIS-20562-2019050313288887 v3), respectively.

2. Lines

Anopheles gambiae

dsRNA-mediated knockdowns and dose-response assays were conducted using the G3 Anopheles gambiae laboratory strain isolated in Gambia in 1975.

To establish new transgenic lines, two differ docking lines were used. Both of them carried an attP site at a known locus on the genome for ΦC31 integrase mediated transgenesis (Table M1). To study the redox homeostasis of GSH, several lines expressing a roGFP2-based construct were generated (Table M2). To knockout TrxR several Cas9 and guide RNA (gRNA) lines were generated (Table M3).

Aedes aegypti

Auranofin feeding assays were performed using the Bangkok strain, a wild type strain isolated in Thailand in 2015. The hGrx1-roGFP2 transgene was integrated randomly into the genome of this line (see below).

Table M1. *A. gambiae* ΦC31 docking lines

Name	Chromosome	Marker	Background	Reference
X1	2L	-	G3	(Volohonsky et al., 2015)
E	3R	ECFP	Keele	(Pondeville et al., 2014)

Table M2. roGFP2-expressing lines

Transgene	Locus	Marker
Actin5c::hGrx1-roGFP2	X1	OpIE2::Puromycin^R
Actin5c::hGrx1-roGFP2	E	OpIE2::Puromycin^R 3P3::CFP
Actin5c::mito-roGFP2-hGrx1	X1	OpIE2::Puromycin^R
AAPP::hGrx1-roGFP2	X1	OpIE2::Puromycin^R
PolyUb::hGrx1-roGFP2	Random (*Aedes)*	–

All lines are *A. gambiae* mosquitoes except when otherwise indicated.

Table M3. *A. gambiae* lines to knockout *TrxR*

System	Transgene	Locus	Marker
Development	Vasa::Cas9	X1	3P3::YFP
Development	Vasa::Cas9	X1	3P3::RFP
Development	Vasa::Cas9	X1	3P3::YFP; 3P3::GFP (Chr. Y)
Development	Vasa::eSpCas9	X1	3P3::RFP
Development	3x(U6::gTrxR)	E	3P3::RFP (nuclear) 3P3::CFP
Midgut	G12::eSpCas9	X1	3P3::RFP
Midgut	G12::3x(tRNA$_{Gly}$-gTrxR)	X1	3P3::CFP
Conditional	Q::Cas9 TrxR::hGrx1-roGFP2-$_{T2A}$-QS-$_{T2A}$-QF	X1	OpIE2::Puromycin^R
Conditional	Q::Cas9 Rpl19::hGrx1-roGFP2-$_{T2A}$-QS-$_{T2A}$-QF	X1	3P3::CFP
Conditional	TrxR::3x(tRNA$_{Gly}$-gTrxR)	X1	3P3::RFP (nuclear)
Conditional	Rpl19::3x(tRNA$_{Gly}$-gTrxR)	X1	3P3::RFP (nuclear)

3. Infections with *P. berghei* parasites

Female mosquitoes were allowed to feed on anesthetized mice infected with transgenic P. berghei parasites expressing fluorescent markers at 21 ºC. For this, 8- to 12-week-old male Hsd:ICR mice (bred in-house from couples purchased from Charles River) were infected with the P. berghei ANKA malaria strain constitutively expressing GFP (Manzoni et al., 2014) or RFP. For this, blood was taken by heart puncture from a donor mouse with a parasitaemia of 3–5 %, diluted in PBS to 10^8 parasitized erythrocytes per ml. 0.2 ml of this suspension was injected intravenously into mice. Parasitaemia was monitored 3 days post passage via FACS analysis (Accuri 6, BD Biosciences) and mosquitoes were allowed to blood feed on mice with

parasitemia between 2-4 %. For this, mice were anaesthetized via an i.p. injection of 8.5 mg/kg of xylazine (Rompun) and 42.5 mg/kg of a mix of tiletamine and zolazepam (w/w 1:1, Zoletil) diluted in saline solution (85 ul of the mix injected per 10 g) and exposed to mosquito bites for 15 min. Fully engorged mosquitoes were sorted and kept at 21 ºC in standard humidity and day/night conditions in a chamber (Percival Scientific) until dissection.

To measure the intensity of infection, females were dissected under a transmission binocular magnifying glass (Nikon) and images taken under a SMZ 18 fluorescent stereomicroscope (Nikon). Parasites were counted manually in ImageJ.

4. Survival assays

Adult females were placed in paper cups and dead mosquitoes counted every 24 h for the duration of the assay. For regular survival assays, females were allowed to feed on 10 % sugar (w/v) ad libitum. For blood feeding survivals, females were sorted 24 h after the blood meal and unfed females, excluded from the assay. In hydrogen peroxide and paraquat feeding assays, the sugar solution was supplemented with the corresponding amount of each chemical. Solutions were prepared and changed every 24 h. In knockdown assays, mosquitoes having died within the first 12 h after injection were removed from the assay.

Graphs were computed using Kaplan-Meier plots in Prism 6 (GraphPad).

5. dsRNA injections

Mosquitoes were briefly anesthetized with CO_2 and immediately placed on ice. With the help of a Nanoject II microinjector (Drummond Scientific) each individual was injected with 69 nL of a dsRNA solution resuspended in H_2O (3 µg/µL). After injection, mosquitoes were immediately placed in the incubator to avoid desiccation.

MOLECULAR BIOLOGY

1. Genomic DNA extraction

DNA was extracted using the NucleoSpin Tissue XS kit (Macherey Nagel) as recommended by the manufacturer. Alternatively, the Phire Tissue Direct PCR Master Mix kit (Thermo Fisher) was used to genotype single females using one leg.

2. Total RNA extraction

Mosquitoes were grinded in RNAzol using a Precellys homogenizer (Bertin instruments), then centrifuged at 15 000 g for 5 min. The supernatant was transferred to a new tube and RNA isolated using the Direct-zol RNA MiniPep kit (Zymo Research) following the manufacturer's recommendation. DNA was removed using the RapidOUT DNA removal kit (Thermo scientific).

3. Complementary DNA (cDNA) synthesis

500 – 1000 ng of total RNA were mixed with 100 pmol of oligo(dT)$_{18}$ (Thermo Scientific) to a final volume of 12.5 µL, then incubated for 5 min at 65 ºC. Then buffer, RiboLock RNase Inhibitor (20 U), dNTPs (1 mM final) and RevertAid H Minus Reverse Transcriptase (200 U) (Thermo Fisher) were added, in that order, to a final volume of 20 µL. The reaction was incubated at 25 ºC for 10 min and then 42 ºC for 1 h. In parallel, a sample containing all the components except the reverse transcriptase was always done as a negative control.

4. PCR amplification

DNA fragments to be used for cloning were amplified using Phusion High-Fidelity DNA Polymerase (Thermo Scientific) following the manufacturer's recommendations. For colony PCR and gel genotyping (high fidelity not required) GoTaq Green Master Mix (Promega) was used instead.

Some primers contained additional sequences at the 5' extremity: T7 promoter (dsRNA templates), BsaI restriction sites (transgenesis) and BamHI/HindII/SphI restriction sites or 15 nucleotides of the destination plasmid (protein expression) (Table M4).

When required for downstream application, fragments were PCR or gel-purified using the NucleoSpin Gel and PCR Clean-up kit (Macherey Nagel).

Table M4. List of primers

Amp.	S	Sequence	Assay
hGrx1-roGFP2	F	**GGTCTC**A<u>TATG</u>GCTCAAGAGTTTGTGAACTGC	Golden gate
	R	**GGTCTC**A<u>AGCT</u>TACTTGTACAGCTCGTCCAT	Golden gate
Mito-roGFP2-hGrx1	F	**GGTCTC**T<u>ATGT</u>CCGTCCTGACGCCG	Golden gate
	R	**GGTCTC**A<u>GAGC</u>GAATTCTCCTCCTGATCCTCCTCC	Golden gate
hGrx1	F	**GGTCTC**A<u>GCTC</u>AAGAGTTTGTGAACTGC	Golden gate
	R	**GGTCTC**A<u>AAGC</u>TTACTGCAGAGCTCCAATCTGC	Golden gate
G12 promoter	F	**GGTCTC**T<u>ATCC</u>GGTACCCACAATACCG	Golden gate
	R	**GGTCTC**A<u>CATT</u>CTCGAGGATGCTAGATT	Golden gate
TrxR promoter	F	CC**GGTCTC**G<u>TATC</u>GCAAGCGCAAGCAGATCCT	Golden gate
	R	CC**GGTCTC**G<u>GAAC</u>CGTCTGCGGAACGCTGT	Golden gate
TrxR promoter	F	CC**GGTCTC**G<u>ATCC</u>GCAAGCGCAAGCAGATCCT	Golden gate
	R	CC**GGTCTC**G<u>ATGG</u>CGCTGCGGAACGCTGT	Golden gate
Rpl19 promoter	F	CC**GGTCTC**G<u>TATC</u>GGATTGATGTGTCGCTGGAAG	Golden gate
	R	CC**GGTCTC**G<u>GAAC</u>GCTGCTGGTTGTTTCCTCGG	Golden gate
Rpl19 promoter	F	CC**GGTCTC**G<u>ATCC</u>GGCATTGATGTGTCGCTGGAGG	Golden gate
	R	CC**GGTCTC**G<u>ATGG</u>GCTGCTGGTTGTTTCCTCGG	Golden gate

Amp.	S	Sequence	Assay
T2A	F	CC**GGTCTC**G<u>GAAG</u>GACGCGGCAGCC	Golden gate
	R	CC**GGTCTC**G<u>AGGG</u>CCAGGGTTCTCTTC	Golden gate
AgTrx1	F	GCGC**GGATCC**GTGTACATGGTGAAAGATTCC	Restriction cloning
	R	GCGC**AAGCTT**TTACGCCGAATGCTGCTGG	Restriction cloning
AaTrxR	F	ATAT**GCATGC**GCGCCCATCAATCAGGAAACTTC	Restriction cloning
	R	ATAT**AAGCTT**TTAACTGCAGCACGTGGCCG	Restriction cloning
AaTrx1	F	ATAT**GGATCC**GTGTACATTGTTAAGGATGCTGCTG	Restriction cloning
	R	ATAT**AAGCTT**CTAGGCGTGCTTCAAGATGTACATC	Restriction cloning
AmTrxR	F	ATAT**GGATCC**CCACCAATTGCTGATCAAAAATTCA	Restriction cloning
	R	ATAT**AAGCTT**TTAACTGCAACAACTTTGTGGCTTA	Restriction cloning
AmTrx2	F	ATAT**GGATCC**GTTTACCAAATTAAGAATGCCAGTG	Restriction cloning
	R	ATAT**AAGCTTT**TATTTGTGCTTCTGAATTGTGCTT	Restriction cloning
CpTrx1	F	caccatcaccATCACGTGTACGTCGTGAAAGATGC	In Fusion cloning
	R	aagctcagctaattaTTATTCGCTATGCTTGGTGAT	In Fusion cloning
CpTrxR	F	caccatcaccATCACGCGCCCATCAATCAGGAA	In Fusion cloning
	R	aagctcagctaattaTTAGCTGCAGCACGTGGC	In Fusion cloning

Amp.	S	Sequence	Assay
TrxR	F	*TAATACGACTCACTATAGGG*CCAGAAGGTGGAGTACGTGAA	dsRNA
	R	*TAATACGACTCACTATAGGG*CACCTCGAGCTTGTCCGACTT	dsRNA
TrxR	F	*TAATACGACTCACTATAGGG*ACGAACGTGCCGCACATCTAC	dsRNA
	R	*TAATACGACTCACTATAGGG*GTTGCAGGCAACGAATTGTCC	dsRNA
LacZ	F	*TAATACGACTCACTATAGGG*TGCCGCTCATCCGCCACATA	dsRNA
	R	*TAATACGACTCACTATAGGG*CACCGATCGCCCTTCCCAACAGT	dsRNA
Rpl19	F	CCAACTCGCGACAAAACATTC	qPCR
	R	ACCGGCTTCTTGATGATCAGA	qPCR
Cas9	F	ACACCACCATCGACCGGAAG	qPCR
	R	TACAGGCCGGTGATGCTCTG	qPCR
roGFP2	F	GGCAAGCTGACCCTGAAGTTC	RT-PCR
QF	R	CCTCGCATTATTCGAGGACG	RT-PCR

Restriction sites in bold; BsaI overhangs underlined; pQE30 complementary sequences in lowercase; T7 promoter sequence in italic.

5. Cloning

Depending on the downstream application, inserts were cloned into different destination vectors.

pJet plasmids

dsRNA template plasmids were cloned into pJET vectors (Thermo Scientific) following the manufacturer's recommendations.

pBluescriptSK-

To assemble transgenesis plasmids, the different inserts were first cloned into the SmaI or the EcoRV site of a pBluescriptSK- (Stratagene) in which the BsaI site had been mutated. To that end, a restriction-ligation was performed at the same time by mixing the PCR fragment, the plasmid, the restriction enzyme (SmaI or EcoRV, Invitrogen or Thermo Scientific) and T4 DNA ligase (Thermo Scientific) and incubating at room temperature for at least 1 h. SmaI or EcoRV buffer supplemented with 1 mM ATP (Thermo Scientific) was used as reaction media. After inactivation of the enzymes, more SmaI/EcoRV was added to cleave the empty vectors for 30 min.

Transgenesis vectors

The final transgenesis plasmids were assembled using GoldenGate cloning (Engler and Marillonnet, 2013). In brief, 40 fmol of each plasmid containing an insert and 40 fmol of the destination vector were mixed with BsaI (NEB) and T4 ligase; reactions took place in the BsaI buffer supplemented with 1mM ATP. Restriction-ligation was achieved by running 3-5 cycles alternating incubation at 37 ºC and 20 ºC for 10 min each. After that, ligation was favored at 20 ºC for 50 min before enzymatic inactivation at 80 ºC. For constructs that did not contain BsaI sites in the final plasmid, a sabotage step was performed to linearize empty vectors. To that end, more BsaI enzyme was added after inactivation and the mixture incubated for 30 min.

Some reactions included linkers to close gaps between incompatible BsaI overhangs (Table M5). To prepare them, 100 mmol of each complementary oligo were diluted in 1 mL of H_2O, then heated at 95 ºC for min and slowly cooled down to 25 ºC. 0.4 µL were used per reaction.

Transgenesis vectors contained a phage Φ31 attB site and a LacZ cassette flanked by BsaI sites. Additionally, they had two selection markers: a kanamycin resistance cassette for the cloning process and a transgenesis marker. The latter consisted of a fluorescent protein driven by the 3xP3 promoter that led to expression in the eyes

and nervous system or a puromycin resistance cassette driven by the OpIE2 promoter to allow for selection under puromycin treatment at the larval stage.

Table M5. List of linkers for Golder gate cloning

Construct	Sense	Sequence
G12::eSpCas9	F	<u>TAAG</u>TTTTACTTAAAGCATTTAAATT
	R	<u>AAGC</u>AATTTAAATGCTTTAAGTAAAA
3x(tRNA_{Gly}-gTrxR)	F	<u>ATAC</u>GGATATCCTTTCGAATCGTT
	R	<u>AAGC</u>AACGATTCGAAAGGATATCC

Overhangs underlined.

Protein expression vector (pQE30)

AgTrx1, AaTrx1, AaTrxR, AmTrx2, AmTrxR, CpTrx1 and CpTrxR were amplified from mosquito samples coming from pools of entire mosquitoes (G3 for *A. gambiae*, Bangkok for *A. aegypti* and wild *C. pipiens* collected in Strasbourg), whereas bee cDNA was kindly provided by Dr. Nicolas Hublot and came from pools of midguts.

AgTrx1, AmTrx2, AmTrxR, and AaTrxR were inserted into the pQE30 vector using restriction enzymes. In brief, genes were amplified with primers containing restriction sites. After purification they were mixed with pQE30 in a 5:1 ratio (insert/vector) and incubated with BamHI/HindIII (*Anopheles* and *Apis*) or SphI/HindIII (*Aedes*). After inactivation of the enzymes, each mix was incubated with T4 ligase in the presence of ATP. AaTrx1, CpTrx1 and CpTrxR were cloned using InFusion cloning (Clonetech). In brief, genes were amplified with primers containing a 15-nt long sequence complementary to the destination plasmid in their 3' end. In parallel, pQE30 was linearized by PCR, leaving the multiple cloning site out of the final product. Each gene was mixed with the linearized vector in a 2:1 ratio and incubated on ice for 15 min. Forward primers did not contain the ATG codon for any of the cloned genes as they were cloned downstream of an His-tag.

All clonings were performed using DH5α bacteria and the CaCl$_2$ transformation method (Manittais et al., 1989) or the Mix&Go kit (Zymoresearch). Bacteria were grown in agar plates containing Luria-Bertani (LB) medium supplemented with the adequate antibiotics for selection (100 μg/mL of carbenicillin/ampicillin for pJet, pBluescriptSK- and pQE30 and 50 μg/mL of kanamycin for the transgenesis vectors).

All plasmids were isolated using the NucleoSpin Plasmid EasyPure kit (Macherey-Nagel) and sequenced-verified.

6. Quantitative PCR (qPCR)

qPCRs were performed on cDNA (final dilution 1:50) using the Fast SYBR Green Master Mix (Thermo Scientific) in 15 µL and a 7500 Fast Real-Time PCR system (Thermo Fisher). All assays included two negative controls (no reverse transcriptase and no template) and melting curves were ran to confirm the absence of primer dimers. Rlp19 was used as housekeeping gene for normalization and the relative quantification done by the double-Ct method. For primers, see Table M4.

7. Reverse transcription PCR (RT-PCR)

RT-PCRs were performed on cDNA obtained from Q::Cas9-TrxR::hGrx1-roGFP2-QS-QF and Q::Cas9-rpl19::hGrx1-roGFP2-QS-QF as described in the cDNA synthesis section. For primers, see Table M4.

8. Double-stranded RNA (dsRNA) synthesis

First, the template was PCR-amplified (see PCR amplification section; see Table M4 for primers) from 1 ng of the plasmids containing the desired sequence. After gel purification, 1 pmol of the product was mixed with NTPs (7.5 mM final concentration of each), buffer at 37 ºC and 2 µL of T7 polymerase (MEGAScript T7 Trasncription kit, Thermo Scientific) to a final volume of 20 µL. The reaction was incubated at 37 ºC over night. The day after, samples were treated with 1 U of DNase I (Thermo Scientific) and incubated at 37 ºC for 15 min. Samples were brought up to a final volume of 100 µL in annealing buffer (100 mM Tris pH 7,7; 10 mM EDTA; 500 mM NaCl) and heated at 95 ºc for 5 min, then allowed to cool down to 25 ºC slowly. The final product was purified using the NucleoSpin RNA XS kit (Macherey Nagel). 1 µL of the purified product was diluted in 9 µL of water and 1 µL was used to measure the concentration in a NanoDrop OneC (Thermo Scientific). To check for the presence of dsRNA, the remaining 9 µL were mixed with loading buffer and split in two; one half was heated at 95 ºC for 5 min and immediately placed on ice. The presence of a shift between the heated and non-heated samples was checked on an agarose gel. The final products were diluted to 3 µg/µL. When required, samples were precipitated in 0.1 volumes of sodium acetate and 1 volume of isopropanol at -

20 ºC for at least 1 h; then, they were resuspended in RNase-free water to the desire concentration.

9. Production of polyclonal antibodies against insect TrxR

Immunogenic, highly conserved peptides were chosen using online tools and performing sequence alignment of various insect TrxRs (see corresponding sections). 3 mg of each peptide were synthesized by Proteogenix and used by Covalab to immunize two rabbits. On day 0, 14, 28 and 42, the animals were injected intradermally with of a mix of the two peptides. On day 39 and 53, 5 mL of blood were extracted and tested on western blot (see following section) for the ability to recognize TrxR in whole mosquito extracts. On day 67, the final sera were extracted from the rabbits and tested again on western blot. The one giving the best signal was purified on affinity columns containing the same peptides that were used for immunization. The peptides were coupled to active sepharose beads, then the serum was loaded for 1 h at 37 ºC; the column was washed and the retained antibodies were eluted to a final concentration of 207 µg/mL. The reactivity of the final, purified product was confirmed in western blots on whole mosquito extracts.

10. Western blot

At least 4 mosquitoes or 10 organs (e.g. midguts) were manually grinded in laemmli buffer (60 mM Tris-Cl pH 6.8, 10 % glycerol, 2 % SDS, 5 % β-mercaptoethanol and 0.01 % bromophenol blue) using a pestle. For non-reducing condition, β-mercaptoethanol was substituted for cOmplete Mini Protease Inhibitor Cocktail (Roche). Proteins were separated in hand-made PAGE gels and transferred to Hybond PVDF (GE Healthcare) membranes using a Pierce G2 Fast Blotter (Thermo Scientific). Membranes were blocked using Blotting-Grade blocker (Bio-rad) or Protein-Free Blocking Buffer (Thermo Scientific). Membranes were washed 3 times for 10 min between incubations with phosphate buffered saline (PBS) containing 0.1 % Tween-20. The signal was revealed using SuperSignal West Pico PLUS chemiluminescent Substrate (Thermo Scientific). For the antibody list and concentrations, see table M6.

Table M6. List of antibodies

Target	Origin	Reference	Western blot	Immunostaining
TrxR	Rabbit	Homemade	1/1000	1/250
Actin	Mouse	Millipore (MAB1501R)	1/1000	
Flag	Mouse	Sigma (F3165)	1/1000	
His	Mouse	Thermo (R930-25)	1/5000	
Rabbit-HRP	Goat	Promega	1/10000	
Mouse-HRP	Goat	Promega	1/10000	
NOS	Rabbit	Thermo (PA1-039)		1/100
Pbs21	Mouse	mAb 13.1		1/1000
Rabbit-Alexa647	Goat	Thermo		1/1000
Mouse-Cy3	Goat	Thermo		1/1000

TRANSGENESIS

1. Plasmids preparation

Bacterial clones carrying the desired plasmid were grown in 50 mL LB + 50 µg/mL kanamycin and the plasmid was purified with the NucleoBlond XtraMidi EF (Macherey-Nagel) kit following the manufacturer's instructions.

For injection, 400 ng/µL of each plasmid were prepared in 0.5x PBS to final volume of 80 µL. Additionally, the mix also contained 80 ng/µL of a plasmid expressing Φ31 recombinase.

2. Plasmids injections

Plasmids were injected into the posterior pole of mosquito eggs using a FemtoJet injector (Eppendorf) as described in Volohonsky et al (Volohonsky et al., 2015).

3. Transgenics selection

Injected mosquitoes were crossed with wild types and their progeny screened under a SMZ 18 fluorescent stereomicroscope (Nikon). Pupae were sorted by sex and crossed to their negative siblings. The next generation was sorted using a Complex Object Parametric Analyzer and Sorter (COPAS) as described in Marois et al (Marois et al., 2012). Fluorescent reporter genes expressed in the eyes and nervous system allowed to sort 1st instar larvae with the COPAS according to their fluorescence level, and thus to distinguish homozygous from heterozygous and wildtype siblings. Alternatively, OpIE::Puromycin^R transgenics were selected by adding 25 µg/mL puromycin to the breeding water.

IMAGING

1. Dissections

Mosquitoes were briefly anesthetized with CO2 and immediately placed on ice until the moment of dissection. Midguts or salivary glands were dissected under a transmission binocular magnifying glass (Nikon) in a drop of phosphate-buffered saline (PBS). In the case of roGFP-expressing midguts and salivary glands, PBS was supplemented with 20 mM N-ethyl-maleimide (NEM) for the samples and 2 mM diamide (DA) or 20 mM dithiothreiol (DTT) for the full oxidation and full reduction controls, respectively.

2. Conservation of roGFP redox state

Dissected midguts and salivary glands were treated as in (Albrecht et al., 2011). In brief, tissues were alkylated in 20 mM NEM for 15 minutes, and then they were fixed in paraformaldehyde (PFA) (4 %) for 20 min. In parallel, full oxidation and reduction controls were prepared by incubating some samples in 2 mM DA or 20 mM (DTT), respectively, prior to alkylation. All compounds were prepared in phosphate-buffered saline. Midguts were mounted with VectaShield and stored at 4ºC in the dark until analysis.

3. Immunostainings

Tissues were fixed in 4% PFA for 40 min, and then permeabilized for 15 min in PBS containing 0.1% Triton-X 100. Samples were blocked in PBS containing 0.1% Triton-X 100 and 1% bovine serum albumin (BSA) for 3 h at room temperature. Primary and

secondary antibodies were diluted in blocking buffer and incubated for 1h at room temperature or overnight at 4ºC. 3 washes of 10 min with PBS were performed after each incubation. For the antibody list, see table M6.

4. Microscopy

Samples were imaged with a Zeiss Axio Observer Z1 Confocal LSM780 microscope equipped with an Evolve™ 412 EMCCD (Photometrics) camera. Images were taken with the Plan-Apochromat 20x/0.8 dry objective or 63x/1.4 oil objective.

For roGFP imaging, the fluorescent probe was excited sequentially at 405 and 488 nm and its emission signal was recorded at 500-530 nm.

5. roGFP images processing

Images were processed in ImageJ following the protocol described in (Kardash et al., 2011). In brief, background was substracted by using the rolling ball procedure set to 50 pixels and images converted to 32-bit. Then, the smooth procedure was applied and images stacked. The intensity of the 488 nm images were thresholded with the default settings in black and white and dark background; values below threshold were set to "not a number". The ratio images were generated by dividing the 405 nm pictures by the 488 nm ones using the Ratio Plus plugin, and colored using the lookup table "fire". For normalization, the obtained intensities were normalized to the DTT control.

To estimate the redox potential of glutathione (E_{GSH}) from these images, we first calculated the degree of oxidation of the roGFP2 probe (OxD_{roGFP2}):

$$OxD_{roGFP2} = \frac{R_{sample} - R_{reduced}}{\frac{I488_{oxidized}}{I488_{reduced}} \left(R_{oxidized} - R_{sample} \right) + \left(R_{sample} - R_{reduced} \right)}$$

where I488 is the intensity of the picture obtained with the 488 laser and R, the ratios. Then, E_{GSH} was calculated using the Nerst equation,

$$E_{roGFP2} = E^{o\prime}_{roGFP2} - \frac{RT}{2F} \ln \left(\frac{1 - OxD_{roGFP2}}{OxD_{roGFP2}} \right)$$

where $E^{o'}_{roGFP2}$ is the midpoint redox potential of roGFP2 (- 280 mV), R is the gas constant (8.315 J K^{-1} mol^{-1}), T the absolute temperature (298.15 k) and F the Faraday constant (96 485 C mol^{-1}).

TRANSCRIPTOMICS

1. Sample preparation

G12::gTrxR and G12::eSpCas9 males and females were mixed and allowed to mate. The progeny was bred together. On day 5 after adult emergence, females were sorted according to their genotype with the help of a SMZ 18 fluorescent stereomicroscope (Nikon). 10 mosquitoes per population were dissected on ice and their midguts immediately placed in 50 μL RNAzol (Sigma) and stored at -80ºC for further RNA extraction; in parallel, 5 additional midguts were dissected, placed in Laemli buffer and stored at -20ºC for western blot analyses. The rest of the mosquitoes were allowed to feed on a mouse (same mouse for the 3 populations). 24 h later, the females that had not fed on blood were removed from the groups, and 3 days after blood feeding, midgut dissections were repeated as for the non-blood fed samples. 1 week after blood feeding, midguts from G12::gTrxR and knockout females were dissected and placed in RNAzol. No western blot samples or G12-Cas9 mosquitoes were taken at this time point.

When all samples had been collected, tissues were disrupted manually using and pestle and RNA was extracted using the Direct-zol RNA MicroPrep kit (Zyme Research) following the manufacturer's instructions. The final elution volume was 25 μL. DNA was removed from the samples using the RapidOut DNA removal kit (Thermo Scientific) and the final RNA concentration measured using a Qubit 2.0 fluorometer (Invitrogen). Additionally, the quality of the RNA was assessed in an Agilent 2100 bioanalyser using an RNA 6000 nano chip (Agilent) according to the manufacturer's instructions.

2. Libraries preparation

Libraries were prepared following the instructions described in NEBNext ultra directional RNS library prep kit for Illumina. In brief, total RNA was fragmented and primed using the NEBNext Poly(A) mRNA magnetic isolation module and a 96S super magnet plate (Alpaqua), to obtain 200 bp fragments. Next, cDNA was

synthesized using actinomycin D (Sigma) and the library enriched using the adaptor and oligos from the NEBNext multiplex oligos for Illumina set 1 and 15 cycles of amplification. CleanNA NGS beads (GC biotech) were used for purification throughout the whole protocol.

Final products were quantified using a Qubit 2.0 fluorometer (Invitrogen) and their profiles assessed in an Agilent bioanalyzer using a High sensitivity DNA kit (Agilent). To improve the selection of fragments >320 bp, samples were pool in equal ratios and purified with CleanNA NGS beads using a 0.7/1 ratio.

PRODUCTION OF RECOMBINANT PROTEINS

1. Expression

M15 bacteria were transformed using the CaCl2 method(Manittais et al., 1989) or the Mix&Go kit (Zymoresearch). Bacteria were grown in LB medium containing 50 µg/mL of carbenicillin and 50 µg/mL kanamycin. One clone from each construct was grown at 37ºC in 3 mL LB medium containing carbenicillin (50 µg/mL) and kanamycin (50 µg/mL), for 8-10h. These cultures were then used to inoculate 250 mL cultures containing the same medium. After overnight incubation under the same conditions, they were used to inoculate 1-L cultues containing the same medium. These cultures were grown at 37ºC until OD_{600} =0.6-0.7. Finally, protein expression was induced for 4h by addition of 1 mM IPTG.

2. Extraction

Bacteria were harvested by centrifugation at 4ºC and 12 000 g for 15 min. Pellet was resuspended in 15 mL of 50 mm Na_2HPO_4 buffer with 300 mm NaCl, pH 8. To avoid degradation, 150 nM pepstatin, 100 µM phenylmethylsulfonyl fluoride and 40 nM cystatin were added. Cells were lysed by sonication (three cycles of 30 sec at 70% and 4ºC) in the presence of 16 mg/L of lysozyme and 100 µg/mL of DNase I. Proteins were recovered after centrifugation at 4ºC and 25 000 g for 30 min.

3. Purification

The extracted proteins were loaded into Ni-NTA (nickel-nitrilotriacetate) agarose columns. Proteins that were bound unspecifically were eluted in the resuspension

buffer and in two concentrations of imidazole (10 mM and 30 mM). The recombinant proteins were eluted in 100, 200 and 500 mM imidazole in the same conditions.

10 μL of each fraction were mixed with 2x Laemmli buffer (4% SDS, 20% glycerol, 10% 2-mercaptoetanol, 0,004% bromophenol blue and 0.125 M Tris HCl pH 6.8) and ran in a SDS-PAGE gel (12.5 % for TrxRs and 15% for Trxs). Coomassie Brilliant Blue was used for staining. Fractions containing the highest amounts of recombinant proteins were mixed and concentrated to a final concentration of 10-30 mg/mL using Viva spin columns (Sartorius) and stored at 4ºC. Protein concentration was determined at 280 nm using the extinction coefficients calculated with Expasy.

INHIBITORS

1. Screening *in vitro*

All compounds were dissolved in 100% dimethyl sulfoxide (DMSO) to a final concentration of 10 mM. Only Compound 32 (Methylene blue) was dissolved in water.

For inhibition assays, TrxR was added to a reaction mixture composed of 100 mM KH_2PO_4, 2mM EDTA pH 7.4 and 0.2 mM NADPH to a final concentration of 0.5 μM. In addition, 10 different concentrations (300 μM – 15 nM) of each compound were added Trx was diluted in the same buffer as TrxR. After baseline measurement, Trx was added to a concentration of 50 μM and the change in absorbance at 340 nm ($\Delta A \cdot min^{-1}$) was monitored to measure NAPDH consumption. A positive control, lacking Trx, and a negative control, with no compound, were also measured. The assays were performed using a Tecan M200 (Maennedorf) plate reader, a HITACHI U-2001 spectrophotometer or an Evolution 300 UV/VIS spectrophotometer (Thermo Fisher).

2. Half inhibitory concentration (IC_{50})

Dose-response curves were computed by non-linear regression using Prism 6 (GraphPad) and IC_{50} obtained from the resulting curves.

3. Dose-response assays

Compounds were dissolved in DMSO to a final concentration of 100 mM or 500 mM and stored at -20ºC until used.

4. Injection

Serial dilutions of the compounds were made ranging from 10 mM to 0.1 mM and keeping the percentage of DMSO constant. Mosquitoes were briefly anesthetized with CO_2 and immediately placed on ice. With the help of a Nanoject II microinjector (Drummond Scientific) each individual was injected with 69 nL of one of these solutions on ice. A negative control containing only DMSO was also injected. A total of 15 mosquitoes were injected with each concentration for each compound. After injection, mosquitoes were immediately placed on a cup containing a sugar pad and placed in the incubator to avoid desiccation. Mortality was followed for one week in 24 h time points. Experiments were performed once.

5. Oral administration

The highest concentrated feeding solution was prepared to obtain 5% sucrose (w/v), 0.5% (v/v) DMSO and 250 µM, 500 µM or 1000 µM. Then, serial dilutions were made until 5 µM, keeping the sugar and DMSO concentrations constant. A negative control solution was prepared with sucrose and DMSO but no compound. Mosquitoes were placed in cups in groups of 10-25 and starved for 6-12 h. To deliver the compounds two methods were used. On one side, cotton swabs were soaked in the solutions and then placed in the cups. Alternatively, solutions were placed in lidless eppendorf tubes, sealed with parafilm, with a protruding strip of filter paper soaked in the solution. 24 h later, dead mosquitoes were counted. Mosquitoes were kept in an incubator at 27ºC and 70% humidity for the duration of the assays. Experiments were repeated independently at least 3 times per condition tested.

6. Median lethal dose (LD_{50})

Dose-response curves were computed by non-linear regression using Prism 6 (GraphPad) and LD_{50} obtained from the resulting curves.

To calculate the LD_{50}, experiments with a mortality of the control groups > 20 % were discarded, unless stated otherwise. The mortality of the treated groups was normalized using Schneider-Orelli's formula:

$$\frac{(mortality\ (\%)\ in\ treated\ group -\ mortality\ (\%)\ in\ control\ group)}{100 -\ mortality\ (\%)\ in\ control\ group} \times 100$$

7. Age experiments

Mosquitoes of 4 different ages were used in these experiments (< 1 week, 1-2 weeks, 2-3 weeks and 3-4 weeks). Groups of 30 mosquitoes were placed in cups and starved for 6-12 h, then they were allowed to feed on a solution containing 5% sucrose (w/v), 0.5% (v/v) DMSO and 200 μM auranofin. In parallel, negative controls were fed with solutions containing 5% sucrose (w/v) and 0.5% (v/v) DMSO. 24 h later, dead mosquitoes were counted in all groups.

BIOINFORMATICS AND *IN SILICO*

1. Transcriptome analysis

Sequencing was aligned on the Anopheles-gambiae-PEST_BASEFEATURES_AgamP4.6 transcript database. The transcript quantification from RNA-seq was done using the Salmon 0.14.1 tool (Patro1 et al., 2017). Specific sequence alignments were done using Bowtie2 (Langmead and Salzberg, 2012).

The quantification was done with selective alignment of the sequencing reads when mapping and then corrected for sequence-specific biases in the input data. Computing bootstrapped abundance estimates over 100 sampling was applied. R [R Core Team] script was then used to analyse transcript abundance using DEseq2 (Love et al., 2014).

2. Alignment

The sequence of A. gambiae TrxR (AGAP000565-RC) was obtained from the VectorBase and Blasted against other insect genomes. The resulting sequences were filtered to eliminate duplicates and the top 30 (including A. gambiae) were aligned in Clustal Omega. Results were visualized and analyzed in CLC Main Workbench (Qiagen).

3. 3D protein structure

The 3D structure of D. melanogaster (2nvk) was obtained from the Protein Data Bank and analyzed in UCSF Chimera (RBVI). The protein sequence was colored according to the degree of conservation using the aforementioned alignment.

4. Online resources

Primers for PCR RT PCR and qPCR were designed and evaluated with Primer3Plus (http://www.bioinformatics.nl/cgi-bin/primer3plus/primer3plus.cgi) (Untergasser et al., 2007); guide RNAs (gRNAs), with CHOPCHOP v2 (http://chopchop.cbu.uib.no) (Labun et al., 2016); immunogenic peptides, with AbDesigner 3D (https://hpcwebapps.cit.nih.gov/AbDesigner3D/) (Saethang et al., 2018).

Gene ontology (GO) enrichment analyses was performed with Panther (http://www.pantherdb.org) (Mi et al., 2019).

The octanol-water partition coefficient (LogP) was calculated in Pirika

(http://pirika.com/ENG/TCPE/index.html).

STATISTICS

All statistical analyses were performed using Prism 6 (GraphPad). Outliers were identified and removed using the ROUT method. Pairwise comparisons were done using Mann-Whitney; group comparisons, using Kruskal-Wallis with Dunn post hoc. The statistical significance of the loss of susceptibility to auranofin in TrxR midgut knockouts was assessed by Chi-square. Statistical differences between LD_{50} were determined using the extra sum-of-squares F test. Long-rank test was used to compare survival curves. P values < 0.05 were considered significant.

RÉSUMÉ EN FRANÇAIS

SOMMAIRE

INTRODUCTION

1. LES MOUSTIQUES

A. Biologie et espèces

Les moustiques, ou *Culicidae*, sont une famille d'insectes de l'ordre des Diptera qui comprend environ 3000 espèces différentes (Rozendaal, 1997). Ces animaux

peuvent être trouvés sous n'importe quelle latitude, à l'exception des régions qui sont gelées en permanence, mais ils peuplent principalement les zones tropicales et subtropicales. Ils présentent un holométabolisme, c'est-à-dire, une métamorphose complète. Les femelles moustiques adultes pondent leurs œufs sur les plans d'eau ou les zones qui seront inondées. À l'intérieur, l'embryon se développe pendant une durée variable (selon l'espèce et les conditions environnementales) jusqu'à l'éclosion d'une larve complètement formée. Le stade larvaire est aquatique et se caractérise par une forme de corps semblable à un ver. Les larves se nourrissent de détritus et de micro-organismes et respirent de l'air, ce qui les oblige à rester à la surface de la masse d'eau ou à proximité. Au total, quatre mues se produisent pendant cette période; les trois premiers donnent des larves d'aspect très similaire, tandis que le dernier implique un développement rapide des disques imaginaires et donne une nymphe qui comprend déjà de nombreuses caractéristiques adultes. Les nymphes sont également aquatiques et présentent un corps très distinctif semblable à une virgule avec un dimorphisme sexuel. Alors que les derniers tissus adultes se sont formés, les pupes ne se nourrissent pas et ne se reposent pas à la surface de l'eau où elles peuvent respirer. Ce processus dure au moins une journée et se traduit par un adulte complètement formé, la dernière étape du cycle de vie et celle qui interagit avec les humains. Les moustiques adultes présentent une forme de corps allongée avec une longue trompe et un dimorphisme sexuel, car les mâles sont plus petits et présentent des antennes touffues. Leur abdomen est également plus mince et se termine par des fermoirs, qu'ils utilisent pour s'accrocher à la femelle. À ce stade, les moustiques se nourrissent principalement du nectar des plantes et contribuent à la pollinisation. Cependant, les femelles doivent se nourrir du sang des vertébrés pour absorber les acides aminés nécessaires à la production d'œufs. En effet, très peu d'espèces de moustiques sont capables de se reproduire sans repas sanguin. Quelques jours après s'être nourrie de sang, les femelles sont prêtes à pondre, fermant ainsi le cycle.

L'alimentation des moustiques par le sang offre aux micro-organismes la possibilité d'être transportés depuis et vers les hôtes vertébrés dont ils se nourrissent. Cette caractéristique a été exploitée par plusieurs agents pathogènes humains, conférant aux moustiques l'honneur douteux d'être les animaux les plus meurtriers sur Terre (Gates, 2018). D'un point de vue biomédical, les moustiques vecteurs les plus importants se répartissent en trois genres: *Anopheles* (paludisme), *Aedes* (dengue, zika chikungunya) et *Culex* (fièvre du Nil occidentale, filariose).

B. Lutte dans le cadre du paludisme

Le paludisme est, de loin, la plus meurtrière de toutes les maladies à transmission vectorielle. Rien qu'en 2017, il a fait 435 000 morts et infecté 290 millions de personnes dans 87 pays. La région la plus touchée est l'Afrique avec 92% de tous les cas, et le groupe le plus vulnérable est celui des enfants de moins de 5 ans, ce qui représente 61% de tous les décès (WHO, 2018).

Parce que le paludisme ne peut pas être transmis entre humains en l'absence de vecteur, éviter les piqûres de moustiques est la prophylaxie la plus efficace. Pour cela, les stratégies actuelles principales consistent à dormir sous des moustiquaires imprégnées d'insecticide (ITN) et pulvériser des insecticides à l'intérieur des maisons (IRS). Ainsi, la lutte contre le paludisme est fortement dépendante de l'utilisation de molécules insecticides.

En 2019, l'Organisation Mondiale de la Santé (WHO) recommande l'utilisation de 13 insecticides pour la lutte contre les vecteurs du paludisme. Ces composés se répartissent en 5 classes chimiques avec trois modes d'action, tous ciblant le système nerveux des moustiques.

(I) Le défi des résistances

La résistance, telle qu'elle est définie par le Comité d'action sur la résistance aux insecticides, est «la sélection d'une caractéristique héréditaire dans une population d'insectes qui entraîne l'échec répété d'un produit insecticide à fournir le niveau de contrôle prévu lorsqu'il est utilisé selon les recommandations» (Résistance aux insecticides Comité d'action (IRAC), 2010). Les premiers rapports sur la résistance aux insecticides dans les populations de moustiques datent des années 1950 (Gjullin et Peters, 1952) ; depuis, la situation n'a fait que se détériorer. En 2016, 77% des pays où le paludisme est endémique ont signalé des résistances dans leurs populations de moustiques à la classe d'insecticides la plus utilisée (pyréthrines) et 25%, aux quatre classes les plus répondues (organochlorés, pyréthrines, carbamates et organophosphorés) (WHO, 2018). Dans le cas des espèces d'*Aedes*, la situation n'est pas non plus encourageante car des résistances ont été trouvées aux États-Unis, en Afrique et en Asie (Moyes et al, 2017).

Étant donné que ces résistances ont un impact sur la transmission du paludisme (Ranson et Lissenden, 2016), la WHO a publié en 2012 un plan mondial pour la gestion de la résistance aux insecticides chez les vecteurs du paludisme. Ce plan d'action était basé sur 5 recommandations clés: (i) gérer les résistances aux insecticides, (ii) les surveiller, (iii) approfondir les connaissances sur les mécanismes et l'impact, (iv) assurer des moyens adéquats et (v) développer de nouveaux outils de lutte anti vectorielle.

2. HOMEOSTASIE REDOX

Les espèces réactives de l'oxygène (ROS) et de l'azote (RNS) sont des molécules produites de manière naturelle dans les cellules qui peuvent infliger des dommages irréversibles aux biomolécules telles que les lipides (Halliwell et Chirico, 1993; Stubbs et Smith, 1984), l'ADN (Pogozelski et Tullius, 1998) et les protéines (Pogozelski et Tullius, 1998). Cependant, elles sont également importantes dans plusieurs processus immunitaires et participent à la signalisation cellulaire par le biais de modifications post-traductionnelles (PTM) dans les cystéines. Ainsi, pour relever le défi que les rôles paradoxaux des ROS / RNS impliquent, les cellules ont développé des systèmes antioxydants pour les contrer et réparer leurs dommages. L'équilibre entre oxydants et antioxydants est ce qu'on appelle communément «l'homéostasie redox» et les conséquences négatives d'un déséquilibre qui favorise les oxydants, le «stress oxydatif». Garder un ton nucléophile intracellulaire correct grâce à des antioxydants est essentiel pour la viabilité cellulaire.

Les systèmes antioxydants sont extrêmement complexes et forment des réseaux interconnectés. Plusieurs types de molécules peuvent agir comme antioxydants dans les cellules en éliminant directement les ROS / RNS ou en réparant les dommages oxydatifs qu'ils génèrent. Néanmoins, les cellules possèdent deux tampons redox principaux : les thiorédoxines (Trxs) et le glutathion (GSH).

A. Les thiorédoxines

Les Trxs sont une classe de petites protéines (12 kDa) thiol actives présentes dans tous les organismes vivants. Elles contiennent un domaine thiorédoxine, et sont impliquées dans la synthèse de l'ADN (Zahedi Avval et Holmgren, 2009) et dans la réduction des ponts disulfure des protéines, participant ainsi au leur repliement (Berndt et al, 2008) ; de plus, elles jouent un rôle clé dans les processus de signalisation cellulaire.

Le rôle des Trxs comme tampon redox est donné par leur capacité à réduire d'autres antioxydants (les peroxirédoxines et la métionine sulfoxide réductase) (Fig. F.1) assurant ainsi un fluxe électronique adéquat. Chez *A. gambiae*, il existe trois gènes codant pour les Trxs, dont deux ont des signaux d'importation mitochondrial. Seul le cytoplasmique, Trx1 (AGAP009584), présente le motif actif redox conservé en tant que tel, tandis que les deux autres ont des résidus Ala et Asp au lieu de Pro. Le génome de la mouche du vinaigre, *D. melanogaster,* code pour plus de Trx, probablement en raison d'événements de duplication après divergence des moustiques (Corona et Robinson, 2006). Au sein de ces gènes supplémentaires, il existe deux Trx spécifiques au sexe (Deadhead, dhd, CG4193; TrxT, CG331) qui sont respectivement présents dans les noyaux des cellules nourricières et des spermatocytes (Pellicena-Pallé et al., 1997; Salz et al. , 1994; Svensson et al., 2007).

Le maintien des Trx dans leur état réduit, c'est-à-dire celui qui leur permet de transférer des électrons, est assuré par la thiorédoxine réductase (TrxR) (Fig F.1). Cette protéine est une flavoenzyme homodimérique qui transfère les électrons du NADPH aux Trxs via un groupe prothétique FAD. Ainsi, TrxR est considéré comme l'enzyme de recyclage du système Trx. De plus, les TrxR peuvent également réduire d'autres substrats tels que des ROS (Björnstedt et al., 1995 ; Zhong et Holmgren, 2000) et d'autres antioxydants (May et al., 1998b ; Johansson et al., 2004).

À la suite de l'évolution, il existe deux types différents de TrxR. Les procaryotes, les archées et les eucaryotes inférieurs présentent de petits TrxR avec un poids moléculaire de 35 kDa. La catalyse de ces petites Mr TrxR repose sur le groupe prothétique FAD et le site thiol actif voisin qui est conservé parmi les espèces (-Cys-Val-Asn-Val-Gly-Cys-) (Williams, 1995). Les eucaryotes supérieurs ont des TrxR plus

grandes (55 kDa) avec un domaine d'interface C-terminal supplémentaire qui contient un autre disulfure redox-actif. Ce motif, codé par les derniers acides aminés C-terminaux de la protéine, n'est pas conservé parmi les espèces. En effet, ce centre redox peut avoir trois formes différentes. Dans la plupart des cas (y compris les mammifères), la catalyse repose sur la présence de sélénium (-Gly-Cys-Sec-Gly) (Arscott et al. 1997; Luthman et Holmgren, 1982) tandis que les orthologues chez *P. falciparum* et les insectes sont indépendants du sélénium. Chez les parasites apicomplexes, ce deuxième site est similaire au site N-terminal (-Gly-Cys-XXXX-Cys-Gly) (Miiller et al. 1996) tandis que chez les insectes les deux Cys sont adjacentes (-Thr / Ser-Cys-Cys -Ser) (Bauer et al. 2003b, 2003a). Toutes les TrxR homodimérisent dans une conformation tête-bêche et chez les grandes Mr TrxR, les électrons circulent entre les deux monomères.

D. melanogaster possède deux gènes codant pour les TrxR, tandis que les moustiques *A. gambiae* n'ont qu'un seul gène. AgTrxR donne lieu à trois variantes d'épissage qui codent pour deux formes cytoplasmiques et une forme mitochondriale qui ont été caractérisées biochimiquement (Bauer et al., 2003a), mais dont les fonctions biologiques in vivo n'ont pas été explorées.

B. Le glutathion

Le GSH est un antioxydant largement distribué dans les organismes vivants. Il est présent en concentrations milli molaires dans la plupart des cellules, est donc il est considéré comme un acteur majeur de l'homéostasie redox. Ce tri peptide est formé de Cys, GLy et Glu et est à la fois un réducteur et un nucléophile. Dans les cellules, il est également présent sous forme oxydée (GSSG); cependant, la forme réduite est beaucoup plus abondante (Abdu et al.; Hazelton et Lang, 1984). Le rapport entre ces deux est généralement utilisé comme mesure du stress oxydatif dans les cellules. Près de 90% de la quantité totale de GSH / GSSG se trouve dans le cytoplasme; environ 10%, dans les mitochondries (Jocelyn et Kamminga, 1974) et un petit pourcentage, dans le réticulum endoplasmique, où les deux formes sont presque aussi abondantes (Hwang et al, 1992).

Le GSH peut directement éliminer certains ROS (Haenen et Bast, 2014). Cependant, comme chez les Trxs, ses principales fonctions antioxydantes proviennent de son

utilisation par des protéines antioxydantes telles que les glutarédoxines (Grxs) (Fig F.1). Il sert également de protection aux thiols partiellement oxydés lorsqu'il est conjugué (S-glutathionylation). En plus d'être un antioxydant clé, le GSH est aussi impliqué dans les voies de détoxification car les glutathion-s-transférases (GSTs) catalysent sa conjugaison à des composés électrophiles pour les rendre solubles dans l'eau et moins réactifs (Enayati et al., 2005). L'augmentation de l'activité des GSTs a été associée à la résistance à certains insecticides (Aravindan et al., 2014; Chen et al., 2003; Gunasekaran et al., 2011; Lumjuan et al., 2011; Olé Sangba et al., 2017; Ranson et al., 2000).

Le GSH est synthétisé *de novo* à partir des trois acides aminés constitutifs dans un processus intracellulaire qui a lieu en deux étapes nécessitant de l'ATP. Chez les moustiques *A. aegypti*, la biosynthèse du GSH diminue avec le vieillissement, entraînant une baisse globale de la quantité totale de GSH chez cette espèce (Hazelton et Lang, 1983, 1984). Étant donné que le Glu et la Cys sont liés par une liaison peptidique avec le groupe γ-carboxyle du Glu, la dégradation du GSH ne peut pas être médiée par des hydrolases régulières. Les seules enzymes capables d'une telle activité sont les γ-glutamyltranspeptidases (GGT), qui sont des protéines liées à la membrane avec le site catalytique tourné vers l'espace extracellulaire. Par conséquent, GSH et GSSG doivent d'abord être exportés afin d'être dégradés. Le nom de ces enzymes est dû à leur capacité à transférer le groupe γ-glutamyle aux peptides et acides aminés dans une réaction de transpeptidation. Alternativement, ils peuvent également utiliser l'eau comme accepteur, générant du Glu (Bachhawat et Kaur, 2017). Les acides aminés résultants peuvent être repris par la cellule pour synthétiser plus de GSH (Bachhawat et al., 2013). Le GSH peut aussi être importé et exporté depuis la cellule. De plus, comme sa biosynthèse a lieu dans le cytoplasme, il doit être importé dans d'autres organites. Ces processus sont médiés par diverses familles de transporteurs, selon le tissu et l'espèce (Bachhawat et al., 2013).

Comme dans le cas du système thiorédoxine, la plupart des organismes possèdent une enzyme de recyclage GSSG appelée glutathione réductase (GR) (Fig F.1 A). Cette flavoenzyme est similaire à TrxR dans sa structure et sa catalyse (Thieme et al., 1981) mais est absente chez les insectes. Dans ces organismes, le système Trx / TrxR serait plutôt responsable du recyclage du GSSG (Bauer et al., 2003a; Kanzok et al., 2001) (Fig. F.1 B).

3. HYPOTHÈSE ET QUESTIONS

De manière générale, les systèmes Trx et GSH sont similaires, à la fois en termes de mécanismes et de fonctions. Ces deux réseaux peuvent interagir l'un avec l'autre comme le montre le fait que la TrxR humaine peut réduire Grx2 (Johansson et al., 2004) qui peut lui-même réduire Prx3 (Hanschmann et al., 2010); de plus, ils peuvent servir de sauvegarde l'un de l'autre, ce qui suggère qu'ils sont (partiellement) redondants (Du et al., 2012; Eriksson et al., 2015; Reichheld et al., 2007; Tan et al., 2010).

Cette diaphonie entre le système est plus évidente dans le cas des insectes où le manque de GR est compensé par les Trx eux-mêmes (Bauer et al., 2003a; Kanzok et al., 2001). Ainsi, dans ces organismes, TrxR est la seule enzyme réduisant à la fois les systèmes Trx et GSH. Cette particularité de la défense antioxydante des insectes, ajoutée au rôle de ces systèmes dans la résistance aux insecticides, offre une nouvelle piste intéressante pour développer des insecticides. De plus, le fait que TrxR soit essentiel à la viabilité de *D. melanogaster* (Missirlis et al., 2002) suggère que TrxR pourrait être un bon candidat comme cible pour développer des nouveaux insecticides.

Ainsi, l'objectif de ma thèse était d'évaluer la pertinence de cette enzyme comme cible contre les moustiques transmetteurs de maladies. À cette fin, j'ai abordé trois questions principales:

Quelle est la dynamique redox générale du glutathion chez les moustiques?

Quel est le rôle de TrxR chez *A. gambiae*?

Les modulateurs chimiques du TrxR tuent-ils les moustiques?
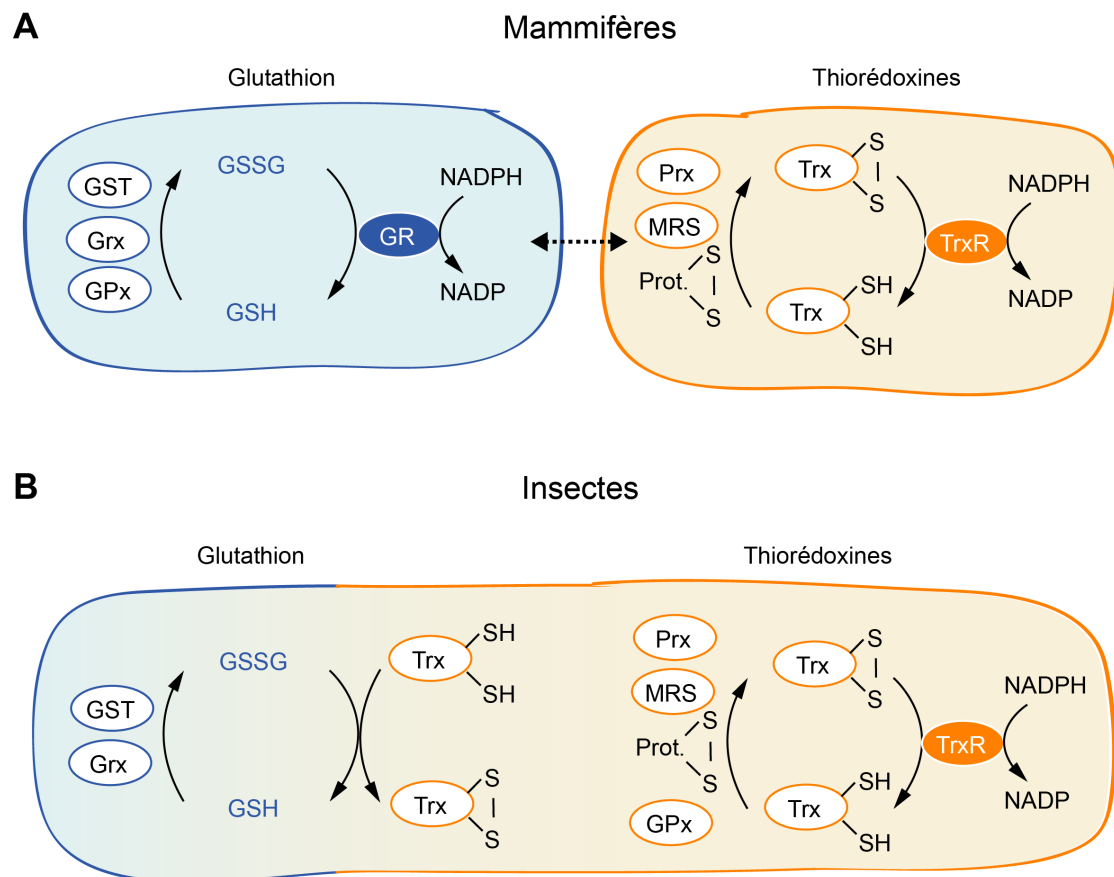
Figure F. 1 Relation entre les systèmes glutathion et thiorédoxine. (A) Chez les mammifères, le glutathione donne des electrons aux glutathione-s-transférases (GST), aux glutarédoxines (Grx) et aux glutathion peroxydases (GPx) et est recyclé par la glutathion réductase (GR). D'autre part, les thiorédoxines réduisent les ponts disulfure dans les proteins, donnent des electrons aux peroxirédoxines (Prx) et aux méthionine sulfoxyde réductases (MRS) et sont recyclées par la thiorédoxine réductase (TrxR). Ces deux systèmes sont séparés, mais ils peuvent interagir et se compenser. (B) Chez les insectes, il n'y a pas de GR; à la place, Trx est responsable du recyclage du GSSG. De plus, GPx utilise Trx au lieu de GSH. Chez ces animaux, le système du glutathion dépend de celui des Trxs.

DISCUSSION

1. Dynamique du glutathion

Pour donner réponse à cette question, nous avons, pour la première fois, exprimé la hGrx1-roGFP2 dans différents compartiments cellulaires, tissus et espèces de moustiques. Le profil d'excitation de cette protéine fluorescente dépend de son état d'oxydation (réduit ou oxydé), qui à la fois est en équilibre avec le degré d'oxydation du glutathion dans la cellule ; ainsi, ce biocapteur permet de mesurer et d'étudier la dynamique du potentiel redox du glutathion (E_{GSH}) en temps réel à l'aide d'un microscope.

A l'aide de ces nouvelles lignées transgéniques, nous avons montré que le E_{GSH} cytoplasmique des entérocytes et de l'épithélium des glandes salivaires des moustiques se situe dans le rang mesurable de la roGFP2. Les mesures réalisées chez *A. gambiae* et *A. aegypti* (-300 – -320 mV) sont cohérentes avec les observations antérieures faites chez d'autres eucaryotes utilisant des outils roGFP De plus, nous avons étudié l'E_{GSH} dans les mitochondries des entérocytes chez *A. gambiae* où nous avons trouvé un potentiel généralement moins réducteur, ce qui est cohérent avec l'idée que les mitochondries sont les principaux producteurs de ROS dans les cellules (Diebold et Chandel, 2016).

De même, dans nos études, nous avons trouvé des différences fondées sur le sexe dans le potentiel redox et le contrôle du glutathion. En général, les mâles possèdent un système plus dynamique, ce qui est cohérent avec les observations selon lesquelles, en général, ils possèdent des niveaux inférieurs d'antioxydants et produisent plus de ROS (Ide et al, 2002; Niveditha et al. 2017). Chez les femelles, l'exposition à des défis oxydatifs (repas sanguin, peroxyde d'hydrogène et paraquat) n'a menée qu'a de petits changements qui n'était pas consistent entre répétitions expérimentales, suggérant une forte régulation de ce système.

Lors du développement, nous avons constaté que les pupes d'*A. gambiae* présentaient un E_{GSH} beaucoup plus oxydant que les larves et les adultes. Les différences dans le degré d'oxydation que nous avons observées entre les individus

et les répétitions expérimentales suggèrent que ce pique d'oxydation à lieu progressivement dans un délai très précis.

Une autre question que nous avons abordée dans le présent travail était l'effet de la réponse antiplasmodiale sur l'homéostasie redox de l'intestin des femelles. 20 - 24 h après l'infection par des parasites de *P. berghei*, nous avons observé la présence de cellules rondes en processus d'expulsion de l'épithélium intestinal, dont la plupart présentaient un E_{GSH} oxydé et co localisaient avec des parasites. Néanmoins, nous n'avons pas observé une corrélation entre cette oxydation et le temps passé depuis l'invasion ou l'expression de la oxyde nitrique synthase (NOS), enzyme pro-oxydante impliquée dans la réponse antiplasmodiale (Han et al., 2000. Nous pouvons donc émettre l'hypothèse que cette oxydation pourrait être transitoire et en relation avec des processus de signalisation cellulaire.

En conclusion, hGrx1-roGFP2 s'est avéré être une méthode utile pour suivre la dynamique de l'oxydation du glutathion dans l'intestin et les glandes salivaires des moustiques. Nous avons montré que le glutathion cytoplasmique et mitochondrial sont pour la plupart réduits et maintenus ainsi même lorsqu'ils sont exposés à des défis oxydatifs. Ces observations indiquent que les moustiques ont de puissants systèmes antioxydants qui maintiennent la réserve de glutathion réduite, ou que les réserves de glutathion ne sont pas sensibles / ne sont pas impliquées dans l'entretien de l'homéostasie intracellulaire des moustiques, au moins dans l'intestin. Les moustiques exprimant hGrx1-roGFP2 nous aideront à approfondir nos recherches sur le stress oxydatif des moustiques et à caractériser leurs systèmes antioxydants.

2. Rôle de la thiorédoxine réductase

Pour explorer cette question, nous avons d'abord développé des anticorps polyclonaux contre AgTrxR qui reconnaissent une protéine de ~ 60 kDa dans les extraits de protéines d'*A. gambiae* ainsi que la TrxR d'autres espèces d'insectes. Ensuite, nous avons produit des mutants pour le seul gène de la TrxR chez *A. gambiae* à l'aide du système CRISPR/Cas9 et nous avons étudié leurs phénotypes.

La présence des deux participants du système CRISPR / Cas9 (c'est-à-dire Cas9 et gRNA) dans les œufs de moustiques a conduit à l'abrogation du développement embryonnaire ; ce rôle essentiel a aussi été observé chez les mammifères (Bondareva et al., 2007; Jakupoglu et al., 2005), où les Trxs sont indispensables car ils sont impliqués dans la prolifération cellulaire et l'apoptose (Matsui et al., 1996; Nonn et al., 2003).

Lorsque Cas9 a été exprimé plus tard au cours du développement larvaire, nous avons obtenu des larves déficientes pour la TrxR dans certains tissus somatiques montrant un phénotype létal fort. En effet, nous avons obtenu des moustiques avec un retard dans le développement de 3 jours qui mouraient principalement sous forme de nymphes ou d'adultes avec les jambes piégées dans la coque nymphale. Lorsque nous avons utilisé eSpCas9 pour la mutagénèse (version moins active, donnant lieu à moins mutations hors cible), le retard a disparu et 17% des descendants sont devenus des adultes avec une espérance de vie très réduite (moins de 10 jours). Ces phénotypes sont similaires à ceux trouvés pour *D. melanogaster* portant des mutations hypomorphiques de TrxR1 (c'est-à-dire qui provoquent une perte partielle de la fonction génique (Missirlis et al., 2001, 2002).

Chez les adultes, nos données ont montré que la TrxR est dispensable dans l'intestin. La réduction sévère des niveaux de TrxR dans ce tissu par mutagenèse CRISPR / Cas9 n'a eu aucun impact sur la survie ou la capacité vectorielle de l'insecte. Au contraire, ces moustiques ont montré une meilleure survie après s'être nourris de sang et du paraquat, ce qui suggère une augmentation de la capacité à résister le stress oxydatif. En plus, la suppression de la TrxR chez les moustiques hGrx1-roGFP2 n'a entraîné aucun changement majeur dans l'équilibre redox du glutathion.

Pour élucider l'origine de ces résultats inattendus, nous avons comparé le transcriptome de l'intestin de ces moustiques mutants à celui des moustiques sauvages (exprimant la TrxR) à trois moments et conditions différents (avant, 3 et 7 jours après un repas sanguin). Nous avons ainsi, détecté une hausse de la transcription de certains gènes correspondent à des enzymes de détoxication, ce qui pourrait expliquer la tolérance accrue à la digestion sanguine et au paraquat des moustiques qui ne possèdent pas la TrxR. Ce phénomène a également été constaté dans les hépatocytes de souris déficients en TrxR1 comme étant médié par la voie Nrf2 (Suvorova et al., 2009). Cette voie de signalisation est activée lors d'un stress

oxydatif (Vomund et al., 2017), ainsi, nos résultats pourraient être révélateurs d'un tel déséquilibre dans l'estomac des moustiques déficients pour la TrxR. Alternativement, le système Trx / TrxR est impliqué dans l'activation de Nrf2 (Schmidt, 2015), ainsi nos résultats pourraient être le résultat d'une activité globale diminuée de ce système. Après l'alimentation en sang, l'expression de deux GSTs été augmentée; ce phénomène a également été observé chez la levure et la souris (Bondareva et al., 2007; Carmel-Harel et al., 2001), où cela a été interprété comme indication d'un déplacement de la charge de l'homéostasie redox vers le système GSH. En effet, une compensation de la perte de la TrxR par le système du GSH pourrait expliquer le phénotype observé, par contre cette hypothèse ouvre une question plus intéressante qui devrait être étudiée à l'avenir : comment peuvent les cellules intestinales maintenir le glutathion réduit en absence de GR et TrxR ?

En conclusion, nous avons montré que TrxR est essentiel pour le développement embryonnaire et larvaire / nymphal, mais dispensable dans l'intestin des moustiques adultes. Étonnamment, nos données suggèrent que l'absence de TrxR dans ce tissu pourrait être compensée par le système GSH. Une caractérisation plus approfondie du rôle des autres effecteurs de la voie GSH mettra en lumière les mécanismes qui régulent l'homéostasie redox chez les insectes. Le rôle de TrxR chez *D. melanogaster* n'a été étudié qu'en cours de développement, nous ne savons donc pas si l'absence d'un phénotype létal chez l'adulte est une caractéristique commune chez les insectes ou plutôt une particularité des moustiques, une question à laquelle il vaudra la peine de répondre.

3. Inhibition chimique

Pour répondre à cette question, nous avons d'abord identifié des inhibiteurs de cette enzyme chez les moustiques *in vitro*, puis nous avons testé leurs effets *in vivo.*

Pour les criblages *in vitro*, nous avons d'abord produit la TrxR et la Trx cytosolique principale des moustiques *Anopheles gambiae* de manière recombinante. Pour tester la sélectivité des inhibiteurs pour l'enzyme chez cette espèce, nous les avons également testés sur d'autres TrxR d'insecte. Ainsi, nous avons, pour la première fois, produit et purifié la TrxR et la Trx des moustiques *Aedes aegypti* et de l'abeille domestique *Apis mellifera*. La caractérisation future de la cinétique de ces TrxR

161

mettra en lumière les différences mécaniques entre les TrxR dépendants et indépendants du sélénium, ce qui nous guidera dans la recherche d'inhibiteurs plus spécifiques.

En total, 37 composés chimiques (sélectionnés au préalable par une de nos collaboratrices) ont été testés sur 4 TrxR (*A. gambiae*, *A. aegypti*, *D. melanogaster*, *A. mellifera*) utilisant les Trx correspondantes ou le réactif d'Ellman (DTNB) comme substrat. 21 de ces composés ont été identifiés comme inhibiteurs d'au moins une des TrxRs dans des concentrations nanomolaires ou micromolaires. Le manque de Sec dans le site actif C-terminal des TrxR d'insectes est compensé par une conformation spécifique qui favorise la protonation du résidu Cys; en conséquence, les TrxR des insectes ne sont pas inhibés, ou pas aussi efficacement, par les inhibiteurs de la disulfure réductase les plus couramment utilisés (Kanzok et al., 2001). Par conséquent, les résultats de nos projections fournissent des informations précieuses sur les inhibiteurs qui pourraient être utilisés contre ces espèces ainsi que sur leurs modes d'action. Le dégrée de conservation de la séquence de la TrxR chez les insectes est très élevée (> 60%). De manière cohérente, notre criblage a montré que, en général, les TrxRs des insectes réagissent de manière similaire; cependant, seule l'auranofine (composé 30) était active contre les 4 TrxRs testées avec les deux types substrats différents que nous avons utilisés. Ainsi, ce criblage pilote a mis en lumière la spécificité de certaines molécules, sur la base desquels de nouvelles molécules avec différents substituants doivent être testées pour augmenter cette spécificité si possible.

Nous avons en outre étudié le potentiel des inhibiteurs de TrxR à exploiter dans une stratégie insecticide contre les moustiques du paludisme. Premièrement, nous avons montré que deux des inhibiteurs identifiés *in* vitro (l'auranofine et la 1,4-naphthoquinone) étaient toxiques d'une manière qui dépend de la dose lorsqu'ils sont directement injectés dans des moustiques *A. gambiae*. Pour mieux caractériser ce phénomène, nous avons étudié plus en détail l'effet de l'auranofine. Ce sel d'or a été initialement approuvé comme traitement contre la polyarthrite rhumatoïde sous le nom de Ridaura; cependant, ces dernières années, ses applications thérapeutiques ont été intensivement étudiées dans le contexte d'autres pathologies telles que le cancer (Carlos Lima et Rodriguez, 2012; Onodera et al., 2019; Ralph et al., 2019), le VIH (Diaz et al. ., 2019) et les infections fongiques (Wiederhold et al., 2017), parasitaires (Capparelli et al., 2016; Fan et al., 2017; Jones et al., 2016) et bactériennes (Jang et Eom, 2019; Marzo et al. ., 2018).

Dans nos tests, l'auranofine a été administrée aux moustiques par voie orale. Étonnamment, ce composé semble avoir un effet répulsif sur les moustiques *A. aegypti* mais pas sur *A. gambiae*. Cette conclusion a été tirée de l'observation que les premiers évitaient le contact avec les solutions contenant cette molécule et ne s'en nourrissaient pas bien. À l'avenir, les expériences devraient être répétées avec différentes doses et en parallèle avec d'autres inhibiteurs de TrxR pour élucider les bases comportementales de ce phénomène et si cela est particulier à l'auranofine ou s'il est commun aux autres inhibiteurs de la TrxR. Chez les moustiques *A. gambiae* âgés de plus d'une semaine (après leur émergence), l'auranofine était toxique en fonction de la dose avec une dose létale moyenne (LD_{50}) de 277 μM. Chez des moustiques plus jeunes, la toxicité était toujours présente mais la LD_{50} était supérieure à 1 mM (concentration maximale testée). Cet effet dépendant de l'âge également été observé pour les insecticides actuels (Collins et al., 2019; Machani et al., 2019; Mbepera et al., 2017; Rajatileka et al., 2011), suggérant ainsi qu'il pourrait être dû à une diminution globale de leur capacité (i) à détoxifier les xénobiotiques et / ou (ii) à surmonter les dommages infligés. Les parasites de *P. falciparum* doivent se développer pendant plus d'une semaine dans le corps du moustique avant de devenir infectieux pour l'homme; cibler ainsi spécifiquement les moustiques de plus d'une semaine pourrait limiter la pression sélective pour le développement de résistances, car ils auraient encore le temps de se reproduire, tout en protégeant les gens contre la transmission du paludisme.

Chez le rat, l'auranofine est connue pour cibler la TrxR et exerce ses effets toxiques sur les cellules lors d'une perturbation de la fonction mitochondriale suivie d'une apoptose (McKeage et al., 2002; Rigobello et al., 2002, 2004). Ceci est concomitant à une augmentation des niveaux de H_2O_2 mitochondrial (Rigobello et al, 2005). Étonnamment, chez les moustiques, l'administration orale de l'auranofine a conduit à une oxydation du glutathion cytoplasmique en fonction de la dose administrée, mais aucun changement a été observé sur le réservoir mitochondrial. D'autres mécanismes associés au traitement par l'auranofine (par exemple l'apoptose) doivent être évalués pour mieux comprendre son mécanisme d'action chez les moustiques.

Les moustiques qui n'expriment pas la TrxR dans les entérocytes ont montré une sensibilité à l'auranofine réduite pendant les 24 premières heures de traitement, mais pas 2 jours après. Ces résultats suggèrent (i) que l'effet toxique que nous observons

163

pour l'auranofine est dû, au moins partiellement, au ciblage de TrxR et (ii) que l'intestin joue un rôle important lorsque le médicament est administré par voie orale. Tester ce composé dans des knockouts complets et / ou en combinaison avec d'autres inhibiteurs de TrxR aidera à élucider si la mortalité observée au jour 2 est due à l'inhibition d'autres enzymes ou à TrxR dans d'autres types de cellules. Au contraire, le dégrée d'oxydation du glutathion cytoplasmique était plus élevé chez les moustiques dépourvus de TrxR dans les entérocytes. Cela suggère que l'oxydation du GSH est due à une cible autre que la TrxR et que la TrxR atténue cette oxydation soit en contrôlant directement le GSH soit en éliminant les ROS (par exemple H_2O_2 à travers les Prxs). L'absence d'oxydation mitochondriale pourrait s'expliquer par l'absence de cette cible dans cet organite. La répétition de ces expériences en combinaison avec des inhibiteurs de la voie de biosynthèse du GSH ou d'autres enzymes redox peut éclairer l'origine de cette oxydation.

En conclusion, nous avons développé un test *in vitro* efficace pour identifier des inhibiteurs des TrxR des insectes et nous avons fourni de nouvelles informations sur la capacité inhibitrice de plusieurs composés connus et nouveaux. De même, nous avons montré que l'inhibiteur de la TrxR, auranofine, a une activité toxique sur les moustiques lors de son ingestion, ce qui pourrait être exploitée pour développer des insecticides. A l'avenir, il serait intéressant de tester ce composée en combinaison avec les insecticides actuels pour évaluer s'il a un effet synergique, notamment dans les souches résistantes. La GST humaine P1-1 est une cible de l'auranofine (De Luca et al., 2013), donc ce composé pourrait aider à briser les résistances dépendantes de ces enzymes.

Bibliography

Abdu, H., Abdussalam, Y., Abduljalal, A., Nabueze, E., Hapca, S., and Deeni, Y. Glutathione Levels and Variations in Anopheles gambiae s . l . from Agricultural and Residential Settings. *5*, 47–51.

Achan, J., Talisuna, A.O., Erhart, A., Yeka, A., Tibenderana, J.K., Baliraine, F.N., Rosenthal, P.J., and D'Alessandro, U. (2011). Quinine, an old anti-malarial drug in a modern world: Role in the treatment of malaria. Malar. J. *10*, 144.

Ahoua Alou, L.P., Koffi, A.A., Adja, M.A., Tia, E., Kouassi, P.K., Koné, M., and Chandre, F. (2010). Distribution of ace-1R and resistance to carbamates and organophosphates in Anopheles gambiae s.s. populations from Côte d'Ivoire. Malar. J. *9*.

Albrecht, S.C., Barata, A.G., Großhans, J., Teleman, A. a., and Dick, T.P. (2011). In vivo mapping of hydrogen peroxide and oxidized glutathione reveals chemical and regional specificity of redox homeostasis. Cell Metab. *14*, 819–829.

de Almeida Oliveira, G., Lieberman, Jo., and Barillas-Mury, C. (2012). Epithelial Nitration by a Peroxidase/NOX5 System Mediates Mosquito Antiplasmodial Immunity. Science (80-.). *335*, 856–859.

Anderson, M.A.E., Gross, T.L., Myles, K.M., and Adelman, Z.N. (2010). Validation of novel promoter sequences derived from two endogenous ubiquitin genes in transgenic Aedes aegypti. Insect Mol. Biol. *19*, 441–449.

Andricopulo, a. D., Akoachere, M.B., Krogh, R., Nickel, C., McLeish, M.J., Kenyon, G.L., Arscott, L.D., Williams, C.H., Davioud-Charvet, E., and Becker, K. (2006). Specific inhibitors of Plasmodium falciparum thioredoxin reductase as potential antimalarial agents. Bioorganic Med. Chem. Lett. *16*, 2283–2292.

Aravindan, V., Muthukumaravel, S., and Gunasekaran, K. (2014). Interaction affinity of delta and epsilon class glutathione-s-transferases (GSTs) to bind with DDT for detoxification and conferring resistance in Anopheles gambiae, a malaria vector. J. Vector Borne Dis. *51*, 8–15.

Arnér, S.J.E., Zhong, L., and Holmgren, A. (1999). Preparation and assay of mammalian thioredoxin and thioredoxin redcutase. Methods Enzymol. *300*, 226–239.

Arscott, L.D., Gromer, S., Schirmer, R.H., Becker, K., and Williams, C.H. (1997). The mechanism of thioredoxin reductase from human placenta is similar to the mechanisms of lipoamide

dehydrogenase and glutathione reductase and is distinct from the mechanism of thioredoxin reductase from Escherichia coli. Proc. Natl. Acad. Sci. U. S. A. *94*, 3621–3626.

Auteri, M., La Russa, F., Blanda, V., and Torina, A. (2018). Insecticide Resistance Associated with kdr Mutations in Aedes albopictus: An Update on Worldwide Evidences. Biomed Res. Int. *2018*.

Bachhawat, A.K., and Kaur, A. (2017). Glutathione Degradation. Antioxidants Redox Signal. *27*, 1200–1216.

Bachhawat, A.K., Thakur, A., Kaur, J., and Zulkifli, M. (2013). Glutathione transporters. Biochim. Biophys. Acta - Gen. Subj. *1830*, 3154–3164.

Balabanidou, V., Kampouraki, A., Maclean, M., Blomquist, G.J., Tittiger, C., Juárez, M.P., Mijailovsky, S.J., Chalepakis, G., Anthousi, A., Lynd, A., et al. (2016). Cytochrome P450 associated with insecticide resistance catalyzes cuticular hydrocarbon production in Anopheles gambiae. Proc. Natl. Acad. Sci. U. S. A. *113*, 9268–9273.

Balabanidou, V., Kefi, M., Aivaliotis, M., Koidou, V., Girotti, J.R., Mijailovsky, S.J., Juárez, M.P., Papadogiorgaki, E., Chalepakis, G., Kampouraki, A., et al. (2019). Mosquitoes cloak their legs to resist insecticides. Proc. R. Soc. B Biol. Sci. *286*, 20191091.

Barbehenn, R. V., Bumgarner, S.L., Roosen, E.F., and Martin, M.M. (2001). Antioxidant defenses in caterpillars: Role of the ascorbate-recycling system in the midgut lumen. J. Insect Physiol. *47*, 349–357.

Bauer, H., Kanzok, S.M., and Heiner Schirmer, R. (2002). Thioredoxin-2 but not thioredoxin-1 is a substrate of thioredoxin peroxidase-1 from Drosophila melanogaster. Isolation and characterization of a second thioredoxin in D. Melanogaster and evidence for distinct biological functions of Trx-1 and Trx-2. J. Biol. Chem. *277*, 17457–17463.

Bauer, H., Gromer, S., Urbani, A., Schnölzer, M., Schirmer, R.H., and Müller, H.M. (2003a). Thioredoxin reductase from the malaria mosquito Anopheles gambiae: Comparisons with the orthologous enzymes of Plasmodium falciparum and the human host. Eur. J. Biochem. *270*, 4272–4281.

Bauer, H., Massey, V., Arscott, L.D., Schirmer, R.H., Ballou, D.P., and Williams, C.H. (2003b). The mechanism of high Mr thioredoxin reductase from Drosophila melanogaster. J. Biol. Chem. *278*, 33020–33028.

Becker, K., Gromer, S., Heiner Schirmer, R., and Müller, S. (2000). Thioredoxin reductase as a pathophysiological factor and drug target. Eur. J. Biochem. *267*, 6118–6125.

Benhar, M., Forrester, M.T., and Stamler, J.S. (2009). Protein denitrosylation: Enzymatic mechanisms and cellular functions. Nat. Rev. Mol. Cell Biol. *10*, 721–732.

Berndt, C., and Lillig, C.H. (2017). Glutathione, Glutaredoxins, and Iron. Antioxidants Redox Signal. *27*, 1235–1251.

Berndt, C., Lillig, C.H., and Holmgren, A. (2008). Thioredoxins and glutaredoxins as facilitators of protein folding. Biochim. Biophys. Acta - Mol. Cell Res. *1783*, 641–650.

Bian, K., Gao, Z., Weisbrodt, N., and Murad, F. (2003). The nature of heme/iron-induced protein tyrosine nitration. Proc. Natl. Acad. Sci. U. S. A. *100*, 5712–5717.

Björnstedt, M., Hamber, M., Kumar, S., Xue, J., and Holmgren, A. (1995). Human Thioredoxin Reductase directly reduces hydroperoxides by NADPH and selenocysteines strongly stimulates the reduction via catalitically generated slenels. J. Biol. Chem. *270*, 11761–11764.

Boissière, A., Tchioffo, M.T., Bachar, D., Abate, L., Marie, A., Nsango, S.E., Shahbazkia, H.R., Awono-Ambene, P.H., Levashina, E.A., Christen, R., et al. (2012). Midgut microbiota of the malaria mosquito vector Anopheles gambiae and interactions with Plasmodium falciparum infection. PLoS Pathog. *8*, 1–12.

Bondareva, A.A., Capecchi, M.R., Iverson, S. V, Li, Y., Lopez, N.I., Lucas, O., Merrill, G.F., Prigge, J.R., Siders, A.M., Wakamiya, M., et al. (2007). Effects of thioredoxin reductase-1 deletion on embryogenesis and transcriptome. Free Radic Biol Med *43*, 911–923.

Bottino-Rojas, V., Talyuli, O.A.C., Carrara, L., Martins, A.J., James, A.A., Oliveira, P.L., and Paiva-Silva, G.O. (2018). The redox-sensing gene Nrf2 affects intestinal homeostasis, insecticide resistance, and Zika virus susceptibility in the mosquito Aedes aegypti. J. Biol. Chem. *293*, 9053–9063.

Brand, M.D. (2010). The sites and topology of mitochondrial superoxide production. Exp Gerontol *45*, 466–472.

Braun, L., Garzó, T., Mandl, J., and Bánhegyi, G. (1994). Ascorbic acid synthesis is stimulated by enhanced glycogenolysis in murine liver. FEBS Lett. *352*, 4–6.

Buettner, G.R. (1993). The Pecking Order of Free Radicals and Antioxidants: Lipid Peroxidation, α-Tocopherol, and Ascorbate. Arch. Biochem. Biophys. *300*, 535–543.

Cao, Y., Q, Y., XH, T., SG, L., and S, L. (2018). Molecular characterization of a typical 2-Cys thioredoxin peroxidase from the Asiatic rice borer Chilo suppressalis and its role in oxidative stress. Arch. Insect Biochem. Physiol. *99*.

Capparelli, E. V, Bricker-ford, R., Rogers, M.J., Mckerrow, J.H., and Reed, L. (2016). Phase I Clinical Trial Results of Auranofin, a Novel Antiparasitic Agent Edmund. Antimicrob. Agents Chemother. *61*, 1–8.

Carlos Lima, J., and Rodriguez, L. (2012). Phosphine-Gold(I) Compounds as Anticancer Agents:

General Description and Mechanisms of Action. Anticancer. Agents Med. Chem. *11*, 921–928.

Carmel-Harel, O., Stearman, R., Gasch, A.P., Botstein, D., Brown, P.O., and Storz, G. (2001). Role of thioredoxin reductase in the Yap1p-dependent response to oxidative stress in Saccharomyces cerevisiae. Mol. Microbiol. *39*, 595–605.

Carrasco, D., Lefèvre, T., Moiroux, N., Pennetier, C., Chandre, F., and Cohuet, A. (2019). Behavioural adaptations of mosquito vectors to insecticide control. Curr. Opin. Insect Sci. *34*, 48–54.

Castello, P.R., Drechsel, D.A., and Patel, M. (2007). Mitochondria are a major source of paraquat-induced reactive oxigen species production in the brain. J. Biol. Chem. *282*, 14186–14193.

Chae, H.Z., Kang, S.W., Kirn, H.J., Kirn, K., Baines, I.C., and Rhee, S.G. (1997). Characterization of three isoforms of mammalian peroxiredoxin that reduce peroxides in the presence of thioredoxin and their role in signal transduction. FASEB J. *11*, 101–112.

Chae, Z., Chungl, S.J., and Rhee, S.G. (1994). Thioredoxin-dependent Peroxide Reductase from Yeast. J. Biol. Chem. *269*, 27670–27678.

Chalfie, M., Tu, Y., Euskirchen, G., Ward, W.W., and Prasher, D.C. (1996). Green fluorescent protein as a marker for gene expression. Science (80-.). *263*, 802–805.

Champer, J., Reeves, R., Oh, S.Y., Liu, C., Liu, J., Clark, A.G., and Messer, P.W. (2017). Novel CRISPR/Cas9 gene drive constructs reveal insights into mechanisms of resistance allele formation and drive efficiency in genetically diverse populations. PLoS Genet. *13*, 1–18.

Charpentier, E., and Doudna, J.A. (2013). Biotechnology: Rewriting a genome. Nature *495*, 50–51.

Chen, L., Hall, P.R., Zhou, X.E., Ranson, H., Hemingway, J., and Meehan, E.J. (2003). Structure of an Insect Delta Class Gst From a Ddt Resistant Strain of the Malaria Vector Anopheles Gambiae. Acta Christallographica *D59*, 2211–2217.

Cibulskis, R.E., Alonso, P., Aponte, J., Aregawi, M., Barrette, A., Bergeron, L., Fergus, C.A., Knox, T., Lynch, M., Patouillard, E., et al. (2016). Malaria: Global progress 2000 - 2015 and future challenges. Infect. Dis. Poverty *5*, 1–8.

Collins, E., Vaselli, N.M., Sylla, M., Beavogui, A.H., Orsborne, J., Lawrence, G., Wiegand, R.E., Irish, S.R., Walker, T., and Messenger, L.A. (2019). The relationship between insecticide resistance, mosquito age and malaria prevalence in Anopheles gambiae s.l. from Guinea. Sci. Rep. *9*, 1–12.

Corona, M., and Robinson, G.E. (2006). Genes of the antioxidant system of the honey bee: Annotation and phylogeny. Insect Mol. Biol. *15*, 687–701.

Cox-Singh, J., Hiu, J., Lucas, S.B., Divis, P.C., Zulkarnaen, M., Chandran, P., Wong, K.T., Adem, P., Zaki, S.R., Singh, B., et al. (2010). Severe malaria - A case of fatal Plasmodium knowlesi infection with post-mortem findings: A case report. Malar. J. *9*, 1–7.

Crawford, J.E., Alves, J.M., Palmer, W.J., Day, J.P., Sylla, M., Ramasamy, R., Surendran, S.N., Black, W.C., Pain, A., and Jiggins, F.M. (2017). Population genomics reveals that an anthropophilic population of Aedes aegypti mosquitoes in West Africa recently gave rise to American and Asian populations of this major disease vector. BMC Biol. *15*, 1–16.

Dansen, T.B., and Wirtz, K.W.A. (2001). The peroxisome in oxidative stress. IUBMB Life *51*, 223–230.

David, J., Ismail, H.M., Chandor-proust, A., John, M., Paine, I., John, M., and Paine, I. (2013). Role of cytochrome P450s in insecticide resistance: impact on the control of mosquito-borne diseases and use of insecticides on Earth. Philos. Trans. R. Soc. *368*, 20120429.

Davies, M.J. (2016). Protein oxidation and peroxidation. Biochem. J. *473*, 805–825.

Davies, T.G.E., Field, L.M., Usherwood, P.N.R., and Williamson, M.S. (2007). DDT, pyrethrins, pyrethroids and insect sodium channels. IUBMB Life *59*, 151–162.

Davioud-Charvet, E., McLeish, M.J., Veine, D.M., Giegel, D., Arscott, L.D., Andricopulo, A.D., Becker, K., Müller, S., Schirmer, R.H., Williams, C.H., et al. (2003). Mechanism-Based Inactivation of Thioredoxin Reductase from Plasmodium falciparum by Mannich Bases. Implication for Cytotoxicity. Biochemistry *42*, 13319–13330.

Debnath, A., Ndao, M., and Reed, S.L. (2013). Reprofiled drug targets ancient protozoans. Gut Microbes *4*, 66–71.

Desideri, E., Filomeni, G., and Ciriolo, M.R. (2012). Glutathione participates in the modulation of starvation-induced autophagy in carcinoma cells. Autophagy *8*, 1769–1781.

Dias, F.A., Gandara, A.C.P., Perdomo, H.D., Gonçalves, R.S., Oliveira, C.R., Oliveira, R.L.L., Citelli, M., Polycarpo, C.R., Santesmasses, D., Mariotti, M., et al. (2016). Identification of a selenium-dependent glutathione peroxidase in the blood-sucking insect Rhodnius prolixus. Insect Biochem. Mol. Biol. *69*, 105–114.

Diaz, R.S., Shytaj, I.L., Giron, L.B., Obermaier, B., Libera, E. della, Galinskas, J., Dias, D., Hunter, J., Janini, M., Gosuen, G., et al. (2019). Potential impact of the antirheumatic agent auranofin on proviral HIV-1 DNA in individuals under intensified antiretroviral therapy: results from a randomized clinical trial. Int. J. Antimicrob. Agents.

Diebold, L., and Chandel, N.S. (2016). Mitochondrial ROS regulation of proliferating cells. Free Radic. Biol. Med. *100*, 86–93.

Ding, Y., Ortelli, F., Rossiter, L.C., Hemingway, J., and Ranson, H. (2003). The Anopheles gambiae glutathione transferase supergene family : annotation , phylogeny and expression profiles. *16*.

Dong, F., Xie, K., Chen, Y., Yang, Y., and Mao, Y. (2017). Polycistronic tRNA and CRIPR guide-RNA enables highly efficient multiplexed genome engineering in human cells. Biochem. Biophys. Res. Commun. *482*, 889–895.

Dong, Y., Simões, M.L., Marois, E., and Dimopoulos, G. (2018). CRISPR/Cas9 -mediated gene knockout of Anopheles gambiae FREP1 suppresses malaria parasite infection. PLoS Pathog. *14*, 1–16.

Dooley, C.T., Dore, T.M., Hanson, G.T., Jackson, W.C., Remington, S.J., and Tsien, R.Y. (2004). Imaging dynamic redox changes in mammalian cells with green fluorescent protein indicators. J. Biol. Chem. *279*, 22284–22293.

Du, Y., Zhang, H., Lu, J., and Holmgren, A. (2012). Glutathione and glutaredoxin act as a backup of human thioredoxin reductase 1 to reduce thioredoxin 1 preventing cell death by aurothioglucose. J. Biol. Chem. *287*, 38210–38219.

Du, Y., Nomura, Y., Zhorov, B.S., and Dong, K. (2016). Sodium channel mutations and pyrethroid resistance in Aedes aegypti. Insects *7*, 1–11.

Eastman, R.T., and Fidock, D.A. (2009). Artemisinin-based combination therapies: a vital tool in efforts to eliminate malaria. *7*, 864–874.

Eckenroth, B.E., Rould, M.A., Hondal, R.J., and Everse, S.J. (2007). Structural and biochemical studies reveal differences in the catalytic mechanisms of mammalian and Drosophila melanogaster thioredoxin reductases. Biochemistry *46*, 4694–4705.

Eklund, H., Gleason, F.K., and Holmgren, A. (1991). Structural and functional relations among thioredoxins of different species. Proteins Struct. Funct. Bioinforma. *11*, 13–28.

Enayati, A.A., Ranson, H., and Hemingway, J. (2005). Insect glutathione transferases and insecticide resistance. Insect Mol. Biol. *14*, 3–8.

Engler, C., and Marillonnet, S. (2013). Combinatorial DNA assembly using Golden Gate cloning. In Synthetic Biology, pp. 141–156.

Enya, S., Yamamoto, C., Mizuno, H., Esaki, T., Lin, H.K., Iga, M., Morohashi, K., Hirano, Y., Kataoka, H., Masujima, T., et al. (2017). Dual roles of glutathione in ecdysone biosynthesis and antioxidant function during larval development in Drosophila. Genetics *207*, 1519–1532.

Eriksson, S., Prigge, J.R., Talago, E.A., Arnér, E.S.J., and Schmidt, E.E. (2015). Dietary methionine can sustain cytosolic redox homeostasis in the mouse liver. Nat. Commun. *6*, 1–9.

Espey, M.G., Xavier, S., Thomas, D.D., Miranda, K.M., and Wink, D.A. (2002). Direct real-time

evaluation of nitration with green fluorescent protein in solution and within human cells reveals the impact of nitrogen dioxide vs. peroxynitrite mechanisms. Proc. Natl. Acad. Sci. U. S. A. *99*, 3481–3486.

Fagbohun, I.K., Oyeniyi, T.A., Idowu, T.E., Otubanjo, O.A., and Awolola, S.T. (2019). Cytochrome P450 Mono-Oxygenase and Resistance Phenotype in DDT and Deltamethrin-Resistant Anopheles gambiae (Diptera: Culicidae) and Culex quinquefasciatus in Kosofe, Lagos, Nigeria. J. Med. Entomol. *56*, 817–821.

Fairhurst, Rick M; Dondorp (2016). Artemisinin resistance review. *33*, 395–401.

Fan, Y., Makar, M., Wang, M.X., and Ai, H. (2017). Monitoring thioredoxin redox with a genetically encoded red fluorescent biosensor. Nat Chem Biol *13*, 1045–1052.

Fang, F.C. (2011). Antimicrobial actions of reactive oxygen species. MBio *2*, 1–6.

Fang, J., Lu, J., and Holmgren, A. (2005). Thioredoxin reductase is irreversibly modified by curcumin: A novel molecular mechanism for its anticancer activity. J. Biol. Chem. *280*, 25284–25290.

Faucon, F., Dusfour, I., Gaude, T., Navratil, V., Boyer, F., Chandre, F., Sirisopa, P., Thanispong, K., Juntarajumnong, W., Poupardin, R., et al. (2015). Identifying genomic changes associated with insecticide resistance in the dengue mosquito Aedes aegypti by deep targeted sequencing. Genome Res. *25*, 1347–1359.

Faurant, C. (2011). From bark to weed: The history of artemisinin. Parasite *18*, 215–218.

Felton, G.W., and Duffey, S.S. (1991). Protective action of midgut catalase in lepidopteran larvae against oxidative plant defenses. J. Chem. Ecol. *17*, 1715–1732.

Feng, X., Zhou, S., Wang, J., and Hu, W. (2018). microRNA profiles and functions in mosquitoes. PLoS Negl. Trop. Dis. *12*, 1–19.

Fernandes, K.M., Neves, C.A., Serrão, J.E., and Martins, G.F. (2014). Aedes aegypti midgut remodeling during metamorphosis. Parasitol. Int. *63*, 506–512.

Feyereisen, R. (1999). Insect P450 Enzymes. Annu. Rev. Entomol. *44*, 507–533.

Finkel, T. (2011). Signal transduction by reactive oxygen species. J. Cell Biol. *194*, 7–15.

Fraenkel, G., and Blewett, M. (1946). Linoleic acid, vitamin E and other fat-soluble substances in the nutrition of certain insects, Ephestia kuehniella, E. elutella, E. cautella and Plodia interpunctella (Lep.). J. Exp. Biol. *22*, 172–190.

Fu, J., Xiong, Z., Huang, C., Li, J., Yang, W., Han, Y., Paiboonrungruan, C., Major, M.B., Chen, K.N., Kang, X., et al. (2019). Hyperactivity of the transcription factor Nrf2 causes metabolic reprogramming in mouse esophagus. J. Biol. Chem. *294*, 327–340.

Gasdaska, P.Y., Gasdaska, J.R., Cochran, S., and Powis, G. (1995). Cloning and sequencing of a human thioredoxin reductase. FEBS Lett. *373*, 5–9.

Gates, Bi. (2018). This animal kills more people in a day than shraks do in a century.

Gjullin, C.M., and Peters, R.F. (1952). recent studies of mosquito resistance to insecticides in California. Mosq. News *12*, 1–7.

Godfray, H.C.J. (2013). Mosquito ecology and control of malaria. J. Anim. Ecol. *82*, 15–25.

Goodman, W.G., and Cusson, M. (2012). The Juvenile Hormones (Elsevier).

Góth, L., and Nagy, T. (2013). Inherited catalase deficiency: Is it benign or a factor in various age related disorders? Mutat. Res. - Rev. Mutat. Res. *753*, 147–154.

Goulson, D. (2013). An overview of the environmental risks posed by neonicotinoid insecticides. J. Appl. Ecol. *50*, 977–987.

Graça-Souza, A. V., Maya-Monteiro, C., Paiva-Silva, G.O., Braz, G.R.C., Paes, M.C., Sorgine, M.H.F., Oliveira, M.F., and Oliveira, P.L. (2006). Adaptations against heme toxicity in blood-feeding arthropods. Insect Biochem. Mol. Biol. *36*, 322–335.

Gravina, S.A., and Mieyal, J.J. (1993). Thioltransferase is a specific glutathionyl mixed disulfide oxidoreductase. Biochemistry *32*, 3368–3376.

Grigoraki, L., Lagnel, J., Kioulos, I., Kampouraki, A., Morou, E., Labbé, P., Weill, M., and Vontas, J. (2015). Transcriptome Profiling and Genetic Study Reveal Amplified Carboxylesterase Genes Implicated in Temephos Resistance, in the Asian Tiger Mosquito Aedes albopictus. PLoS Negl. Trop. Dis. *9*, 1–17.

Grigoraki, L., Balabanidou, V., Meristoudis, C., Miridakis, A., Ranson, H., Swevers, L., and Vontas, J. (2016). Functional and immunohistochemical characterization of CCEae3a, a carboxylesterase associated with temephos resistance in the major arbovirus vectors Aedes aegypti and Ae. albopictus. Insect Biochem. Mol. Biol. *74*, 61–67.

Gromer, S., Arscott, L.D., Williams, C.H., Schirmer, R.H., and Becker, K. (1998). Human Placenta Thioredoxin Reductase. J. Biol. Chem. *273*, 20096–20101.

Gromer, S., Johansson, L., Bauer, H., Arscott, L.D., Rauch, S., Ballou, D.P., Williams, C.H., Schirmer, R.H., and Arnér, E.S.J. (2003). Active sites of thioredoxin reductases: Why selenoproteins? Proc. Natl. Acad. Sci. U. S. A. *100*, 12618–12623.

Gross, E., Sevier, C.S., Heldman, N., Vitu, E., Bentzur, M., Kaiser, C.A., Thorpe, C., and Fass, D. (2006). Generating disulfides enzymatically: Reaction products and electron acceptors of the endoplasmic reticulum thiol oxidase Ero1p. Proc. Natl. Acad. Sci. U. S. A. *103*, 299–304.

Gunasekaran, K., Muthukumaravel, S., Sahu, S.S., Vijayakumar, T., and Jambulingam, P. (2011).

Glutathione S Transferase Activity in Indian Vectors of Malaria: A Defense Mechanism Against DDT. J. Med. Entomol. *48*, 561–569.

Gurgueira, S.A., Lawrence, J., Coull, B., Krishna Murthy, G.G., and González-Flecha, B. (2002). Rapid increases in the steady-state concentration of reactive oxygen species in the lungs and heart after particulate air pollution inhalation. Environ. Health Perspect. *110*, 749–755.

Gutscher, M., Pauleau, A.-L., Marty, L., Brach, T., Wabnitz, G.H., Samstag, Y., Meyer, A.J., and Dick, T.P. (2008). Real-time imaging of the intracellular glutathione redox potential. Nat. Methods *5*, 553–559.

Haenen, G.R.M.M., and Bast, A. (2014). Glutathione revisited: A better scavenger than previously thought. Front. Pharmacol. *5*, 1–5.

Hall, A.G. (1999). The role of glutathione in the regulation of apoptosis. Eur. J. Clin. Invest. *29*, 238–245.

Halliwell, B., and Chirico, S. (1993). Lipid peroxidation : significance and its mechanism. Am. J. Clin. Nutr. *7*, 715–725.

Han, Y.S., Thompson, J., Kafatos, F.C., and Barillas-Mury, C. (2000). Molecular interactions between Anopheles stephensi midgut cells and Plasmodium berghei: The time bomb theory of ookinete invasion. Mem. Inst. Oswaldo Cruz *95*, 28–29.

Hanschmann, E.-M., Godoy, J.R., Berndt, C., Hudemann, C., and Lillig, C.H. (2013). Thioredoxins, Glutaredoxins, and Peroxiredoxins—Molecular Mechanisms and Health Significance: from Cofactors to Antioxidants to Redox Signaling. Antioxid. Redox Signal. *19*, 1539–1605.

Hanschmann, E.M., Lönn, M.E., Schütte, L.D., Funke, M., Godoy, J.R., Eitner, S., Hudemann, C., and Lillig, C.H. (2010). Both thioredoxin 2 and glutaredoxin 2 contribute to the reduction of the mitochondrial 2-Cys peroxiredoxin Prx3. J. Biol. Chem. *285*, 40699–40705.

Hanson, G.T., Aggeler, R., Oglesbee, D., Cannon, M., Capaldi, R.A., Tsien, R.Y., and Remington, S.J. (2004). Investigating Mitochondrial Redox Potential with Redox-sensitive Green Fluorescent Protein Indicators. J. Biol. Chem. *279*, 13044–13053.

Harbut, M.B., Vilchèze, C., Luo, X., Hensler, M.E., Guo, H., Yang, B., Chatterjee, A.K., Nizet, V., Jacobs, W.R., Schultz, P.G., et al. (2015). Auranofin exerts broad-spectrum bactericidal activities by targeting thiol-redox homeostasis. Proc. Natl. Acad. Sci. U. S. A. *112*, 4453–4458.

Harman, D. (2003). The Free Radical Theory of Aging. Antioxidants Redox Signal. *5*, 557–561.

Hayes, J.D., Flanagan, J.U., and Jowsey, I.R. (2005). Glutathione transferases. Annu Rev Phasmacol Toxicol *45*, 51–88.

Hazelton, G.A., and Lang, C.A. (1983). Glutathione biosynthesis in the aging adult yellow-fever mosquito [Aedes aegypti (Louisville)]. Biochem. J. *210*, 289–295.

Hazelton, G.A., and Lang, C.A. (1984). Glutathione levels during the mosquito life span with emphais on senescence. Proceeding Soc. Experimetnal Biol. Med. *256*, 249–256.

Heck, D.E., Vetrano, A.M., Mariano, T.M., and Laskin, J.D. (2003). UVB light stimulates production of reactive oxygen species: Unexpected role for catalase. J. Biol. Chem. *278*, 22432–22436.

Hernández-García, D., Wood, C.D., Castro-Obregón, S., and Covarrubias, L. (2010). Reactive oxygen species: A radical role in development? Free Radic. Biol. Med. *49*, 130–143.

Holmström, K.M., and Finkel, T. (2014). Cellular mechanisms and physiological consequences of redox-dependent signalling. Nat. Rev. Mol. Cell Biol. *15*, 411–421.

House, H.L. (1966). Effects of vitamins E and A on growth and development, and the necessity of vitamin E for reproduction in the parasitoid Agria affinis (Fallén) (Diptera, Sarcophagidae). J. Insect Physiol. *12*, 409–417.

Hrycay, E.G., and Bandiera, S.M. (2012). The monooxygenase, peroxidase, and peroxygenase properties of cytochrome P450. Arch. Biochem. Biophys. *522*, 71–89.

Huang, H., Arscott, L.D., Ballou, D.P., and Jr, C.H.W. (2008). Function of Glu-469 # in the Acid # Base Catalysis of Thioredoxin Reductase from Drosophila melanogaster Function of Glu-469 ′ in the Acid - Base Catalysis of Thioredoxin Reductase from. *47*, 12769–12776.

Huang, Y., Guo, Q., Sun, X., Zhang, C., Xu, N., Xu, Y., Zhou, D., Sun, Y., Ma, L., Zhu, C., et al. (2018). Culex pipiens pallens cuticular protein CPLCG5 participates in pyrethroid resistance by forming a rigid matrix. Parasites and Vectors *11*, 1–10.

Huaxia, Y., Wang, F., Yan, Y., Liu, F., Wang, H., Guo, X., and Xu, B. (2015). A novel 1-Cys thioredoxin peroxidase gene in Apis cerana cerana: characterization of AccTpx4 and its role in oxidative stresses. Cell Stress Chaperones *20*, 663–672.

Hwang, C., Sinskey, A.J., and Lodish, H.F. (1992). Oxidized redox state of glutathione in the endoplasmic reticulum. Science (80-.). *257*, 1496–1502.

Ibrahim, S.S., Ndula, M., Riveron, J.M., Irving, H., and Wondji, C.S. (2016a). The P450 CYP6Z1 confers carbamate/pyrethroid cross-resistance in a major African malaria vector beside a novel carbamate-insensitive N485I acetylcholinesterase-1 mutation. Mol. Ecol. *25*, 3436–3452.

Ibrahim, S.S., Riveron, J.M., Stott, R., Irving, H., and Wondji, C.S. (2016b). The cytochrome P450 CYP6P4 is responsible for the high pyrethroid resistance in knockdown resistance-free Anopheles arabiensis. Insect Biochem. Mol. Biol. *68*, 23–32.

Ide, T., Tsutsui, H., Ohashi, N., Hayashidani, S., Suematsu, N., Tsuchihashi, M., Tamai, H., and Takeshita, A. (2002). Greater oxidative stress in healthy young men compared with premenopausal women. Arterioscler. Thromb. Vasc. Biol. *22*, 438–442.

Insecticide Resistance Action Committee (IRAC) (2010). Prevention and management of insecticide resistance in vectors and pests of public health importance A manual produced by Insecticide Resistance Action Committee (IRAC) Resistance Management for Sustainable Agriculture and Improved Public Health. Insectic. Resist. Action Comm. 3–26.

Ishak, I.H., Kamgang, B., Ibrahim, S.S., Riveron, J.M., Irving, H., and Wondji, C.S. (2017). Pyrethroid Resistance in Malaysian Populations of Dengue Vector Aedes aegypti Is Mediated by CYP9 Family of Cytochrome P450 Genes. PLoS Negl. Trop. Dis. *11*, 1–20.

Jakupoglu, C., Przemeck, G.K.H., Schneider, M., Moreno, S.G., Mayr, N., Hatzopoulos, A.K., de Angelis, M.H., Wurst, W., Bornkamm, G.W., Brielmeier, M., et al. (2005). Cytoplasmic Thioredoxin Reductase Is Essential for Embryogenesis but Dispensable for Cardiac Development. Mol. Cell. Biol. *25*, 1980–1988.

Jang, H.I., and Eom, Y.B. (2019). Repurposing auranofin to combat uropathogenic Escherichia coli biofilms. J. Appl. Microbiol. *127*, 459–471.

Jena, K., Kar, P.K., Babu, C.S., Giri, S., Singh, S.S., and Prasad, B.C. (2013). Comparative Study of Total Hydroperoxides and Antioxidant Defense System in the Indian Tropical Tasar Silkworm, Antheraea mylitta , in Diapausing and Non-Diapausing Generations . J. Insect Sci. *13*, 1–11.

Jocelyn, P., and Kamminga, A. (1974). The non-protein thiol of rat liver mitochondria. Biochim. Biophys. Acta *343*, 356–362.

Johansson, C., Lillig, C.H., and Holmgren, A. (2004). Human Mitochondrial Glutaredoxin Reduces S-Glutathionylated Proteins with High Affinity Accepting Electrons from Either Glutathione or Thioredoxin Reductase. J. Biol. Chem. *279*, 7537–7543.

Jones, M.K., Grau, K.R., Costantini, V., Kolawole, A.O., Graaf, D., Freiden, P., Graves, C.L., Koopmans, M., Wallet, S.M., Tibbetts, S.A., et al. (2016). Auranofin inactivates Trichomonas vaginalis thioredoxin. Int J Antimicrob Agents *48*, 690–694.

Jortzik, E., Farhadi, M., Ahmadi, R., Tóth, K., Lohr, J., Helmke, B.M., Kehr, S., Unterberg, A., Ott, I., Gust, R., et al. (2014). Antiglioma activity of GoPI-sugar, a novel gold(I)-phosphole inhibitor: Chemical synthesis, mechanistic studies, and effectiveness in vivo. Biochim. Biophys. Acta - Proteins Proteomics *1844*, 1415–1426.

Jourd'heuil, D., Jourd'heuil, F.L., and Feelisch, M. (2003). Oxidation and nitrosation of thiols at low micromolar exposure to nitric oxide: Evidence for a free radical mechanism. J. Biol. Chem.

278, 15720–15726.

Jovanović-Galović, A., Blagojević, D.P., Grubor-Lajšić, G., Worland, R., and Spasić, M.B. (2004). Role of antioxidant defense during different stages of preadult life cycle in European corn borer (Ostrinia nubilalis, Hubn.): Diapause and metamorphosis. Arch. Insect Biochem. Physiol. *55*, 79–89.

Kanzok, S.M., Fechner, A., and Bauer, H. (2001). Substitution of the Thioredoxin System for Glutathione Reductase in Drosophila melanogaster. *291*, 643–647.

Kardash, E., Bandemer, J., and Raz, E. (2011). Imaging protein activity in live embryos using fluorescence resonance energy transfer biosensors. Nat. Protoc. *6*, 1835–1846.

Kasozi, D., Mohring, F., Rahlfs, S., Meyer, A.J., and Becker, K. (2013). Real-Time Imaging of the Intracellular Glutathione Redox Potential in the Malaria Parasite Plasmodium falciparum. PLoS Pathog. *9*, 1–18.

Ketterman, A.J., Saisawang, C., and Wongsantichon, J. (2011). Insect glutathione transferases. Drug Metab. Rev. *43*, 253–265.

Killeen, G.F., Fillinger, U., Kiche, I., Gouagna, L.C., and Knols, B.G.J. (2002). Eradication of Anopheles gambiae from Brazil: Lessons for malaria control in Africa? Lancet Infect. Dis. *2*, 618–627.

Kiššová, I.B., and Camougrand, N. (2009). Glutathione participates in the regulation of mitophagy in yeast. Autophagy *5*, 872–873.

Kobayashi, A., Ohta, T., and Yamamoto, M. (2004). Unique Function of the Nrf2-Keap1 Pathway in the Inducible Expression of Antioxidant and Detoxifying Enzymes. Methods Enzymol. *378*, 273–286.

Kraemer, M.U.G., Sinka, M.E., Duda, K.A., Mylne, A.Q.N., Shearer, F.M., Barker, C.M., Moore, C.G., Carvalho, R.G., Coelho, G.E., Van Bortel, W., et al. (2015). The global distribution of the arbovirus vectors Aedes aegypti and Ae. Albopictus. Elife *4*, 1–18.

Kumar, S., Molina-Cruz, A., Gupta, L., Rodrigues, J., and Barillas-Mury, C. (2001). A Peroxidase/Dual Oxidase System Modulates Midgut Epithelial Immunity in Anopheles gambiae. Science (80-.). *327*, 1644–1648.

Kumar, S., Christophides, G.K., Cantera, R., Charles, B., Han, Y.S., Meister, S., Dimopoulos, G., Kafatos, F.C., and Barillas-Mury, C. (2003). The role of reactive oxygen species on Plasmodium melanotic encapsulation in Anopheles gambiae. Proc. Natl. Acad. Sci. U. S. A. *100*, 14139–14144.

Kumar, S., Gupta, L., Yeon, S.H., and Barillas-Mury, C. (2004). Inducible peroxidases mediate

nitration of Anopheles midgut cells undergoing apoptosis in response to Plasmodium invasion. J. Biol. Chem. *279*, 53475–53482.

Labun, K., Montague, T.G., Gagnon, J.A., Thyme, S.B., and Valen, E. (2016). CHOPCHOP v2: a web tool for the next generation of CRISPR genome engineering. Nucleic Acids Res. *44*, W272–W276.

Lacey, B.M., Eckenroth, B.E., Flemer, S.J., and Hondal, R.J. (2008). Selenium in Thioredoxin Reductase: A Mechanistic Perspective. Bciohemistry *47*, 12810–12821.

Langmead, B., and Salzberg, S.L. (2012). Fast gapped-read alignment with Bowtie 2. Nat. Methods *9*, 357–359.

Lavine, M.D., and Strand, M.R. (2002). Insect Hemocytes and Their Role in Immunity. Insect Biochem. Mol. Biol. *32*, 1292–1309.

Lee, K. (1991). Glutathione S-transferase activities in phytophagous insects: Induction and inhibition by plant phototoxins and phenols. Insect Biochem. *21*, 353–361.

Lee, K.S., Ryul Kim, S., Sook Park, N., Kim, I., Dong Kang, P., Hee Sohn, B., Ho Choi, K., Woo Kang, S., Ho Je, Y., Mong Lee, S., et al. (2005). Characterization of a silkworm thioredoxin peroxidase that is induced by external temperature stimulus and viral infection. Insect Biochem. Mol. Biol. *35*, 73–84.

Lewis, D.F.V. (2002). Oxidative stress: The role of cytochromes P450 in oxygen activation. J. Chem. Technol. Biotechnol. *77*, 1095–1100.

Lin, G.G., and Scott, J.G. (2012). Ros function in redox signaling. *100*, 130–134.

Lindsay, S.W., and Gibson, M.E. (1988). Bednets revisited- old idea, new angle. Parasitol. Today *4*, 270–272.

Linenberg, I., Christophides, G.K., and Gendrin, M. (2016). Larval diet affects mosquito development and permissiveness to Plasmodium infection. Sci. Rep. *6*, 1–10.

Little, C., and O'Brien, P.J. (1968). An intracellular GSH-peroxidase with a lipid peroxide substrate. Biochem. Biophys. Res. Commun. *31*, 145–150.

Liu, Z., Du, Z.Y., Huang, Z.S., Lee, K.S., and Gu, L.Q. (2008). Inhibition of thioredoxin reductase by curcumin analogs. Biosci. Biotechnol. Biochem. *72*, 2214–2218.

Liu, Z., Chen, O., Wall, J.B.J., Zheng, M., Zhou, Y., Wang, L., Ruth Vaseghi, H., Qian, L., and Liu, J. (2017). Systematic comparison of 2A peptides for cloning multi-genes in a polycistronic vector. Sci. Rep. *7*, 1–9.

Lothrop, A.P., Ruggles, E.L., and Hondal, R.J. (2009). No Selenium Required: Reactions Catalyzed By Mammalian Thioredoxin Reductase That Are Independent of a Selenocysteine Residue.

Biochemistry *48*, 6213–6223.

Love, M.I., Huber, W., and Anders, S. (2014). Moderated estimation of fold change and dispersion for RNA-seq data with DESeq2. Genome Biol. *15*, 1–21.

Lu, J., and Holmgren, A. (2012). Thioredoxin system in cell death progression. Antioxidants Redox Signal. *17*, 1738–1747.

Lu, J., and Holmgren, A. (2014). The thioredoxin antioxidant system. Free Radic. Biol. Med. *66*, 75–87.

Lu SC (2013). Glutathione synthesis. Biochim. Biophys. Acta *1830*, 3143–3153.

De Luca, A., Hartinger, C.G., Dyson, P.J., Lo Bello, M., and Casini, A. (2013). A new target for gold(I) compounds: Glutathione-S-transferase inhibition by auranofin. J. Inorg. Biochem. *119*, 38–42.

Luckhart, T.M.L.P. and S. (2008). A mosquito 2-Cys peroxiredoxin protects against nitrosative and oxidative stresses associated with malaria parasite infection. Free Radic. Biol. Med. *40*, 1067–1082.

Lumjuan, N., Rajatileka, S., Changsom, D., Wicheer, J., Leelapat, P., Prapanthadara, L. aied, Somboon, P., Lycett, G., and Ranson, H. (2011). The role of the Aedes aegypti Epsilon glutathione transferases in conferring resistance to DDT and pyrethroid insecticides. Insect Biochem. Mol. Biol. *41*, 203–209.

Lundberg, J.O., Weitzberg, E., and Gladwin, M.T. (2008). The nitrate-nitrite-nitric oxide pathway in physiology and therapeutics. Nat. Rev. Drug Discov. *7*, 156–167.

Luthman, M., and Holmgren, A. (1982). Rat Liver Thioredoxin and Thioredoxin Reductase: Purification and Characterization. Biochemistry *21*, 6628–6633.

Machani, M.G., Ochomo, E., Sang, D., Bonizzoni, M., Zhou, G., Githeko, A.K., Yan, G., and Afrane, Y.A. (2019). Influence of blood meal and age of mosquitoes on susceptibility to pyrethroids in Anopheles gambiae from Western Kenya. Malar. J. *18*, 1–9.

Mack, S.R., Foley, D.A., and Vanderberg, J.P. (1979). Hemolymph volume of noninfected and Plasmodium berghei-infected Anopheles stephensi. J. Invertebr. Pathol. *34*, 105–109.

Magalhaes, T., Brackney, D.E., Beier, J.C., and Foy, B.D. (2008). Silencing an Anopheles gambiae catalase and sulfhydryl oxidase increases msoquito mortality after a blood meal. Arch. Insect Biochem. Physiol. *68*, 134–143.

Maiorino, M., Ursini, F., Bosello, V., Toppo, S., Tosatto, S.C.E., Mauri, P., Becker, K., Roveri, A., Bulato, C., Benazzi, L., et al. (2007). The Thioredoxin Specificity of Drosophila GPx : A Paradigm for a Peroxiredoxin-like Mechanism of many Glutathione Peroxidases. *4*, 1033–

1046.

Mancilla, H., Maldonado, R., Cereceda, K., Villarroel-Espíndola, F., Montes De Oca, M., Angulo, C., Castro, M.A., Slebe, J.C., Vera, J.C., Lavandero, S., et al. (2015). Glutathione Depletion Induces Spermatogonial Cell Autophagy. J. Cell. Biochem. *116*, 2283–2292.

Manittais, T., Sambrook, J., and Fritsch, E.F. (1989). Molecular cloning: a laboratory manual (Cold Spring Harbor Laboratory Press).

Manzoni, G., Briquet, S., Risco-Castillo, V., Gaultier, C., Topçu, S., Ivănescu, M.L., Franetich, J.F., Hoareau-Coudert, B., Mazier, D., and Silvie, O. (2014). A rapid and robust selection procedure for generating drug-selectable marker-free recombinant malaria parasites. Sci. Rep. *4*, 1–10.

Marois, E., Scali, C., Soichot, J., Kappler, C., Levashina, E.A., and Catteruccia, F. (2012). High-throughput sorting of mosquito larvae for laboratory studies and for future vector control interventions. Malar. J. *11*, 1.

Marzo, T., Cirri, D., Pollini, S., Prato, M., Fallani, S., Cassetta, M.I., Novelli, A., Rossolini, G.M., and Messori, L. (2018). Auranofin and its Analogues Show Potent Antimicrobial Activity against Multidrug-Resistant Pathogens: Structure–Activity Relationships. ChemMedChem *13*, 2448–2454.

Matsui, M., Oshima, M., Oshima, H., Takaku, K., Maruyama, T., Yodoi, J., and Taketo, M.M. (1996). Early Embryonic Lethality Caused by Targeted Disruption of the Mouse Thioredoxin Gene. Dev. Biol. *178*, 179–185.

May, J.M., Cobb, C.E., Mendiratta, S., Hill, K.E., and Burk, R.F. (1998a). Reduction of the ascorbyl free radical to ascorbate by thioredoxin reductase. J. Biol. Chem. *273*, 23039–23045.

May, J.M., Cobb, C.E., Mendiratta, S., Hill, K.E., and Burk, R.F. (1998b). Reduction of the ascorbyl free radical to ascorbate by thioredoxin reductase. J. Biol. Chem. *273*, 23039–23045.

Mbepera, S., Nkwengulila, G., Peter, R., Mausa, E.A., Mahande, A.M., Coetzee, M., and Kweka, E.J. (2017). The influence of age on insecticide susceptibility of Anopheles arabiensis during dry and rainy seasons in rice irrigation schemes of Northern Tanzania. Malar. J. *16*, 1–9.

McCarty, S.E., Schellenberger, A., Goodwin, D.C., Fuanta, N.R., Tekwani, B.L., and Calderón, A.I. (2015). Plasmodium falciparum thioredoxin reductase (PfTrxR) and Its role as a target for new antimalarial discovery. Molecules *20*, 11459–11473.

McDermott, E.G., Morris, E.K., and Garver, L.S. (2019). Sodium Ascorbate as a Potential Toxicant in Attractive Sugar Baits for Control of Adult Mosquitoes (Diptera: Culicidae) and Sand Flies (Diptera: Psychodidae). J. Med. Entomol. *56*, 1359–1367.

McKeage, M.J., Maharaj, L., and Berners-Price, S.J. (2002). Mechanisms of cytotoxicity and antitumor activity of gold(I) phosphine complexes: The possible role of mitochondria. Coord. Chem. Rev. *232*, 127–135.

Menon, D., and Board, P.G. (2013). A role for glutathione transferase omega 1 (GSTO1-1) in the glutathionylation cycle. J. Biol. Chem. *288*, 25769–25779.

Mercer, S.W., and Burke, R. (2016). Evidence for a role for the putative Drosophila hGRX1 orthologue in copper homeostasis. BioMetals *29*, 705–713.

Meyer, A.J., and Dick, T.P. (2010). Fluorescent protein-based redox probes. Antioxid. Redox Signal. *13*, 621–650.

Mhamdi, A., and Van Breusegem, F. (2018). Reactive oxygen species in plant development. Dev. *145*.

Mi, H., Muruganujan, A., Ebert, D., Huang, X., and Thomas, P.D. (2019). PANTHER version 14: More genomes, a new PANTHER GO-slim and improvements in enrichment analysis tools. Nucleic Acids Res. *47*, D419–D426.

Miiller, S., Gilberger, T., Petra, M.F., Beckerb, K., Schirmerb, R.H., and Walter, R.D. (1996). Recombinant putative glutathione reductase of Plasmodium falciparum. Mol. Biochem. Parasitol. *80*, 215–219.

Miller, R.L., Ikram, S., Armelagoss, G.J., Walker, R., Harers, W.B., Shiffi, C.J., Baggett, D., Carrigan, M., and Maret, S.M. (1994). Diagnosis of Plasmodium falciparum infections in mummies using the rapid manual ParaSightTM-F test. Trans. R. Soc. Trop. Med. Hyg. *88*, 31–32.

Mills, G.C. (1957). Glutathione peroxidase, an erythrocyte enzyme which protects hemoglobin from oxidative breakdown. J. Biol. Chem *229*, 189–197.

Missirlis, F., Phillips, J.P., and Jäckle, H. (2001). Cooperative action of antioxidant defense systems in Drosophila. Curr. Biol. *11*, 1272–1277.

Missirlis, F., Ulschmid, J.K., Hirosawa-Takamori, M., Nke, S.G., Fer, U.S., Becker, K., Phillips, J.P., and Ckle, H.J. (2002). Mitochondrial and cytoplasmic thioredoxin reductase variants encoded by a single Drosophila gene are both essential for viability. J. Biol. Chem. *277*, 11521–11526.

Mitsuishi, Y., Taguchi, K., Kawatani, Y., Shibata, T., Nukiwa, T., Aburatani, H., Yamamoto, M., and Motohashi, H. (2012). Nrf2 Redirects Glucose and Glutamine into Anabolic Pathways in Metabolic Reprogramming. Cancer Cell *22*, 66–79.

Miyawaki, A., Llopis, J., Heim, R., McCaffery, M.J., Adams, J.A., Ikurak, M., and Tsien, R.Y. (1997). Fluorescent indicators for Ca2+ based on green fluorescent proteins and calmodulin.

Nature *388*, 882–887.

Molina-Cruz, A., DeJong, R.J., Charles, B., Gupta, L., Kumar, S., Jaramillo-Gutierrez, G., and Barillas-Mury, C. (2008). Reactive oxygen species modulate Anopheles gambiae immunity against bacteria and Plasmodium. J. Biol. Chem. *283*, 3217–3223.

Morin, C., Besset, T., Moutet, J.-C., Fayolle, M., Brückner, M., Limosin, D., Becker, K., and Davioud-Charvet, E. (2008). The aza-analogues of 1,4-naphthoquinones are potent substrates and inhibitors of plasmodial thioredoxin and glutathione reductases and of human erythrocyte glutathione reductase. Org. Biomol. Chem. *6*, 2731–2742.

Moyes, C.L., Vontas, J., Martins, A.J., Ng, L.C., Koou, S.Y., Dusfour, I., Raghavendra, K., Pinto, J., Corbel, V., David, J.P., et al. (2017). Contemporary status of insecticide resistance in the major Aedes vectors of arboviruses infecting humans. PLoS Negl. Trop. Dis. *11*, 1–20.

Muri, J., Heer, S., Matsushita, M., Pohlmeier, L., Tortola, L., Fuhrer, T., Conrad, M., Zamboni, N., Kisielow, J., and Kopf, M. (2018). The thioredoxin-1 system is essential for fueling DNA synthesis during T-cell metabolic reprogramming and proliferation. Nat. Commun. *9*, 1–16.

N'Guessan, R., Darriet, F., Guillet, P., Carnevale, P., Traore-Lamizana, M., Corbel, V., Koffi, A.A., and Chandre, F. (2003). Resistance to carbosulfan in Anopheles gambiae from Ivory Coast, based on reduced sensitivity of acetylcholinesterase. Med. Vet. Entomol. *17*, 19–25.

Neumman, R., and Peter, H. (1987). Insecticidal organophosphates : Nature made them first. Experientia *43*, 1235–1237.

Niveditha, S., Deepashree, S., Ramesh, S.R., and Shivanandappa, T. (2017). Sex differences in oxidative stress resistance in relation to longevity in Drosophila melanogaster. J. Comp. Physiol. B Biochem. Syst. Environ. Physiol. *187*, 899–909.

Nonn, L., Williams, R.R., Erickson, R.P., and Powis, G. (2003). The Absence of Mitochondrial Thioredoxin 2 Causes Massive Apoptosis, Exencephaly, and Early Embryonic Lethality in Homozygous Mice. Mol. Cell. Biol. *23*, 916–922.

Nordberg, J., and Arnér, E.S.J. (2001). Reactive oxygen species, antioxidants, and the mammalian thioredoxin system. Free Radic. Biol. Med. *31*, 1287–1312.

Odnokoz, O., Nakatsuka, K., Klichko, V.I., Nguyen, J., Solis, L.C., Ostling, K., Badinloo, M., Orr, W.C., and Radyuk, S.N. (2017). Mitochondrial peroxiredoxins are essential in regulating the relationship between Drosophila immunity and aging. Biochim. Biophys. Acta - Mol. Basis Dis. *1863*, 68–80.

Ohl, K., Fragoulis, A., Klemm, P., Baumeister, J., Klock, W., Verjans, E., Böll, S., Möllmann, J., Lehrke, M., Costa, I., et al. (2018). Nrf2 is a central regulator of metabolic reprogramming of myeloid-derived suppressor cells in steady state and sepsis. Front. Immunol. *9*, 1–17.

Olé Sangba, M.L., Sidick, A., Govoetchan, R., Dide-Agossou, C., Ossè, R.A., Akogbeto, M., and Ndiath, M.O. (2017). Evidence of multiple insecticide resistance mechanisms in Anopheles gambiae populations in Bangui, Central African Republic. Parasites and Vectors *10*, 1–10.

Oliveira, H.M., Kubota, M.S., Arau, H.R.C., Bahia, A.C., Vinı, M., Lacerda, G., Oliveira, P.L., Traub-, Y.M., and Rı, C.M. (2013). The Role of Reactive Oxygen Species in Anopheles aquasalis Response to Plasmodium vivax Infection. *8*, 1–10.

Oliveira, J.H.M., Gonçalves, R.L.S., Lara, F.A., Dias, F.A., Gandara, A.C.P., Menna-Barreto, R.F.S., Edwards, M.C., Laurindo, F.R.M., Silva-Neto, M.A.C., Sorgine, M.H.F., et al. (2011). Blood meal-derived heme decreases ROS levels in the midgut of Aedes aegypti and allows proliferation of intestinal microbiota. PLoS Pathog. *7*.

Oliveira, J.H.M., Talyuli, O.A.C., Goncalves, R.L.S., Paiva-Silva, G.O., Sorgine, M.H.F., Alvarenga, P.H., and Oliveira, P.L. (2017). Catalase protects Aedes aegypti from oxidative stress and increases midgut infection prevalence of Dengue but not Zika. PLoS Negl. Trop. Dis. *11*, 1–13.

Oliver, S. V., and Brooke, B.D. (2016). The Role of Oxidative Stress in the Longevity and Insecticide Resistance Phenotype of the Major Malaria Vectors Anopheles arabiensis and Anopheles funestus. PLoS One *11*, e0151049.

Onodera, T., Momose, I., and Kawada, M. (2019). Drug Discovery : Recent Progress and the Future Potential Anticancer Activity of Auranofin. *67*, 186–191.

Ormö, M., Cubitt, A.B., Kallio, K., Gross, L. a, Tsien, R.Y., Remington, S.J., Ormo, M., Cubitt, A.B., Kallio, K., Gross, L. a, et al. (1996). Crystal structure of the Aequorea victoria green fluorescent protein. Science *273*, 1392–1395.

Østergaard, H., Henriksen, A., Hansen, F.G., and Winther, J.R. (2001). Shedding light on disulfide bond formation: Engineering a redox switch in green fluorescent protein. EMBO J. *20*, 5853–5862.

Owings, J.P., McNair, N.N., Mui, Y.F., Gustafsson, T.N., Holmgren, A., Contel, M., Goldberg, J.B., and Mead, J.R. (2016). Auranofin and N-heterocyclic carbene gold-analogs are potent inhibitors of the bacteria Helicobacter pylori. FEMS Microbiol. Lett. *363*, 1–6.

Panday, A., Sahoo, M.K., Osorio, D., and Batra, S. (2015). NADPH oxidases: An overview from structure to innate immunity-associated pathologies. Cell. Mol. Immunol. *12*, 5–23.

Papathanos, P.A., Windbichler, N., Menichelli, M., Burt, A., and Crisanti, A. (2009). The vasa regulatory region mediates germline expression and maternal transmission of proteins in the malaria mosquito Anopheles gambiae: A versatile tool for genetic control strategies. BMC Mol. Biol. *10*, 1–13.

Patro1, R., Duggal, G., Love, M.I., Irizarry, R.A., and Kingsford, C. (2017). Salmon: fast and bias-aware quantification of transcript expression using dual-phase inference. Nat. Methods *14*, 417–419.

Pavlidi, N., Vontas, J., and Van Leeuwen, T. (2018). The role of glutathione S-transferases (GSTs) in insecticide resistance in crop pests and disease vectors. Curr. Opin. Insect Sci. *27*, 97–102.

Pellicena-Pallé, A., Stitzinger, S.M., and Salz, H.K. (1997). The function of the Drosophila thioredoxin homologue encoded by the deadhead gene is redox-dependent and blocks the initiation of development but not DNA synthesis. Mech. Dev. *62*, 61–65.

Peltoniemi, M.J., Karala, A.R., Jurvansuu, J.K., Kinnula, V.L., and Ruddock, L.W. (2006). Insights into deglutathionylation reactions: Different intermediates in the glutaredoxin and protein disulfide isomerase catalyzed reactions are defined by the γ-linkage present in glutathione. J. Biol. Chem. *281*, 33107–33114.

Peng, X., Giménez-Cassina, A., Petrus, P., Conrad, M., Rydén, M., and Arnér, E.S.J. (2016). Thioredoxin reductase 1 suppresses adipocyte differentiation and insulin responsiveness. Sci. Rep. *6*, 1–17.

Perkins, A., Poole, L.B., and Karplus, P.A. (2014). Tuning of peroxiredoxin catalysis for various physiological roles. Biochemistry *53*, 7693–7705.

Peterson, T.M.L., Gow, A.J., and Luckhart, S. (2007). Nitric oxide metabolites induced in Anopheles stephensi control malaria parasite infection. Free Radic Biol Med *42*, 132–142.

Pias, E.K., and Tak Yee, A.W. (2002). Apoptosis in mitotic competent undifferentiated cells is induced by cellular redox imbalance independent of reactive oxygen species production. FASEB J. *16*, 781–790.

Piermarini, P.M., Esquivel, C.J., and Denton, J.S. (2017). Malpighian tubules as novel targets for mosquito control. Int. J. Environ. Res. Public Health *14*.

Pogozelski, W.K., and Tullius, T.D. (1998). Oxidative strand scission of nucleic acids: Routes initiated by hydrogen abstraction from the sugar moiety. Chem. Rev. *98*, 1089–1107.

Pondeville, E., Puchot, N., Meredith, J.M., Lynd, A., Vernick, K.D., Lycett, G.J., Eggleston, P., and Bourgouin, C. (2014). Efficient φc31 integrase-mediated site-specific germline transformation of Anopheles gambiae. Nat. Protoc. *9*, 1698–1712.

Popham, H.J.R., and Shelby, K.S. (2009). Ascorbic acid influences the development and immunocompetence of larval Heliothis virescens. Entomol. Exp. Appl. *133*, 57–64.

Port, F., and Bullock, S.L. (2017). Augmenting CRISPR applications in Drosophila with tRNA-flanked Cas9 and Cpf1 sgRNAs. *13*, 852–854.

Port, F., Chen, H.-M., Lee, T., and Bullock, S.L. (2014). Optimized CRISPR/Cas tools for efficient germline and somatic genome engineering in Drosophila. Proc. Natl. Acad. Sci. *111*, E2967–E2976.

Potter, C.J., Tasic, B., Russler, E. V, and Liang, L. (2010). The Q system: a repressible binary system for transgene expression, lineage tracing and mosaic analysis. Cell *141*, 536–548.

Poupardin, R., Srisukontarat, W., Yunta, C., and Ranson, H. (2014). Identification of Carboxylesterase Genes Implicated in Temephos Resistance in the Dengue Vector Aedes aegypti. PLoS Negl. Trop. Dis. *8*.

Pragya, P., Shukla, A.K., Murthy, R.C., Abdin, M.Z., and Chowdhuri, D.K. (2014). Over-expression of superoxide dismutase ameliorates Cr(VI) induced adverse effects via modulating cellular immune system of Drosophila melanogaster. PLoS One *9*.

Pryce, J., Richardson, M., and Lengeler, C. (2018). Insecticide-treated nets for preventing malaria (Review) SUMMARY OF FINDINGS FOR THE MAIN COMPARISON. Cochrane Database Syst. Rev. 1–85.

Pryor, W. a (1986). Oxy-radicals and related species: their formation, lifetimes and reactions. Annu. Rev. Physiol. *48*, 657–667.

Putchala, M.C., Ramani, P., Sherlin, H.J., Premkumar, P., and Natesan, A. (2013). Ascorbic acid and its pro-oxidant activity as a therapy for tumours of oral cavity-A systematic review. Arch. Oral Biol. *58*, 563–574.

Rackham, O., Shearwood, A.M.J., Thyer, R., McNamara, E., Davies, S.M.K., Callus, B.A., Miranda-Vizuete, A., Berners-Price, S.J., Cheng, Q., Arnér, E.S.J., et al. (2011). Substrate and inhibitor specificities differ between human cytosolic and mitochondrial thioredoxin reductases: Implications for development of specific inhibitors. Free Radic. Biol. Med. *50*, 689–699.

Radi, R. (2018). Oxygen radicals, nitric oxide, and peroxynitrite: Redox pathways in molecular medicine. Proc. Natl. Acad. Sci. U. S. A. *115*, 5839–5848.

Radyuk, S.N., Klichko, V.I., Spinola, B., Sohal, R.S., and Orr, W.C. (2001). The peroxiredoxin gene family in Drosophila melanogaster. Free Radic. Biol. Med. *31*, 1090–1100.

Radyuk, S.N., Michalak, K., Klichko, V.I., Benes, J., Rebrin, I., Sohal, R.S., and Orr, W.C. (2009). Peroxiredoxin 5 confers protection against oxidative stress and apoptosis and also promotes longevity in Drosophila. Biochem. J. *419*, 437–445.

Radyuk, S.N., Rebrin, I., Klichko, V.I., Sohal, B.H., Michalak, K., Benes, J., Sohal, R.S., and Orr, W.C. (2010). Mitochondrial peroxiredoxins are critical for the maintenance of redox state and the survival of adult Drosophila. Free Radic. Biol. Med. *49*, 1892–1902.

Radyuk, S.N., Klichko, V.I., Michalak, K., and Orr, W.C. (2013). The effect of peroxiredoxin 4 on fly physiology is a complex interplay of antioxidant and signaling functions. FASEB J. *27*, 1426–1438.

Ragu, S., Dardalhon, M., Sharma, S., Iraqui, I., Buhagiar-Labarchéde, G., Grondin, V., Kienda, G., Vernis, L., Chanet, R., Kolodner, R.D., et al. (2014). Loss of the thioredoxin reductase Trr1 suppresses the genomic instability of peroxiredoxin TSA1 mutants. PLoS One *9*.

Rajatileka, S., Burhani, J., and Ranson, H. (2011). Mosquito age and susceptibility to insecticides. Trans. R. Soc. Trop. Med. Hyg. *105*, 247–253.

Ralph, S.J., Nozuhur, S., ALHulais, R.A., Rodríguez‐Enríquez, S., and Moreno‐Sánchez, R. (2019). Repurposing drugs as pro‐oxidant redox modifiers to eliminate cancer stem cells and improve the treatment of advanced stage cancers. Med. Res. Rev. *1*, 1–30.

Ranson, H., and Lissenden, N. (2016). Insecticide Resistance in African Anopheles Mosquitoes: A Worsening Situation that Needs Urgent Action to Maintain Malaria Control. Trends Parasitol. *32*, 187–196.

Ranson, H., Collins, F., and Hemingway, J. (1998). The role of alternative mRNA splicing in generating heterogeneity within the Anopheles gambiae class I glutathione S-transferase family. Proc. Natl. Acad. Sci. U. S. A. *95*, 14284–14289.

Ranson, H., Jensen, B., Wang, X., Prapanthadara, L., Hemingway, J., and Collins, F.H. (2000). Genetic mapping of two loci affecting DDT resistance in the malaria vector Anopheles gambiae. Insect Mol. Biol. *9*, 499–507.

Ranson, H., Rossiter, L., Ortelli, F., Jensen, B., Wang, X., Roth, C.W., Collins, F.H., and Hemingway, J. (2001). in resistance to DDT in the malaria vector Anopheles gambiae. *304*, 295–304.

Redza-Dutordoir, M., and Averill-Bates, D.A. (2016). Activation of apoptosis signalling pathways by reactive oxygen species. Biochim. Biophys. Acta - Mol. Cell Res. *1863*, 2977–2992.

Reed, T.T. (2011). Lipid peroxidation and neurodegenerative disease. Free Radic. Biol. Med. *51*, 1302–1319.

Regina, I., Capoci, G., Sakita, K.M., Faria, D.R., Rodrigues-vendramini, F.A.V., Arita, G.S., Bonfim-mendonça, P.D.S., and Kioshima, E.S. (2019). Two New 1 , 3 , 4-Oxadiazoles With Effective Antifungal Activity Against Candida albicans. *10*, 1–11.

Reichheld, J.P., Khafif, M., Riondet, C., Droux, M., Bonnard, G., and Meyer, Y. (2007). Inactivation of thioredoxin reductases reveals a complex interplay between thioredoxin and glutathione pathways in arabidopsis development. Plant Cell *19*, 1851–1865.

Renn, S.C.P., Park, J.H., Rosbash, M., Hall, J.C., and Taghert, P.H. (1999). A pdf neuropeptide gene mutation and ablation of PDF neurons each cause severe abnormalities of behavioral circadian rhythms in Drosophila. Cell *99*, 791–802.

Riabinina, O., Task, D., Marr, E., Lin, C.C., Alford, R., O'Brochta, D.A., and Potter, C.J. (2016). Organization of olfactory centres in the malaria mosquito Anopheles gambiae. Nat. Commun. *7*.

Ribeiro, J.M.C. (2003). A catalogue of Anopheles gambiae transcripts significantly more or less expressed following a blood meal. Insect Biochem. Mol. Biol. *33*, 865–882.

Ribeiro, J.M.C., and Nussenzveig, R.H. (1993). Nitric oxide synthase activity from a hematophagous insect salivary gland. FEBS Lett. *330*, 165–168.

Rigobello, M.P., Scutari, G., Boscolo, R., and Bindoli, A. (2002). Induction of mitochondrial permeability transition by auranofin, a Gold(I)-phosphine derivative. Br. J. Pharmacol. *136*, 1162–1168.

Rigobello, M.P., Scutari, G., Folda, A., and Bindoli, A. (2004). Mitochondrial thioredoxin reductase inhibition by gold(I) compounds and concurrent stimulation of permeability transition and release of cytochrome c. Biochem. Pharmacol. *67*, 689–696.

Rigobello, M.P., Folda, A., Baldoin, M.C., Scutari, G., and Bindoli, A. (2005). Effect of Auranofin on the mitochondrial generation of hydrogen peroxide. Role of thioredoxin reductase. Free Radic. Res. *39*, 687–695.

Riley, P.A. (1994). Free radicals in biology: Oxidative stress and the effects of ionizing radiation. Int. J. Radiat. Biol. *65*, 27–33.

Rinkevich, F.D., Du, Y., and Dong, K. (2013). Diversity and Convergence of Sodium Channel Mutations Involved in Resistance to Pyrethroids. Pestic Biochem Pyhsiol *106*, 93–100.

Roll Back Malaria Partnership (2008). The gobal malaria actin plan: for a malaria-free world (Geneva).

Rosenwasser, S., Rot, I., Meyer, A.J., Feldman, L., Jiang, K., and Friedman, H. (2010). A fluorometer-based method for monitoring oxidation of redox-sensitive GFP (roGFP) during development and extended dark stress. Physiol. Plant. *138*, 493–502.

Rozendaal, J.A. (1997). Mosquitoes and other bitting Diptera. In Vector Control: Methods for Use by Individuals and Communities, (Geneva), pp. 10–17.

RTS, S.C.T.P. (2017). Efficacy and safety of RTS , S / AS01 malaria vaccine with or without a booster dose in infants and children in Africa : final results of a phase 3 , individually randomised , controlled trial. Lancet *386*, 31–45.

Ryter, S, W. Tyrrell, R, M. (2000). the Heme Synthesis and Degradation Pathways: role in oxidant sensitivity. Free Radic. Biol. Med. *28*, 289–309.

Saethang, T., Hodge, K., Kimkong, I., Payne, D.M., Knepper, M.A., and Pisitkun, T. (2018). AbDesigner3D: A structure-guided tool for peptide-based antibody production. Bioinformatics *34*, 2158–2160.

Sahoo, A., Sahu, S., Dandapat, J., and Samanta, L. (2016). Pro-oxidative challenges and antioxidant protection during larval development of non-mulberry silkworm, Antheraea mylitta (Lepidoptera: Saturniidae). Ital. J. Zool. *83*, 3–14.

Saillenfait, A.M., Ndiaye, D., and Sabaté, J.P. (2015). Pyrethroids: Exposure and health effects - An update. Int. J. Hyg. Environ. Health *218*, 281–292.

Salz, H.K., Flickinger, T.W., Mittendorf, E., Pellicena-Palle, A., Petschek, J.P., and Albrecht, E.B. (1994). The Drosophila maternal effect locus deadhead encodes a thioredoxin homolog required for female meiosis and early embryonic development. Genetics *136*, 1075–1086.

Scherz-Shouval, R., Shvets, E., Fass, E., Shorer, H., Gil, L., and Elazar, Z. (2007). Reactive oxygen species are essential for autophagy and specifically regulate the activity of Atg4. EMBO J. *26*, 1749–1760.

Schirmer, R.H., Coulibaly, B., Stich, A., Scheiwein, M., Merkle, H., Eubel, J., Becker, K., Becher, H., Müller, O., Zich, T., et al. (2003). Methylene blue as an antimalarial agent. Redox Rep. *8*, 272–275.

Schmidt, E.E. (2015). Interplay between cytosolic disulfide reductase systems and the Nrf2/Keap1 pathway. Biochem. Soc. Trans. *43*, 632–638.

Seaman, J.A., Alout, H., Meyers, J.I., Stenglein, M.D., Dabiré, R.K., Lozano-Fuentes, S., Burton, T.A., Kuklinski, W.S., Black, W.C., and Foy, B.D. (2015). Age and prior blood feeding of Anopheles gambiae influences their susceptibility and gene expression patterns to ivermectin-containing blood meals. BMC Genomics *16*, 1–18.

Sebastià, J., Cristòfol, R., Martín, M., Rodriguez-Farré, E., and Sanfeliu, C. (2003). Evaluation of Fluorescent Dyes for Measuring Intracellular Glutathione Content in Primary Cultures of Human Neurons and Neuroblastoma SH-SY5Y. Cytom. Part A *51*, 16–25.

Shi, G.Q., Yu, Q.Y., Shi, L., and Zhang, Z. (2012). Molecular cloning and characterization of peroxiredoxin 4 involved in protection against oxidative stress in the silkworm Bombyx mori. Insect Mol. Biol. *21*, 581–592.

Shivanandappa, S.N.S.R.R.T. (2017). Paraquat-Induced Movement Disorder in Relation to Oxidative Stress-Mediated Neurodegeneration in the Brain of Drosophila melanogaster. Neurochem. Res. *0*, 0.

Silva-Adaya, D., Gonsebatt, M.E., and Guevara, J. (2014). Thioredoxin system regulation in the central nervous system: Experimental models and clinical evidence. Oxid. Med. Cell. Longev. *2014*.

Silva, A.P.B., Santos, J.M.M., and Martins, A.J. (2014). Mutations in the voltage-gated sodium channel gene of anophelines and their association with resistance to pyrethroids - A review. Parasites and Vectors *7*, 1–14.

Sim, C., and Denlinger, D.L. (2011). Pipiens, Catalase and superoxide dismutase-2 enhance survival and protect ovaries during overwintering diapause in the msoquito Culex. J. Insect Physiol. *57*, 628–634.

Slater, A. (1993). Chloroquine. XPharm Compr. Pharmacol. Ref. *57*, 203–235.

Slaymaker, I.M., Gao, L., Zetsche, B., Scott, D.A., Yan, W.X., and Zhang, F. (2016). Rationally engineered Cas9 nucleases with improved specificity. Science (80-.). *351*, 84–88.

Spielman, A., and Williams, C.M. (1966). Lethal effects of synthetic juvenile hormone on larvae of the yellow fever mosquito, Aedes aegypti. Science (80-.). *154*, 1043–1044.

Stenvall, J., Fierro-González, J.C., Swoboda, P., Saamarthy, K., Cheng, Q., Cacho-Valadez, B., Arnér, E.S.J., Persson, O.P., Miranda-Vizuete, A., and Tuck, S. (2011). Selenoprotein TRXR-1 and GSR-1 are essential for removal of old cuticle during molting in Caenorhabditis elegans. Proc. Natl. Acad. Sci. U. S. A. *108*, 1064–1069.

Stubbs, C.D., and Smith, A.D. (1984). The modification of mammalian membrane polyunsaturated fatty acid composition in relation to membrane fluidity and function. BBA - Rev. Biomembr. *779*, 89–137.

Sumayao, R., Newsholme, P., and McMorrow, T. (2018). The role of cystinosin in the intermediary thiol metabolism and redox homeostasis in kidney proximal tubular cells. Antioxidants *7*.

Sun, Y., and Rigas, B. (2008). The thioredoxin system mediates redox-induced cell death in human colon cancer cells: Implications for the mechanism of action of anticancer agents. Cancer Res. *68*, 8269–8277.

Sun, J., Folk, D., Bradley, T.J., and Tower, J. (2002). Induced overexpression of mitochondrial Mn-superoxide dismutase extends the life span of adult Drosophila melanogaster. Genetics *161*, 661–672.

Suvorova, E.S., Lucas, O., Weisend, C.M., Rollins, M.C.F., Merrill, G.F., Capecchi, M.R., and Schmidt, E.E. (2009). Cytoprotective Nrf2 pathway is induced in chronically Txnrd 1-deficient hepatocytes. PLoS One *4*.

Svensson, M.J., and Larsson, J. (2007). Thioredoxin-2 affects lifespan and oxidative stress in

Drosophila. Hereditas *144*, 25–32.

Svensson, M.J., Don Chen, J., Pirrotta, V., and Larsson, J. (2003). The ThioredoxinT and deadhead gene pair encode testis- and ovary-specific thioredoxins in Drosophila melanogaster. Chromosoma *112*, 133–143.

Svensson, M.J., Stenberg, P., and Larsson, J. (2007). Organization and regulation of sex-specific thioredoxin encoding genes in the genus Drosophila. Dev. Genes Evol. *217*, 639–650.

Ta, T.H., Hisam, S., Lanza, M., Jiram, A.I., Ismail, N., and Rubio, J.M. (2014). First case of a naturally acquired human infection with Plasmodium cynomolgi. Malar. J. *13*, 1–7.

Talsma, A.D., Christov, C.P., Terriente-Felix, A., Linneweber, G.A., Perea, D., Wayland, M., Shafer, O.T., and Miguel-Aliaga, I. (2012). Remote control of renal physiology by the intestinal neuropeptide pigment-dispersing factor in Drosophila. Proc. Natl. Acad. Sci. U. S. A. *109*, 12177–12182.

Tan, S.X., Greetham, D., Raeth, S., Grant, C.M., Dawes, I.W., and Perrone, G.G. (2010). The thioredoxin-thioredoxin reductase system can function in vivo as an alternative system to reduce oxidized glutathione in Saccharomyces cerevisiae. J. Biol. Chem. *285*, 6118–6126.

Tappel, A.L. (1962). Vitamin E as the biological lipid antioxidant. Vitam. Horm. *20*, 493–510.

Tarimo, B., Law, H., Tao, D., Pastrana-Mena, R., Kanzok, S., Buza, J., and Dinglasan, R. (2018). Paraquat-Mediated Oxidative Stress in Anopheles gambiae Mosquitoes Is Regulated by An Endoplasmic Reticulum (ER) Stress Response. Proteomes *6*, 47.

Tchigossou, G., Djouaka, R., Akoton, R., Riveron, J.M., Irving, H., Atoyebi, S., Moutairou, K., Yessoufou, A., and Wondji, C.S. (2018). Molecular basis of permethrin and DDT resistance in an Anopheles funestus population from Benin. Parasites and Vectors *11*, 1–13.

Thannickal, V.J., and Fanburg, B.L. (2010). Reactive oxygen species in cell signaling. Am J Physiol Lung Cell Mol Physiol *279*, 1005–1028.

Thieme, R., Pai, E.F., Schirmer, R.H., and Schulz, G.E. (1981). Three-dimensional structure of glutathione reductase at 2 Å resolution. J. Mol. Biol. *152*, 763–782.

Thimmulappa, R.K., Kensler, T.W., Thimmulappa, R.K., Lee, H., Rangasamy, T., and Reddy, S.P. (2016). Nrf2 is a critical regulator of the innate immune response and survival during experimental sepsis Find the latest version : Nrf2 is a critical regulator of the innate immune response and survival during experimental sepsis. *116*.

Thomas, D.C. (2017). The phagocyte respiratory burst: Historical perspectives and recent advances. Immunol. Lett. *192*, 88–96.

Thomas, J.A., Poland, B., and Honzatko, R. (1995). Protein sulfhydryls and their role in the

antioxidant function of protein S-thiolation. Arch. Biochem. Biophys. *319*, 1–9.

Tiwari, N.K., Reynolds, P.J., and Calderón, A.I. (2016). Preliminary LC-MS Based Screening for Inhibitors of Plasmodium falciparum Thioredoxin Reductase (PfTrxR) among a Set of Antimalarials from the Malaria Box. Molecules *21*.

Torres, M., and Forman, H.J. (2003). Redox signaling and the MAP kinase pathways. BioFactors *17*, 287–296.

Tuladhar, A., and Rein, K.S. (2018). Manumycin A Is a Potent Inhibitor of Mammalian Thioredoxin Reductase-1 (TrxR-1). ACS Med. Chem. Lett. *9*, 318–322.

Tuladhar, R., Yeu, Y., Tyler Piazza, J., Tan, Z., Rene Clemenceau, J., Wu, X., Barrett, Q., Herbert, J., Mathews, D.H., Kim, J., et al. (2019). CRISPR-Cas9-based mutagenesis frequently provokes on-target mRNA misregulation. Nat. Commun. *10*, 1–10.

Untergasser, A., Nijveen, H., Rao, X., Bisseling, T., Geurts, R., and Leunissen, J.A.M. (2007). Primer3Plus, an enhanced web interface to Primer3. Nucleic Acids Res. *35*, 71–74.

Urig, S., and Becker, K. (2006). On the potential of thioredoxin reductase inhibitors for cancer therapy. Semin. Cancer Biol. *16*, 452–465.

Vannini, L., Reed, T.W., and Willis, J.H. (2014). Temporal and spatial expression of cuticular proteins of Anopheles gambiae implicated in insecticide resistance or differentiation of M/S incipient species. Parasites and Vectors *7*, 1–11.

Vaughan, A., Hawkes, N., and Hemingway, J. (1997). Co-amplification explains linkage disequilibrium of two mosquito esterase genes in insecticide-resistant Culex quinquefasciatus. Biochem. J. *325*, 359–365.

Venturi, G., Di Luca, M., Fortuna, C., Elena Remoli, M., Riccardo, F., Severini, F., Toma, L., Del Manso, M., Benedetti, E., Grazia Caporali, M., et al. (2017). Detection of a chikungunya outbreak in Central Italy Detection of a chikungunya outbreak in Central. Euro Surveill. *22*, 1–4.

Vincent, S.R. (2010). Nitric oxide neurons and neurotransmission. Prog. Neurobiol. *90*, 246–255.

Volohonsky, G., Terenzi, O., Soichot, J., Naujoks, D. a, Nolan, T., Windbichler, N., Kapps, D., Smidler, A.L., Vittu, A., Costa, G., et al. (2015). Tools for Anopheles gambiae Transgenesis. G3 (Bethesda). 1–47.

Vomund, S., Schäfer, A., Parnham, M.J., Brüne, B., and Von Knethen, A. (2017). Nrf2, the master regulator of anti-oxidative responses. Int. J. Mol. Sci. *18*, 1–19.

Wagener, K.C., Kolbrink, B., Dietrich, K., Kizina, K.M., Terwitte, L.S., Kempkes, B., Bao, G., and Müller, M. (2016). Redox Indicator Mice Stably Expressing Genetically Encoded Neuronal

roGFP: Versatile Tools to Decipher Subcellular Redox Dynamics in Neuropathophysiology. Antioxidants Redox Signal. *25*, 41–58.

Wan, H., Kang, T., Zhan, S., You, H., Zhu, F., Lee, K.S., Zhao, H., Jin, B.R., and Li, J. (2014). Peroxiredoxin 5 from common cutworm (Spodoptera litura) acts as a potent antioxidant enzyme. Comp. Biochem. Physiol. Part - B Biochem. Mol. Biol. *175*, 53–61.

Wang, L., Yang, Z., Fu, J., Yin, H., Xiong, K., Tan, Q., Jin, H., Li, J., Wang, T., Tang, W., et al. (2012). Ethaselen: A potent mammalian thioredoxin reductase 1 inhibitor and novel organoselenium anticancer agent. Free Radic. Biol. Med. *52*, 898–908.

Wang, X., Campos, C.R., Peart, J.C., Smith, L.K., Boni, J.L., Cannon, R.E., and Miller, D.S. (2014). Nrf2 upregulates ATP binding cassette transporter expression and activity at the blood-brain and blood-spinal cord barriers. J. Neurosci. *34*, 8585–8593.

Wang, Y.Y., Chen, J., Liu, X.M., Zhao, R., and Zhe, H. (2018). Nrf2-mediated metabolic reprogramming in cancer. Oxid. Med. Cell. Longev. *2018*.

Wazen, R.M., Kuroda, S., Nishio, C., Sellin, K., Brunski, J.B., and Nanci, A. (2014). Inhibiton of Thioredoxin Reductase 1 by Porphyrins and Other Small Molecules Iddentified By a High Throughput Screening Assay. Free Radic. Biol. Med. *8*, 1385–1395.

WEBB, J.E., and GREEN, R.A. (1945). On the penetration of insecticides through the insect cuticle. J. Exp. Biol. *22*, 8–20.

Weill, M., Malcolm, C., Chandre, F., Mogensen, K., Berthomieu, A., Marquine, M., and Raymond, M. (2004). The unique mutation in ace-1 giving high insecticide resistance is easily detectable in mosquito vectors. Insect Mol. Biol. *13*, 1–7.

Wells, W.W., Xu, D.P., Yang, Y., and Rocque, P.A. (1990). Mammalian thioltransferase (glutaredoxin) and protein disulfide isomerase have dehydroascorbate reductase activity. J. Biol. Chem. *265*, 15361–15364.

Wessing, A., and Zierold, K. (1999). The formation of type-I concretions in Drosophila Malpighian tubules studied by electron microscopy and X-ray microanalysis. J. Insect Physiol. *45*, 39–44.

Whitbread, A.K., Masoumi, A., Tetlow, N., Schmuck, E., Coggan, M., and Board, P.G. (2005). Characterization of the omega class of glutathione transferases. Methods Enzymol. *401*, 78–99.

WHO (2005). Safety of Pyrethroids for Public Health Use. World Heal. Organ. , WHOPES (WHO Pestic. Eval. Scheme) PCS (Programme Chem. Safety) 49.

WHO (2006). Indoor residual spraying: Use of indoor residual spraying for scaling up global malaria control and elimination. Glob. Malar. Program. World Heal. Organ.

WHO (2012). World Malaria Report 2012 (Geneva).

WHO (2018). World malaria report 2018 (Geneva).

Wiederhold, N.P., Patterson, T.F., Srinivasan, A., Chaturvedi, A.K., Fothergill, A.W., Wormley, F.L., Ramasubramanian, A.K., and Lopez-Ribot, J.L. (2017). Repurposing auranofin as an antifungal: In vitro activity against a variety of medically important fungi. Virulence *8*, 138–142.

William, T., Menon, J., Rajahram, G., Chan, L., Ma, G., Donaldson, S., Khoo, S., Fredrick, C., Jelip, J., Anstey, N.M., et al. (2011). Severe Plasmodium knowlesi malaria in a tertiary care hospital, Sabah, Malaysia. Emerg. Infect. Dis. *17*, 1248–1255.

Williams, C.H. (1995). Mechanism and structure of thioredoxin reductase from Escherichia coli. FASEB J. *9*, 1267–1276.

Winter, F., Edaye, S., Hüttenhofer, A., and Brunel, C. (2007). Anopheles gambiae miRNAs as actors of defence reaction against Plasmodium invasion. Nucleic Acids Res. *35*, 6953–6962.

Winterbourn, C.C. (2008). Reconciling the chemistry and biology of reactive oxygen species. Nat. Chem. Biol. *4*, 278–286.

World Health Organization (2018). Global report on insecticide resistance in malaria vectors: 2010-2016.

World Health Organization (2019). Guidelines for Malaria Vector Control.

Wu, C., Parrott, A.M., Fu, C., Liu, T., Marino, S.M., Gladyshev, V.N., Jain, M.R., Baykal, A.T., Li, Q., Oka, S., et al. (2011). Thioredoxin 1-mediated post-translational modifications: Reduction, transnitrosylation, denitrosylation, and related proteomics methodologies. Antioxidants Redox Signal. *15*, 2565–2604.

Yan, Y., Zhang, Y., Huaxia, Y., Wang, X., Yao, P., Guo, X., and Xu, B. (2014). Identification and characterisation of a novel 1-Cys thioredoxin peroxidase gene (AccTpx5) from Apis cerana cerana. Comp. Biochem. Physiol. Part - B Biochem. Mol. Biol. *172–173*, 39–48.

Yao, P., Lu, W., Meng, F., Wang, X., Xu, B., and Guo, X. (2013). Molecular cloning, Expression and oxidative stress response of a mitochondrial thioredoxin peroxidase gene (AccTpx-3) from Apis cerana cerana. J. Insect Physiol. *59*, 273–282.

Yoo, M.H., Carlson, B.A., Gladyshev, V.N., and Hatfield, D.L. (2013). Abrogated Thioredoxin System Causes Increased Sensitivity to TNF-α-Induced Apoptosis via Enrichment of p-ERK 1/2 in the Nucleus. PLoS One *8*, 1–10.

Zahedi Avval, F., and Holmgren, A. (2009). Molecular mechanisms of thioredoxin and glutaredoxin as hydrogen donors for mammalian S phase ribonucleotide reductase. J. Biol. Chem. *284*,

8233–8240.

Zelko, I.N., Mariani, T.J., and Folz, R.J. (2002). Superoxide dismutase multigene family: A comparison of the CuZn-SOD (SOD1), Mn-SOD (SOD2), and EC-SOD (SOD3) gene structures, evolution, and expression. Free Radic. Biol. Med. *33*, 337–349.

Zhang, Y., and Lu, Z. (2015). Peroxiredoxin 1 protects the pea aphid Acyrthosiphon pisum from oxidative stress induced by Micrococcus luteus infection. J. Invertebr. Pathol. *127*, 115–121.

Zhang, J., Campbell, R.E., Ting, A.Y., and Tsien, R.Y. (2002). Creating new fluorescent probes for cell biology. Nat. Rev. Mol. Cell Biol. *3*, 906–918.

Zhang, J., Wang, X., Vikash, V., Ye, Q., Wu, D., Liu, Y., and Dong, W. (2016a). ROS and ROS-Mediated Cellular Signaling. Oxid. Med. Cell. Longev. *2016*.

Zhang, J., Zhang, B., Li, X., Han, X., Liu, R., and Fang, J. (2019a). Small molecule inhibitors of mammalian thioredoxin reductase as potential anticancer agents: An update. Med. Res. Rev. *39*, 5–39.

Zhang, S., Li, Z., Nian, X., Wu, F., Shen, Z., and Zhang, B. (2015). Sequence analysis , expression profiles and function of thioredoxin 2 and thioredoxin reductase 1 in resistance to nucleopolyhedrovirus in Helicoverpa armigera. Nat. Publ. Gr. 1–16.

Zhang, S.D., Shen, Z.J., Liu, X.M., Li, Z., Zhang, Q.W., and Liu, X.X. (2016b). Molecular identification of three novel glutaredoxin genes that play important roles in antioxidant defense in Helicoverpa armigera. Insect Biochem. Mol. Biol. *75*, 107–116.

Zhang, Y., Wang, J., Wang, Z., Zhang, Y., Shi, S., Nielsen, J., and Liu, Z. (2019b). A gRNA-tRNA array for CRISPR-Cas9 based rapid multiplexed genome editing in Saccharomyces cerevisiae. Nat. Commun. *10*, 1–10.

Zhong, L., and Holmgren, A. (2000). Essential role of selenium in the catalytic activities of mammalian thioredoxin reductase revealed by characterization of recombinant enzymes with selenocysteine mutations. J. Biol. Chem. *275*, 18121–18128.

Zhong, L., Arne, E.S.J., and Holmgren, A. (2000). Structure and mechanism of mammalian thioredoxin reductase: The active site is a redox-active selenolthiol/selenenylsulfide formed from the conserved cysteine-selenocysteine sequence. Proc. Natl. Acad. Sci. *97*, 5854–5859.

Zhou, G., Kohlhepp, P., Geiser, D., Frasquillo, M. del C., Vazquez-Moreno, L., and Winzerling, J.J. (2007). Fate of blood meal iron in mosquitoes. J. Insect Physiol. *53*, 1169–1178.

Zhou, Y., Liu, Y., Yan, H., Li, Y., Zhang, H., Xu, J., Puthiyakunnon, S., and Chen, X. (2014). MIR-281, an abundant midgut-specific miRNA of the vector mosquito Aedes albopictus enhances dengue virus replication. Parasites and Vectors *7*, 1–11.

Zhu, J., and Noriega, F.G. (2016). The Role of Juvenile Hormone in Mosquito Development and Reproduction (Elsevier Ltd.).

Zou, L., Wang, J., Gao, Y., Ren, X., Rottenberg, M.E., Lu, J., and Holmgren, A. (2018). Synergistic antibacterial activity of silver with antibiotics correlating with the upregulation of the ROS production. Sci. Rep. *8*, 1–11.

SUPPLEMENTARY

S.1 Codon optimized *AgTrx*

GGATCCGTGTATATGGTCAAAGACTCGGAAGATTTCAACAATAAGCTGGAAGCT
GCAGGCGATCAACTGGTTGTAGTGGACTTCTTTGCCACGTGGTGTGGTCCGTG
CAAAGTGATTGCGCCGAAATTGGAAGAGTTTCAGAACAAGTATGCGGACAAAAT
CGTGGTTGTGAAAGTCGATGTTGATGAATGCGAAGAATTAGCTGCCCAGTACAA
CATTGCGAGCATGCCAACCTTTCTCTTTATCAAACGCAAAGAAGTCGTAGGGCA
GTTTAGTGGCGCAAATGCGGAGAAACTGGAGAATTTCATTCAGCAACATTCCGC
CTAAAAGCTT

S.2 Codon optimized *AgTrxR*

GGATCCGCGCCTCTCAACCAGGAGAACTACGAATACGACCTGGTGGTAATTGG
CGGTGGCAGTGGCGGTTTGGCGTGTGCTAAGCAGGCAGTACAACTGGGTGCAA
AAGTTGCCGTTCTGGACTTCGTGAAACCGAGCCCTCGTGGCACCAAATGGGGT
CTTGGTGGCACATGCGTTAACGTAGGCTGTATTCCGAAGAAACTCATGCATCAG
GCTAGTCTGCTCGGCGAAGCGATTCACGACTCACAACCGTATGGCTGGCAGCT
CCCAGATCCGGCTGCCATTCGTCATGACTGGGCGACGTTAACAGAGAGCGTGC
AGAACCACATCAAGTCGGTGAATTGGGTGACCCGCGTCGATCTGCGCGACCAG
AAAGTGGAATATGTGAACGGGTTAGGCTACTTCAAAGACGATCACACCGTGGTC
GCCGTAATGAAGAACCAGACGGAACGCGAACTCCGTGCCAAACATGTTGTCAT
CGCGGTTGGTGGTCGTCCACGCTATCCGGATATCCCTGGTGCGGCGGAGTATG
GCATTACCTCTGATGACATCTTTTCGCTGCCGCAAGCTCCCGGTCGGACGTTGC
TGGTTGGTGCGGGATACATTGGGCTGGAATGCGCCGGCTTTCTGAAAGGGTTG
GGATACGACGTCAGCGTGATGGTCCGGAGCATTTTGCTGCGCGGATTCGACCA
ACAGATGGCAACTATGGTTGGGGATAGCATGGTTGAGAAAGGTATCCGCTTTCA
CCATCGTTCTCGCCCGTTAGCCGTAGAGAAACAGCCGGATGGCCGTCTGCTGG
TGCGTTACGAAACTGTTGATGAGGCGGGTACTGCCACAAATGGCGAAGATGTG

TTCGATACCGTGCTGTTCGCGATTGGCCGCCAAGCCGAGACTGGCACCCTGAA
ACTTGCGAATGCTGGAGTGGTGACCGCGGAAGGTGGTAAGTCCGATAAACTGG
AAGTCGATGAAACCGATCATCGCACGAATGTGCCGCATATCTACGCAGTCGGC
GATGTTCTGTATCGCAAACCGGAACTGACCCCAGTTGCGATTCATGCTGGCCGC
ATTATTGCGCGTCGCCTGTTTGGCGGGAGTGAAGAACGCATGGACTATGCTGAT
GTAGCGACTACGGTGTTTACCCCGCTGGAATATGGGTGTGTCGGGCTGTCCGA
AGAAGCAGCAGAGGCAGCCCATGGCAAAGATGGGATCGAAGTCTATCACGCAT
ATTACAAACCTACCGAATTCTTTGTGCCACAGCGTTCGGTACGGTATTGCTATTT
GAAAGCCGTTGCGCTGCGCGAGGGTAACCAGCGCGTGTTAGGACTGCACTTTC
TGGGTCCCGCAGCCGGCGAAGTCATCCAGGGATTTGCAGCCGCGTTAAAATGC

S.3 Codon optimized *AaTrx*

GTGTATATCGTTAAGGATGCAGCCGATTTTGATAGCAAACTGGAAAGCGCCGGT
GACAAACTGGTGGTTGTGGATTTCTTTGCCACCTGGTGCGGTCCGTGCAAAGTT
ATTGCACCGAAACTGGAAGAATTTCAGAATAAGTATGCAGAAAAGGTTCTGATTA
TCAAAGTGGATGTTGATGAATGCGAAGATCTGGCAGCAAAATATGAAATTAGCA
GTATGCCGACCTTTCTGTTTATTAAGGGTAAAAAGTGGTGTATCAGTTTAGTGG
CGCCAATGATCAGAAACTGGAAATGTATATTCTGAAACATGCCTAA

Table S.4. Tested compound and IC$_{50}$ values (µM) on different insect TrxR using the cognate Trx or DTNB as substrate in two different assays (microplate reader and spectrophotometer)

#	Mw (g/mol)	Anopheles gambiae Trx Micro.	Anopheles gambiae Trx Spect.	Anopheles gambiae DTNB Spect.	Aedes aegypti Trx Spect.	Aedes aegypti DTNB Spect.	Drosophila melanogaster Trx Micro.	Drosophila melanogaster Trx Spect.	Apis mellifera Trx Micro.	Apis mellifera Trx Spect.	Apis mellifera DTNB Micro.	Apis mellifera DTNB Spect.
1	414,93	>300		> 300	162,9	> 300	>300		> 300		> 300	
2	486,55	>300		94,88	46,21	82,16	>300		> 300		281,4	109,9
3	271,39	>300		147,7	>300	> 300	>300		> 300		> 300	
4	514,67	>300		243,7	>300	388,3	>300		361,8		> 300	
5	275,22	>300		> 300	>300	> 300	>300		> 300		> 300	
6	310,27	>300		> 300	172,4	73,75	>300		311,2		> 300	
7	267,22	>300		94,38	>300	146,7	>300		> 300		> 300	
8	467,22	>300		> 300	93,9	> 300	88,8	26,7	647,4		> 300	
9	460,51	>300		98,62	66,45	63,39	>300		> 300		> 300	
10	342,35	>300		> 300	>300	> 300	>300		> 300		> 300	
11	403,52	>300		> 300	>300	> 300	>300		> 300		> 300	
12	260,25	>300		> 300	>300	> 300	>300		> 300		> 300	
13	486,55	243		197,5	124,1	84,59	>300		425,7		> 300	
14	245,2	>300		> 300	>300	> 300	>300		> 300		> 300	
15	229,23	>300		> 300	>300	> 300	>300		> 300		> 300	
16	152,15	>300		> 300	>300	> 300	>300		> 300		> 300	
17	248,2	>300		> 300	>300	> 300	>300		> 300		> 300	
18	264,24	234		24,8	133,9	43,02	255		397,6		278,9	72
19	254,36	>300		295,2	>300	> 300	>300		> 300		> 300	
20	335,47	>300		> 300	>300	> 300	>300		> 300		> 300	
21	336,19	>300		55,9	41,78	55,58	>300		112,1		101,6	169,7
22	344,07	>300		> 300	>300	> 300	>300		> 300	> 300	> 300	
23	338,52	>300		> 300	317,1	233,1	>300		305,8		> 300	
24	344,52	13,5	44,8	35,8	47,48	66,46	31,7	n.d.	61,5	> 300	150,2	> 300
25	220,36	>300		> 300	>300	> 300	>300		> 300		> 300	
26	264,33	>300		> 300	>300	> 300	>300		> 300		> 300	
27	368,38	325		73,97	36,47	> 60	345	42,4	124		59,55	91,78
28	158,16	0,12	0,28	1,148	0,3722	89,77	>300		0,231	0,4124	197,3	308,2
29	172,18	133	285	> 300	> 300	> 300	68	128	358,6	120,7	> 300	

III

Table S.4. (continued)

#	Mw (g/mol)	Anopheles gambiae Trx Micro.	Anopheles gambiae Trx Spect.	Anopheles gambiae DTNB Spect.	Aedes aegypti Trx Spect.	Aedes aegypti DTNB Spect.	Drosophila melanogaster Trx Micro.	Drosophila melanogaster Trx Spect.	Apis mellifera Trx Micro.	Apis mellifera Trx Spect.	Apis mellifera DTNB Micro.	Apis mellifera DTNB Spect.
30	678,49	0,017	0,114	0,01965	0,0188	0,1318	0,7	0,11	0,04368	0,111	0,0997	n.d.
31	928,74	0,007	0,034	0,1175	1,001	0,08784	>300		0,1164	0,05143	0,6584	65,39
32	373,9	>300		> 300	> 100	> 300	0,13	327	> 300	> 300	> 300	
33	357,2	329		> 300	78,73	> 200	>300		210,1		> 300	
34	341,2	>300		111	95,06	54,38	>300		154,7	49,78	> 300	
35	355,18	310		> 300	27,09	278	189		115,8	25,17	> 300	
36	322,44	>300		71,04	222,2	44,73	>300		490,9	114,5	> 300	
37	354,51	>300		88,29	137,4	70,01	>300		203,7	> 300	> 300	

Raquel MELA LÓPEZ

Université de Strasbourg

JUSTUS-LIEBIG-UNIVERSITÄT GIESSEN

Thioredoxin reductase in *Anopheles gambiae* **mosquitoes:**
ROLE IN REDOX HOMEOSTASIS MAINTENANCE
AND MANIPULATION FOR VECTOR CONTROL

Résumé en français

L'émergence et la propagation des résistances aux insecticides chez les populations de moustiques constituent une menace majeure pour les programmes de contrôle du paludisme. Il existe donc un besoin urgent de développer des nouveaux insecticides à modes d'action novateurs. Les insectes ne possèdent pas l'enzyme antioxydante clé glutathion réductase, dont on pense que le rôle est compensé par le système thiorédoxine / thioredoxine reductase.

L'objectif de ma thèse était d'étudier le rôle de la thiroedoxine réductase chez le moustique vecteur du paludisme *Anopheles gambiae* et d'évaluer son potentiel en tant que nouvelle cible insecticide. J'ai mis en place de nouvelles lignées transgéniques reportrices de l'état redox et j'ai montré qu'en général, le maintien de l'homéostasie redox est étroitement réglementé chez ces espèces tout au long de leur cycle de vie. J'ai en outre généré des mutants CRISPR / Cas9 pour la *thiorédoxine réductase* et montré qu'elle est essentiel pour le développement des moustiques, mais qu'elle n'est pas indispensable dans l'intestin des adultes. Enfin, j'ai identifié des inhibiteurs de cette enzyme *in vitro* et montré qu'ils sont mortels pour les moustiques *Anopheles gambiae.*

Mots clés : thiorédoxine réductase – roGFP – insecticides – Anopheles gambiae – homéostasie redox

Summary in English

The emergence and spreading of insecticide resistances in mosquito populations is a major threat to malaria control programs. There is, therefore, an urge to develop new insecticides with novels modes of action. Insects lack the key antioxidant enzyme glutathione reductase, whose role is believed to be compensated by the thioredoxin / thioredoxin reductase system.

The aim of my PhD was to study the role of thiroedoxin reductase in the malaria mosquito *Anopheles gambiae* and to assess its potential as a new insecticidal target. I have established new transgenic redox reporter mosquito lines and shown that, in general, the maintenance of the redo homeostasis is tightly regulated in these species over their entire life cycle. I have further generated CRISPR/Cas9 mutants for *thioredoxin reductase* and demonstrated that it is essential for mosquito development, but dispensable in the midgut of the adults. Finally, I have identified inhibitors of this enzyme *in vitro* and shown that they are lethal to *Anopheles gambiae* mosquitoes.

Key words: thioredoxin reductase – roGFP – insecticides – Anopheles gambiae – redox homeostasis